MOLECULAR DISSECTION OF LIGHT PERCEPTION

IN ZEBRAFISH

DISSERTATION

ZUR

ERLANGUNG DER NATURWISSENSCHAFTLICHEN DOKTORWÜRDE

(DR. SC. NAT.)

VORGELEGT DER

MATHEMATISCH-NATURWISSENSCHAFTLICHEN FAKULTÄT

DER

UNIVERSITÄT ZÜRICH

VON

MARION HAUG

VON

WEININGEN ZH

PROMOTIONSKOMITEE

PROF. DR. STEPHAN C. F. NEUHAUSS (LEITUNG DER DISSERTATION)

PROF. DR. CHRISTIAN GRIMM

PROF. DR. STEVEN A. BROWN

ZÜRICH, 2012

I TABLE OF CONTENT

II PREFACE

„Man muss noch Chaos in sich haben, um einen tanzenden

Stern gebären zu können.“

---

aus „Also sprach Zarathustra“ von Friedrich Nietzsche, 1844 – 1900

III SUMMARY

The perception of light enables animals to coordinate behavior and physiology to changes in their surrounding. In my thesis, I exploited the advantages of the vertebrate model organism zebrafish to investigate different aspects of light perception.

Glutamate is the principal excitatory neurotransmitter in the brain, implicating that glutamate receptors play crucial roles in signal transmission. Nevertheless, the knowledge about metabotropic glutamate receptors (mGluRs) in zebrafish is scarce. While mammals possess eight mGluRs, our phylogenetic analysis revealed that the zebrafish genome harbors a larger mGluR family of 13 genes, which likely originate from the teleost specific additional whole genome duplication. As they phylogenetically segregate in the same subfamilies as mammals, conserved functions are expected. An accurate mRNA expression study revealed a unique distribution of all *mglurs* within the zebrafish nervous system, suggesting highly distinct functions for each of the receptor subtypes.

Photoreceptors release glutamate in the dark. Sign inversion for the detection of light increments is mediated via the inhibitory mGluR6 on ON-bipolar cell dendrites. We found that the zebrafish harbors two mGluR6 paralogs and that the mGluR6 signaling pathway is likely conserved in this animal. This enables the use of zebrafish as a model to elucidate mGluR6 mediated ON-signaling properties. A functional analysis in mGluR6b-depleted larvae revealed a significant contribution of mGluR6b to the cone ON-response. In addition, we suggest that at least part of the remaining cone ON-response is generated via EAAT7. Excitatory amino acid transporters (EAATs) are hypothesized to be involved in direct retinal ON-signaling by hyperpolarizing ON-bipolar cells via an inhibitory chloride conductance.

Almost all organisms possess some form of biological time keeping mechanism that provides an internal representation of time. This circadian clock sets the phases at which behavioral and physiological events occur and allows fine-tuning to the environment. Visual sensitivity was found to be regulated by such internal rhythms, being highest at dusk. To our surprise, we found *mglur6* pathway members to be under circadian control, suggesting a molecular mechanism for the increased visual sensitivity in the evening.

Another part of my thesis deals with non-visual light perception, also important for driving the circadian clock. Cryptochromes (Crys), photopigments absorbing light in the UV- and blue range, were found to be involved in many light-guided processes. This includes circadian rhythmicity where Crys regulate the negative limb of the transcriptional feedback loop or even act as light sensor for the circadian clock. A comparative bioinformatic analysis allowed us to decipher the correct phylogeny of all eight zebrafish Crys. We confirmed a rhythmic expression of all *crys* in the zebrafish retina, which however does not necessarily implicate an involvement in the input pathway to the circadian clock.

Non-visual photoreception is mediated via ocular and extraocular photopigments, which have likely different contributions to light-guided behavioral mechanisms. Using eyeless mutants helped us to decipher between ocular and extraocular input to locomotor activity responses upon changing illumination under different light spec-

tra. We could show that the startle OFF-response is likely mediated via the retina, while the ON-response includes extraocular photopigments that absorb light in the blue to green range. This shows that such experiments are a useful tool to predict spectral properties of photopigments that mediate light-guided behaviors.

IV ZUSAMMENFASSUNG

Die Wahrnehmung unterschiedlicher Lichtreize erlaubt es Tieren ihr Verhalten und ihre Physiologie verändernden Umweltbedingungen anzupassen. In dieser Arbeit nutzte ich die Vorzüge des Modellorganismus Zebrafisch um verschiedene Aspekte der neuronalen Lichtverarbeitung zu untersuchen.

Glutamat gehört zu den wichtigsten Neurotransmittern des Gehirns, was zur Folge hat, dass Glutamatezeptoren bedeutende Rollen in der Signalübermittlung spielen. Dennoch ist noch wenig über metabotrope Glutamatrezeptoren (mGluRs) im Wirbeltier Zebrafisch bekannt. Unsere phylogenetische Untersuchung hat ergeben, dass diese Genfamilie im Zebrafisch umfangreicher ist als in Säugetieren. Die fünf zusätzlichen mGluRs entstanden wahrscheinlich während der nachträglichen Genomduplikation der Teleosten, zu denen auch der Zebrafisch gehört. Da alle mGluRs von Zebrafischen und Säugetieren in die phylogenetisch gleichen Subfamilien segregieren, erwarten wir ähnliche Funktionen dieser Gene. Detaillierte Expressionsstudien zeigten eine spezifische Verteilung der einzelnen *mglurs* im Zentralnervensystem des Zebrafisches, was darauf hinweist, dass jeder Subtyp eine spezielle Funktion ausführt.

Photorezeptoren schütten in der Dunkelheit Glutamat aus. Dieses Signal wird mithilfe des inhibierenden mGluR6 in den Dendriten von ON-Bipolarzellen umgekehrt, um ansteigende Helligkeit zu detektieren. Der Zebrafisch besitzt zwei *mglur6* Gene, die beide in ON-Bipolarzellen exprimiert sind. Weitere Lokalisationsstudien zeigten, dass der intrazelluläre mGluR6 Signalweg im Zebrafisch konserviert ist, was eine genauere Studie der Bestandteile der mGluR6-abhängigen ON-Signale ermöglichte. Mithilfe einer funktionellen Analyse in Larven konnten wir eine bedeutende Beteiligung von mGluR6b in der von Zapfen gesteuerten ON-Antwort finden. Weiterführende Experimente zeigten, dass zumindest ein Teil der restlichen ON-Antwort durch den Glutamattransporter EAAT7 vermittelt wird. Es wird angenommen, dass diese Transporter mit Hilfe eines hemmenden Chloridstroms ON-Bipolarzellen in der Dunkelheit inhibieren.

Desweiteren spielt bei der Lichtwahrnehmung die zirkadiane Uhr eine wichtige Rolle. Fast alle Organismen besitzen eine Art biologische innere Zeitmessung. Sie steuert die Anpassung von Verhalten und Physiologie über den Tag hinweg und erlaubt eine Abstimmung mit der Umwelt. Auch die Empfindlichkeit des visuellen Systems, die während der Abenddämmerung am höchsten ist, wird durch einen internen Rhythmus gesteuert. Interessanterweise fanden wir, dass die Expression einiger der am mGluR6 Signalweg beteiligten Gene zirkadian reguliert ist. Dies könnte ein bislang unbekannter molekularer Mechanismus sein, der die höhere visuelle Empfindlichkeit am Abend bedingt.

Ein weiterer Teil meiner Arbeit befasst sich mit nicht-visueller Lichtwahrnehmung. Cryptochrome (Crys), Photopigmente die Licht im UV- und Blau-Bereich absorbieren, sind an vielen lichtabhängigen Prozessen beteiligt. Dies beinhaltet auch die zirkadian Rhythmik, wo Crys den negativen Teil des Regelkreises regulieren oder sogar direkt den Lichtsensor für die zirkadiane Uhr bilden. Mittels einer vergleichenden bioinformatischen Analyse konnten wir die korrekte Phylogenie aller acht Zebrafisch-spezifischen Cryptochrome bestimmen. Desweiteren wiesen wir eine rhythmische Exprimierung aller *crys* in der Netzhaut des Fisches nach.

Nicht-visuelle Lichtwahrnehmung kann durch Photopigmente erfolgen die in den Augen oder auch anderswo am Körper angebracht sind. Welche Photopigmente an welchen lichtgesteuerten Verhaltensmechanismen beteiligt sind, ist nicht bekannt. Um zu unterscheiden welche Photopigmente zu motorischen Aktivitätsrhythmen beitragen, verglichen wir Wildtypen mit augenlosen Mutanten unter verschiedenen Lichtverhältnissen. So konnten wir zeigen, dass die typisch erhöhte motorische Aktivität bei Ausstellen des Lichtes über die Augen generiert wird, während beim Anstellen des Lichtes die erhöhte Aktivität eher durch Photopigmente des restlichen Körpers, welche Licht im Blau- bis Grünbereich absorbieren, vermittelt wird. Diese Experimente sind sehr hilfreich um spektrale Eigenschaften von Photopigmenten vorherzusagen, die lichtabhängige Verhaltensmechanismen steuern.

Chapter 1

General Introduction

1.1 Light perception

Processing and interpreting visible light generates visual sensation. To accomplish this, animals use their eyes and brains, however, light is not only perceived for conscious form vision but also guides a large number of physiological tasks we are mostly unaware of. Almost all living beings on earth from plants, to bacteria and animals use specific photopigments to perceive light that mediate such unconscious tasks. In the following sections I will discuss several aspects of visual and non-visual photoreception.

1.1.1 Architecture of the eye

All vertebrate eyes are composed of three nuclear and two synaptic layers. Light enters the eye trough the pupil, traverses the vitreous and several cell layers before it falls on an array of photoreceptors located in the back of the eye (Fig. 1). The cornea, a transparent surface that covers the pupil and the iris, together with the crystalline lens form an optical system that enables the production of a focused image at the photoreceptor level (reviewed in Purves *et al.*, 2004). In mammals, birds, and reptiles, a changing shape of the lens accomplished via muscle contractions leads to accommodation and helps focusing on a specific depth. The fovea is a small pit in the human retina that consists of the highest density of cone photoreceptors. This is the central point for image focusing during the day and enables resolution of the finest details.

The retina that perceives and processes the incoming light is located at the back of the eye. It develops as an evagination from the neural tube, therefore it is part of the central nervous system. The retina is built of three layers of nerve cell bodies and two interplexiform layers where synaptic contacts occur. The outermost outer nuclear layer (ONL) consists of two types of photoreceptors, rods and cones, which possess visual pigments in their outer segments. They consist of opsin and a bound chromophore, the 11-cis retinal that is able to absorb light and start a signaling cascade by conformational change to its all-trans form. Structurally different cone opsins enable light absorption at different wavelengths to generate color vision. Cones are less sensitive to light than rods, thus start to contribute to vision at higher light intensity and are mostly used during the day. At such bright light levels rods are already saturated. As they are able to detect very few photons their main task is to provide vision at very low light intensities as it occurs during the night. To rely their information both rod and cone photoreceptors form synapses with bipolar cells in the outer plexiform layer (OPL), which in turn are connected to ganglion cells in the inner plexiform layer (IPL). Ganglion cells are the output neurons of the retina and their axons bundle to form the nerve fibers which leave the eye as optic nerve. Since at this spot no photorecep-

tors can be placed, it is also called the blind spot. In addition, the retina harbors horizontal and amacrine cells that enable horizontal information flow through the retina. Although less apparent, two more non-neural cell types are crucial for continuous visual function, Muller glia cells and cells of the retinal pigment epithelium (RPE). Besides that numerous subgroups in every cell type and sublaminae in each layer add to the complexity of the vertebrate retina. Muller glia cells are important not only for transmitter homeostasis but also for retinal regeneration (Yurco & Cameron, 2005; Fausett & Goldman, 2006), and the RPE harbors many functions such as "recharging" of visual pigments, phagocytosis and renewal of photoreceptor outer segments, and the transport of metabolites to and from the subretinal space (Sparrow *et al.*, 2010; Strauss, 2005).

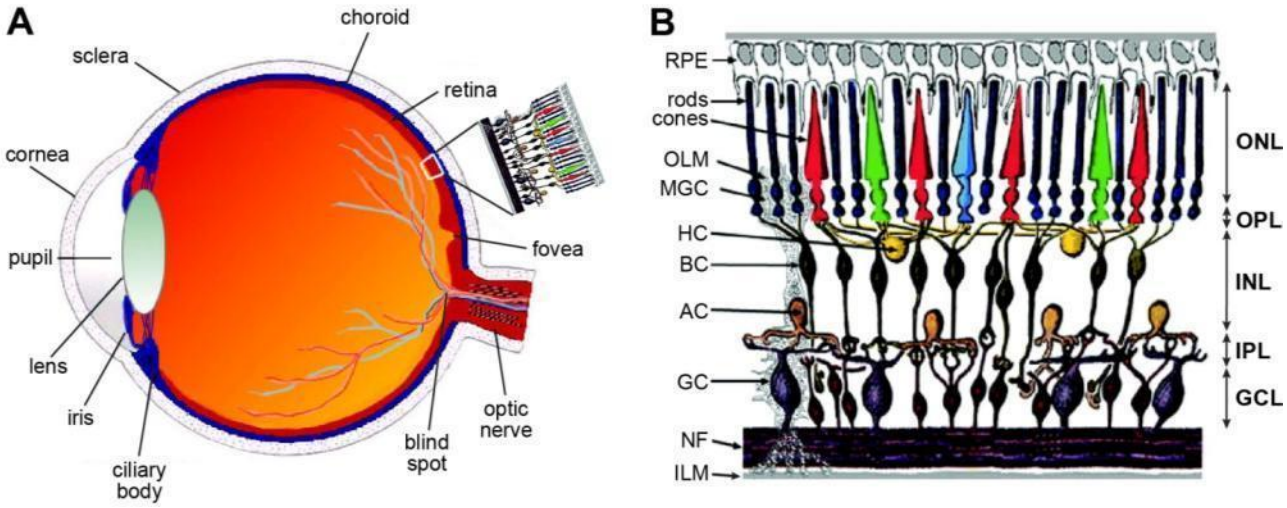

Fig. 1: Anatomy of the eye.
A: *Schematic radial section through the human eye.* ***B:*** *Enlargement of the retina as depicted in A. AC, amacrine cells; BC, bipolar cells; GC, ganglion cells; GCL, ganglion cell layer; HC, horizontal cells; ILM, inner limiting membrane; INL, inner nuclear layer; IPL, inner plexiform layer; MGC, muller glia cells; NF, nerve fibers; OLM, outer limiting membrane; ONL, outer nuclear layer; OPL, outer plexiform layer; RPE, retinal pigment epithelium. Adapted from webvision.med.utah.edu.*

1.1.2 Generation of retinal ON- and OFF-responses

Glutamate is the most abundant neurotransmitter in the central nervous system. The visual signaling cascade initiated by light absorption of the chromophore in photoreceptor outer segments leads to a hyperpolarization of photoreceptors, thereby decreasing glutamate release into the synaptic cleft. This signal is not only propagated through the following cell layers and finally to the brain, it rather is highly processed already within the retina. The parallel processing of for example color or motion into different channels is fundamental for vision and already occurs at the first visual synapse (reviewed in Wässle, 2004). Also the detection of brighter or lower than background illumination fundamental for contrast perception segregates into two opposite pathways in the OPL which are reinforced by lateral inhibiting horizontal cells. As all photoreceptors respond with hyperpolarization and a decreased glutamate release on light absorption, the separation is mediated via two different types of glutamate receptors on bipolar cell dendrites. The OFF-response is mediated via AMPA/kainate type of ionotropic glutamate receptors, thereby conserving the signal from photoreceptors. ON-signaling on the other hand needs an opposite response onto glutamate, which is accomplished via mGluR6, an inhibitory metabotropic glutamate

receptor (Fig. 2A). Here, an increase in glutamate starts an intracellular G-protein coupled signaling cascade that leads to the closure of a transient receptor potential channel (TRPM1) and hyperpolarizes the cell (Fig. 2B). Recently, nyctalopin (NYX) and G protein-coupled receptors (GPR158/179) have been discovered to play crucial roles in compartmentalization of pathway members (Cao *et al.*, 2011; Orlandi *et al.*, 2012). However, their precise role in the mGluR6 pathway is still unknown. Mutations in any of the genes involved in that pathway manifest in lacking ERG b-waves and lead to night blindness in humans (Dryja *et al.*, 2005; Zeitz *et al.*, 2005; Bech-Hansen *et al.*, 2000; Audo *et al.*, 2012). In addition to mGluR6 signaling, another way to hyperpolarize ON-bipolar cells upon light decreases has been discovered in lower vertebrates. Inhibitory chloride conductances of excitatory amino acid transporters (EAATs) located on bipolar cell dendrites likely also contribute to ON-signaling (Fig. 2C; Grant & Dowling, 1995, 1996; Wong *et al.*, 2005; Wong *et al.*, 2004). However, the main task of these glutamate transporters mostly located on presynapses and glia cells is to prevent glutamate spillover (Huang & Bergles, 2004).

While cones synapse to ON- and OFF-bipolar cells, rods are only connected to ON-type bipolar cells, which then conduct the obtained signal over amacrine cells to ON- and OFF-cone bipolar cells. However, there is evidence for direct synaptic connections between rods and OFF-cone bipolar cells, which would provide an alternative rod pathway (Li *et al.*, 2004; Li *et al.*, 2010).

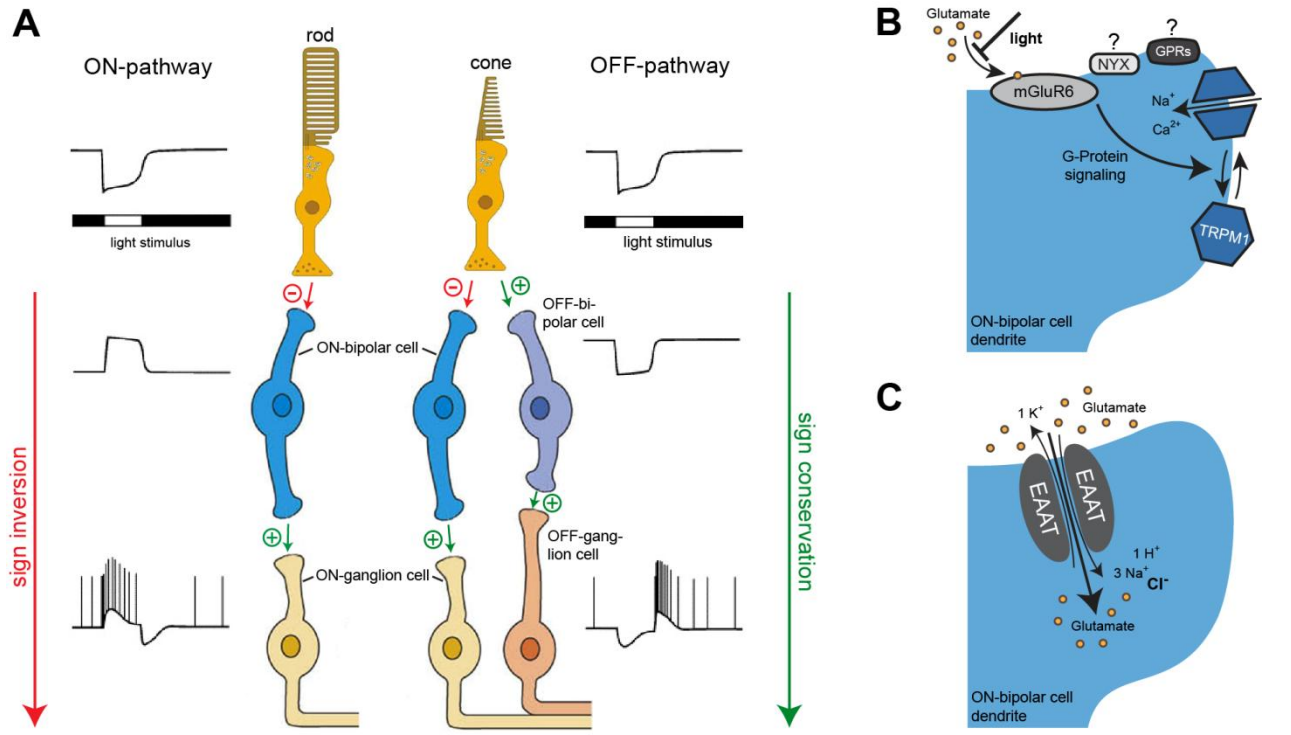

Fig. 2: Parallel ON- and OFF-pathways.
A: *Drawing of retina ON- and OFF-responses showing sign inversing (red) and sign conserving (green) synapses. Electrical responses from photoreceptors, bipolar cells, and ganglion cells to a light stimulus are indicated on either side, showing the separation into ON- and OFF-pathways at the level of bipolar cells as a reaction to light increases or light decreases, respectively. This dichotomy is reflected at the level of ganglion cells which respond with an increased or decreased firing pattern during the light stimulus.* ***B,C:*** *Enlargement of the ON-bipolar cell dendrite depicting the two possibilities to generate a sign inversion. The mGluR6 pathway leads to a closure of a cation channel (TRPM1), thereby hyperpolarizing the cell (B), while the opening of glutamate transporters (EAATs) hyperpolarizes the cell via a co-conductance of chloride (C). A: adapted from (Purves et al., 2004; La Cour & Ehinger, 2005).*

1.1.3 Light perception of the circadian system

As early as in 1729 the French astronomer Jean-Jacques Ortous de Mairan described that the daily opening and closure of the leaves of a flowering plant was not only a simple response to sunlight but rather a rhythmic motion that persisted even in the absence of light. Such robust day-night oscillations in behavior and physiology are found in nearly all living organisms and are called circadian rhythms. Most of these rhythms persist under constant external conditions and allow organisms to anticipate and adapt to the daily changing environment. The importance of biological clocks is reflected by the huge amount of physiological processes that underlay circadian rhythms. Besides hormone release and metabolism also many aspects of the visual system such as electrical coupling of rods and cones or visual sensitivity undergo daily changes (reviewed in Guido *et al.*, 2010). To stay synchronized with the 24 hour cycle given by the sun, the circadian system is mainly reset by light. While the architecture of our eyes enables highly accurate temporal and spatial vision at a point of interest it is not suited to measure gross changes in irradiance levels (reviewed in Foster & Hankins, 2002). Therefore other sensors are needed to fulfill this task. Fruit flies solved this problem by expressing the blue-light absorbing photopigment cryptochrome (CRY) in every cell (Emery *et al.*, 1998; Plautz *et al.*, 1997). Induced by light, it drives a transcriptional-translational-feedback loop that leads to rhythmic gene expression and subsequently behavior (Fig. 3A). Mammals still possess cell-autonomous circadian clocks, however, they are not directly entrained by light but need to be synchronized from a hierarchically higher center. Specific photosensitive retinal ganglion cells expressing the photopigment melanopsin absorb light unconsciously and send their information via the retinohypothalamic tract (RHT) to the hypothalamic suprachiasmatic nucleus (SCN), also called the master clock (Hattar *et al.*, 2002; Berson *et al.*, 2002). There, two interspersed molecular feedback loops are activated which drive rhythmic gene expression (Fig. 3B). Similar to the fruit fly, lower vertebrates such as zebrafish still maintain directly light-responsive, cell-autonomous circadian clocks that use cryptochrome 1a as light sensor (Whitmore *et al.*, 2000). Likely, other photopigments such as other cryptochromes or opsin variants located in peripheral tissues or the eye contribute to clock entrainment as well, as a large variety of photoreceptors enables a more reliable indication of light.

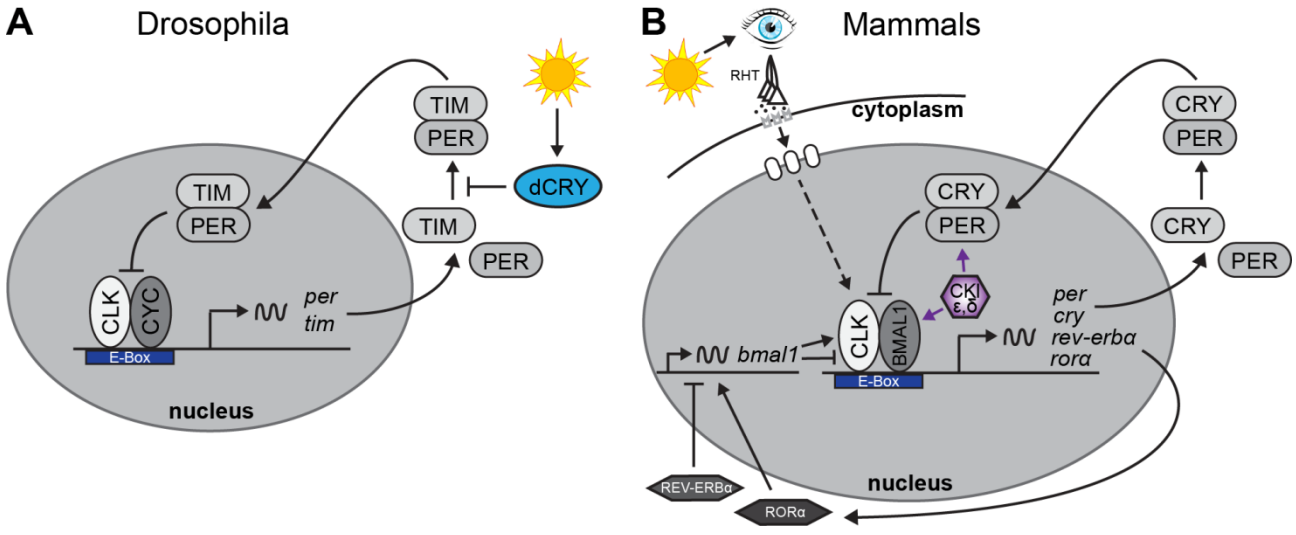

Fig. 3: Regulation of circadian clocks in Drosophila and mammals.
Simplified models of the Drosophila and mammalian circadian clock mechanism. ***A:*** *In Drosophila, cryptochrome (dCRY) suppresses the negative feedback loop of the circadian clock by binding to timeless (TIM) in a light-dependent manner. This results to TIM degradation and prevents heterodimerization with period (PER).Without dCRY the PER:TIM complex would enter the nucleus and inhibit the binding of clock (CLK) and cycle (CYC) proteins to the E-box in the promoters of clock genes, preventing their expression. B: Light entrains the mammalian circadian pacemaker by light input over the retina and the retinohypothalamic tract (RHT) that results in expression of immediate early genes that phase shift the circadian clock (not shown). Similar to Drosophila negative feedback loops control rhythmic clock gene expression, however, here cryptochromes are integral parts of the loop. Posttranslational modifications mediated by casein kinase I (CKI isoform ε and δ) regulate PER, CRY, and BMAL1 protein stability, thereby regulating the action of clock proteins. BMAL1 is the mammalian ortholog of cycle. Adapted from (Albrecht, 2004; Lin & Todo, 2005; Guido et al., 2010).*

1.2 The zebrafish in vision research

When about 20 years ago George Streisinger, a scientist working on the genetics of phages, started to introduce the zebrafish (*Danio rerio*) as a model system, he could hardly imagine the large success of this little fish in the scientific world. His idea was to use zebrafish for a genetic analysis of the vertebrate nervous system. Some of the first publications about zebrafish already described its visual pigments (Nawrocki *et al.*, 1985) and the early development of the retina (Streisinger *et al.*, 1989) which paved the way for this model organism in vision research.

The zebrafish retina develops extraordinarily fast enabling vision-based foraging already at 5 days post fertilization (dpf). At that stage all retinal cell types are present in a layered structure which changes only marginally in adulthood (Fig. 4). Larval fish have an excellent color vision adapted to their diurnal habitat and show nearly adult-like visual performances (Branchek, 1984; Branchek & Bremiller, 1984). Similar to humans, zebrafish harbor cones that absorb light in the red, green and blue range (Robinson *et al.*, 1995). However, in their retina the red- and the green-cone are merged to a red-green doublecone and they possess in addition a forth UV-cone type (Robinson *et al.*, 1993). Nevertheless, there are more than only four cone types present in the zebrafish retina, as recent studies detected two red- (LWS1, -2) , four green- (RH2-1 to 2-4), one blue- (SWS2) and one UV- (SWS1) opsin (Chinen *et al.*, 2003). As rods are not crucial for vision during early larval stages, they start to integrate later. Their structure appears adult-like from around day 15 on, and first functions can be measured at 12 dpf (Branchek, 1984; Branchek & Bremiller, 1984). The larval zebrafish retina is thus cone-dominated, in contrast to the rod-dominated retinae of nocturnal mammals like mice. In that respect the teleost retina is more closely related to that of humans than the retina of rodents and is ideally suited to study cone-related mechanisms. Moreover, the large number of offspring, the external development of the embryo and its transparency facilitates experimental manipulations and observations.

A large number of mutant strains were produced by incorporation of random mutations via ENU-mutagenesis (Mullins *et al.*, 1994) or retroviruses (Gaiano *et al.*, 1996). This forward genetic strategy led to the identification of many retina specific phenotypes that enable the study of specific mutations of interest (Malicki *et al.*, 1996). However, without the ability to test the fish's visual behavior and detect particular phenotypes, such screens would not have been very successful. Scientists make use of innate behaviors elicited by moving visual stimuli. One widely used technique that generates reliable readouts of visual function is the optokinetic response (OKR; reviewed in Huang & Neuhauss, 2008). It is characterized as a stereotypic compensating eye movement to track

moving objects of the surround. In the lab it is imitated by a rotating paper drum around an immobilized fish (Fig. 5A,B). By changing properties of the moving grate such as contrast, color and temporal or spatial frequency, different aspects of visual function, e.g. visual acuity (Haug *et al.*, 2010) or more subtle defects such as color blindness (Brockerhoff *et al.*, 1997), can be measured. Another possibility is to measure motor responses triggered by fast changes of illumination. The read out of these visual motor responses (VMR) gives information about ON- and OFF-pathways (Fig. 5C,D), however, as zebrafish are able to gain information about light via peripheral photoreceptors (Fernandes *et al.*, 2012), the read out might not be as straight forward as previously thought. Patch clamp or electroretinogram (ERG; Fig. 5E,F) recordings allow the measurement of retinal properties on a physiological level. Combined with pharmacological tools aspects of specific signaling pathways can be dissected and individually studied. As genomic information for the zebrafish is available, in recent years reverse genetic tools have been developed allowing precise analysis of certain structures and genes. Nowadays, morpholino-based gene downregulation and transposon-mediated creation of stable transgenics are just two technologies widely used among the zebrafish community. The recently developed TALENs system even promises reliable and fast targeted gene knock out and will greatly enhance the power of zebrafish as a genetic model organism. In addition, optogenetics is currently revolutionizing behavioral neuroscience (reviewed in del Bene & Wyart, 2012). As this technique is based on light-activated molecules and allows the monitoring and controlling of neuronal activity in living animals, the small, transparent, and genetically accessible zebrafish is perfectly suitet for exploiting this new method.

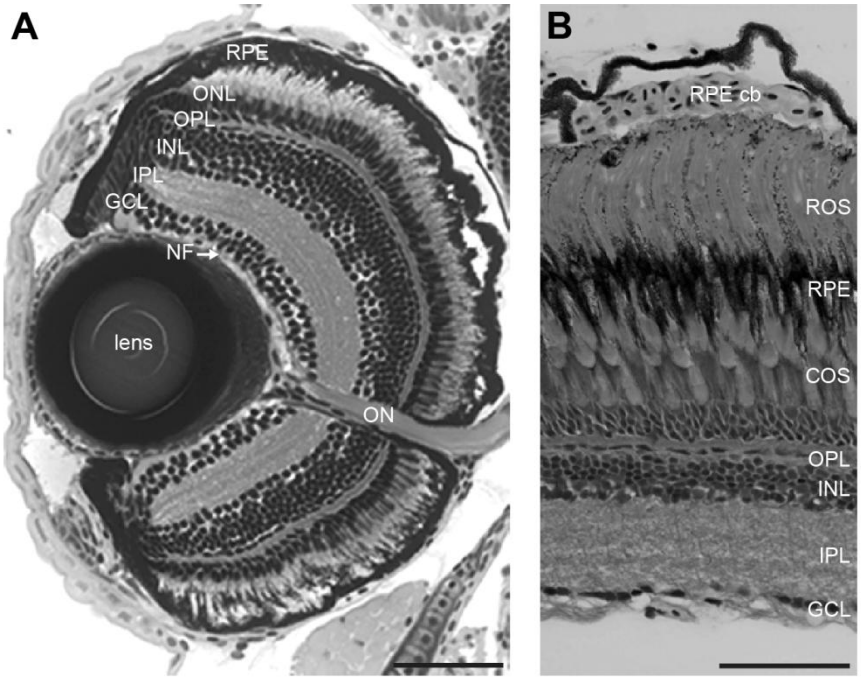

Fig. 4: Light micrographs of radial sections through the zebrafish retina.
A: *Already at 5 dpf the zebrafish retina is fully functional and shows a layered structure similar to the adult retina (**B**). COS, cone outer segments; GCL, ganglion cell layer; INL, inner nuclear layer; IPL, inner plexiform layer; NF, nerve fibers; ON, optic nerve; ONL, outer nuclear layer; OPL, outer plexiform layer; ROS, rod outer segments; RPE, retinal pigment epithelium; RPE cb, cell bodies of the RPE. Scale bars = 50 µm.*

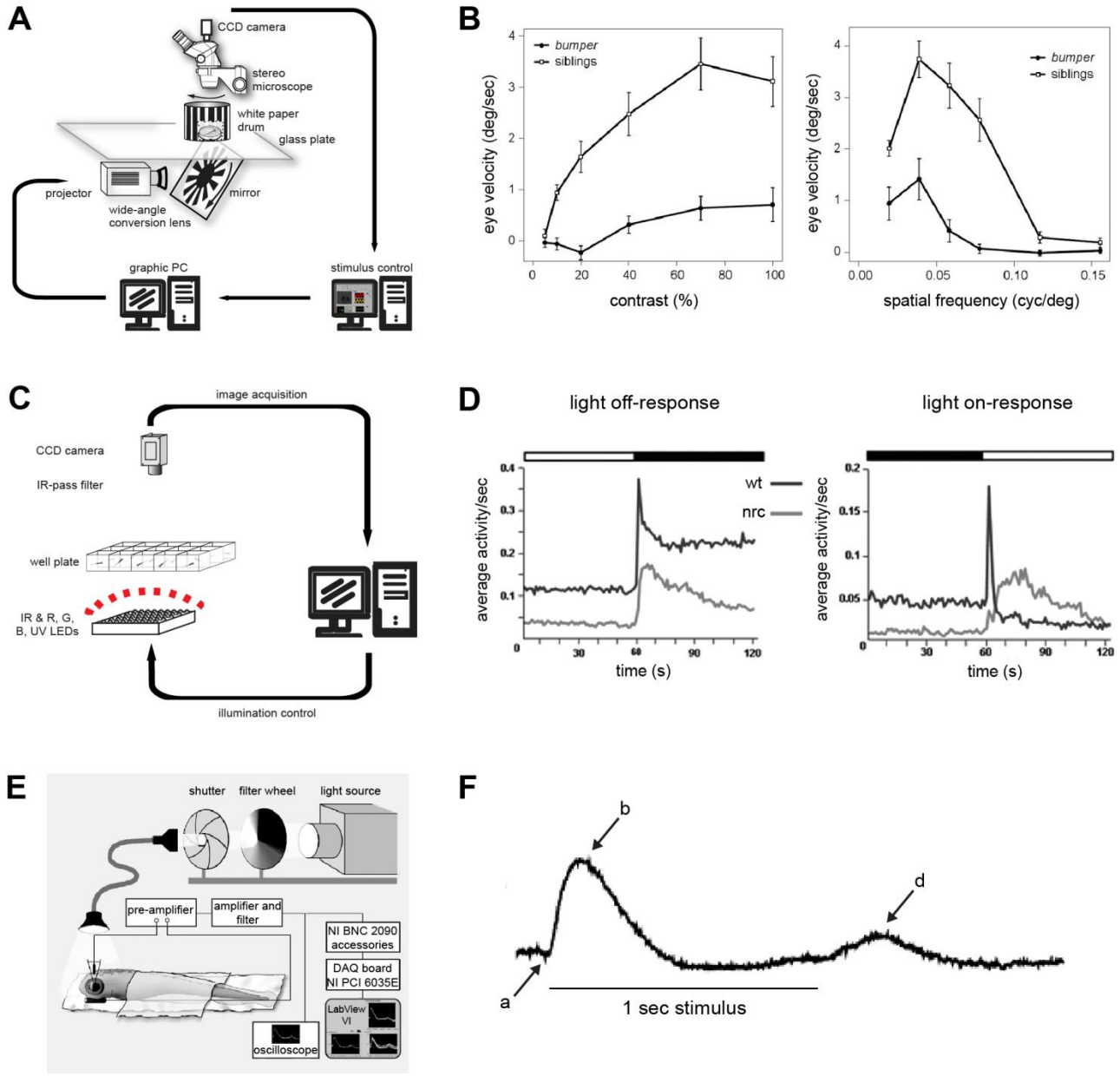

Fig. 5: Tools for testing visual performance in zebrafish.
A: *Setup for measuring the optokinetic response (OKR).* ***B:*** *Zebrafish larval eye velocity depends on contrast and spatial frequency as depicted in wild-type and bumper mutant fish that have a lens defect.* ***C:*** *Experimental device for testing visual motor responses (VMR).* ***D:*** *Changing illumination leads to fast startle responses in fish larvae measured with the VMR-setup. Weaker but robust startle response could be measured in no optokinetic response c (nrc) mutants that were previously reported to be completely blind.* ***E:*** *For measuring the electroretinogram (ERG) an electrode is placed directly onto the cornea.* ***F:*** *light stimulus leads to the generation of an a-, a b-, and a d-wave reflecting responses generated by photoreceptors, the ON- and OFF-pathway, respectively. A,B: adapted from (Mueller & Neuhauss, 2010; Mueller et al., 2011); C: by K. Mueller; D: adapted from (Emran et al., 2008); E,F: adapted from (Makhankov et al., 2004).*

1.3 Genome duplications as driving force in evolution

In all three domains of life, large proportions of genes were generated by genome duplications. While many of these duplicated genes accumulate deleterious mutations and later become pseudogenes, some are maintained within the genome. If no gene dosage constrains keeps those genes functional, their release from selective pres-

sure could lead to the acquisition of new functions. In a whole genome duplication (WGD) event not only single genes but the whole genome including regulatory elements is duplicated. Here, mutations in regulatory subunits could split the ancestral function onto both genes (Force *et al.*, 1999). Gene duplications do not necessarily have to be a dead end but provide opportunities for evolutionary success. In plants and yeast polyploidy likely accelerated evolution and builds the basis for speciation (Blanc & Wolfe, 2004; Kellis *et al.*, 2004).

Although WGDs are less frequent in vertebrates two round of WGD are believed to stand at the beginning of the vertebrate evolution (Fig. 6) (Hoegg & Meyer, 2005; Dehal & Boore, 2005), however, the evolutionary effects of these events are still debated (reviewed in Crow & Wagner, 2006; van de Peer *et al.*, 2009). Teleosts underwent a third round of whole genome duplication right at the basis of their lineage about 350 Mya (million years ago; Fig. 6) (Amores *et al.*, 1998; Vandepoele *et al.*, 2004). Nowadays, the class of teleosts comprises over 23'000 species and is the most diverse and evolutionary successful group of vertebrates (Basden *et al.*, 2000). Whether this triumphant radiation was facilitated by the additional WGD is unclear since fossil records propose that 100 – 150 million years separate the duplication event and teleost radiation (reviewed in Ohno, 1999, Postlethwait *et al.*, 2004, Volff, 2005). Nevertheless, gene loss or partitioning of gene function can still occur many millions of years after a WGD (Scannell *et al.*, 2006; Sémon & Wolfe, 2007, 2008). Likely, a change in the ecological situation built the basis for speciation of teleosts. As the above mentioned models for gene preservation possibly led to the retainment of around 20% of all duplicated genes in teleosts (Force *et al.*, 1999; Woods *et al.*, 2005), the use of zebrafish in molecular genetics is exacerbated. While redundant gene function of duplicated genes complicates loss-of-function studies, the partitioning ancestral gene function can bring the opportunity to identify tissue-specific regulatory elements. Moreover, the investigation of sub- or neofunctionalization events helps identifying the evolution of gene function.

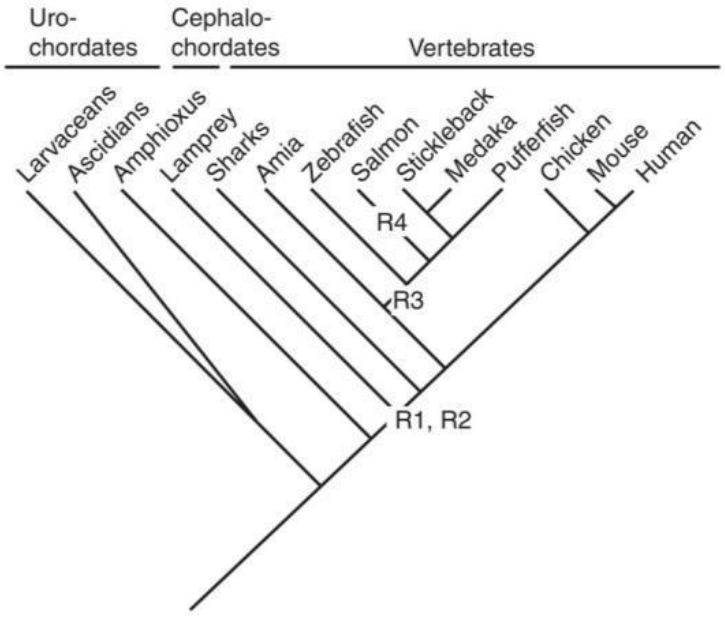

Fig. 6: Chordate phylogeny indicating probable genome duplication events.
Two rounds of whole genome duplications (R1 and R2) occurred approximately 500 Mya at the very base of the vertebrate taxa. An additional third duplication event (R3) was specific to the class of ray-finned fish and happened around 350 Mya. A further duplication event, R4, presumably occurred about 50 Mya at the base of the salmonid radiation. Adapted from (Postlethwait, 2007).

1.4 Objectives of the thesis

This thesis aims to enlighten different aspects of light perception in zebrafish by exploiting bioinformatic, molecular, and behavioral techniques.

Although glutamate is one of the main neurotransmitters in the central nervous system and its receptors are essential for many signal pathways, the knowledge about metabotropic glutamate receptors (mGluRs) in zebrafish is scarce. Chapter 2 of my thesis deals with the family of glutamate receptors, its phylogenetic relationship and detailed expression in the zebrafish central nervous system.

As the contribution of mGluR6 to the retinal ON-response is still under debate, the focus of Chapters 3 and 4 lies on the molecular dissection of the retinal ON-signaling in the cone-dominant larval zebrafish retina. Chapter 3 describes the retinal expression of both zebrafish *mglur6* paralogs in larval and adult fish. In addition, the function of mGluR6b was investigated by a morpholino mediated gene knockdown and subsequent ERG analysis. In Chapter 4 we examined signal transmission at the first visual synapse in a broader manner. First, we studied the co-expression of molecules involved in the mGluR6 signaling pathway to find whether this pathway is also conserved in zebrafish. Next, we investigated the possible contribution of mGluR6a and -6b to the ON-response on a morphological level. Besides that, as glutamate transporters (EAATs) are hypothesized to be involved in direct ON-signaling, we examined EAAT7 in combination with mGluR6b by a double knockdown approach.

Many retinal mechanisms are regulated by a circadian clock. Visual sensitivity was found to be highest at dusk, however, no molecular mechanism has been found yet. In Chapter 5 we describe a possible mechanism that could explain this phenomenon.

Chapters 6 and 7 focus on cryptochromes (Crys), the blue-light receptors involved in many photoreactive pathways. As to date Cry phylogeny has been ambiguous, a preceding analysis of this gene family's phylogeny was essential. Therefore, these studies were initiated by bioinformatic analysis of *cry* sequences in zebrafish and further comparison to data of other species. Furthermore, mRNA expression analysis of *crys* in zebrafish was accomplished to find hints for an involvement of a cryptochrome in non-visual photoreception mediated via the retina.

As zebrafish not only possess photoreceptive cells in their eyes, the last Chapter 8 deals with light perception of ocular and extraocular photoreceptors. Locomotor activity patterns as well as responses to fast changes in illumination were measured under different light conditions with the VMR-setup. The use of the eyeless *chokh* mutant allowed us to distinguish between behaviors mediated by ocular or peripheral photopigments.

1.5 References

Albrecht, U. (2004) Human molecular chronotyping in sight? Genome Biol., 5, 246.

Amores, A., Force, A., Yan, Y.L., Joly, L., Amemiya, C., Fritz, A., Ho, R.K., Langeland, J., Prince, V., Wang, Y.L., Westerfield, M., Ekker, M. & Postlethwait, J.H. (1998) Zebrafish hox clusters and vertebrate genome evolution. Science, 282, 1711–1714.

Audo, I., Bujakowska, K., Orhan, E., Poloschek, C.M., Defoort-Dhellemmes, S., et. al. (2012) Whole-exome sequencing identifies mutations in GPR179 leading to autosomal-recessive complete congenital stationary night blindness. Am. J. Hum. Genet., 90, 321–330.

Basden, A.M., Young, G.C., Coates, M.I. & Ritchie, A. (2000) The most primitive osteichthyan braincase? Nature, 403, 185–188.

Bech-Hansen, N.T., Naylor, M.J., Maybaum, T.A., Sparkes, R.L., Koop, B., Birch, D.G., Bergen, A.A., Prinsen, C.F., Polomeno, R.C., Gal, A., Drack, A.V., Musarella, M.A., Jacobson, S.G., Young, R.S. & Weleber, R.G. (2000) Mutations in NYX, encoding the leucine-rich proteoglycan nyctalopin, cause X-linked complete congenital stationary night blindness. Nat. Genet., 26, 319–323.

Berson, D.M., Dunn, F.A. & Takao, M. (2002) Phototransduction by retinal ganglion cells that set the circadian clock. Science, 295, 1070–1073.

Blanc, G. & Wolfe, K.H. (2004) Functional divergence of duplicated genes formed by polyploidy during Arabidopsis evolution. Plant Cell, 16, 1679–1691.

Branchek, T. (1984) The development of photoreceptors in the zebrafish, brachydanio rerio. II. Function. J. Comp. Neurol, 224, 116–122.

Branchek, T. & Bremiller, R. (1984) The development of photoreceptors in the zebrafish, Brachydanio rerio. I. Structure. J Comp Neurol, 224, 107–115.

Brockerhoff, S.E., Hurley, J.B., Niemi, G.A. & Dowling, J.E. (1997) A new form of inherited red-blindness identified in zebrafish. J. Neurosci., 17, 4236–4242.

Cao, Y., Posokhova, E. & Martemyanov, K.A. (2011) TRPM1 forms complexes with nyctalopin in vivo and accumulates in postsynaptic compartment of ON-bipolar neurons in mGluR6-dependent manner. J. Neurosci., 31, 11521–11526.

Chinen, A., Hamaoka, T., Yamada, Y. & Kawamura, S. (2003) Gene duplication and spectral diversification of cone visual pigments of zebrafish. Genetics, 163, 663–675.

Crow, K. & Wagner, G. (2006) What Is the Role of Genome Duplication in the Evolution of Complexity and Diversity? Mol. Biol. Evol., 23, 887–892.

del Bene, F. & Wyart, C. (2012) Optogenetics: a new enlightenment age for zebrafish neurobiology. Dev Neurobiol 72 (3), 404–414.

Dehal, P. & Boore, J.L. (2005) Two rounds of whole genome duplication in the ancestral vertebrate. PLoS Biol., 3, e314.

Dryja, T.P., McGee, T.L., Berson, E.L., Fishman, G.A., Sandberg, M.A., Alexander, K.R., Derlacki, D.J. & Rajagopalan, A.S. (2005) Night blindness and abnormal cone electroretinogram ON responses in patients with mutations in the GRM6 gene encoding mGluR6. Proc. Natl. Acad. Sci. U.S.A., 102, 4884–4889.

Emery, P., So, W.V., Kaneko, M., Hall, J.C. & Rosbash, M. (1998) CRY, a Drosophila clock and light-regulated cryptochrome, is a major contributor to circadian rhythm resetting and photosensitivity. Cell, 95, 669–679.

Emran, F., Rihel, J. & Dowling, J.E. (2008) A behavioral assay to measure responsiveness of zebrafish to changes in light intensities. J Vis Exp.

Fausett, B.V. & Goldman, D. (2006) A role for alpha1 tubulin-expressing Müller glia in regeneration of the injured zebrafish retina. J. Neurosci., 26, 6303–6313.

Fernandes, A.M; Fero K.; Arrenberg, A.B; Bergeron, S.A; Driever, W.; Burgess, H.A (2012) Deep brain photoreceptors control light seeking behavior in zebrafish larvae. Current Biology. In press.

Force, A., Lynch, M., Pickett, F.B., Amores, A., Yan, Y.L. & Postlethwait, J. (1999) Preservation of duplicate genes by complementary, degenerative mutations. Genetics, 151, 1531–1545.

Foster, R.G. & Hankins, M.W. (2002) Non-rod, non-cone photoreception in the vertebrates. Prog Retin Eye Res, 21, 507–527.

Gaiano, N., Amsterdam, A., Kawakami, K., Allende, M., Becker, T. & Hopkins, N. (1996) Insertional mutagenesis and rapid cloning of essential genes in zebrafish. Nature, 383, 829–832.

Grant, G.B. & Dowling, J.E. (1995) A glutamate-activated chloride current in cone-driven ON bipolar cells of the white perch retina. J Neurosci, 15, 3852–3862.

Grant, G.B. & Dowling, J.E. (1996) On bipolar cell responses in the teleost retina are generated by two distinct mechanisms. J Neurophysiol, 76, 3842–3849.

Guido, M.E., Garbarino-Pico, E., Contin, M.A., Valdez, D.J., Nieto, P.S., Verra, D.M., Acosta-Rodriguez, V.A., Zavalía, N. de & Rosenstein, R.E. (2010) Inner retinal circadian clocks and non-visual photoreceptors: novel players in the circadian system. Prog. Neurobiol., 92, 484–504.

Hattar, S., Liao, H.W., Takao, M., Berson, D.M. & Yau, K.W. (2002) Melanopsin-containing retinal ganglion cells: architecture, projections, and intrinsic photosensitivity. Science, 295, 1065–1070.

Haug, M.F., Biehlmaier, O., Mueller, K.P. & Neuhauss, S.C. (2010) Visual acuity in larval zebrafish: behavior and histology. Front. Zool., 7, 8.

Hoegg, S. & Meyer, A. (2005) Hox clusters as models for vertebrate genome evolution. Trends Genet., 21, 421–424.

Huang, Y.H. & Bergles, D.E. (2004) Glutamate transporters bring competition to the synapse. Curr. Opin. Neurobiol., 14, 346–352.

Huang, Y.-Y. & Neuhauss, S.C.F. (2008) The optokinetic response in zebrafish and its applications. Front. Biosci., 13, 1899–1916.

Kellis, M., Birren, B.W. & Lander, E.S. (2004) Proof and evolutionary analysis of ancient genome duplication in the yeast Saccharomyces cerevisiae. Nature, 428, 617–624.

La Cour, M. & Ehinger, B. (2005) The Biology of the Eye. The Retina. Elsevier, 195–252.

Li, W., Chen, S. & DeVries, S.H. (2010) A fast rod photoreceptor signaling pathway in the mammalian retina. Nat. Neurosci., 13, 414–416.

Li, W., Keung, J.W. & Massey, S.C. (2004) Direct synaptic connections between rods and OFF cone bipolar cells in the rabbit retina. J. Comp. Neurol., 474, 1–12.

Lin, C. & Todo, T. (2005) The cryptochromes. Genome Biol., 6, 220.

Makhankov, Y.V., Rinner, O. & Neuhauss, S.C.F. (2004) An inexpensive device for non-invasive electroretinography in small aquatic vertebrates. J. Neurosci. Methods, 135, 205–210.

Malicki, J., Neuhauss, S. C., Schier, A. F., Solnica-Krezel, L., Stemple, D. L., Stainier, D. Y., Abdelilah, S., Zwartkruis, F., Rangini, Z., Driever, W. (1996). Mutations affecting development of the zebrafish retina. Development 123, pp. 263–273.

Mueller, K.P. & Neuhauss, S.C.F. (2010) Quantitative measurements of the optokinetic response in adult fish. J. Neurosci. Methods, 186, 29–34.

Mueller, K.P., Schnaedelbach, O.D.R., Russig, H.D. & Neuhauss, S.C.F. (2011) VisioTracker, an innovative automated approach to oculomotor analysis. J Vis Exp.

Mullins, M.C., Hammerschmidt, M., Haffter, P. & Nüsslein-Volhard, C. (1994) Large-scale mutagenesis in the zebrafish: in search of genes controlling development in a vertebrate. Curr. Biol., 4, 189–202.

Nawrocki, L., Bremiller, R., Streisinger, G. & Kaplan, M. (1985) Larval and adult visual pigments of the zebrafish, Brachydanio rerio. Vision Res., 25, 1569–1576.

Ohno, S. (1999) Gene duplication and the uniqueness of vertebrate genomes circa 1970-1999. Semin. Cell Dev. Biol., 10, 517–522.

Orlandi, C., Posokhova, E., Masuho, I., Ray, T.A., Hasan, N., Gregg, R.G. & Martemyanov, K.A. (2012) GPR158/179 regulate G protein signaling by controlling localization and activity of the RGS7 complexes. J. Cell Biol., 197, 711–719.

Plautz, J.D., Kaneko, M., Hall, J.C. & Kay, S.A. (1997) Independent photoreceptive circadian clocks throughout Drosophila. Science, 278, 1632–1635.

Postlethwait, J., Amores, A., Cresko, W., Singer, A. & Yan, Y.-L. (2004) Subfunction partitioning, the teleost radiation and the annotation of the human genome. Trends Genet., 20, 481–490.

Postlethwait, J.H. (2007) The zebrafish genome in context: ohnologs gone missing. J. Exp. Zool. B Mol. Dev. Evol., 308, 563–577.

Purves, D., Augustine G.J., Fitzpatrick, D., Hall, W., LaMantia, A.-S., McNamara, J. & Williams, S. (2004) Neuroscience, third edition. Sinauer Associates, Inc. Publishers, Sunderland, Massachusetts, U.S.A.

Robinson, J., Schmitt, E.A. & Dowling, J.E. (1995) Temporal and spatial patterns of opsin gene expression in zebrafish (Danio rerio). Vis. Neurosci., 12, 895–906.

Robinson, J., Schmitt, E.A., Hárosi, F.I., Reece, R.J. & Dowling, J.E. (1993) Zebrafish ultraviolet visual pigment: absorption spectrum, sequence, and localization. Proc. Natl. Acad. Sci. U.S.A., 90, 6009–6012.

Scannell, D.R., Byrne, K.P., Gordon, J.L., Wong, S. & Wolfe, K.H. (2006) Multiple rounds of speciation associated with reciprocal gene loss in polyploid yeasts. Nature, 440, 341–345.

Sémon, M. & Wolfe, K.H. (2007) Reciprocal gene loss between Tetraodon and zebrafish after whole genome duplication in their ancestor. Trends Genet., 23, 108–112.

Sémon, M. & Wolfe, K.H. (2008) Preferential subfunctionalization of slow-evolving genes after allopolyploidization in Xenopus laevis. Proc. Natl. Acad. Sci. U.S.A., 105, 8333–8338.

Sparrow, J.R., Hicks, D. & Hamel, C.P. (2010) The retinal pigment epithelium in health and disease. Curr. Mol. Med., 10, 802–823.

Strauss, O. (2005) The retinal pigment epithelium in visual function. Physiol. Rev., 85, 845–881.

Streisinger, G., Coale, F., Taggart, C., Walker, C. & Grunwald, D.J. (1989) Clonal origins of cells in the pigmented retina of the zebrafish eye. Dev. Biol., 131, 60–69.

van de Peer, Y., Maere, S. & Meyer, A. (2009) The evolutionary significance of ancient genome duplications. Nat. Rev. Genet., 10, 725–732.

Vandepoele, K., Vos, W. de, Taylor, J.S., Meyer, A. & van de Peer, Y. (2004) Major events in the genome evolution of vertebrates: paranome age and size differ considerably between ray-finned fishes and land vertebrates. Proc. Natl. Acad. Sci. U.S.A., 101, 1638–1643.

Volff, J.-N. (2005) Genome evolution and biodiversity in teleost fish. Heredity (Edinb), 94, 280–294.

Wässle, H. (2004) Parallel processing in the mammalian retina. Nat. Rev. Neurosci., 5, 747–757.

Whitmore, D., Foulkes, N.S. & Sassone-Corsi, P. (2000) Light acts directly on organs and cells in culture to set the vertebrate circadian clock. Nature, 404, 87–91.

Wong, K.Y., Adolph, A.R. & Dowling, J.E. (2005) Retinal bipolar cell input mechanisms in giant danio. I. Electroretinographic analysis. J Neurophysiol, 93, 84–93.

Wong, K.Y., Gray, J., Hayward, C.J.C., Adolph, A.R. & Dowling, J.E. (2004) Glutamatergic mechanisms in the outer retina of larval zebrafish: analysis of electroretinogram b- and d-waves using a novel preparation. Zebrafish, 1, 121–131.

Woods, I.G., Wilson, C., Friedlander, B., Chang, P., Reyes, D.K., Nix, R., Kelly, P.D., Chu, F., Postlethwait, J.H. & Talbot, W.S. (2005) The zebrafish gene map defines ancestral vertebrate chromosomes. Genome Res., 15, 1307–1314.

Yurco, P. & Cameron, D.A. (2005) Responses of Müller glia to retinal injury in adult zebrafish. Vision Res., 45, 991–1002.

Zeitz, C., van Genderen, M., Neidhardt, J., Luhmann, U.F.O., Hoeben, F., Forster, U., Wycisk, K., Mátyás, G., Hoyng, C.B., Riemslag, F., Meire, F., Cremers, F.P.M. & Berger, W. (2005) Mutations in GRM6 cause autosomal recessive congenital stationary night blindness with a distinctive scotopic 15-Hz flicker electroretinogram. Invest. Ophthalmol. Vis. Sci., 46, 4328–4335.

Chapter 2

Phylogeny and Expression Divergence of Metabotropic Glutamate Receptor Genes in the Brain of Zebrafish (*Danio rerio*)

Marion F. Haug[1], Matthias Gesemann[1], Thomas Mueller[2], Stephan C. F. Neuhauss[1δ]

[1]Institute of Molecular Life Sciences, University of Zurich, Winterthurerstrasse 190, 8057 Zurich, Switzerland

[2]Institute of Biology I, Department of Developmental Biology, University of Freiburg, Hauptgasse 1, 79104 Freiburg, Germany

[δ] corresponding author

Manuscript accepted for publication in *the Journal of Comparative Neurology*

Personal contribution:

cloning, sequence analysis and *in situ* hybridization experiments, preparation of all figures and tables, except figure 1, writing and editing of the manuscript

2.1 Abstract

Glutamate, the most abundant excitatory neurotransmitter of the central nervous system, modulates synaptic transmission and neuronal excitability via metabotropic glutamate receptors (mGluRs). These receptors are essential components for diverse cognitive functions and they represent potential drug targets for the treatment of a number of neurological and psychiatric disorders.

Here, we describe the phylogenetic relation and mRNA distribution of zebrafish mGluRs. In comparison to the eight *mglurs* present in the mammalian genome, we identified 13 different *mglur* genes in the zebrafish genome. *In situ* hybridization experiments in zebrafish revealed widespread expression patterns for the different *mglurs* in the central nervous system, implicating their significance in diverse neuronal functions. Prominent *mglur* expression is found in the olfactory bulb, the optic tectum, the hypothalamus, the cerebellum, and the retina. We show that expression pattern of paralogs generated by the teleost specific whole genome duplication is overlapping in some brain regions but complementary in others, suggesting sub- and/or neofunctionalization in the latter. Group I *mglurs* are similarly expressed in brain areas of both larval and adult zebrafish, suggesting that their functions are comparable during these stages.

2.2 Introduction

In recent years the zebrafish Danio rerio has emerged as one of the favorite model organisms for genetic studies. Particularly well studied are genes involved in nervous system development and function (e.g. Schweitzer & Driever, 2009; Lillesaar, 2011). However, despite the fact that glutamate is the main excitatory neurotransmitter of the vertebrate nervous system, little is known about glutamatergic systems in zebrafish or other teleosts.

In general, glutamate receptors fall into three broad classes: the ionotropic NMDA and AMPA/kainate receptors, the excitatory amino acid transporters (EAATs) and the mGluRs. mGluRs are seven-transmembrane proteins with an intracellular G-protein coupled signal transduction pathway, which activates a second messenger cascade upon glutamate binding (Nakanishi & Masu, 1994). In mammals, the mGluR family consists of eight different subtypes that can be classified into three distinct groups (I-III) based on their structural homology, pharmacological properties and second messenger cascade. While receptor subtypes -1 and -5 comprise the group I, mGluR2 and -3 are members of group II, and mGluR4, -6, -7 and -8 are constituting the group III. Group I members are positively coupled to the phosphoinositol transduction pathway whereas group II and group III mGluRs are negatively linked to adenyl cyclase and thus downregulate cyclic nucleotide synthesis. Group III mGluRs can be distinguished from group II mGluRs due to their distinctive sensitivity for the agonist L-2-amino-4-phosphonobutyrate (APB or L-AP4) (Pin & Duvoisin, 1995; Rosemond *et al*., 2004).

By modulating signal transduction at pre- and postsynaptic sides, glutamate acting via mGluRs plays a crucial role in neuronal synaptic transmission. Consequently, mGluRs can be found in diverse neuronal cell types of the central and peripheral nervous system and they have been considered potential targets for therapeutic approaches in various neurodegenerative disorders (Byrnes *et al*., 2009; Knackstedt & Kalivas, 2009; Luscher & Huber, 2010; reviewed in Niswender & Conn, 2010).

The functions of group I mGluRs have been especially well-studied as they are expressed in many excitatory synapses (reviewed in Ferraguti & Shigemoto, 2006). Group I mGluRs are implicated in long term potentiation (LTP) influencing plasticity of behavior, learning and memory. Moreover, mGluR-induced LTP might be linked to aspects of mental retardation as well as Parkinson's and Alzheimer's disease (reviewed in Luscher & Huber, 2010). In this study, we cloned and phylogenetically characterized all members of the *mglur* family in the zebrafish *Danio rerio*. Similar to mammals, the zebrafish mGluR subtypes fall into the three distinct groups, however, *mglur1, -2, -5, -6,* and *-8* are present as two paralogs. Using *in situ* hybridization, we analyzed their expression patterns during development and found a unique pattern for all *mglurs* in larval zebrafish. Paralogous genes show overlapping but also mutually exclusive expression domains, suggesting potential sub- or neofunctionalization between duplicated genes (Force *et al*., 1999). In addition, we studied gene expression patterns of group I *mglurs*, namely *mglur1a* and *-1b*, as well as *mglur5a* and *-5b*, on brain sections of adult zebrafish in order to compare expression patterns between larval and adult stages. These transcript patterns, here exemplified for the cerebellum and the hypothalamus, show similarities between embryonic and adult zebrafish indicating conserved functions throughout the stages.

2.3 Materials and Methods

2.3.1 Fish maintenance and breeding

Fish were kept under a 14h/10h light/dark cycle and bred as previously described (Mullins *et al*., 1994). The wild-type strain used for all studies was WIK. Embryos were raised at 28 °C in E3 medium and staged according to development in days post fertilization (dpf). Experiments were performed in accordance with the ARVO Statement for the Use of Animals in Ophthalmic and Vision Research and were approved by the local authorities (Veterinäramt Zürich TV4206).

2.3.2 Annotation of *mglur* cDNAs

As gene predictions within GenBank are produced by automated processes which have been shown to contain numerous errors, mGluR cDNA sequences used in this study were manually annotated. Sequences were identified and annotated using combined information from expressed sequence tags and genome databases (GeneBank, http://www.ncbi.nlm.nih.gov; Ensembl, http://www.ensembl.org/ index.html). Human and mouse sequences were used as initial query (for more details on sequence annotation see Gesemann *et al*., 2010).

2.3.3 Phylogenetic analysis

The phylogenetic analysis was performed on the Phylogeny.fr platform (http://www.phylogeny.fr) comprising the following steps (Dereeper *et al*., 2008). Sequences were aligned using MUSCLE (v3.7) (Edgar, 2004) configured for highest accuracy (MUSCLE with default settings). Sequences length varied between 727 and 1199 amino acids. After alignment, ambiguous regions (i.e. containing gaps and/or are poorly aligned) were removed using Gblocks (v0.91b) (Castresana, 2000). The following parameters were implemented. The minimum length of a block after gap cleaning was set to 5; positions with a gap in less than 50% of the sequences were selected in the final alignment if they were within an appropriate block; all segments with contiguous nonconserved positions bigger than 8 were rejected; minimum number of sequences for a flank position were 55%. After curation 703 amino acids were chosen for further analysis. The phylogenetic tree was reconstructed using the maximum likelihood method implemented in the PhyML program (v3.0 aLRT) (Guindon & Gascuel, 2003). The default substitution model was selected assuming an estimated proportion of invariant sites (of 0.000) and 4 gamma-distributed rate categories to account for rate heterogeneity across sites. The gamma shape parameter was estimated directly from the data (gamma = 0.728). Reliability for internal branch was assessed using the aLRT test (Anisimova & Gascuel, 2006). Graphical representation and edition of the phylogenetic tree were performed with TreeDyn (v198.3) and the svg file imported into CorelDraw (version x4; Corel Corporation Ottawa, Canada) for final editing.

2.3.4 Cloning of *mglur* full-length cDNAs

Using the QIAShredder and the RNeasy kit (Qiagen, Hombrechtikon, Switzerland), the total mRNA of approximately 80 7-day-old wild-type zebrafish heads was isolated and reverse transcribed using oligo-dT primers (First Strand Kit; Stratagene, La Jolla, CA, USA). For Polymerase Chain Reaction (PCR) Taq polymerase (Taq Gold;

Applied Biosystems, Switzerland) and sequence-specific oligonucleotide primers were used (Tab. 1). Amplified DNA pieces were subcloned into the TOPO pCRII vector (TA Cloning Kit Dual Promoter; Invitrogen, Basel, Switzerland) and subsequently sequenced.

Gene	Primer	5' to 3'
mglur1a	1a_dr_1475s	AGGAGATAGGCCGCTTTG
mglur1a	1a_dr_3479as	AGTGATTGATTAATAAACAGCG
mglug1b	1b_dr_1497s	GTGGCATGAAGGCATTTTG
mglug1b	1b_dr_3501as	ACAAAAAGCTGCGGTAAATC
mglur2a	2a_dr_-0002s	CCATGGCTCAGAGGTCAG
mglur2a	2a_dr_2689as	GGCAAACAAACAGGAATCC
mglur2b	2b_dr_0141	GCACGAGAAGGGAAAAGG
mglur2b	2b_dr_2662	GTGATGACGGGATATAAAATTG
mglur3	3a_dr_-0018s	CTCTTCTGTCCTTAAACGATG
mglur3	3a_dr_1652as	CAGGGCATGCAGGTAAAC
mglur4	4a_dr_-0001s	CATGGGGAAAATGATTGG
mglur4	4a_dr_1698as	GTTAGGTCTCAAATCGAAGC
mglur5a	5a_dr_0670s	CACACTGAAGGGAATTATGG
mglur5a	5a_dr_1614s	GACCTGCACTCCATGTAAAG
mglur5a	5a_dr_1931as	TTGGCAATGAGGCAGAAG
mglur5a	5a_dr_3581as	GACATTTACAGCAGGATTTTG
mglur5b	5b_dr_-0001s	ATGGTCATTTTGTGTTCTCTC
mglur5b	5b_dr_3622as	AACACCGCTTAGAATTTTCC
mglur6a	6a_dr_-0003s	AGGATGTTTCGAGTTTTAAGC
mglur6a	6a_dr_1345s	CGCGCTGTCAACTTTAATG
mglur6a	6a_dr_1657as	CGTCTGCTTGGAACTGATAG
mglur6a	6a_dr_2424as	TGCTGTGCCAAAGAAAATG
mglur6b	6b_dr_-0010s	GCCAGCAACTATGACATCAC
mglur6b	6b_dr_1675as	CATCACAGAGCTCACAATGC
mglur7	7a_dr_-0006s	GAGACCATGGCTTGCTTTC
mglur7	7a_dr_1745as	GCCAGGAAGACTGAAATGAC
mglur8a	8a_dr_1300s	AGCAACATCAATGGGAAAG
mglur8a	8a_dr_2733as	TCCTCATATGGCGTGATTG
mglur8b	8b_dr_-0003s	ACCATGTTGAGTGCCTTTG
mglur8b	8b_dr_2785as	AGGATGTTCGCTCATATGG

Table 1:
Primer sites used for the generation of sense and antisense RNA probes.

2.3.5 Whole mount *in situ* hybridization

In vitro transcription of DNA probes was performed using the Roche DIG-RNA Labeling Kit (Roche Diagnostics, Rotkreuz, Switzerland). Probes longer than 1000 bp were hydrolyzed. To suppress pigmentation, embryos were treated with 3 µM PTU (1-phenyl-2-thiourea; Sigma-Aldrich, St. Louis, MO, USA). Zebrafish larvae were collected at 3 or 5 dpf, anesthetized on ice, and immediately fixed in 4% paraformaldehyde (PFA) in phosphate buffered saline (PBS, freshly prepared, pH 7.4) over night (ON) at 4 °C. Fixed tissue was washed twice for 5 min with PBT (PBS containing 0.1% Tween 20; Sigma-Aldrich) and dehydrated in a graded series of methanol/PBT mixtures each for 5 min at room temperature (RT). Larvae were stored at -20 °C in 100% methanol until required. Whole mount i*n situ* hybridization was performed according to Thisse and Thisse (Thisse & Thisse, 2008) with slight adaptations of the protocol: permeabilization by proteinase K (10 µg/ml) was accomplished for 60 min for three-day-old fish and for 75 min for five-day-old fish. From day two on TNT (100 mM Tris HCl pH 7.5, 150 mM NaCl, 0.5% Tween 20) was used for all washing steps instead of PBT. AP-conjugated anti-DIG antibody (Roche) was diluted 1:5'000 in blocking solution (Roche) in TNT. After the staining was stopped, larvae were postfixed in 4% PFA in PBS ON at 4 °C. The next day, stained larvae were washed twice for 5 min in PBT and placed in successive dilutions of PBT/methanol and methanol/glycerol each for 5 min at RT to the final step of 100% glycerol (Sigma-Aldrich). For obtaining optimal pictures, larvae were mounted on an adapted glass slide in 100% glycerol (Sigma-Aldrich) and the DIC modus of a light microscope (Olympus BX61) and a color camera (ColorView IIIu; Soft Imaging System, Olympus) were used. Representative whole mount stained larvae were placed in 30% sucrose

ON at 4 °C and embedded in cryomatrix (Tissue Tek O.C.T., Sakura, Zoeterwonde, NL) in an aluminum mold. 12 µm thick transverse sections were cut using a Microm microtome (HM 550) collected on glass slides and cover-slipped with Kaiser's glycerol gelatine (Merck KGaA, Darmstadt, Germany). Images were taken in the bright field modus of a light microscope (Olympus BX61) and were processed and arranged using Adobe Photoshop and Adobe Illustrator CS5.

2.3.6 *In situ* hybridization on sections

Adult zebrafish were euthanized using tricaine (MS-222; Sigma-Aldrich) and iced water. The head was cut, briefly washed in PBS and fixed in 4% PFA ON at 4 °C. After washing the tissue twice with PBT for 5 min at RT, it was placed in 30% sucrose ON and treated similar to the whole mount stained larvae. Eventually, 16 µm thick transverse and sagital sections were cut and mounted on glass slides. *In situ* hybridization was performed as described for larval fish, but proteinase K permeabilization time was reduced to 2.5 min and PBT was used for the washing steps and to dissolve the blocking reagent. The staining was stopped by a brief washing step with PBS pH 5.5 followed by two washing steps with PBS pH 7.4. Before the cover-slip was mounted, the stained tissue was postfixed in 4% PFA at RT for 1 h and washed twice with PBS pH 7.4. Images were taken with the DIC modus of a light microscope (Olympus BX61) and were processed and arranged using Adobe Photoshop and Adobe Illustrator CS5.

2.4 List of Abbreviations

A	anterior thalamic nucleus
ad	adult
ac	anterior commissure
ALLG	anterior lateral line ganglion
CC	cerebellar crest
CCe	corpus cerebelli
CeP	cerebellar plate
CePl	lateral part of cerebellar plate
CNS	central nervous system
CIL	central nucleus of inferior lobe
CM	corpus mamillare
CNS	central nervous system
CP	central posterior thalamic nucleus
Cpop	commissural postoptica
D	dorsal telencephalic area
Dc	central zone of D
Dd	dorsal zone of D
DIL	diffuse nucleus of inferior lobe
Dl	lateral zone of D
Dm	medial zone of D
DON	descending octaval nucleus
Dp	posterior zone of D
DP	dorsal posterior thalamic nucleus
DT	dorsal thalamus
E	epiphysis
EG	eminentia granularis

EmT	eminentia thalami
ET	entopeduncular nucleus
FG	facial ganglion
FL	facial lobe
GCL	ganglion cell layer (retina); granule cell layer (cerebellum)
GG	glossopharyngeal ganglion
GT	griseum tectale
Ha	habenula
Hc (larvae)	caudal hypothalamus
Hc (adult)	caudal zone of periventricular hypothalamus
Hd	dorsal zone of periventricular hypothalamus
Hi	intermediate hypothalamus
Hr	rostral hypothalamus
Hv	ventral zone of periventricular hypothalamus
INL	inner nuclear layer
IO	inferior olive
l	lateral tectal proliferation zone
LCa	lobus caudalis cerebellum
lfb	lateral forebrain bundle
LH	lateral hypothalamic nucleus
LVe	lateral ventricular recess of hypothalamus
mn	motor neurons
ML	molecular layer (cerebellum)
MC	mauthner cells
MO	medulla oblongata
MOc	caudal part of MO
MOl	lateral part of MO
MOn	nucleus in MO
MON	medial octavolateralis nucleus
MOp	posterior part of MO
M2	migrated posterior tubercular area
M3	migrated area of EmT
Nln	nucleus interpeduncularis
NLV	nucleus lateralis valvulae
OA	octaval area
OB	olfactory bulb
OG	otic ganglion
ON	optic nerve
P	pallium
PCL	Purkinje cell layer (cerebellum)
PGa	anterior preglomerular nucleus
PGl	lateral preglomerular nucleus
PGm	medial preglomerular nucleus
PGZ (L1/2, L3)	periventricular gray zone of TeO (layer 1/2, layer 3)
PLLG	posterior lateral line ganglion
Po	preoptic region
poc	postoptic commissure
PPa	parvocellular preoptic nucleus, anterior part
PPp	parvocellular preoptic nucleus, posterior part
Pr	pretectum
PSp	parvocellular superficial pretectal nucleus
PT	posterior tuberculum
PTd	dorsal part of posterior tuberculum
PTN	posterior tubercular nucleus
PTv	ventral part of posterior tuberculum
PVe	posterior recess ventricle of hypothalamus

RF	reticular formation
RVe	rhombencephalic ventricle
PVO	paraventricular organ
S	subpallium
Sd	dorsal division of subpallium
SFGS	superficial gray/fibrous layer of TeO
SO	optic layer of TeO
SR	superior raphe
Sv	ventral division of subpallium
T	midbrain tegmentum
TeO	tectum opticum
TeVe	tectal ventricle
TG	trigeminal ganglion
TL	torus longitunidalis
TLa	torus lateralis
TN	tegmental nucleus
TPp	periventricular nucleus of PT
TS	torus semicircularis
TVe	telencephalic ventricle
Va	valvula cerebelli
Val/m	lateral/medial division of Va
V	ventral telencephalic area
Vc	central nucleus of V
VG	vagal ganglion
Vl	lateral nucleus of V
VL	vagal lobe
VM	ventromedial thalamic nucleus
VT	ventral thalamus
Vv	ventral nucleus of V

2.5 Results

2.5.1 mGluRs in the zebrafish *Danio rerio*

The family of metabotropic glutamate receptors in mammals consists of eight different members which are categorized into three subgroups according to their sequence homology, pharmacology, and associated signal transduction pathways (Pin & Duvoisin, 1995). Based on sequence similarity, we annotated and cloned 13 zebrafish mGluR family members. Except for some single nucleotide polymorphisms, sequencing of the amplified cDNA fragments revealed no significant alterations from our annotated sequences. We distinguished three distinct subgroups of zebrafish mGluRs which correspond to their mammalian counterparts (Fig. 1). While we found no evidence for a second zebrafish paralog of *mglur3*, *-4*, and *-7*, we detected two paralogs for *mglur1*, *-2*, *-5*, *-6*, and *-8*. The location of duplicated *mglurs* on different chromosomes supports the notion that they originated from the teleost specific whole genome duplication rather from tandem duplication (Meyer & van de Peer, 2005; Ohno, 1999; Postlethwait, 2007).

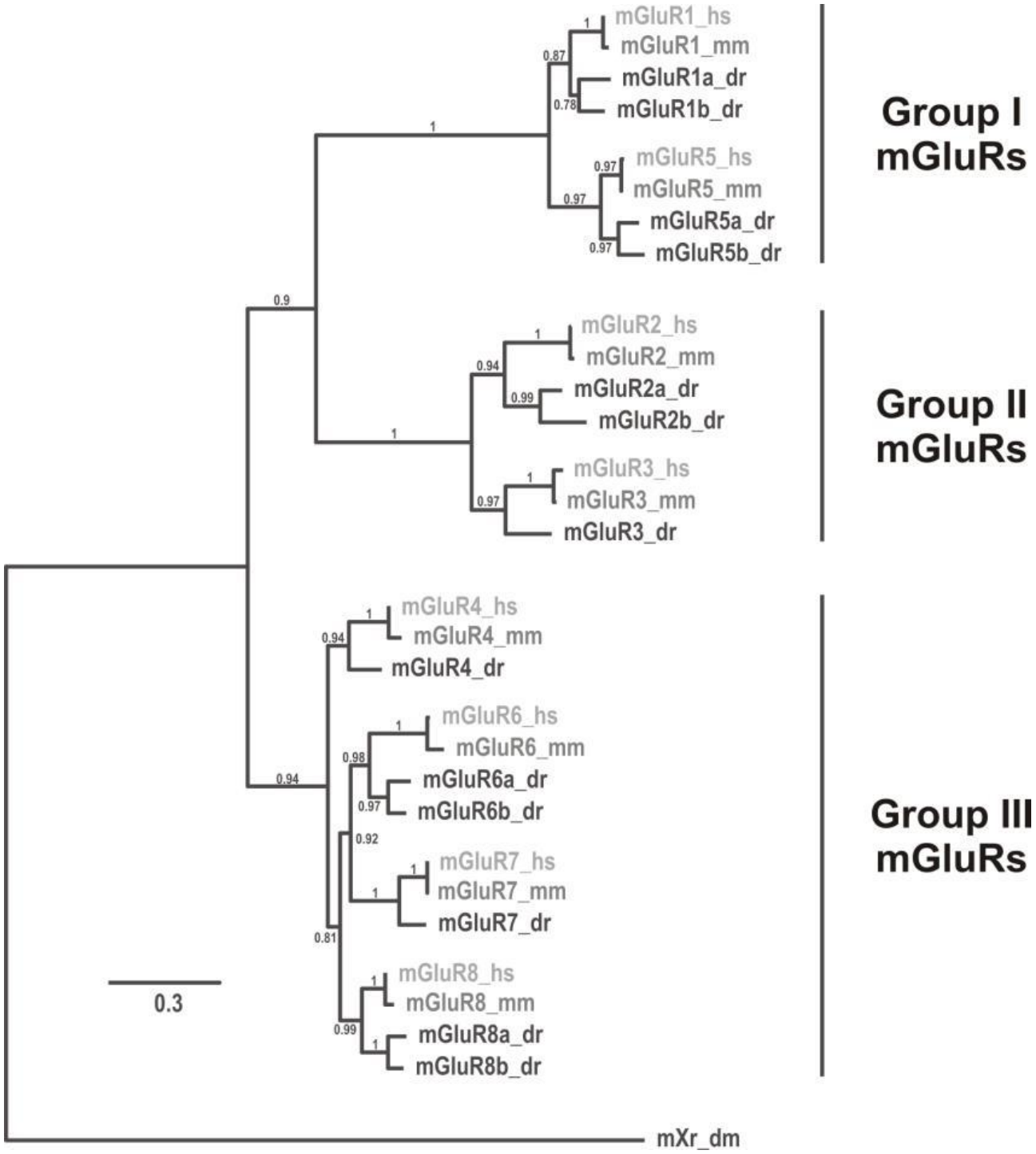

Figure 1: Zebrafish mGluR subfamilies have retained duplicated genes.
MGluR sequences of the following species were used in phylogenetic reconstructions: hs = Homo sapiens; mm = Mus musculus and dr = Danio rerio. While zebrafish mGluRs are shown in dark gray, mouse mGluRs are given in middle gray, and human mGluRs in light gray. As an outgroup the Drosophila melanogaster (dm) mXr receptor gene, which shares about 40% homology with vertebrate mGluRs, was used. Note that except for mGluR3, -4, and -7 the zebrafish has retained gene duplicates for all other mGluRs.

2.5.2 Distinct expression patterns for *mglurs* in the larval and adult zebrafish nervous system

To determine the expression pattern of members of the metabotropic glutamate receptor family, we performed *in situ* hybridization experiments on five-day-old zebrafish. An overview of *mglur* expressions in larval zebrafish is shown in Table 2. We generally followed the nomenclature of the zebrafish brain atlas of larval (Mueller & Wullimann, 2005) and adult (Wullimann *et al*., 1996) zebrafish and followed some modifications suggested by other authors (Bae *et al*., 2009; Wullimann & Mueller, 2004; Yamamoto *et al*., 2011; Mueller *et al*., 2006).

Transcripts for both *mglur1* paralogs are located in the region of the cerebellar plate (Fig. 2,3). However, the expression domains of *mglur1a* transcripts are broader and the expression levels appear to be higher compared to its paralog *mglur1b*. In the adult cerebellum, *mglur1a* is exclusively expressed in the Purkinje cells (PCL; Fig. 4A1,A8-A11). In contrast, *mglur1b* is located in Purkinje cells but additionally in the granule cell layer of the corpus cerebelli and in the lobus caudalis cerebelli (GCL, LCa; Fig. 4B1,B7-9). Expression of *mglur1b* in the eminentia granularis is seen throughout development (EG; Fig. 3) and persists into adulthood (Fig. 4B8). While *mglur1a* is strongly expressed in the olfactory bulb of the mature brain (OB; Fig. 4A1), expression in the larval telencephalon was found to be in the subpalliar region (Sd; Fig. 2J1) although at 3 dpf expression in the olfactory bulb cannot be excluded (OB, Sd; Fig. 2B,F). The faint *mglur1a* expression in diencephalic regions of zebrafish larvae (Fig. 2E,J,J2-4) stands in contrast to the strong labeling of diencephalic, especially hypothalamic, structures in the adult fish (Fig. 4A1,A6-11). *mglur1b* is largely expressed in the same diencephalic regions but shows an additional staining of the epiphysis at 5 dpf (E; Fig. 3G,I,I1). It is furthermore expressed in the lateral tectal proliferation zone as well as in the optic tectum, of three- and five-day-old larval zebrafish (l, TeO; Fig. 2A,D,E,I2-5). The optic tectum of adult fish shows *mglur1b* expression domains comparable to larval ones (TeO; Fig. 4B1,B5-7) No *mglur1b* labeling, however, was found in telencephalic and medial to ventral diencephalic regions at larval stages in contrast to the adult CNS (Fig. 4B1,B4-8). Moreover, cells of the medial octavolateralis nucleus display a very prominent *mglur1b* labeling (MON; Fig. 4B1,B9).

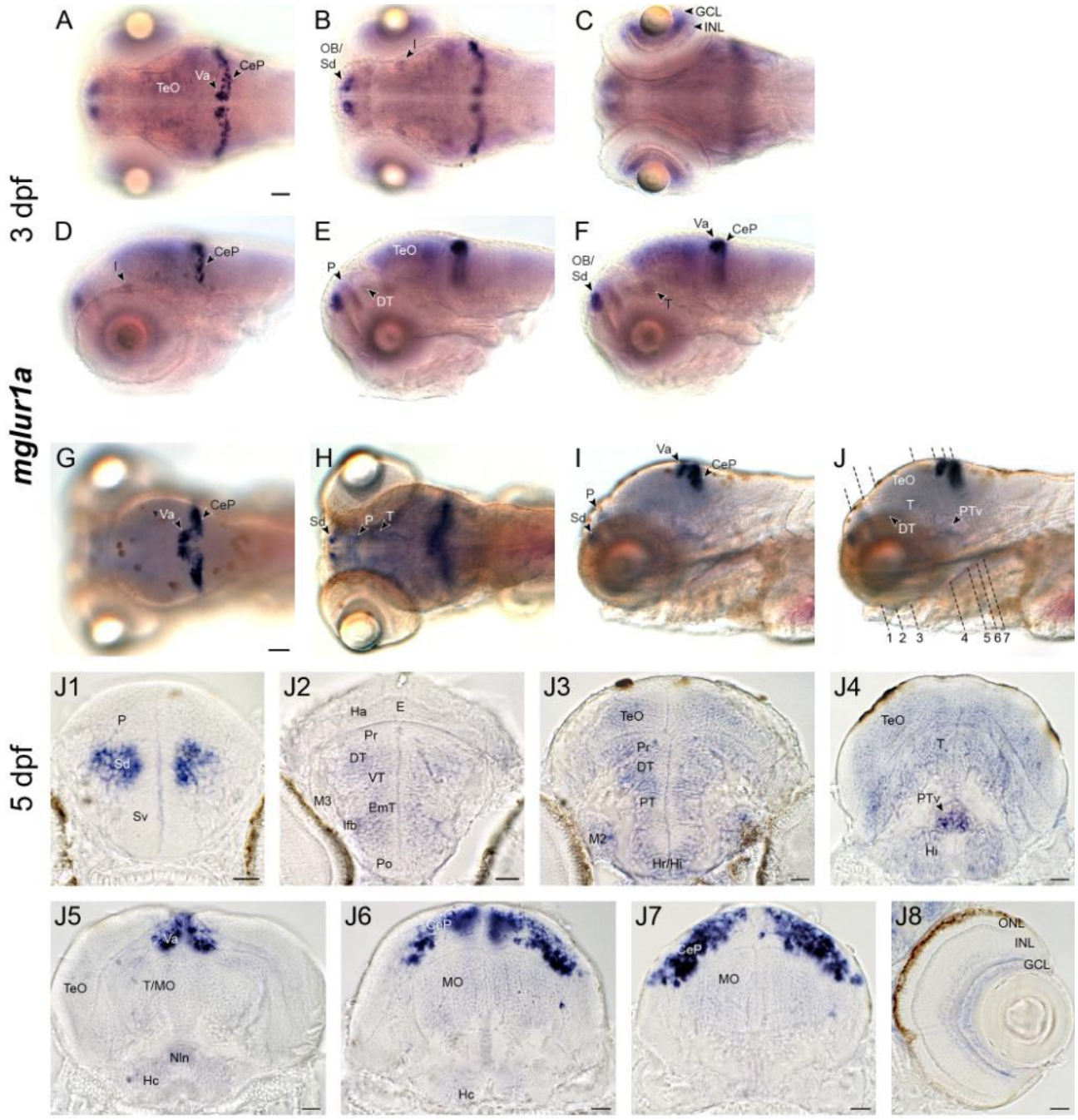

Figure 2: Expression pattern of mglur1a in three- and five-day-old zebrafish

Expression of mglur1a transcripts detected by in situ hybridization in three-day-old whole mounts (A-F), five-day-old whole mounts (G-J) and the respective cross sections (J1-8) of the zebrafish head. At 3 dpf both the dorsal (A-C) and the lateral (D-F) views reveal strongest mglur1a expression in the telencephalon (OB and Sd) and the cerebellar region (Va, CeP) as well as in the retina (INL, GCL). Cross sections of five-day-old fish stained with the mglur1a riboprobe only reveal staining in the Sd but not in the OB (J1). In addition strong expression is also found in the cerebellum (Va, CeP) in both dorsal (G) and lateral (I) views as well as in cross sections (J5-7).Levels of the cross sections J1-7 are indicated in J. For abbreviations see list. Scale bar in A (applies to A-F) and in G (applies to G-J) = 50 µm, scale bars in J1-8 = 20 µm.

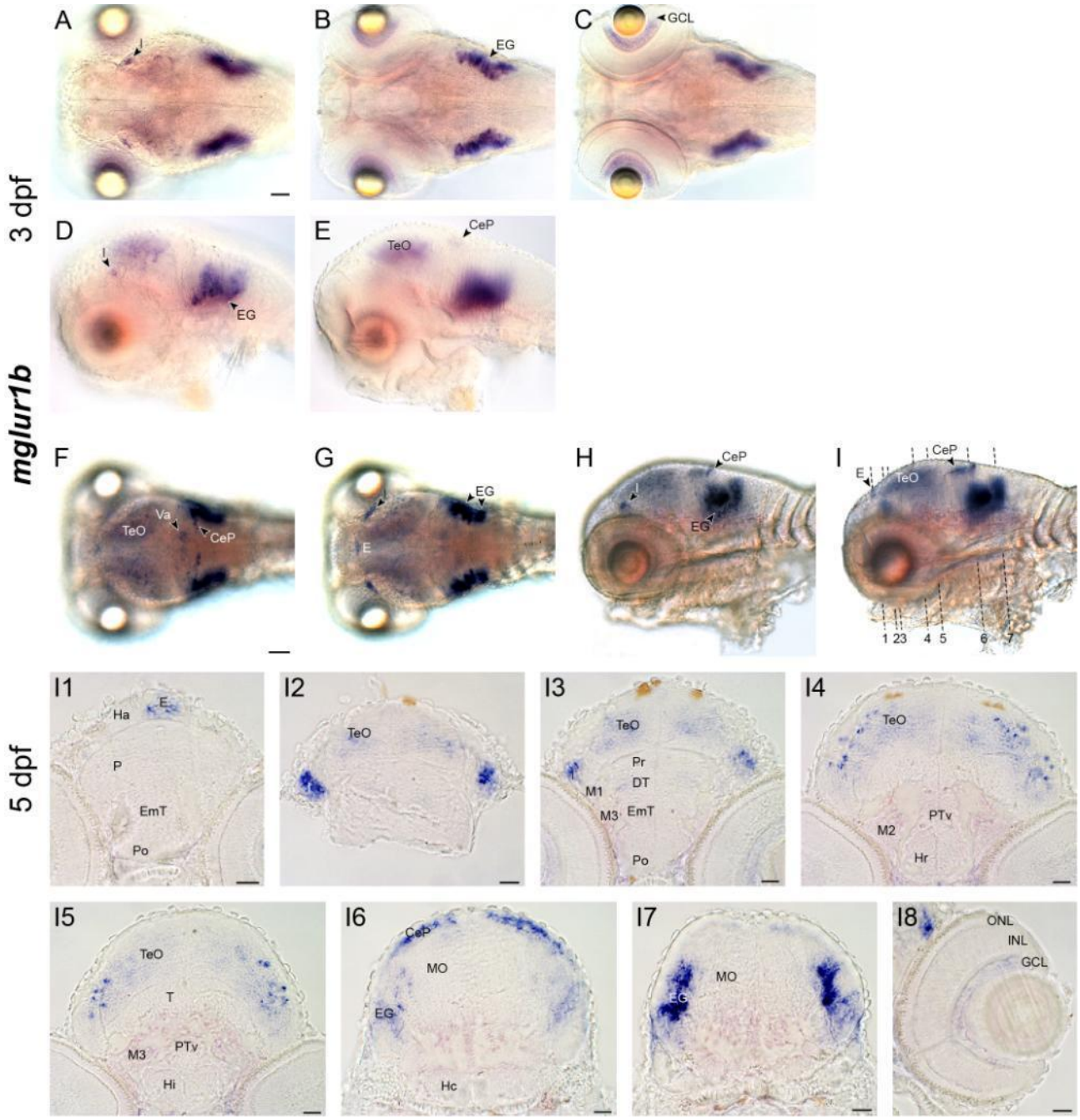

Figure 3: Expression pattern of mglur1b in three- and five-day-old zebrafish

Expression of the mglur1b riboprobe detected by in situ hybridization in three- (A-E) and five- (F-I) day-old fish larvae on whole mounts as well as on cross sections of five-day-old fish heads (I1-8).

Whole mount expression of mglur1b in three-day-old fish in dorsal (A-C) and lateral views (D,E) shows strongest staining in the retinal ganglion cell layer (GCL) and the eminentia granularis (EG) of the cerebellum. In five-day-old fish the dorsal (F,G) and lateral (H,I) views show a similar pattern with highest expression in the eminentia granularis (EG). This expression is confirmed in cross sections (I6-7). In addition, distinctive expression of mglur1b is found in the lateral tectal proliferation zone (l), the epiphysis (E), and the cerebellar plate (CeP). Levels of the cross sections I1-7 are indicated in I. For abbreviations see list. Scale bar in A (applies to A-E) and in F (applies to F-I) = 50 µm, scale bars in I1-8 = 20 µm.

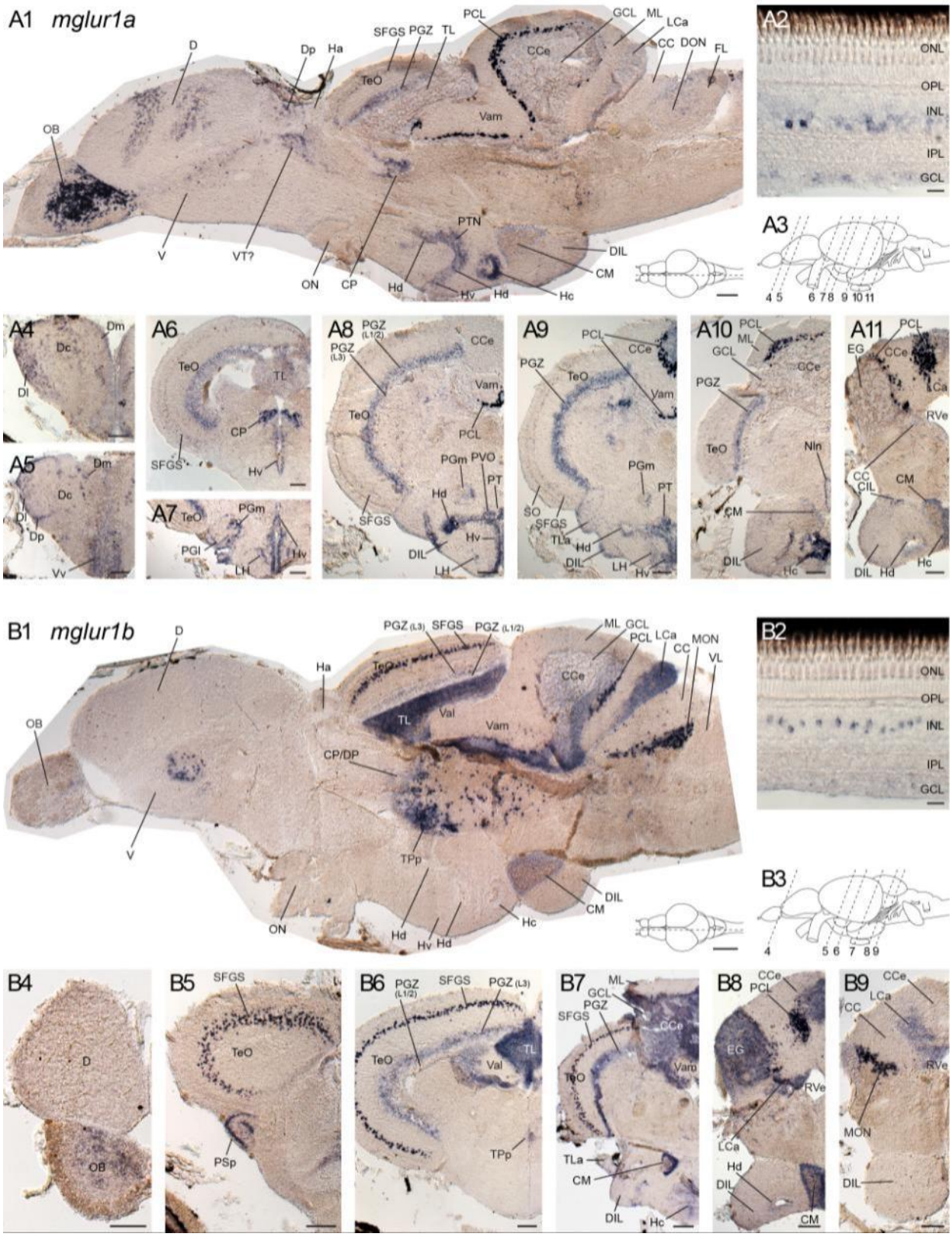

Figure 4: Expression pattern of group I mglur1 paralogs in adult zebrafish brain

mglur1 expression in sagital (A1,B1), retinal (A2,B2), and cross sections (A4-11,B4-9) of 5.5 months old zebrafish.
While a sagital section (A1) shows mglur1a labeling in the olfactory bulb (OB), the dorsal and ventral telencephalic area (D, V), the central posterior thalamic nucleus (CP), the cerebellar region (CCe with PCL, ML, and GCL, LCa) as well as the hypothalamus (Hd, Hv, Hc, DIL), cross sections (A4-11) demonstrate that also lateral parts of the hypothalamic region (LH, TLa; A7-9) are

stained. In the retina cells of the proximal INL and the GCL are stained by the mglur1a riboprobe (A2). Prominent mglur1b expression in the dorsal (TeO, TL) and medial (TPp) diencephalon was seen a sagital section (B1). Compared to mglur1a an even broader part of the cerebellum shows mglur1b expression (CCe with PCL, ML, and GCL, LCa). While the INL of the retina, most likely the bipolar cells, reveals a strong labeling of mglur1b, expression in the retinal ganglion cell layer (GCL) is only weak (B2). The cross sections (B4-9) confirm the strong mglur1b labeling in the cerebellum (CCe with PCL, ML and GCL, LCa, EG; B7-9). They additionally show mglur1b expression in the caudal (Hc; B7) and dorsal (Hd; B8) hypothalamus.
The levels of the sagital sections are illustrated at the bottom right of A1 and B1. Note that the axis of section A1 and B1 is slightly moved laterally. Levels of the cross sections are indicated in A3 and B3. All scale bars = 100 µm.

In larval fish *mglur5* paralogs are strongly expressed in the pallium (P), in hypothalamic parts of the brain (Hi, Hr, DIL,TLA), and weakly expressed in the cerebellar plate (CeP) and the nucleus interpeduncularis (Nln; all in Fig. 5,6). Paralog specific staining for *mglur5a* can be found in a ventral part of the hindbrain, most likely in the inferior olive (IO, Fig. 5B,F,H,J,J7) The localization of *mglur5a* riboprobes in adult tissue highly resembles the larval situation. In adult fish a prominent labeling of dorsal telencephalic regions (Dd, Dm, Dl, Dp; Fig. 7A1,A4-6), hypothalamic structures (Hd, Hv, LH, CIL, DIL, TLa; Fig. 6A1,A8-11) and the nucleus interpeduncularis (Fig. 7A11) was found. In lateral sections even cell bodies of the inferior olive are *mglur5a* positive (data not shown). While the weak labeling of the cerebellar granular cell layer seems unspecific because it is not consistent on all sections, labeling of Purkinje cells is observed (PCL; Fig. 7A1). In addition, the olfactory bulb (OB; Fig. 6A1) and the caudal part of the periventricular hypothalamus (Hc; Fig. 7A1,A10) is stained in adult tissue. In contrast to this, *mglur5b* reveals is broadly expressed in various parts of the diencephalon (DT, EmT, M2; Fig. 6), and the medulla oblongata (MO; Fig. 6) in three- and five-day-old fish. In the adult CNS, *mglur5b* expression is restricted to frontal brain regions such as the olfactory bulb and the dorsal and ventral telencephalic areas (OB, Vc, Vd, Vl, Vv; Fig. 7B1, B4-6). The periventricular gray zone of the optic tectum (PGZ; Fig. 7B8-12) and some diencephalic structures such as the preglomerular nucleus (PGl, PGm; Fig. 7B9), and hypothalamic nuclei (Hc, Hd, Hv, LH, TLa, DIL; Fig. 7B1,B9-12) are strongly labeled.

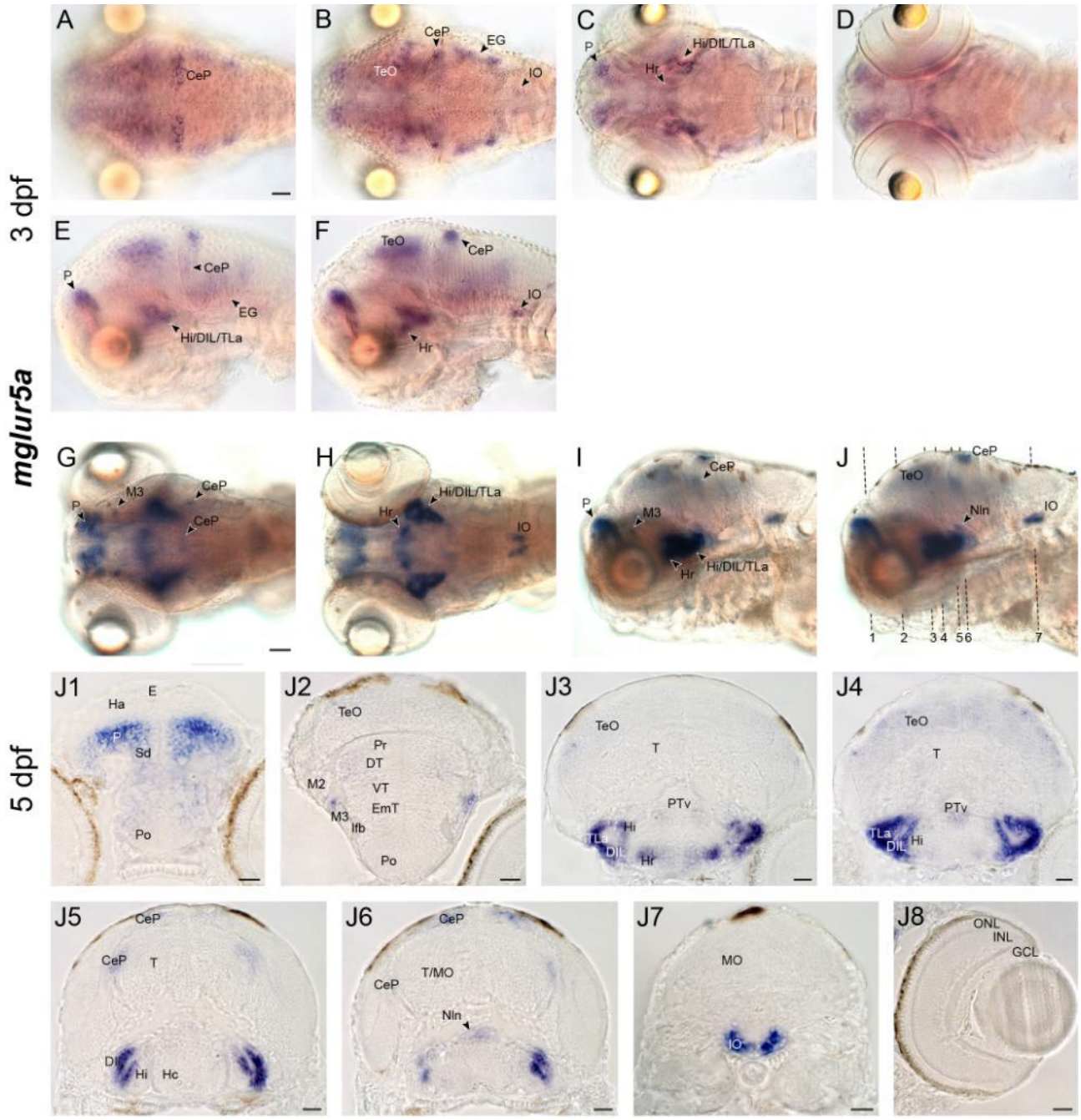

Figure 5: Expression pattern of mglur5a in three- and five-day-old zebrafish

Dorsal (A-D,G,H) and lateral (E,F,I,J) views of mglur5a expression in three- (A-F) and five- (G-J) day-old whole mounts and in cross sections of larval zebrafish at 5 dpf (J1-8).

The mglur5a riboprobe strongly labels hypothalamic (Hr, Hi, TLa, DIL) and cerebellar structures (CeP, CePl, EG) as well as the pallium (P), the optic tectum (TeO) and the inferior olive (IO) in three-day-old fish larvae. This expression is consistent until 5 dpf where similar structures are labeled (G-J). Cross sections confirm the location of mglur5a in the pallium (P), the cerebellar plate (CeP), the hypothalamus (Hi, Hr, TLa, DIL), and the inferior olive (IO). Levels of the cross sections J1-7 are indicated in J. For abbreviations see list. Scale bar in A (applies to A-F) and in G (applies to G-J) = 50 µm, scale bars in J1-8 = 20 µm.

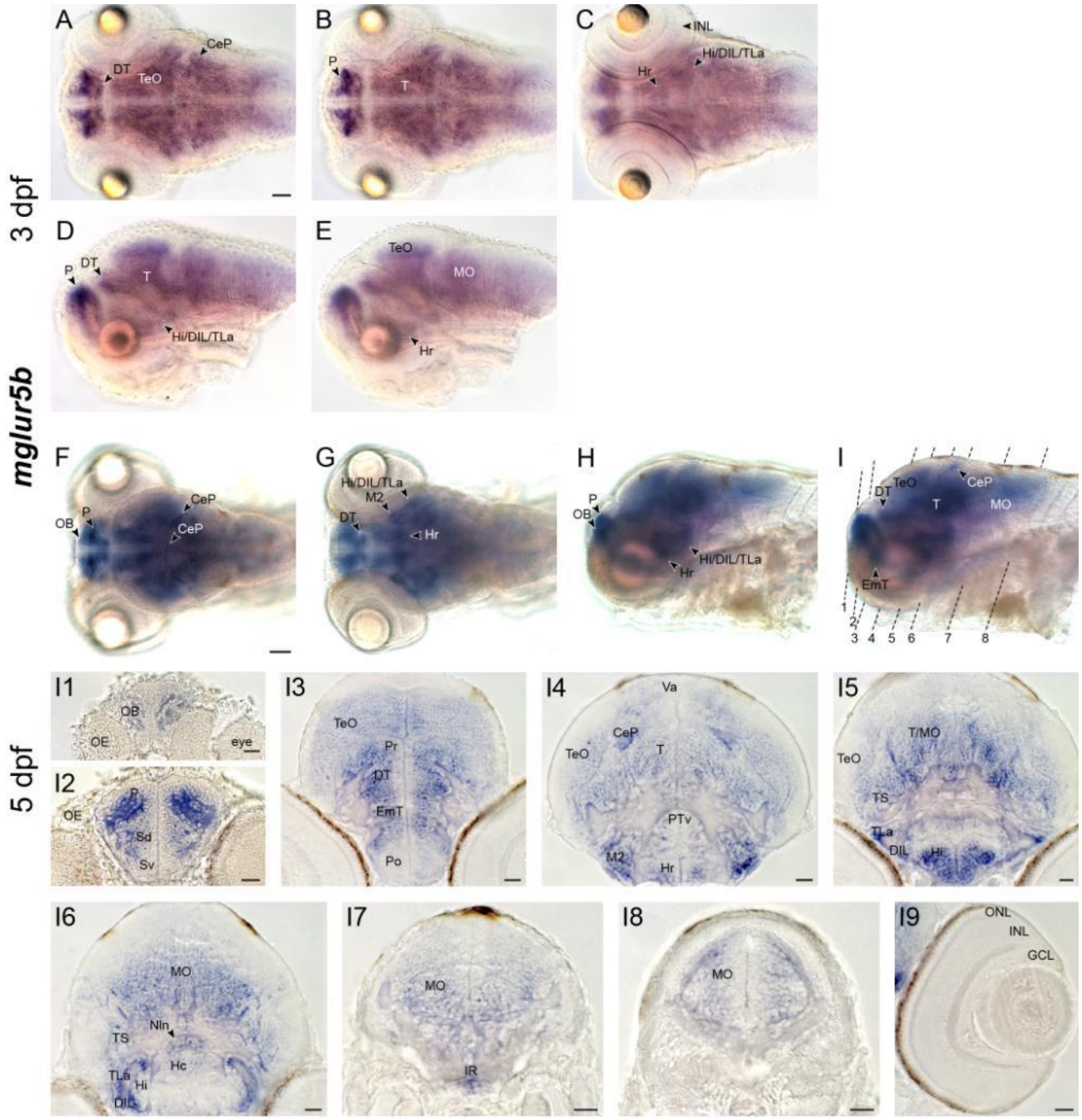

Figure 6: Expression pattern of mglur5b in three-and five-day-old zebrafish

Expression of mglur5a transcripts detected by in situ hybridization in three-day-old whole mounts (A-E), five-day-old whole mounts (G-I) and the respective cross sections (I1-9) of the zebrafish head.

In dorsal (A-C) and lateral (D,E) views of three-day-old larvae stained with the mglur5b riboprobes a high expression in the region of the pallium (P), in hypothalamic structures (Hi, Hr, TLa, DIL), and throughout the mid- and hindbrain is seen. A weak expression is found in the inner nuclear layer of the retina (INL). At 5 dpf a similar broad distribution of mglur5b transcripts is visible in both dorsal (F,G) and lateral (H,I) views. Cross sections confirm the labeling of the pallium (P) and the hypothalamus (Hi, Hr, TLa, DIL) but show additional clear labeling in the olfactory bulb (OB) and in anterior parts of the diencephalon (Pr, DT, EmT, M2). Levels of the cross sections I1-8 are indicated in I. For abbreviations see list. Scale bar in A (applies to A-E) and in F (applies to F-I) = 50 µm, scale bars in I1-9 = 20 µm.

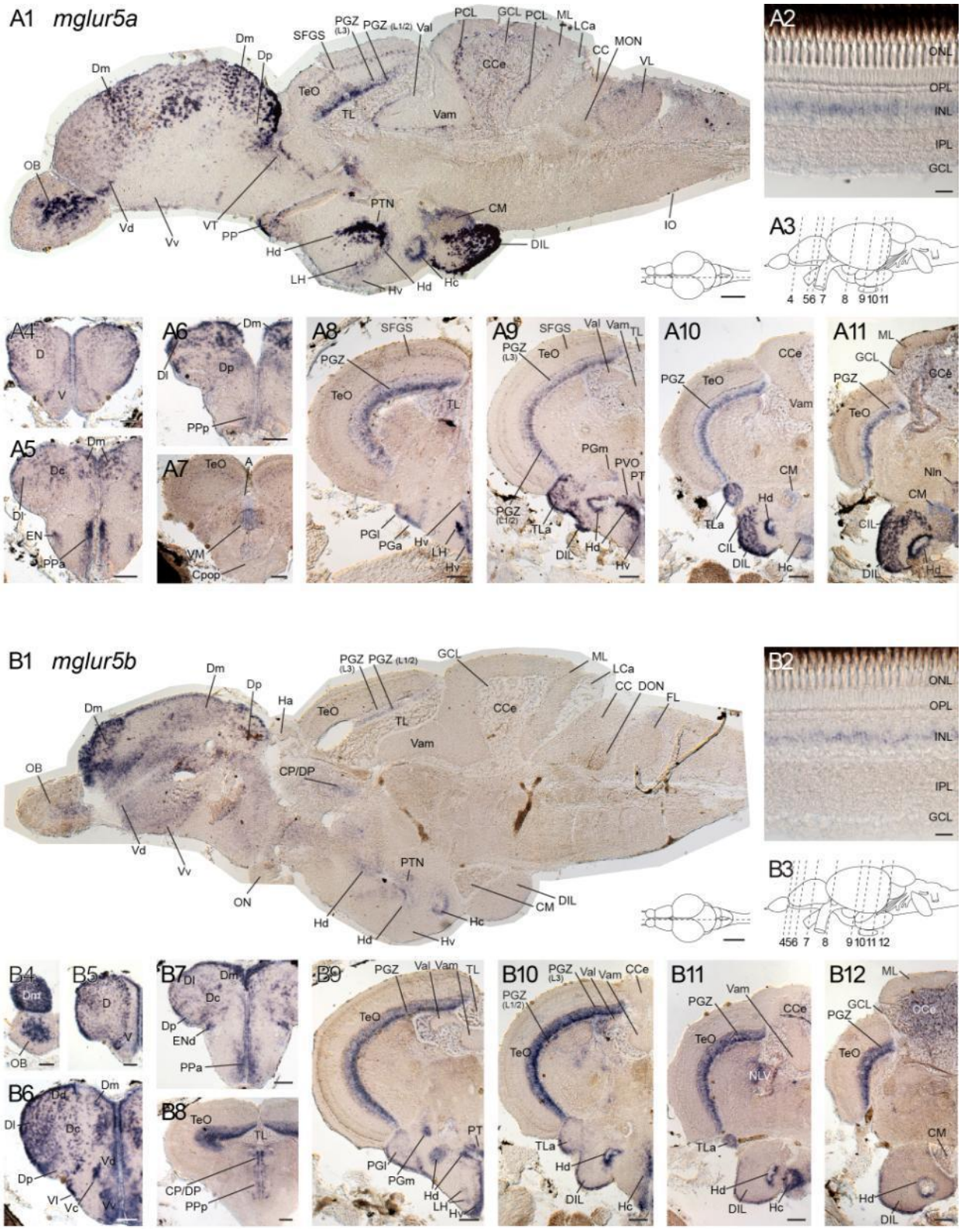

Figure 7: Expression pattern of group I mglur5 paralogs in adult zebrafish brain

mglur5 expression in sagital (A1,B1), retinal (A2,B2), and cross sections (A4-11,B4-12) of 5.5 months old zebrafish.

The mglur5a riboprobe strongly labels the telencephalic region (OB, several parts of Dand V A1,A4-6), and layers of the optic tectum (SFGS and PGZ in TeO; A1,A7-11). While expression in some ventral diencephalic regions (PTN, Hd, Hv, Hc, DIL, CM) is clearly seen in a sagital section (A1), the cross sections reveal additional staining in lateral hypothalamic regions (LH, TLa, CIL; A8-11). Moreover, some cell bodies of the inferior olive are mglur5a-positive (IO; A1). A retinal cross section reveals mglur5a expression in the medial INL where bipolar cell bodies are expressed (A2). mglur5b shows the most prominent expression in

several areas of the dorsal telencephalon (Dc, Dd, Dl, Dm, Dp; B1,B4-7) and the ventral telencephalic area (Vc, Vd, Vl, Vv; B1,B4-6). Similar to its paralog, mglur5b reveals an expression in the medial INL of the retina (B2). Cross sections depict strong labeling in the olfactory bulb (OB; B4).Compared to sagital sections, a stronger labeling in hypothalamic regions is visible (Hv, Hd, Hc. LH, TLa, DIL; B9-12). Moreover, the periventricular grey zone of the optic tectum (PGZ; B9-12) reveals prominent mglur5b expression.The levels of the sagital sections are illustrated at the bottom right of A1 and B1. Note that the axis of section A1 and B1 is slightly moved to the lateral side. The levels of the cross sections are indicated in A3 and B3. All scale bars = 100 µm.

The group II mGluRs in zebrafish consist of two mGluR2 paralogs and mGluR3. The *mglur2a* riboprobe labels cells in the olfactory bulb (OB), migrated neurons of the eminentia thalami (M3), as well as lateral parts of the cerebellar plate (CeP), and the trigeminal ganglion (TG). In addition, a weak staining in several parts of the midbrain (DT, VT, PTv) and in the caudal tegmentum/rostral medulla oblongata (T, MO; all in Fig. 8) is visible. Sections show additional *mglur2a*-positive cells in the eminentia granularis (EG; Fig. 8J7). Similar to *mglur2a*, *mglur2b* is expressed in the olfactory bulb, however, expression of this paralog is restricted to the medial part of the olfactory bulb (OB; Fig. 9). Besides that the paralogous genes do not share other expression domains. In the telencephalon, *mglur2b* is expressed in the pallium (P) and in a medial part of the olfactory bulb (OB; both in Fig. 9). Their expression is restricted here to proliferative cells around the ventricular zones (TVe, TeVe, RVe), the epiphysis (E), the intermediate and caudal hypothalamus (Hi, Hc), the reticular formation (RF), and in a nucleus in the lateral part of medulla oblongata (MO; all in Fig. 9). In three-day-old larvae *mglur2b* is also expressed in a structure which might be the Mauthner cells (MC; Fig. 9C,F). To conclude, *mglur2b* is expressed in medial part of the olfactory bulb (Fig. 9), whereas *mglur2a* is expressed within the entire OB (Fig. 8). Otherwise, these two paralogous genes are expressed mutually exclusive in the brain of larval fish.

Riboprobes for *mglur3* highlight the ventricular boundaries of the larval zebrafish brain, ranging from the telencephalic- , to the tectal- , and the rhombencephalic ventricle (TeV, TeVe, RVe; all in Fig. 10). Even the lateral ventricular recess of the hypothalamus are faintly stainined (LVe; Fig. 10K4). Apart from that, *mglur3* is also expressed in the pallium (P), the hypothalamus (Hi, Hc), the cerebellum (Va, CeP). Some weak *mglur3* expression is found in the habenula (Ha), the migrated part of the posterior tubercular area (M2), and the superior raphe (SR; all in Fig. 10).

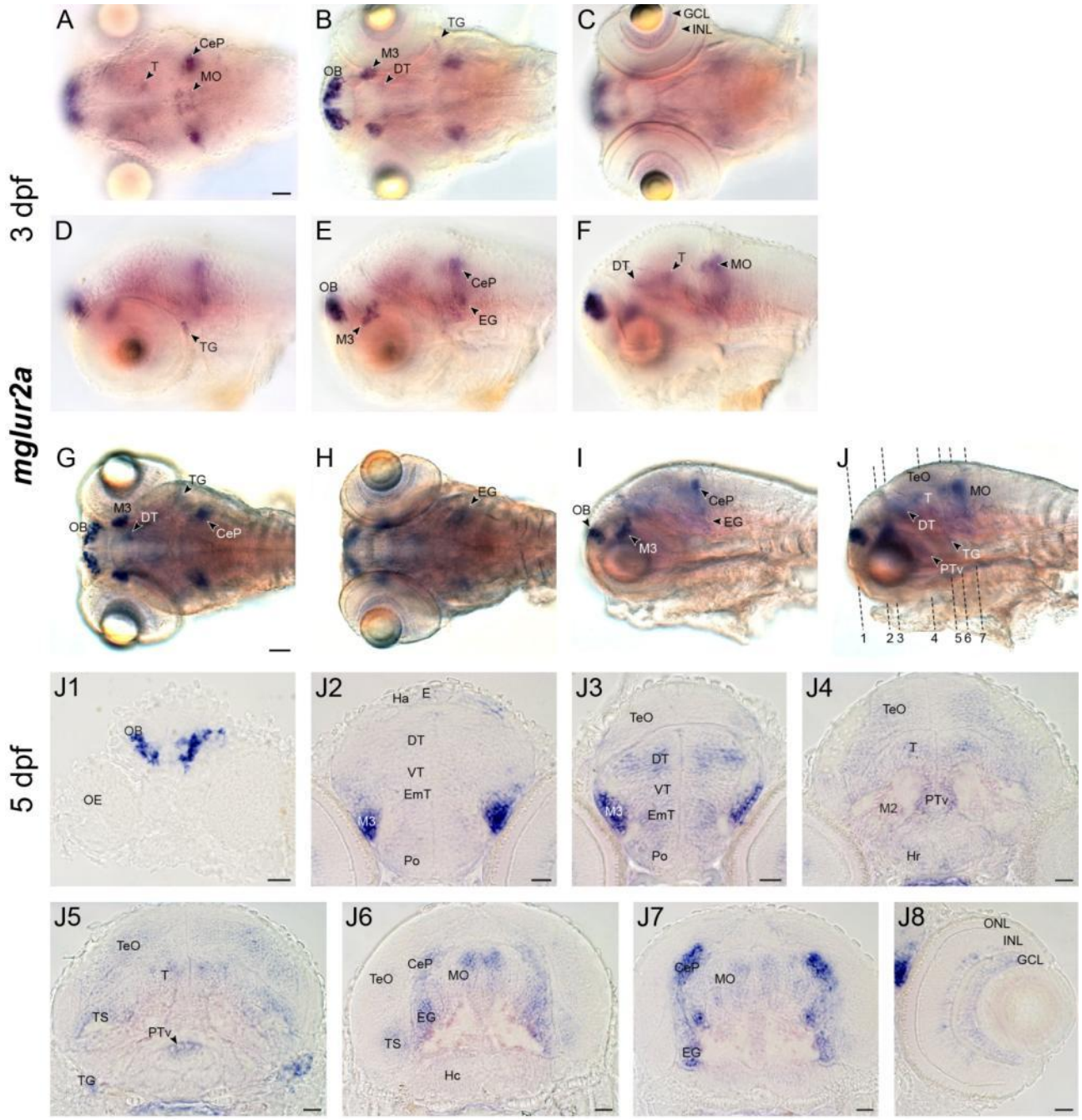

Figure 8: Expression pattern of mglur2a in three- and five-day-old zebrafish

Expression of mglur2a transcripts in three- (A-F) and five- (G-J) day-old zebrafish whole mounts depicted in dorsal (A-C,G,H) and lateral views (D-F,I,J) as well as in cross sections through the head of five-day-old whole mounts (J1-8).

Expression of mglur2a in three-day-old fish shows prominent labeling in the olfactory bulb (OB) but also in various parts of the diencephalon and the hindbrain (A-F). At 5 dpf mglur2a transcripts are expressed in similar regions as in three-day-old fish (G-J). Sections of mglur2a hybridized five-day-old larvae (J1-8) show highest expression in nuclei of the olfactory bulb nuclei (OB), in the migrated area of the eminentia thalami (M3), and in lateral cerebellar parts (CeP, EG). Besides that, mglur2a is expressed in inner retinal layers (INL and GCL) as depicted in J8. Levels of the cross sections J1-7 are indicated in J. For abbreviations see list. Scale bar in A (applies to A-F) and in G (applies to G-J) = 50 µm, scale bars in J1-8 = 20 µm.

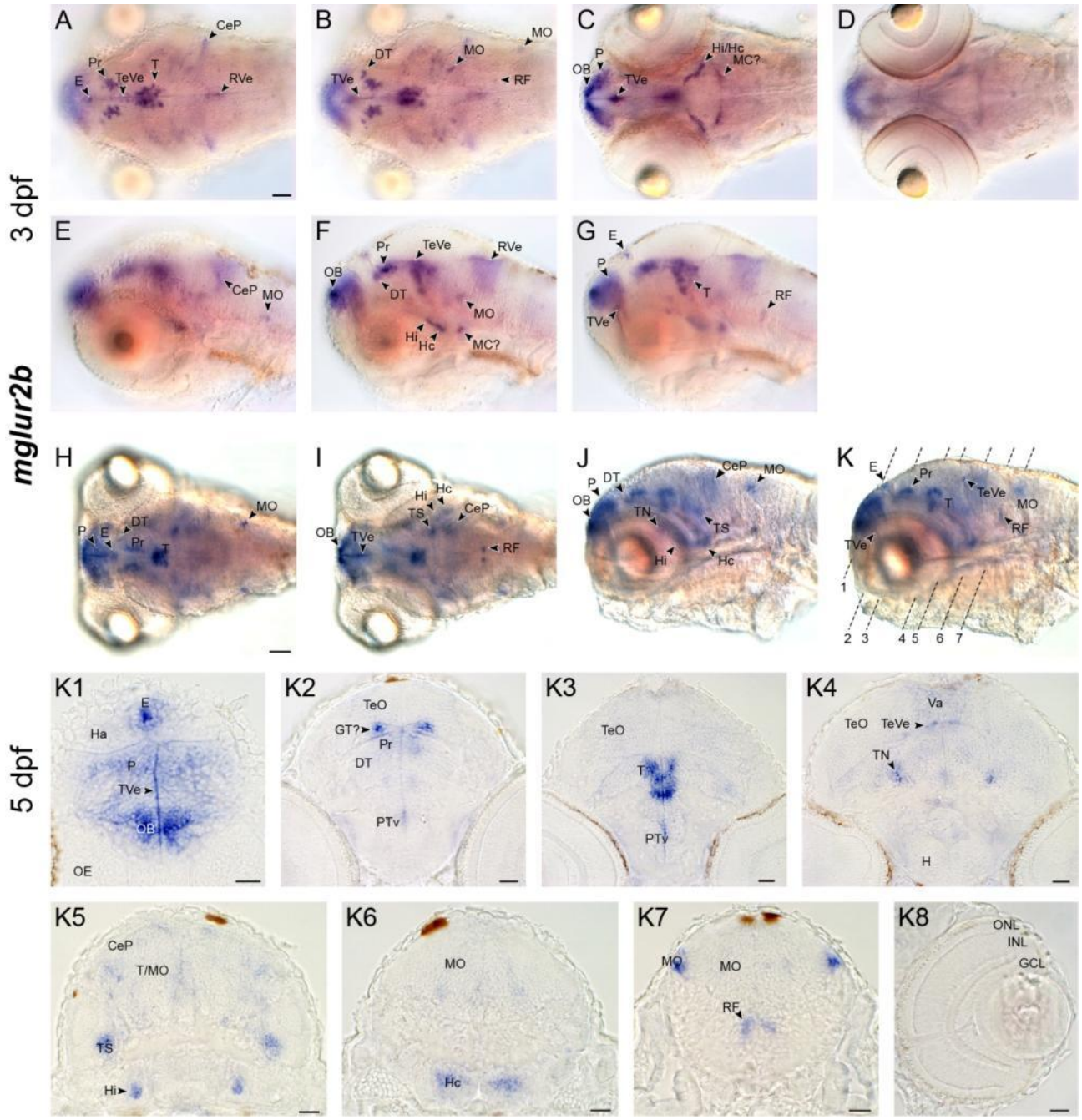

Figure 9: Expression pattern of mglur2b in three- and five-day-old zebrafish

In situ hybridization of three- (A-G) and five- (H-K) day-old zebrafish larvae using the mglur2b riboprobe. K1-8 depict cross sections through a zebrafish at 5 dpf stained with mglur2b.

Dorsal (A-D) and lateral (E-G) views of three-day-old whole mounts show high mglur2b expression in the telencephalon (OB, E, P), in specific diencephalic regions (DT, Pr, T, Hi, Hc), as well as the hindbrain (CeP, MO, MC, RF). In addition expression around ventricular zones is visible (TVe, TeVe, RVe). Five-day-old zebrafish tissues labeled with mglur2b transcripts (H-K) indicate a very similar expression pattern as at 3 dpf. The most prominent expression in found in regions around the telencephalic ventricle (TVe), in the hypothalamus (Hi, Hc), and the hindbrain (e.g. CeP, TS, RF). Cross sections of five-day-old fish stained with the mglur2b probe (K1-8) confirm its very distinct expression profile. Levels of the cross sections K1-7are indicated in K. For abbreviations see list. Scale bar in A (applies to A-G) and scale bar in H (applies to H-K) = 50 µm, scale bars in K1-8 = 20 µm.

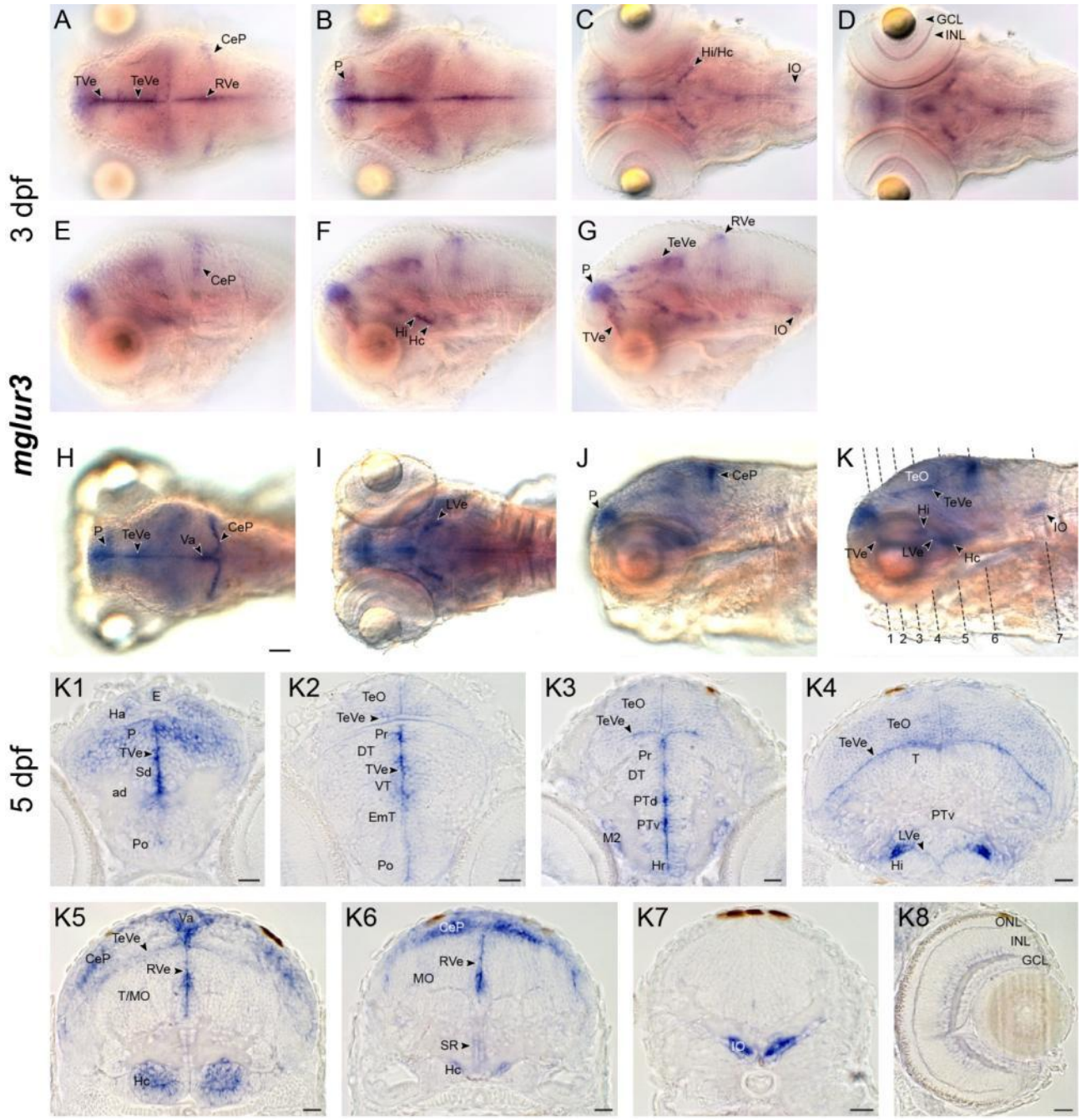

Figure 10: Expression pattern of mglur3 in three- and five-day-old zebrafish

Expression of mglur3 transcripts in whole mounts at 3 (A-G) and 5 dpf (H-K) as well as in cross sections of a five-day-old larvae (K1-8).

Dorsal (A-D) and lateral (E-G) views of a three-day-old zebrafish show strongest mglur3 labeling in the pallium (P), periventricular zones (TVe, TeVe, RVe) and in hypothalamic areas (Hi, Hc). At 5 dpf expression of mglur3 in dorsal (H,K) and lateral (J,K) views indicate a distinctive labeling in periventricular zones (TeV, TeVe, LVe) similar to the staining at 3 dpf. In addition the cerebellum (Va, CeP) and the hypothalamus are mglur3 positive as well. Sections of an mglur3 hybridized larvae at 5 dpf confirm the pronounced staining of all periventricular (TVe, TeVe, LVe, RVe) and some cerebellar (Va, CeP) and hypothalamic (Hi, Hc) regions. Additional expression is detected in the inferior olive (IO) and the inner retina (INL, GCL).Levels of the cross sections K1-7 are indicated in K. For abbreviations see list. Scale bar in A (applies to A-G), and scale bar in H (applies to H-K) = 50 µm, scale bars in K1-8 = 20 µm.

Group III *mglur4* transcripts are located in multiple regions of the CNS. The telecephalic part shows a staining in the olfactory bulb (OB), the dorsal division of the subpallium (Sd), and the preoptic region (Po; all in Fig. 11). Besides intense staining of the optic tectum (TeO) and the tegmentum (T), diencephalic regions (Ha, PT, Hr, Hi, TLa; all in Fig. 11) are also stained with the *mglur4* riboprobe. The hindbrain reveals staining in the lateral cerebellar plate (CeP), in a lateral nucleus, and a broad part of the medulla oblongata (MO; all Fig. 11). In addition, *mglur4* is strongly expressed in diverse cranial ganglia (TG, ALLG, FG, GG, VG, PLLG; all Fig. 11) at 3 and 5 dpf while expression in motor neurons (mn; Fig. 11A,E) is only found at 3 dpf.

Expression of both *mglur6* paralogs is limited in the CNS. The *mglur6a* probe strongly labels the habenula (Ha), the nucleus interpeduncularis (Nln), the lateral cerebellar plate (CeP), and the inferior olive (IO; all Fig. 12). In cross sections additional weak staining can be observed in the subpalliar region (Sd), in various parts of the diencephalon (between DT and PT, TeO, Hc) and in substructures of the medulla oblongata (MO; all Fig. 12). Besides staining in some scattered neurons of the olfactory bulb (OB) and the habenula (Ha), *mglur6b* reveals strong labeling in the rostral part of the hypothalamus (Hr; all Fig. 13). Both *mglur6* paralogs are highly expressed in inner retinal layers in both three- and five-day-old larvae (GCL, INL; Fig. 12,13).

mglur7 transcripts are broadly expressed throughout the CNS in three- and five-day-old fish larvae. The telencephalon shows staining in the pallium (P) and the preoptic region (Po; both Fig. 14). Further expression is visible in diencephalic regions such as the eminentia thalami (EmT), the migrated area of the EmT (M3), the posterior tuberculus (M2), the optic tectum (TeO), the hypothalamus (Hr, TLa, DIL), and the nucleus of the inferior lobe (IO; all in Fig. 14). In addition, *mglur7* transcripts can also be seen in cerebellar regions (CeP), two cranial ganglia (TG, VG), the nucleus interpeduncularis (Nln), and in a lateral part of the medulla oblongata (MO; all in Fig. 14). Although staining in the habenula (Ha) is not seen in the cross section I1 of Figure 14, other sections reveal *mglur7* positive cells in this region (data not shown). In the retina *mglur7* is highly expressed in inner layers (GCL, INL; Fig. 14I8). At 3 dpf, motor neurons of the hindbrain reveal a faint labeling (mn; Fig. 14A) but apart from that *mglur7* expression in younger zebrafish larvae is identical to the one observed at 5 dpf.

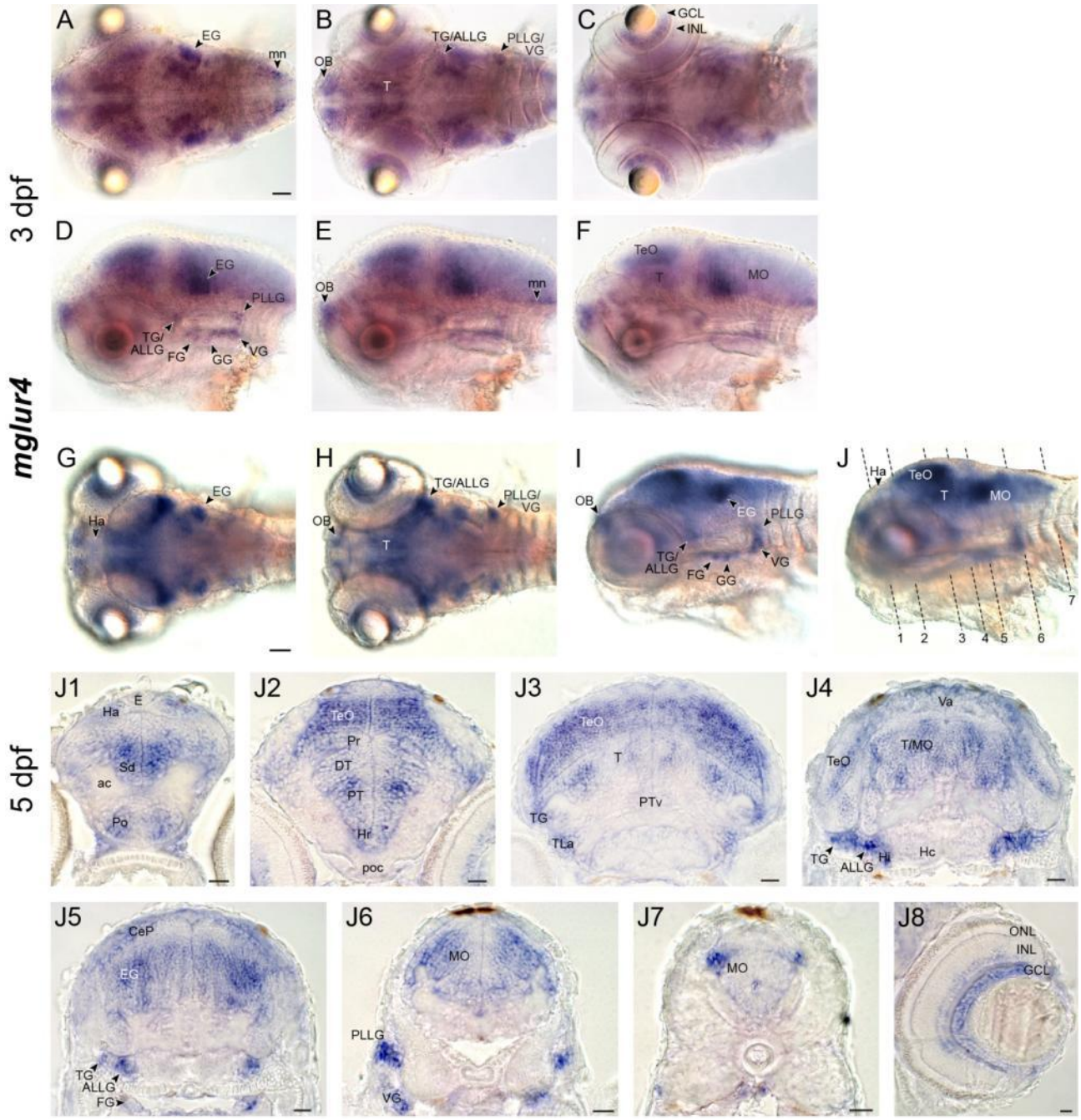

Figure 11: Expression pattern of mglur4 in three- and five-day-old zebrafish

Expression of the mglur4 riboprobe detected by in situ hybridization in three- (A-F) and five- (G-J) day-old fish larvae on whole mounts as well as on cross sections of five-day-old fish heads (J1-8).

Dorsal (A-C) and lateral (D-F) views of mglur4 expression in three-day-old fish reveals strong staining in the cranial ganglia (TG, ALLG, FG, VG, PLLG), in the olfactory bulb (OB), and in broad regions of the diencephalon (T, TeO) and the hindbrain (EG, MO, mn). Additional expression is seen in the inner nuclear layer (INL) and the ganglion cell layer (GCL) of the retina. At 5 dpf dorsal (G,H) and lateral (I,J) views show additional expression in the habenula (Ha). The cross sections through five-day-old fish heads stained with mglur4 probes (J1-8) confirm the broad labeling of brain structures but additionally show expression in the subpallium (Sd), the preoptic region (Po), the posterior tuberculum (PT), the cerebellum (CeP) and the hypothalamus (Hr, Hi, TLa). Levels of the cross sections J1-7 are indicated in J. For abbreviations see list. Scale bar in A (applies to A-F) and scale bar in G (applies to F-J) = 50 µm, scale bars in J1-8 = 20 µm.

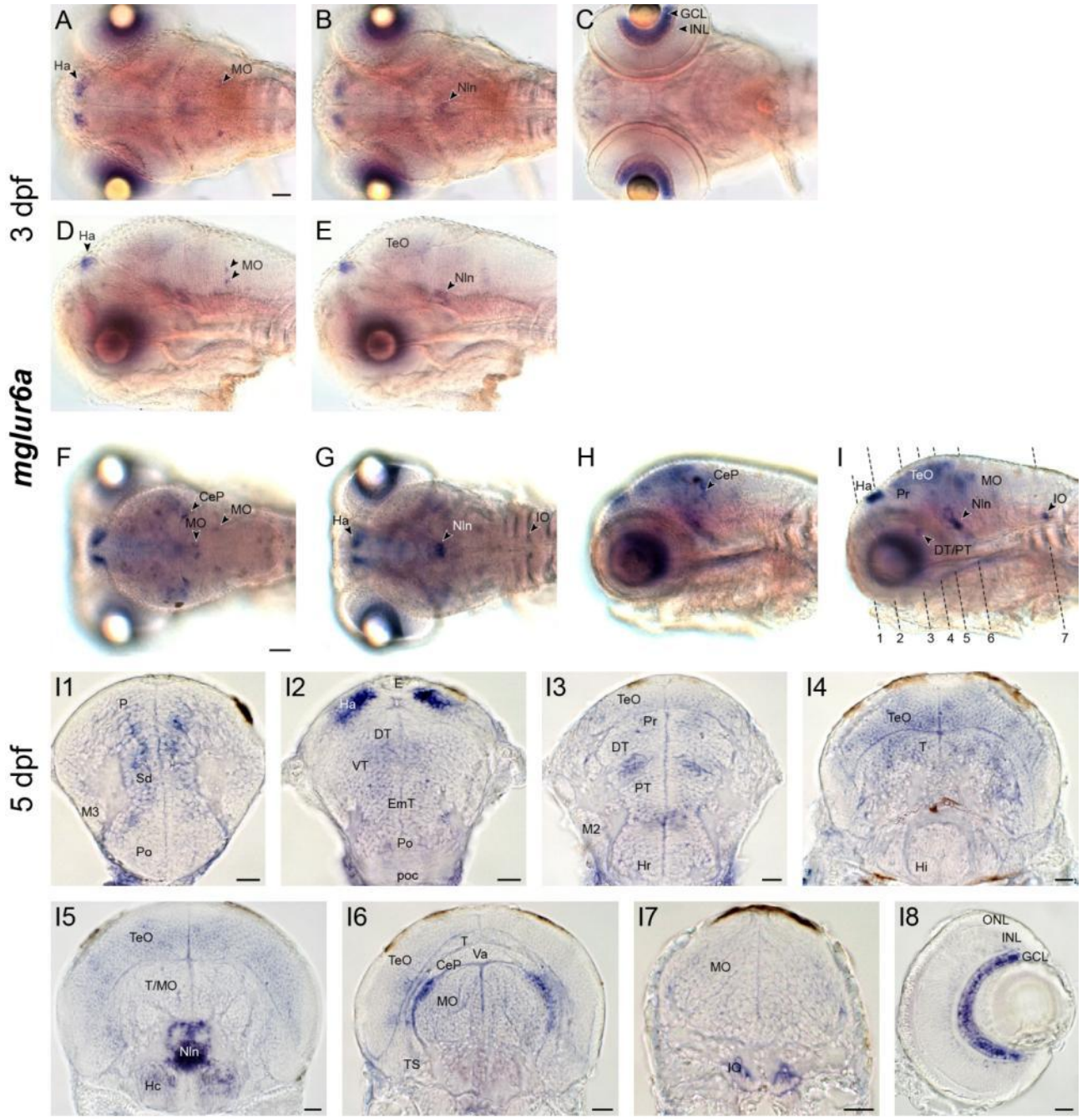

Figure 12: Expression pattern of mglur6a in three- and five-day-old zebrafish

Expression of mglur6a transcripts detected by in situ hybridization on whole mount larvae at 3 (A-E) and at 5 dpf (F-I) as well as in cross sections (I1-8) throught the head of a five-day-old fish expressing mglur6a.Whole mount expression of mglur6a in zebrafish larvae at 3 dpf in dorsal (A-C) and lateral views (D,E) revealing an intense labeling of the retinal ganglion cell layer (GCL) and the habenula (Ha). Dorsal (F,G) and lateral (H,I) views and cross sections (I1-8) of five-day-old fish expressing mglur6a show additional staining in the subpalliar region (Sd), the thalamus (TeO, DT, VT, PT, T), the cerebellum (CeP), the nucleus interpeduncularis (Nln), and in two nuclei of the medulla oblongata (MO).Levels of the cross sections I1-7 are indicated in I. For abbreviations see list. Scale bar in A (applies to A-E) and scale bar in F (applies to F-I) = 50 µm, scale bars in I1-8 = 20 µm.

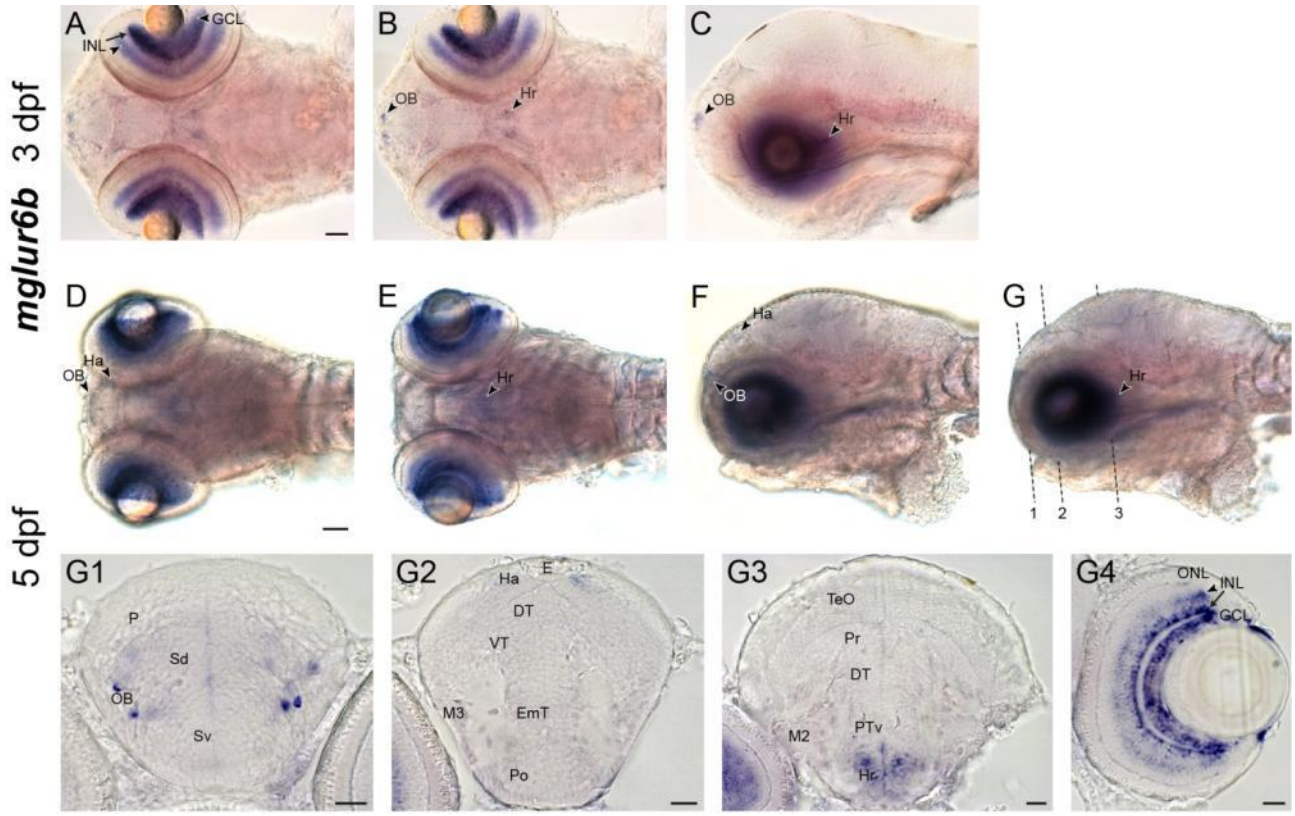

Figure 13: Expression pattern of mglur6b in three- and five-day-old zebrafish

Expression of mglur6b transcripts in three- (A-F) and five- (G-J) day-old zebrafish whole mounts depicted in dorsal (A,B,D,E) and lateral views (C,F,G) as well as in cross sections through the head of five-day-old whole mounts (G1-4).

The mglur6b riboprobe strongly labels the retinal ganglion cell layer (GCL) and the medial (arrow) and the proximal part (arrowhead) of inner nuclear layer (INL) at 3 dpf (A-C). Weak staining is also found in the olfactory bulb (OB) and the hypothalamus (Hr). Similar staining is found five-day-old larvae (D-G). Cross sections of a five-day-old larvae stained with the mglur6b riboprobe (G1-4) confirm labeling of few cells in the olfactory bulb (OB), the habenula (Ha), the rostral hypothalamus (Hr) as well as the inner retinal layers (GCL, INL; medial: arrow, proximal: arrowhead). Levels of the cross sections G1-3 are indicated in G. For abbreviations see list. Scale bar in A (applies to A-C) and scale bar in D (applies to D-G) = 50 µm, scale bars in G1-4 = 20 µm.

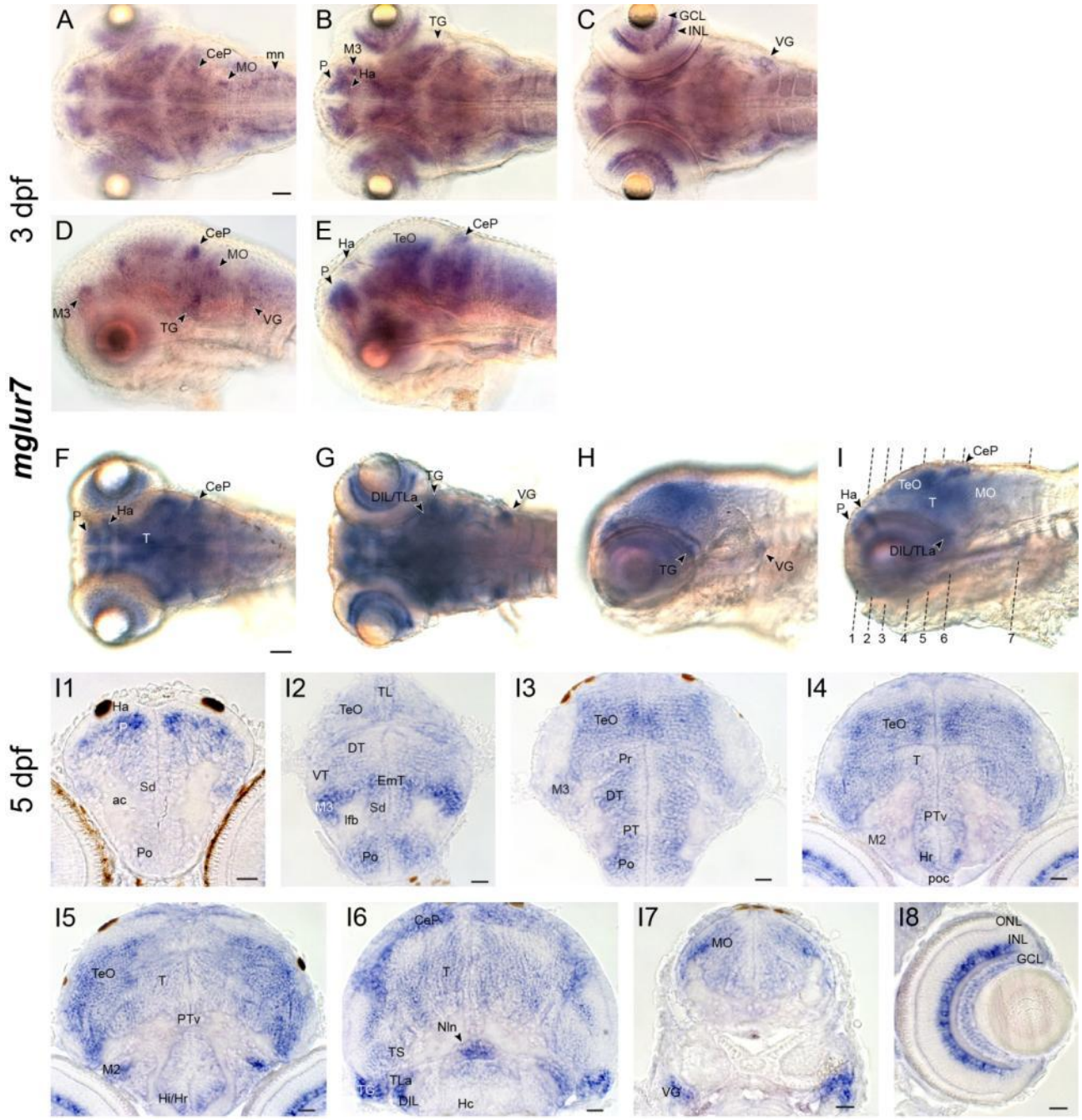

Figure 14 - Expression pattern of mglur7 in three-and five-day-old zebrafish

In situ hybridization of three- (A-E) and five- (F-I) day-old zebrafish larvae using the mglur7 riboprobe. I1-8 depict cross sections through a zebrafish at 5 dpf stained with mglur7.

Dorsal (A-C) and lateral views (D,E) of a fish larvae expressing mglur7 shows staining in broad regions of the CNS from the telencephalon (P) over the diencephalon (Ha, M3, TeO) to the hindbrain (CeP, TG, MO, mn). Additionally, the vagal ganglion (VG) and two layers in the retina (INL, GCL) are stained. Expression of mglur7 transcripts in the CNS at 5 dpf is even broader compared to 3 dpf as depicted in dorsal (F,G) and lateral (H,I) views of whole mount larvae. In cross sections (I1-8) prominent expression was found in the pallium (P), in diverse diencephalic structures such as the optic tectum (TeO) or the hypothalamus (Hr, TLa, DIL), in the nucleus interpeduncularis (Nln), in the cerebellar plate (CeP), in two cranial ganglia (TG, VG), and in the inner part of the INL and the GCL of the retina (I8). Levels of the cross sections I1-7 are indicated in I. For abbreviations see list. Scale bar in A (applies to A-E) and scale bar in F (applies to F-I) = 50 µm, scale bars in I1-8 = 20 µm.

mglur8a antisense RNA specifically labels the olfactory bulb (OB), the pallium (P, Sd), and the preoptic region of the forebrain (Po; all in Fig. 15). Transcripts are also found around migrated neurons of the eminentia thalami (M3), possibly in the ventral thalamus (VT?)and in the dorsal thalamus (DT), as well as in the optic tectum (TeO) the rostral part of the hypothalamus (Hr), and in the torus semicircularis (TS; all in Fig. 15). *mglur8a* expression in the hindbrain is confined to the cerebellar region (CeP) and parts of the medulla oblongata (MO; both in Fig. 15). While *mglur8a* is expressed in the proximal part of the inner nuclear layer (INL) and in the ganglion cell layer (GCL; Fig. 15J8), its paralog is only found in the proximal INL (Fig. 16K8). Overall, *mglur8b* shows a similar but weaker expression than *mglur8a* (Fig. 16). It is expressed in some additional structures such as the habenula (Ha), the posterior tuberculum (PT), the anterior tegmentum (T), and two cranial ganglia (OG, PLLG; all in Fig. 16).

At larval stages, besides *mglur2b* and *mglur5a*, all *mglurs* are expressed in the zebrafish retina. A closer analysis of *mglur5* paralogs in the adult retina reveals an expression of them in the inner nuclear layer (INL). In contrast to findings in mammals, *mglurs* are located in either the inner nuclear layer (INL), or the ganglion cell layer (GCL), or in both, but never in photoreceptors.

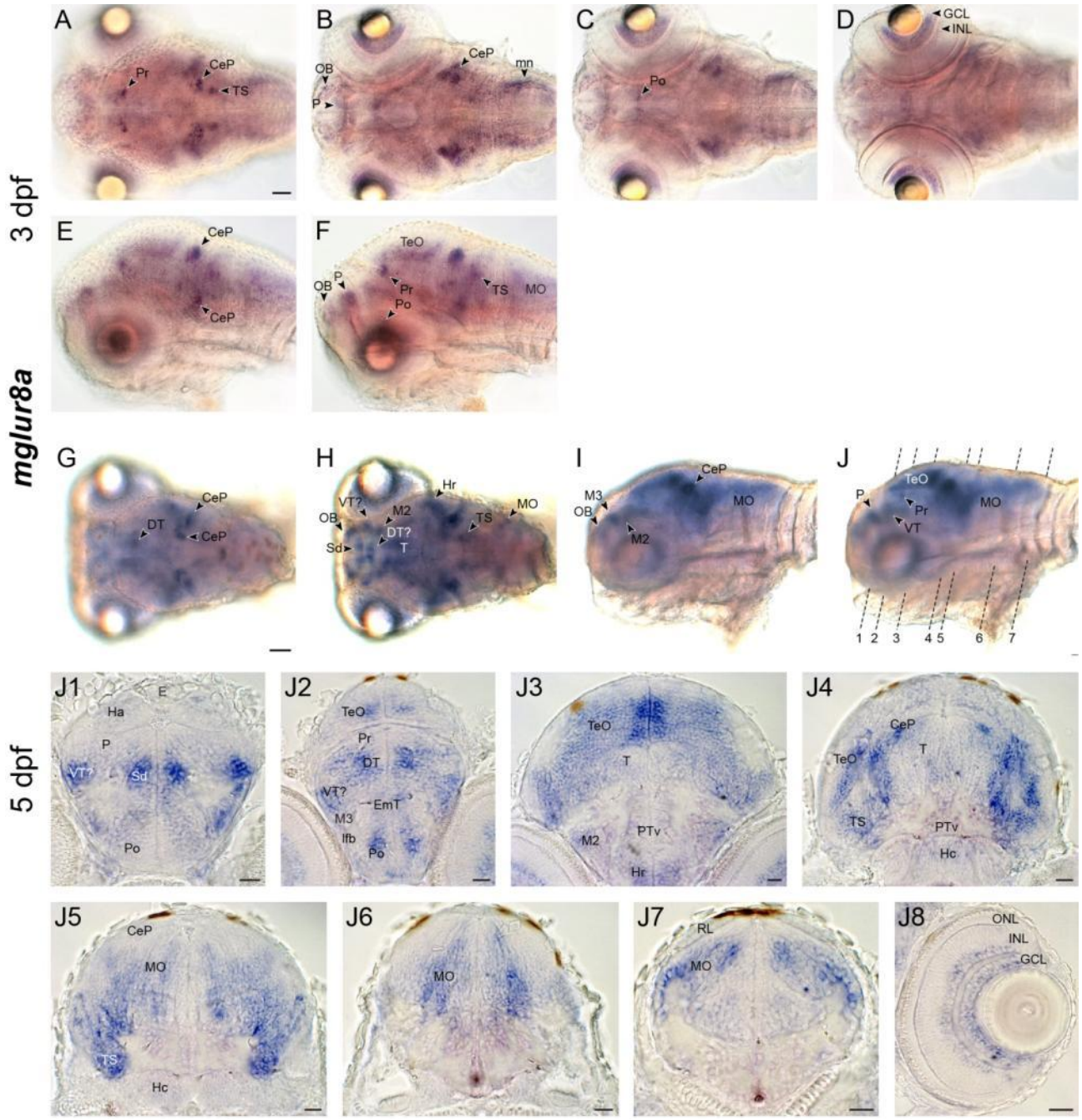

Figure 15: Expression pattern of mglur8a in three- and five-day-old zebrafish

Expression of mglur8a transcripts detected by in situ hybridization in three- (A-F) and five- (G-J) day-old fish larvae on whole mounts as well as on cross sections of five-day-old fish heads (J1-8).

Whole mount expression of mglur8a in dorsal (A-D) and lateral views (E,F) at 3 dpf shows prominent labeling of the preoptic tectum (Po), the cerebellum (CeP), presumably motor neurons (mn) in the hindbrain as well as the retinal ganglion cell layer (GCL). Although the expression seems broader dorsal (G,H) and lateral (I,J) views of mglur8a labeled, five-day-old larvae reveal an expression in similar regions of the CNS as three-day-old larvae. Cross sections (J1-8) indicate prominent staining in diencephalic areas (e.g. Sd, DT, Po), the medial optic tectum (TeO), the lateral cerebellum (CeP), the torus semicircularis (TS), and the medulla oblongata (MO).Levels of the cross sections J1-7 are indicated in J. For abbreviations see list. Scale bar in A (applies to A-F) and scale bar in G (applies to F-J) = 50 µm, scale bars in J1-8 = 20 µm.

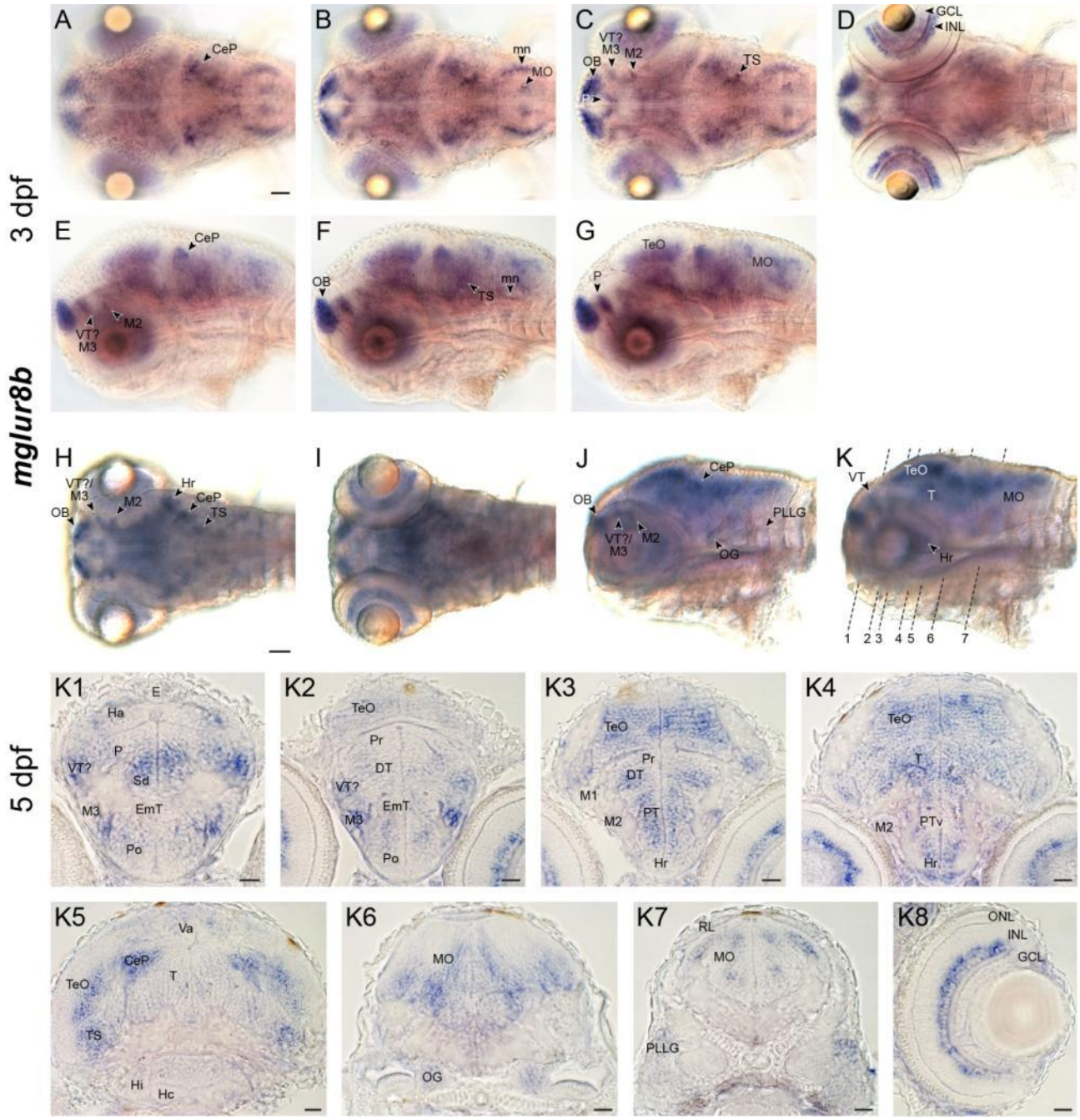

Figure 16: Expression pattern of mglur8b in three- and five-day-old zebrafish

Expression of mglur8b transcripts in three- (A-G) and five- (H-K) day-old zebrafish whole mounts depicted in dorsal (A-D,H,I) and lateral views (E-G,J,K) as well as in cross sections through the head of five-day-old whole mounts (K1-8).

At 3 dpf mglur8b is detected in broad regions of the CNS (A-G). Most prominent labeling is found in the olfactory bulb (OB), the optic tectum (TeO), the cerebellum (CeP), in motor neurons (mn) as well as in the retina (GCL, INL). The five-day-old whole mounts (H-K) reveal similar mglur8b expression. Cross sections (K1-8) confirm the broad expression of mglur8b in the diencephalic (e.g. M3, TeO, DT, PT) and hindbrain region (CeP, TS, MO) of five-day-old fish. In addition, these sections reveal mglur8b staining in two cranial ganglia (OG, PLLG). Levels of the cross sections K1-7 are indicated in K. For abbreviations see list. Scale bar in A (applies to A-G) and scale bar in H (applies to H-K) = 50 µm, scale bars in K1-8 = 20 µm.

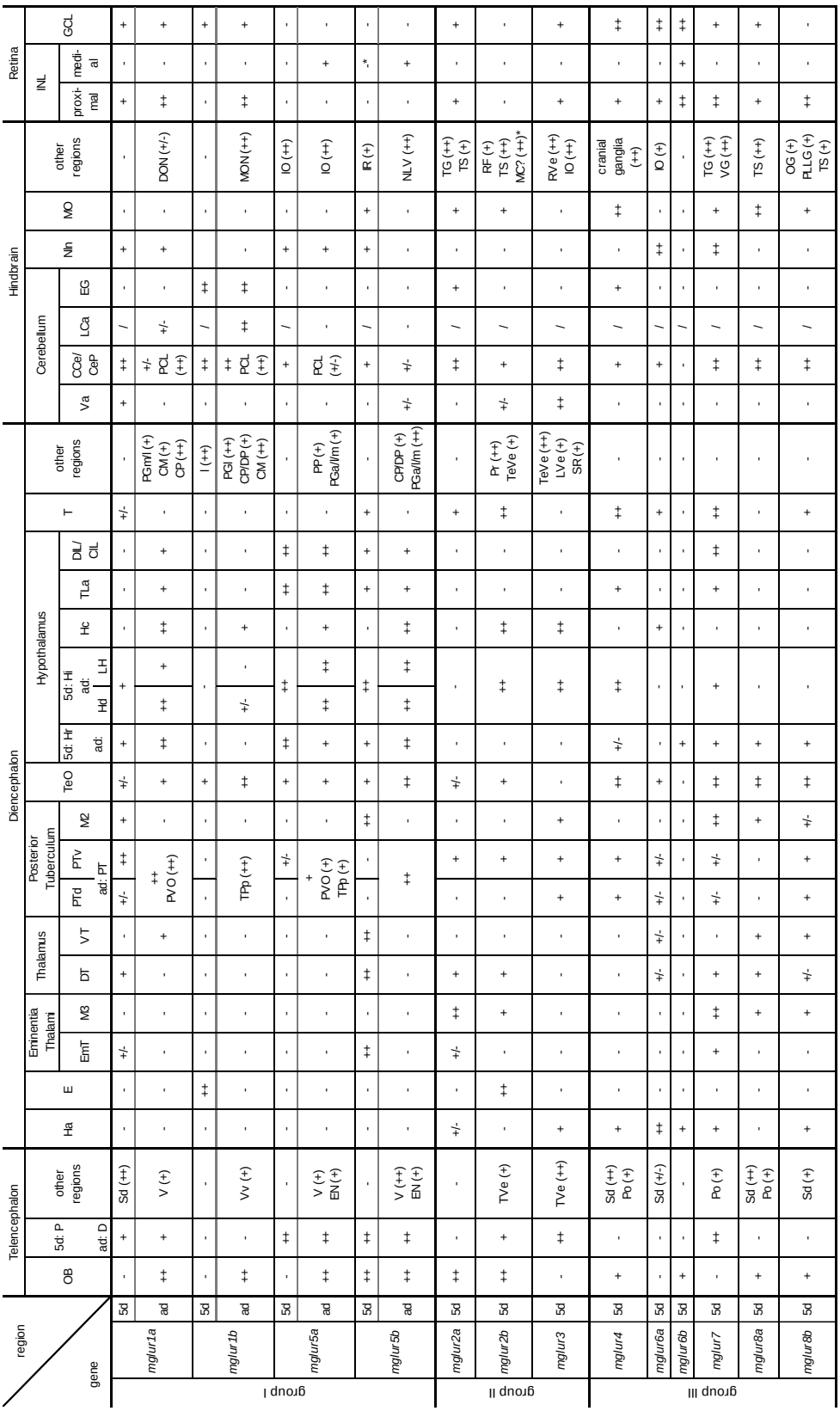

Table 2: Overview of mglur expression in zebrafish.

Overview of mglur RNA expression in the zebrafish CNS. For group I mglurs expression in adult tissue is included as well. See list for abbreviations.

2.6 Discussion

While the mammalian genome contains eight *mglur* genes (Nakanishi & Masu 1994), we found 13 mGluRs to be present in zebrafish. This increase in number can be readily explained by the whole genome duplication in teleosts (Meyer & van de Peer, 2005; Ohno, 1999; Postlethwait, 2007). The high amino acid sequence similarity as well as the segregation of the 13 zebrafish mGluRs into the corresponding subgroups suggests functional conservation of these receptors between zebrafish and mammals. Moreover, some of the *mglur* genes in zebrafish are known to be expressed in corresponding brain regions of mammals (reviewed in Ferraguti & Shigemoto, 2006), indicating that these genes are also similarly regulated.

The 13 zebrafish mGluRs are expressed in different but overlapping regions of the developing CNS, best explained by the duplication-degeneration-complementation (DDC) model of Force and colleagues (Force *et al*., 1999). This model explains the fate of initial redundant genes following genome duplications. Accumulation of mutations in regulatory regions may lead to a split in gene function among gene paralogs (subfunctionalization) or even to the uptake of a novel, non-redundant function of either one paralog (neofunctionalization). In the following paragraphs brain regions with prominent *mglur* labeling and their expression patterns are discussed particularly with those described for mammals.

In this study we determined the expression patterns of every single *mglur* in the zebrafish central nervous system (CNS). While expression of paralogous genes is overlapping in some brain regions, other areas are exclusively stained by the riboprobe of one paralog, suggesting evolutionary events such as sub- or neofunctionalization. Such events are best explained by the duplication-degeneration-complementation (DDC) model of Force and colleagues (Force et al., 1999). It states that accumulation of mutations in regulatory regions may lead to a split in gene function among gene paralogs (subfunctionalization) or even to the uptake of a novel, non-redundant function of either one paralog (neofunctionalization). In general, zebrafish *mglur* expression patterns often resemble the mammalian situation, which is also true for group I *mglurs* which were investigated in both adult as well as larval tissue. In the following paragraphs we will discuss how class I mGluRs expression patterns in the brain of zebrafish compare to orthologous gene expression patterns described for mammals. *mglurs* of other classes will be discussed in case they are prominently expressed in distinct brain regions.

2.6.1 Group I mGluRs

Group I *mglurs* are amongst the best studied members of the *mglur* family. Interestingly, our experiments indicated that the distribution of group I mGluRs as described in the rodent brain (reviewed in Ferraguti and Shigemoto, 2006) is strikingly similar to those of their orthologous genes in the zebrafish CNS. This suggests that these receptors have conserved functions between different vertebrates. In addition, group I *mglurs* are similarly expressed in both larval and adult zebrafish, suggesting that mGluR functions are established early during development. Early establishment may reflect the fact that neural circuits do not switch their receptor expression pattern once they have developed. The high resemblance between larval, adult as well as mammalian *mglur* transcript expression patterns speaks to the he possibility to use zebrafish across different developmental stages to study mGluR function.

In rats, mGluR1 expression is strongest in the olfactory bulb, hippocampus, thalamus and cerebellar Purkinje cells, mGluR5 expression is present in many telencephalic and thalamic regions as well as in the superior colliculus (reviewed in Ferraguti and Shigemoto, 2006). In contrast to mammals, zebrafish possess two *mglur1* and *mglur5* paralogs each, so some of the functions may have been distributed onto only one paralogous gene. mGluR1 for example is involved in learning and memory in mammals (Aiba et al., 1994a; Gil-Sanz et al., 2008), a hypothesis that is supported by the expression of both mammalian *mglur1* splice variants in the hippocampus (Martin et al., 1992; Baude et al., 1993; Ferraguti et al., 1998, 2004). In zebrafish, only *mglur1a* but not *-1b* is expressed in the lateral dorsal telencephalic area, the regions that corresponds to the mammalian hippocampus (Wullimann and Mueller, 2004b; Northcutt, 2006). We therefore hypothesize that a possible mGluR1 involvement in learning and memory in this area is solely transferred onto the zebrafish mGluR1a.

2.6.2 Olfactory bulb

The OB of larval zebrafish reveals a prominent expression of several *mglurs*. While the riboprobes of group II and III *mglurs 2b*, *-4*, *-6b*, *-7*, and *-8a* only partially stain the OB, *mglur2b* and *-8b* are highly expressed in this structure. Expression of some *mglurs* in this region, for instance *mglurs 2b* and *-8b*, are highly similar, suggesting that many neurons of the OB express a variety of *mglur* subtypes. In addition, in the innermost layer of the OB in adult fish all four group I *mglur* genes are expressed. Therefore, the granule and periglomerular cells, located in this area, likely express different types of the group I *mglurs*. In contrast to that, larval tissue only reveals expression of the group I *mglurs 1a* and *-5b* in the OB, suggesting that the other two members function in the adult but not during development.

The finding of such a variety of *mglurs* in the zebrafish OB is comparable to the situation in mammals, where expression for all mGluRs has been described (Dong et al., 2009; Vardi et al., 2011). Similar to our results in adult zebrafish, group I mGluRs are highly expressed in the granule cell layer of the rodent OB (Romano et al., 1995; Shigemoto et al., 1993; Sahara et al., 2001), where they likely participate in regulating the excitability of neurons (Jian et al., 2010; Heinbockel et al., 2007). In contrast to zebrafish, group I mGluRs are additionally located in other layers of the mammalian OB bulb (Shigemoto et al., 1992; Heinbockel et al., 2004; Sahara et al., 2001), mostly on mitral cells (Nakanishi and Masu, 1994; Saugstad et al., 1997; Ohishi et al., 1993; Sahara et al., 2001; Kinzie et al., 1997; Duvoisin et al., 1995) that convey information from the OB to higher brain regions.

2.6.3 Optic tectum

Organized in a layered structure, the optic tectum (TeO) mediates complex visually evoked behaviors by integrating multisensory information (Nevin *et al.*, 2010). Most retinal afferents enter the uppermost tectal layer where they make excitatory glutamatergic synaptic contact with interneurons (Kageyama & Meyer, 1989; van Keuren-Jensen & Cline, 2006). These send the information along vertically oriented dendrites into deeper tectal areas via inhibitory GABAergic or excitatory glutamatergic or cholinergic synapses (Kinoshita & Ito, 2006). As information is highly processed and filtered within tectal layers, recent research focused more on the investigation of distinct microcircuits (e.g. Del Bene *et al.*, 2010; Ramdya & Engert, 2008). However, to understand circuit

formation and processing in this multilaminar structure, it is necessary to know about its general features such as neuron- or receptor subtypes.

Besides *mglur2b* and *-6b*, all *mglur* subtypes show expression in the TeO of larval zebrafish. While group I *mglurs* are still expressed in the TeO at 5 dpf, they reveal a stronger and broader expression in three-day-old larvae, suggesting tight developmental regulation. In the adult zebrafish TeO group I *mglurs* are expressed at varying intensities in the layers of the periventricular grey zone (PGZ). Noteworthy is the prominent expression of *mglur1b* in the superficial gray/fibrous layer (SFGS). Group II *mglur2a* and *-3* show a faint expression and group III *mglur4*, *-6a*, *-7* and both *mglur8* paralogs are strongly expressed in the TeO. Most published studies discuss expression but not function of mGluR family members in the superior colliculus, which is homologous to the TeO of non-anamniote vertebrates (e.g. Ohishi *et al*., 1993; Kinoshita *et al*., 1998; Cirone *et al*., 2002b). At the functional level a contribution of mGluRs to the modulation of synaptic signaling in the superior colliculus of rats (Cirone & Salt 2000, 2001; Cirone *et al*., 2002a) and the TeO of chicken (Tasca *et al*., 1995) has been reported. However, except for a study demonstrating that visually evoked mGluR1-activation indirectly affects AMPAR synaptic plasticity, no functional details are known (van Keuren-Jensen & Cline, 2006).

2.6.4 Hypothalamus

The hypothalamus, located in the ventral part of the diencephalon, is the central organizing structure for the regulation of homeostatic functions. Various studies report the presence of mGluRs in the hypothalamus (Kiss *et al*., 1996; Schrader & Tasker, 1997; Chen & van den Pol, 1998; Pampillo *et al*., 2002; Panatier *et al*., 2004), implying a significant role for them in the modulation of signal transduction and thereby influencing homeostasis (reviewed in Kuzmiski & Bains, 2010). Given the conserved hypothalamic development of teleosts and mammals (Machluf *et al*., 2011), fish represent a suitable model to study hypothalamic function and signaling.

In larval zebrafish a variety of *mglurs* are expressed in hypothalamic regions (*mglur1a*, *-2b*, *-3*, *-5a*, *-5b,* and all group III *mglurs*). Amongst them, the members of group I mGluRs seem to play crucial roles in various areas of the hypothalamus pathways (Caruso *et al*., 2006; Huang & van den Pol, 2007). Both *mglur5* paralogs reveal a very prominent and defined expression in the rostral and intermediate hypothalamus as well as in the torus lateralis and the inferior lobe. In rats a physiological study demonstrates an influence of astrocytic group I mGluRs on synaptic plasticity of neighboring hypothalamic neurons (Gordon *et al*., 2009). Since the expression of both, mGluR1 and -5 in hypothalamic glia cells is described (Silva *et al*., 1999; van den Pol *et al*., 1995) it is likely that both receptors mediate plasticity. Besides that, group I mGluRs influence signal transduction in many other hypothalamic signaling pathways (Caruso *et al*., 2006; Huang & van den Pol, 2007; Dewing *et al*., 2007). The low expression of *mglur1b* in only a few adult hypothalamic structures indicates that in zebrafish the major role in hypothalamic signal modulation is likely controlled by mGluR1a, and the two mGluR5 paralogs.

Group II *mglur2b* and *-3* are strongly expressed in the caudal hypothalamus. However, neither an involvement in the modulation of GABA release in suprachiasmatic neurons of rats (Chen & van den Pol, 1998) no other specific functions have been described in the literature. Although expression of all group III mGluRs in the hypothalamus is described (Ghosh *et al*., 1997; Chen & van den Pol, 1998), specific functions for receptor subtypes are unknown due to the lack of specific agonists (Schrader and Tasker, 1997; Chen & van den Pol, 1998; Panatier *et al*.,

2004; Kuzmiski *et al*., 2009). The mRNA expression analysis demonstrates that all group III *mglurs* are present in the larval zebrafish hypothalamus albeit with a variation of the regions and the expression level.

2.6.5 Cerebellum

The most extensively studied mGluR in the cerebellum of mammals is mGluR1. Its knockout leads to problems in motor coordination and spatial learning (Aiba *et al.*, 1994b; Conquet *et al.*, 1994), demonstrating a crucial role in long term potentiation and –depression (Aiba *et al.*, 1994b; Conquet *et al*., 1994). Consistent with that we find prominent expression for both *mglur1* paralogs in the zebrafish cerebellum. At larval stages the cerebellar *mglur1a*-riboprobe detects cells that resemble a Purkinje cell staining of an antibody against Parvalbumin7 (Bae *et al*., 2009). In contrast to Parvalbumin 7, *mglur1b* is additionally expressed in a subpopulation of granule cells in the dorsal and lateral part of the cerebellum. The staining pattern for *mglur1b* seems to coincide partially with the vesicular glutamate transporter 1 (Vglut1), arguing for a presynaptic function as observed for Vglut1 (Bae *et al*., 2009). Expression of *mglur1s* in these regions persists into adulthood where both *mglur1* transcripts are present in Purkinje cells, and the granule cell layer of the corpus cerebelli as well as the eminentia granularis are *mglur1b*-positive. Interestingly, human mRNA expression studies of *mglur1* splice variants show only expression for certain variants in cerebellar granule, Purkinje and basket cells, whereas another isoform is exclusively present in granule cells (Makoff *et al*., 1997). This suggests that the cerebellar subdivision of zebrafish *mglur1* paralogs may be similar to the subdivision of *mglur1* splice variants in humans, even though in zebrafish the two variants originate from a whole genome duplication event and not from the same gene. The expression of *mglur1* in corresponding structures in fish and mammals may indicate some conservation in functional aspects of these receptors. While the ancestral gene presumably fulfilled the combined function of both paralogs, functions may have later been subdivided between the two paralogs by subfunctionalization (Force *et al*., 1999). Zebrafish *mglur1* paralogs are also expressed in regions of the brain where the corresponding mammalian ortholog might not be expressed. However, as *mglur1* variants have a very broad expression range it remains to be determined whether some of the zebrafish mRNA patterns are due to newly acquired gene functions.

Similar to mGluR1, the second group I mGluR, mGluR5, is also in involved in synaptic plasticity of the cerebellum, although not in exactly the same way as is apparent when comparing the different phenotypes of knockout mice (Aiba *et al.*, 1994b; Conquet *et al.*, 1994; Lu *et al.*, 1997). In line with that, we find *mglur5a* and *-5b* expression in the larval and adult zebrafish cerebellum, albeit not in such a broad manner as for the *mglur1* paralogs. Moreover, except for *mglur6b*, we localize all *mglur* subtypes in at least parts of the cerebellar structures of zebrafish larvae. Since both group II (Ghose *et al*., 1997; Knoflach and Kemp, 1998; Watanabe and Nakanishi, 2003) and group III mGluRs are known to act in cerebellar signaling pathways (Pekhletski *et al*., 1996; Cartmell *et al*., 1997; Abitbol *et al*., 2008; Zhang *et al*., 2008), and are assumed to be involved in synaptic plasticity and motor learning (Anwyl, 1999; Zhu *et al*., 2005) the presence of transcripts for these *mglur* subtypes in the zebrafish cerebellum are hardly astonishing. However, an exception is mGluR6, which is expressed in lateral cerebellar regions of 5-day-old zebrafish larvae but has not been reported yet to be present in developing or mature cerebellar structures in mammals (Berthele *et al*., 1999).

2.6.6 Retina

Since glutamate is the main neurotransmitter in the retina, various mGluRs can be found in the eye. In other species mGluRs have been shown to be involved in signal modulation of the first visual synapse (Higgs *et al*., 2002; Higgs & Lukasiewicz, 2002; Hirasawa *et al*., 2002; Hosoi *et al*., 2005). However, the zebrafish retina does not express any *mglur* in the outermost layers of the retina where photoreceptors (ONL) and horizontal cell bodies (outermost INL close to OPL) are located.

Both *mglur1* paralogs are expressed in inner retinal layers of larval zebrafish. While we could not detect any *mglur5a* transcripts in the larval retina, *mglur5b* shows a faint expression in the inner retina at 3 but not at 5 dpf. Expression of *mglur1a* and *-5b* is consistent between embryonic and adult tissue, whereas *mglur1b* and *-5a* are additionally expressed in the medial INL in adult retinas, indicating an additional role for these genes in adulthood. An immunohistochemical study performed in adult goldfish retinae showed expression of mGluR1α mainly in ON-bipolar cell dendrites (Joselevitch *et al.,* 2007). This study also reported mGluR5 immunoreactivity in glia cells and in the OPL, INL, and IPL. While the expression pattern for zebrafish *mglur1b* is consistent with the one found for goldfish mGluR1α, the expression we found for the *mglur5* paralogs is concentrated on the INL and does not resemble glia cell labeling. However, a direct comparison to our results is not possible since the antibodies used by Joselevitch and colleagues were not specifically designed against teleost tissue and therefore also not against a specific mGluR paralog.

Group II mGluRs are involved in the presynaptic inhibition of retinotectal transmission in goldfish (Zhang & Schmidt, 1999) which explains the presence of two of the three zebrafish group II mGluRs in the ganglion cell layer. However, as mGluR3 is – in contrast to our data – not expressed in the retina of cat and goldfish (Cai & Pourcho, 1999; Joselevitch *et al.,* 2007), and as we could not find *mglur2b*-positive labeling in the larval fish retina, this function seems to be exclusively mediated by zebrafish mGluR2a. In addition, the expression of *mglur2* mRNA in rat amacrine and ganglion cells (Hartveit *et al.*, 1995) agrees well with the expression of *mglur2a* in the proximal INL and GCL.

Other interesting differences in expression exist for the *mglur6* paralogs: Vertebrate mGluR6 is known to be involved in the ON-bipolar cell signaling, being exclusively expressed in ON-bipolar cell dendrites (Nomura *et al*., 1994; Hartveit *et al*., 1995; Masu *et al*., 1995; Ueda *et al*., 1997; Vardi & Morigiwa, 1997; Vardi *et al*., 2000). We only found expression of *mglur6b* in the medial INL, where bipolar cell bodies are located, whereas *mglur6a* is not expressed in this layer at larval stages. This suggests that the known function in the ON-bipolar cell pathway of the mammalian mGluR6 is fulfilled exclusively by the zebrafish mGluR6b in the larval retina. The expression of both *mglur6* paralogs in the retinal bipolar cell layer of adult zebrafish (Huang *et al.,* 2012) suggests – at least for *mglur6a* – a developmental regulation of gene expression in this retinal cell layer. *Mglur6* paralogs may have separate roles in the ON-bipolar cell pathway. Since rods mature later than cones (Branchek & Bremiller 1984), one could envision a scenario where the cone ON-pathway mainly relies on *mglur6b* and the rod ON-pathway on *mglur6a*, which is not expressed until rods are functionally mature. MGluR6 was thought of being exclusively involved in the postsynaptic reception of the ON-pathway signal, however, our finding of *mglur6* expression in the inner retina proposes an additional modulatory role (Huang *et al*., 2012). The fact that *mglur6* was recently

detected in human retinal ganglion cell bodies (Klooster *et al*., 2011) indicates that this role might be more widespread in vertebrates than originally anticipated.

Various studies in mammals detected *mglur8* throughout different retinal layers from the OPL to the GCL (Duvoisin *et al*., 1995; Koulen & Brandstätter, 2002; Duvoisin *et al*., 1995; Quraishi *et al*., 2007). Our expression analysis demonstrates an identical expression of both *mglur8* paralogs in the inner part of the INL but only *mglur8a* is additionally expressed in the GCL and none of the paralogs is located in the outer retinal layers. The immunohistochemical analysis of mGluR8 in rats revealed a developmentally distinct expression, starting with the labeling of ganglion cell somata at postnatal day 5. Immunoreactivity in the OPL was only detected from postnatal day 10 on (Koulen & Brandstätter, 2002), however, analyzing larval zebrafish we locate *mglur8* mRNA only in inner retinal layers, an expression in the outer retina at later stages cannot be excluded.

The photopic retina of zebrafish is already highly developed and nearly fully functional at 5 dpf, when rods just begin to functionally integrate into the retina at that stage (Branchek, 1984; Branchek & Bremiller, 1984). A developmental regulation of gene expression – as proposed for *mglur6b* and the *mglur8* paralogs – could explain the restricted expression pattern we find for most *mglurs*. Except for mGluR6, which directly acts as glutamate receptor in the ON-bipolar cell pathway (Masu *et al*., 1995), all other mGluRs are known to indirectly modulate synaptic signaling in the retina at pre- and postsynapses, for example by changing presynaptic calcium concentration in photoreceptor synaptic terminals (Akopian & Witkovsky, 1996; Koulen *et al*., 1999) or even by directly influencing transmitter release (Hirasawa *et al*., 2002). However, the expression of almost all zebrafish *mglurs* in the retina shows their important impact in visual signal transmission.

2.6.7 Conclusion

Glutamate mediates most of the excitatory signaling of the nervous system and is of prime importance for the functioning of neuronal circuits. Knowledge of glutamatergic signaling, in particular of its receptors, helps deciphering underlying mechanisms and organizations of these circuits. Our detailed analysis of zebrafish metabotropic glutamate receptors showed comparably broad expression in similar regions as their mammalian orthologs, implicating their significance in diverse neuronal functions. The paralogous zebrafish *mglurs* are all expressed in overlapping but also in exclusive brain regions, suggesting functional specialization. Moreover, the high coincidence between larval and adult gene expression makes larval zebrafish suitable as a model to study mGluR function and may helps to facilitate the disentanglement of neuronal circuits.

2.7 References

Abitbol, K, Acher, F, Daniel, H. 2008. Depression of excitatory transmission at PF-PC synapse by group III metabotropic glutamate receptors is provided exclusively by mGluR4 in the rodent cerebellar cortex. J. Neurochem, 105, 2069–2079.

Aiba, A, Chen, C, Herrup, K, Rosenmund, C, Stevens, CF, Tonegawa, S. 1994a. Reduced hippocampal long-term potentiation and context-specific deficit in associative learning in mGluR1 mutant mice. Cell, 79, 365–375.

Aiba, A, Kano, M., Chen, C, Stanton, ME, Fox, GD, Herrup, K., Zwingman, TA, Tonegawa, S. 1994b. Deficient cerebellar long-term depression and impaired motor learning in mGluR1 mutant mice. Cell, 79, 377–388.

Akazawa, C, Ohishi, H, Nakajima, Y, Okamoto, N, Shigemoto, R, Nakanishi, S, Mizuno, N. 1994. Expression of mRNAs of L-AP4-sensitive metabotropic glutamate receptors (mGluR4, mGluR6, mGluR7) in the rat retina. Neurosci Lett, 171, 52–54.

Akopian, A, Witkovsky, P. 1996. Activation of metabotropic glutamate receptors decreases a high-threshold calcium current in spiking neurons of the Xenopus retina. Vis. Neurosci, 13, 549–557.

Alioto, TS, Ngai, J. 2005. The odorant receptor repertoire of teleost fish. BMC Genomics, 6, 173.

Amsterdam, A, Lin, S, Hopkins, N. 1995. The Aequorea victoria green fluorescent protein can be used as a reporter in live zebrafish embryos. Dev Biol, 171, 123–129.

Anisimova, M, Gascuel, O. 2006. Approximate likelihood-ratio test for branches: A fast, accurate, and powerful alternative. Syst. Biol, 55, 539–552.

Anwyl, R. 1999. Metabotropic glutamate receptors: electrophysiological properties and role in plasticity. Brain Res. Brain Res. Rev, 29, 83–120.

Bae, Y-K, Kani, S, Shimizu, T, Tanabe, K, Nojima, H, Kimura, Y, Higashijima, S-I, Hibi, M. 2009. Anatomy of zebrafish cerebellum and screen for mutations affecting its development. Dev. Biol, 330, 406–426.

Baude, A, Nusser, Z, Roberts, JD, Mulvihill, E, McIlhinney, RA, Somogyi, P. 1993. The metabotropic glutamate receptor (mGluR1 alpha) is concentrated at perisynaptic membrane of neuronal subpopulations as detected by immunogold reaction. Neuron, 11, 771–787.

Berthele, A, Platzer, S, Laurie, DJ, Weis, S, Sommer, B, Zieglgänsberger, W, Conrad, B, Tölle, TR. 1999. Expression of metabotropic glutamate receptor subtype mRNA (mGluR1-8) in human cerebellum. Neuroreport, 10, 3861–3867.

Branchek, T. 1984. The development of photoreceptors in the zebrafish, brachydanio rerio. II. Function. J. Comp. Neurol, 224, 116–122.

Branchek, T, Bremiller, R. 1984. The development of photoreceptors in the zebrafish, Brachydanio rerio. I. Structure. J Comp Neurol, 224, 107–115.

Brandstätter, JH, Koulen, P, Kuhn, R., van der Putten, H, Wässle, H. 1996. Compartmental localization of a metabotropic glutamate receptor (mGluR7): two different active sites at a retinal synapse. J Neurosci, 16, 4749–4756.

Byrnes, KR, Loane, DJ, Faden, AI. 2009. Metabotropic glutamate receptors as targets for multipotential treatment of neurological disorders. Neurotherapeutics, 6, 94–107.

Cai, W, Pourcho, RG. 1999. Localization of metabotropic glutamate receptors mGluR1alpha and mGluR2/3 in the cat retina. J. Comp. Neurol, 407, 427–437.

Cartmell, J, Kemp, JA, Mutel, V. 1997. L-AP4 inhibition of depolarization-evoked cGMP formation in rat cerebellum. Neurosci. Lett, 228, 191–194.

Caruso, C, Durand, D, Watanobe, H, Lasaga, M. 2006. NMDA and group I metabotropic glutamate receptors activation modulates substance P release from the arcuate nucleus and median eminence. Neurosci. Lett, 393, 60–64.

Castresana, J. 2000. Selection of conserved blocks from multiple alignments for their use in phylogenetic analysis. Mol. Biol. Evol, 17, 540–552.

Chen, G, van den Pol, AN. 1998. Coexpression of multiple metabotropic glutamate receptors in axon terminals of single suprachiasmatic nucleus neurons. J. Neurophysiol, 80, 1932–1938.

Cirone, J, Salt, TE. 2000. Physiological role of group III metabotropic glutamate receptors in visually responsive neurons of the rat superficial superior colliculus. Eur. J. Neurosci, 12, 847–855.

Cirone, J, Salt, TE. 2001. Group II and III metabotropic glutamate receptors contribute to different aspects of visual response processing in the rat superior colliculus. J. Physiol. (Lond.), 534, 169–178.

Cirone, J, Pothecary, CA, Turner, JP, Salt, TE. 2002a. Group I metabotropic glutamate receptors (mGluRs) modulate visual responses in the superficial superior colliculus of the rat. J. Physiol. (Lond.), 541, 895–903.

Cirone, J, Sharp, C, Jeffery, G, Salt, TE. 2002b. Distribution of metabotropic glutamate receptors in the superior colliculus of the adult rat, ferret and cat. Neuroscience, 109, 779–786.

Conquet, F, Bashir, ZI, Davies, CH, Daniel, H, Ferraguti, F, Bordi, F, Franz-Bacon, K, Reggiani, A, Matarese, V, Condé, F. 1994. Motor deficit and impairment of synaptic plasticity in mice lacking mGluR1. Nature, 372, 237–243.

Corrêa, S.A.L. and Zupanc, G.K.H. 2004. Re-evaluation of the afferent connections of the pituitary in the weakly electric fish Apteronotus leptorhynchus: an in vitro tract-tracing study. J. Comp. Neurol., 470, 39–49.

Del Bene, F, Wyart, C, Robles, E, Tran, A, Looger, L, Scott, EK, Isacoff, EY, Baier, H. 2010. Filtering of visual information in the tectum by an identified neural circuit. Science, 330, 669–673.

Dereeper, A, Guignon, V, Blanc, G, Audic, S, Buffet, S, Chevenet, F, Dufayard, JF, Guindon, S, Lefort, V, Lescot, M, Claverie, JM, Gascuel, O. 2008. Phylogeny.fr: robust phylogenetic analysis for the non-specialist. Nucleic Acids Res, 36, W465-9.

Dewing, P, Boulware, MI, Sinchak, K, Christensen, A, Mermelstein, PG, Micevych, P. 2007. Membrane estrogen receptor-alpha interactions with metabotropic glutamate receptor 1a modulate female sexual receptivity in rats. J. Neurosci, 27, 9294–9300.

Dong, H-W, Heinbockel, T, Hamilton, KA, Hayar, A, Ennis, M. 2009. Metabotropic glutamate receptors and dendrodendritic synapses in the main olfactory bulb. Ann. N. Y. Acad. Sci, 1170, 224–238.

Duvoisin, RM, Zhang, C, Ramonell, K. 1995. A novel metabotropic glutamate receptor expressed in the retina and olfactory bulb. J Neurosci, 15, 3075–3083.

Edgar, R.C. 2004. MUSCLE: a multiple sequence alignment method with reduced time and space complexity. BMC Bioinformatics, 5, 113.

Ferraguti, F, Conquet, F, Corti, C, Grandes, P, Kuhn, R, Knopfel, T. 1998. Immunohistochemical localization of the mGluR1beta metabotropic glutamate receptor in the adult rodent forebrain: evidence for a differential distribution of mGluR1 splice variants. J. Comp. Neurol., 400, 391–407.

Ferraguti, F, Cobden, P, Pollard, M, Cope, D, Shigemoto, R, Watanabe, M, Somogyi, P. 2004. Immunolocalization of metabotropic glutamate receptor 1alpha (mGluR1alpha) in distinct classes of interneuron in the CA1 region of the rat hippocampus. Hippocampus, 14, 193–215.

Ferraguti, F., Shigemoto, R. 2006. Metabotropic glutamate receptors. Cell Tissue Res., 326, 483–504.

Force, A, Lynch, M, Pickett, FB, Amores, A, Yan, YL, Postlethwait, J. 1999. Preservation of duplicate genes by complementary, degenerative mutations. Genetics, 151, 1531–1545.

Gesemann, M, Lesslauer, A, Maurer, CM, Schönthaler, HB, Neuhauss, SCF. 2010. Phylogenetic analysis of the vertebrate excitatory/neutral amino acid transporter (SLC1/EAAT) family reveals lineage specific subfamilies. BMC Evol. Biol, 10, 117.

Ghose, S, Wroblewska, B, Corsi, L, Grayson, DR, de Blas, AL, Vicini, S, Neale, JH. 1997. N-acetylaspartylglutamate stimulates metabotropic glutamate receptor 3 to regulate expression of the GABA(A) alpha6 subunit in cerebellar granule cells. J. Neurochem, 69, 2326–2335.

Ghosh, P.K, Baskaran, N, van den Pol, AN. 1997. Developmentally regulated gene expression of all eight metabotropic glutamate receptors in hypothalamic suprachiasmatic and arcuate nuclei--a PCR analysis. Brain Res. Dev. Brain Res, 102, 1–12.

Gil-Sanz, C, Delgado-García, JM, Fairén, A and Gruart, A. 2008. Involvement of the mGluR1 receptor in hippocampal synaptic plasticity and associative learning in behaving mice. Cereb. Cortex, 18, 1653–1663.

Gordon, GRJ, Iremonger, KJ, Kantevari, S, Ellis-Davies, GCR, MacVicar, BA, Bains, JS. 2009. Astrocyte-mediated distributed plasticity at hypothalamic glutamate synapses. Neuron, 64, 391–403.

Grant, GB, Dowling, JE. 1995. A glutamate-activated chloride current in cone-driven ON bipolar cells of the white perch retina. J Neurosci, 15, 3852–3862.

Grant, GB, Dowling, JE. 1996. On bipolar cell responses in the teleost retina are generated by two distinct mechanisms. J Neurophysiol, 76, 3842–3849.

Guindon, S, Gascuel, O. 2003. A simple, fast, and accurate algorithm to estimate large phylogenies by maximum likelihood. Syst. Biol, 52, 696–704.

Hartveit, E, Brandstätter, JH, Enz, R, Wässle, H. 1995. Expression of the mRNA of seven metabotropic glutamate receptors (mGluR1 to 7) in the rat retina. An in situ hybridization study on tissue sections and isolated cells. Eur J Neurosci, 7, 1472–1483.

Heinbockel, T, Heyward, P, Conquet, F, Ennis, M. 2004. Regulation of main olfactory bulb mitral cell excitability by metabotropic glutamate receptor mGluR1. J. Neurophysiol., 92, 3085–3096.

Heinbockel, T, Laaris, N, Ennis, M. 2007. Metabotropic glutamate receptors in the main olfactory bulb drive granule cell-mediated inhibition. J. Neurophysiol, 97, 858–870.

Higgs, MH, Romano, C, Lukasiewicz, PD. 2002. Presynaptic effects of group III metabotropic glutamate receptors on excitatory synaptic transmission in the retina. Neuroscience, 115, 163–172.

Higgs, MH, Lukasiewicz, PD. 2002. Activation of group II metabotropic glutamate receptors inhibits glutamate release from salamander retinal photoreceptors. Vis. Neurosci, 19, 275–281.

Hirasawa, H, Shiells, R, Yamada, M. 2002. A metabotropic glutamate receptor regulates transmitter release from cone presynaptic terminals in carp retinal slices. J. Gen. Physiol, 119, 55–68.

Hosoi, N, Arai, I, Tachibana, M. 2005. Group III metabotropic glutamate receptors and exocytosed protons inhibit L-type calcium currents in cones but not in rods. J. Neurosci, 25, 4062–4072.

Huang, H, van den Pol, AN. 2007. Rapid direct excitation and long-lasting enhancement of NMDA response by group I metabotropic glutamate receptor activation of hypothalamic melanin-concentrating hormone neurons. J. Neurosci, 27, 11560–11572.

Huang, Y-Y, Haug, MF, Gesemann, M, Neuhauss, SCF. 2012. Novel Expression Patterns of Metabotropic Glutamate Receptor 6 in the Zebrafish Nervous System. PLoS ONE, 7, 135-143.

Iwakabe, H, Katsuura, G, Ishibashi, C, Nakanishi, S. 1997. Impairment of pupillary responses and optokinetic nystagmus in the mGluR6-deficient mouse. Neuropharmacology, 36, 135–143.

Jian, K, Cifelli, P, Pignatelli, A, Frigato, E, Belluzzi, O. 2010. Metabotropic glutamate receptors 1 and 5 differentially regulate bulbar dopaminergic cell function. Brain Res, 1354, 47–63.

Joselevitch, C, Klooster, J, Kamermans, M. 2007. Localization of metabotropic glutamate receptors in the outer plexiform layer of the goldfish retina. Cell Tissue Res, 330, 389–403.

Kageyama, GH, Meyer, RL. 1989. Glutamate-immunoreactivity in the retina and optic tectum of goldfish. Brain Res., 503, 118–127.

Kawakami, K, Shima, A. 1999. Identification of the Tol2 transposase of the medaka fish Oryzias latipes that catalyzes excision of a nonautonomous Tol2 element in zebrafish Danio rerio. Gene, 240, 239–244.

Kikuta, H, Laplante, M, Navratilova, P, Komisarczuk, AZ, Engstrom, PG, Fredman, D, Akalin, A, Caccamo, M, Sealy, I, Howe, K, Ghislain, J, Pezeron, G, Mourrain, P, Ellingsen, S, Oates, AC, Thisse, C, Thisse, B, Foucher, I, Adolf, B, Geling, A, Lenhard, B, Becker, TS. 2007. Genomic regulatory blocks encompass multiple neighboring genes and maintain conserved synteny in vertebrates. Genome Research, 17, 545–555.

Kinoshita, A, Shigemoto, R, Ohishi, H, van der Putten, H, Mizuno, N. 1998. Immunohistochemical localization of metabotropic glutamate receptors, mGluR7a and mGluR7b, in the central nervous system of the adult rat and mouse: a light and electron microscopic study. J. Comp. Neurol, 393, 332–352.

Kinoshita, M., Ito, E. 2006 Roles of periventricular neurons in retinotectal transmission in the optic tectum. Prog. Neurobiol., 79, 112–121.

Kinzie, JM, Shinohara, MM, van den Pol, AN, Westbrook, GL, Segerson, TP. 1997. Immunolocalization of metabotropic glutamate receptor 7 in the rat olfactory bulb. J. Comp. Neurol, 385, 372–384.

Kiss, J, Görcs, TJ, Kuhn, R, Knöpfel, T, Csáky, A, Halász, B. 1996. Distribution of metabotropic glutamate receptor 1a in the rat hypothalamus: an immunocytochemical study using monoclonal and polyclonal antibody. Acta. Biol. Hung, 47, 221–237.

Klooster, J, Yazulla, S, Kamermans, M. 2009. Ultrastructural analysis of the glutamatergic system in the outer plexiform layer of zebrafish retina. J Chem Neuroanat, 37, 254–265.

Klooster, J, Blokker, J, Ten Brink, JB, Unmehopa, U, Fluiter, K, Bergen, AAB, Kamermans, M. 2011. Ultrastructural Localization and Expression of Trpm1 in the Human Retina. Invest. Ophthalmol. Vis. Sci.

Knackstedt, LA, Kalivas, PW. 2009. Glutamate and reinstatement. Curr Opin Pharmacol, 9, 59–64.

Knoflach, F, Kemp, JA. 1998. Metabotropic glutamate group II receptors activate a G protein-coupled inwardly rectifying K+ current in neurones of the rat cerebellum. J. Physiol. (Lond.), 509 (Pt 2), 347–354.

Koulen, P, Brandstätter, JH. 2002. Pre- and Postsynaptic Sites of Action of mGluR8a in the mammalian retina. Invest Ophthalmol Vis Sci, 43, 1933–1940.

Koulen, P, Kuhn, R, Wässle, H, Brandstätter, JH. 1999. Modulation of the intracellular calcium concentration in photoreceptor terminals by a presynaptic metabotropic glutamate receptor. Proc. Natl. Acad. Sci. U.S.A, 96, 9909–9914.

Kuzmiski, JB, Bains, JS. 2010. Metabotropic glutamate receptors: gatekeepers of homeostasis. J. Neuroendocrinol, 22, 785–792.

Kuzmiski, JB, Pittman, QJ, Bains, JS. 2009. Metaplasticity of hypothalamic synapses following in vivo challenge. Neuron, 62, 839–849.

Li, W-H, Yang, J, Gu, X. 2005. Expression divergence between duplicate genes. Trends Genet, 21, 602–607.

Lillesaar, C. (2011) The serotonergic system in fish. J. Chem. Neuroanat., 41, 294–308.

Lu, YM, Jia, Z, Janus, C, Henderson, JT, Gerlai, R, Wojtowicz, JM, Roder, JC. 1997. Mice lacking metabotropic glutamate receptor 5 show impaired learning and reduced CA1 long-term potentiation (LTP) but normal CA3 LTP. J. Neurosci., 17, 5196–5205.

Luscher, C, Huber, KM. 2010. Group 1 mGluR-dependent synaptic long-term depression: mechanisms and implications for circuitry and disease. Neuron, 65, 445–459.

Machluf, Y, Gutnick, A, Levkowitz, G. 2011. Development of the zebrafish hypothalamus. Ann. N. Y. Acad. Sci, 1220, 93–105.

Makoff, AJ, Phillips, T, Pilling, C, Emson, P. 1997. Expression of a novel splice variant of human mGluR1 in the cerebellum. Neuroreport, 8, 2943–2947.

Martin, LJ, Blackstone, CD, Huganir, RL, Price, DL. 1992. Cellular localization of a metabotropic glutamate receptor in rat brain. Neuron, 9, 259–270.

Masu, M, Iwakabe, H, Tagawa, Y, Miyoshi, T, Yamashita, M, Fukuda, Y, Sasaki, H, Hiroi, K, Nakamura, Y, Shigemoto, R, et al. 1995. Specific deficit of the ON response in visual transmission by targeted disruption of the mGluR6 gene. Cell, 80, 757–765.

Meyer, A, van de Peer, Y. 2005. From 2R to 3R: evidence for a fish-specific genome duplication (FSGD). Bioessays, 27, 937–945.

Mills, IA, Adolph, AR, Dowling, JE. 2009. Rods are Functional in 5-6 Day Old Larval Zebrafish. ARVO e-abstract 4566.

Mueller, T, Vernier, P, Wullimann, MF. 2006. A phylotypic stage in vertebrate brain development: GABA cell patterns in zebrafish compared with mouse. J. Comp. Neurol, 494, 620–634.

Mueller, T, Wullimann, MF. 2005. Atlas of Early Zebrafish Brain Development. A Tool for Molecular Neurogenetics, Elsevier.

Mullins, MC, Hammerschmidt, M, Haffter, P, Nüsslein-Volhard, C. 1994. Large-scale mutagenesis in the zebrafish: in search of genes controlling development in a vertebrate. Curr Biol, 4, 189–202.

Nakajima, Y, Iwakabe, H, Akazawa, C, Nawa, H, Shigemoto, R, Mizuno, N, Nakanishi, S. 1993. Molecular characterization of a novel retinal metabotropic glutamate receptor mGluR6 with a high agonist selectivity for L-2-amino-4-phosphonobutyrate. J Biol Chem, 268, 11868–11873.

Nakanishi, S, Masu, M. 1994. Molecular diversity and functions of glutamate receptors. Annu Rev Biophys Biomol Struct, 23, 319–348.

Nevin, LM, Robles, E, Baier, H, Scott, EK. 2010. Focusing on optic tectum circuitry through the lens of genetics. BMC Biol., 8, 126.

Niswender, CM, Conn, PJ. 2010. Metabotropic glutamate receptors: physiology, pharmacology, and disease. Annu. Rev. Pharmacol. Toxicol., 50, 295–322.

Nomura, A, Shigemoto, R, Nakamura, Y, Okamoto, N, Mizuno, N, Nakanishi, S. 1994. Developmentally regulated postsynaptic localization of a metabotropic glutamate receptor in rat rod bipolar cells. Cell, 77, 361–369.

Northcutt, RG. 2006. Connections of the lateral and medial divisions of the goldfish telencephalic pallium. J. Comp. Neurol., 494, 903–943.

Ohishi, H, Shigemoto, R, Nakanishi, S, Mizuno, N. 1993. Distribution of the mRNA for a metabotropic glutamate receptor (mGluR3) in the rat brain: an in situ hybridization study. J. Comp. Neurol, 335, 252–266.

Ohno, S. 1999. Gene duplication and the uniqueness of vertebrate genomes circa 1970-1999. Semin Cell Dev Biol, 10, 517–522.

Page, RD. 1996. TreeView: an application to display phylogenetic trees on personal computers. Comput Appl Biosci, 12, 357–358.

Pampillo, M, Scimonelli, T, Duvilanski, BH, Celis, ME, Seilicovich, A, Lasaga, M. 2002. The activation of metabotropic glutamate receptors differentially affects GABA and alpha-melanocyte stimulating hormone release from the hypothalamus and the posterior pituitary of male rats. Neurosci. Lett, 327, 95–98.

Panatier, A, Poulain, DA, Oliet, SHR. 2004. Regulation of transmitter release by high-affinity group III mGluRs in the supraoptic nucleus of the rat hypothalamus. Neuropharmacology, 47, 333–341.

Pekhletski, R, Gerlai, R, Overstreet, LS, Huang, XP, Agopyan, N, Slater, NT, Abramow-Newerly, W, Roder, JC, Hampson, DR. 1996. Impaired cerebellar synaptic plasticity and motor performance in mice lacking the mGluR4 subtype of metabotropic glutamate receptor. J. Neurosci, 16, 6364–6373.

Pin, JP, Duvoisin, R. 1995. The metabotropic glutamate receptors: structure and functions. Neuropharmacology, 34, 1–26.

Postlethwait, JH. 2007. The zebrafish genome in context: ohnologs gone missing. J Exp Zoolog B Mol Dev Evol, 308, 563–577.

Quraishi, S, Gayet, J, Morgans, CW, Duvoisin, RM. 2007. Distribution of group-III metabotropic glutamate receptors in the retina. J Comp Neurol, 501, 931–943.Ramdya, P, Engert, F. 2008. Emergence of binocular functional properties in a monocular neural circuit. Nat. Neurosci., 11, 1083–1090.

Ramdya, P, Engert, F. 2008. Emergence of binocular functional properties in a monocular neural circuit. Nat. Neurosci., 11, 1083–1090.

Romano, C, Sesma, MA, McDonald, CT, O'Malley, K, van den Pol, AN, Olney, JW. 1995. Distribution of metabotropic glutamate receptor mGluR5 immunoreactivity in rat brain. J. Comp. Neurol., 355, 455–469.

Rosemond, E, Wang, M, Yao, Y, Storjohann, L, Stormann, T, Johnson, EC, Hampson, DR. 2004. Molecular basis for the differential agonist affinities of group III metabotropic glutamate receptors. Mol Pharmacol, 66, 834–842.

Sahara, Y, Kubota, T, Ichikawa, M. 2001. Cellular localization of metabotropic glutamate receptors mGluR1, 2/3, 5 and 7 in the main and accessory olfactory bulb of the rat. Neurosci. Lett, 312, 59–62.

Saugstad, JA, Kinzie, JM, Shinohara, MM, Segerson, TP, Westbrook, GL. 1997. Cloning and expression of rat metabotropic glutamate receptor 8 reveals a distinct pharmacological profile. Mol. Pharmacol, 51, 119–125.

Schrader, LA, Tasker, JG. 1997. Presynaptic modulation by metabotropic glutamate receptors of excitatory and inhibitory synaptic inputs to hypothalamic magnocellular neurons. J. Neurophysiol, 77, 527–536.

Schweitzer, J. & Driever, W. (2009) Development of the dopamine systems in zebrafish. Adv. Exp. Med. Biol., 651, 1–14.

Sen, M, Gleason, E. 2006. Immunolocalization of metabotropic glutamate receptors 1 and 5 in the synaptic layers of the chicken retina. Vis Neurosci, 23, 221–231.

Shigemoto, R, Nakanishi, S, Mizuno, N. 1992. Distribution of the mRNA for a metabotropic glutamate receptor (mGluR1) in the central nervous system: an in situ hybridization study in adult and developing rat. J. Comp. Neurol., 322, 121–135.

Shigemoto, R, Nomura, S, Ohishi, H, Sugihara, H, Nakanishi, S, Mizuno, N. 1993. Immunohistochemical localization of a metabotropic glutamate receptor, mGluR5, in the rat brain. Neurosci. Lett., 163, 53–57.

Silva, GA, Theriault, E, Mills, LR, Pennefather, PS, Feeney, CJ. 1999. Group I and II metabotropic glutamate receptor expression in cultured rat spinal cord astrocytes. Neurosci. Lett, 263, 117–120.

Tasca, CI, Vendite, D, Martini, LH, Cardoso, LF, Souza, DO. 1995. Modulation of adenosine-induced cAMP accumulation via metabotropic glutamate receptors in chick optic tectum. Neurochem. Res, 20, 1033–1039.

Thisse, C, Thisse, B. 2008. High-resolution in situ hybridization to whole-mount zebrafish embryos. Nat Protoc, 3, 59–69.

Thoreson, WB, Witkovsky, P. 1999. Glutamate receptors and circuits in the vertebrate retina. Prog Retin Eye Res, 18, 765–810.

Ueda, Y, Iwakabe, H, Masu, M, Suzuki, M, Nakanishi, S. 1997. The mGluR6 5' upstream transgene sequence directs a cell-specific and developmentally regulated expression in retinal rod and ON-type cone bipolar cells. J Neurosci, 17, 3014–3023.

van den Pol, AN, Romano, C, Ghosh, P. 1995. Metabotropic glutamate receptor mGluR5 subcellular distribution and developmental expression in hypothalamus. J. Comp. Neurol, 362, 134–150.

van Keuren-Jensen, K, Cline, HT. 2006. Visual experience regulates metabotropic glutamate receptor-mediated plasticity of AMPA receptor synaptic transmission by homer1a induction. J. Neurosci, 26, 7575–7580.

Vardi, N, Duvoisin, R, Wu, G, Sterling, P. 2000. Localization of mGluR6 to dendrites of ON bipolar cells in primate retina. J Comp Neurol, 423, 402–412.

Vardi, N, Morigiwa, K. 1997. ON cone bipolar cells in rat express the metabotropic receptor mGluR6. Vis Neurosci, 14, 789–794.

Vardi, T, Fina, M, Zhang, L, Dhingra, A, Vardi, N. 2011. mGluR6 transcripts in non-neuronal tissues. J. Histochem. Cytochem., 59, 1076–1086.

Watanabe, D, Nakanishi, S. 2003. mGluR2 postsynaptically senses granule cell inputs at Golgi cell synapses. Neuron, 39, 821–829.

Wersinger, E, Schwab, Y, Sahel, JA, Rendon, A, Pow, DV, Picaud, S, Roux, MJ. 2006. The glutamate transporter EAAT5 works as a presynaptic receptor in mouse rod bipolar cells. J Physiol, 577, 221–234.

Westerfield, M. 2000. The zebrafish book. A guide for the laboratory use of zebrafish (Danio rerio). 4th ed., Univ. of Oregon Press, Eugene.

Wullimann, MF, Mueller, T. 2004a. Identification and morphogenesis of the eminentia thalami in the zebrafish. J. Comp. Neurol, 471, 37–48.

Wullimann, MF, Mueller, T. 2004b. Teleostean and mammalian forebrains contrasted: Evidence from genes to behavior. J. Comp. Neurol., 475, 143–162.

Wullimann, MF, Rupp, B, Reichert, H. 1996. Neuroanatomy of the Zebrafish Brain: A Topological Atlas, Birkhäuser.Yamamoto, K, Ruuskanen, JO, Wullimann, MF, Vernier, P. 2011. Differential expression of dopaminergic cell markers in the adult zebrafish forebrain. J. Comp. Neurol, 519, 576–598.

Zhang, C, Schmidt, JT. 1999. Adenosine A1 and class II metabotropic glutamate receptors mediate shared presynaptic inhibition of retinotectal transmission. J. Neurophysiol., 82, 2947–2955.

Zhang, C-S, Bertaso, F, Eulenburg, V, Lerner-Natoli, M, Herin, GA, Bauer, L, Bockaert, J, Fagni, L, Betz, H, and Scheschonka, A. 2008. Knock-in mice lacking the PDZ-ligand motif of mGluR7a show impaired PKC-dependent autoinhibition of glutamate release, spatial working memory deficits, and increased susceptibility to pentylenetetrazol. J. Neurosci, 28, 8604–8614.

Zhu, L, Strata, P, Andjus, PR. 2005. Pharmacology of the metabotropic glutamate receptor mediated current at the climbing fiber to Purkinje cell synapse. Prog. Brain Res, 148, 299–306.

Chapter 3

Novel Expression Patterns of mGluR6 in the Zebrafish Nervous System

Marion F. Haug*[1], Matthias Gesemann*[1], Ying-Yu Huang*[1†], Stephan C. F. Neuhauss[1δ]

[1]Institute of Molecular Life Sciences, University of Zurich, Winterthurerstrasse 190, 8057 Zurich, Switzerland

[†]present address: Neurology Department, University Hospital Zurich, Frauenklinikstrasse 26, 8091 Zurich, Switzerland

* these authors contributed equally to this work

[δ] corresponding author

Article published in *PloS ONE*

Personal contribution:

cloning, sequence analysis and *in situ* hybridization of *mglur6* and *gnao* paralogs, immunehistochemical analysis, ERG recordings, writing of the corresponding methods sections, preparation of figures 2, 3, and 4 and supplemental figures 1 and 2 and writing of the corresponding legends, editing of the manuscript

OPEN ACCESS Freely available online PLoS one

Novel Expression Patterns of Metabotropic Glutamate Receptor 6 in the Zebrafish Nervous System

Ying-Yu Huang[◑¤], Marion F. Haug[◑], Matthias Gesemann[◑], Stephan C. F. Neuhauss*

Institute of Molecular Life Sciences, Neuroscience Center Zürich and Center for Integrative Human Physiology, University of Zürich, Zürich, Switzerland

Abstract

The metabotropic glutamate receptor 6 (mGluR6 or GRM6) belongs to the class III of the metabotropic glutamate receptor family. It is the only known mGluR that mediates direct synaptic transmission in the nervous system and is thought to mediate the ON-response in the ON-pathway of the vertebrate retina. Phylogenetic and gene structure analysis indicated that the zebrafish genome harbours two *mglur6* paralogs, *mglur6a* and *mglur6b*. Besides expression in the inner nuclear layer and distinct regions in the brain, both *mglur6* paralogs are expressed in ganglion cells of the retina, an expression pattern which can also be observed in the downstream effector molecules gnaoa and gnaob. This unexpected expression pattern is consistent with immunohistological labeling using a peptide antibody specific for the mGluR6b paralog. These expression patterns contradict the existing view that mGluR6 is solely located on ON-bipolar cells where it functions in signal transmission. Consistent with expression in ON-bipolar cells, we report a decreased b-wave amplitude in the electroretinogram after morpholino-based downregulation of mGluR6b, showing a function in the ON response. Our data suggest more widespread functions of mGluR6 mediated signaling in the central nervous system, possibly including sign reversing synapses in the inner retina.

Citation: Huang Y-Y, Haug MF, Gesemann M, Neuhauss SCF (2012) Novel Expression Patterns of Metabotropic Glutamate Receptor 6 in the Zebrafish Nervous System. PLoS ONE 7(4): e35256. doi:10.1371/journal.pone.0035256

Editor: Olivier Jacques Manzoni, Institut National de la Santé et de la Recherche Médicale, France

Received November 1, 2011; **Accepted** March 14, 2012; **Published** April 16, 2012

Funding: This study was partially funded by EU framework7 projects RETICIRC and ZF-HEALTH and the Swiss National Science Foundation (31003A_135598/1). The funders had no role in study design, data collection and analysis, decision to publish, or preparation of the manuscript.

Competing Interests: The authors have declared that no competing interests exist.

* E-mail: stephan.neuhauss@imls.uzh.ch

◑ These authors contributed equally to this work.

¤ Current address: Neurology Department, University Hospital Zürich, Zürich, Switzerland

Introduction

Like in other parts of the central nervous system, glutamate is known to be the major excitatory neurotransmitter in the vertebrate retina. The main types of neurons in the retina that use glutamate as a neurotransmitter are photoreceptors (rods and cones), bipolar cells (ON and OFF types), and ganglion cells. These cells form the vertical pathway to convey visual information from the retina to the brain, specifically from photoreceptors via bipolar cells to ganglion cells. Both rod and cone photoreceptors tonically release glutamate in darkness. Upon light exposure they hyperpolarize due to the closure of cation channels leading to a light dependent reduction of glutamate release.

Already at the first visual synapse this signal is parceled into two parallel streams of information: the ON-pathway that is activated by an increase in light (decrease in glutamate) and the OFF-pathway that in turn is activated by a decrease in light (increase in glutamate). Consequently bipolar cells of these two pathways express different glutamate receptors.

The OFF-response is mediated by non-NMDA (AMPA/kainate) ionotropic glutamate receptors expressed on OFF-bipolar cells [1]. This sign-conserving synaptic transmission functions similar to many other excitatory synapses of the central nervous system. In contrast, ON-bipolar cells mediate a sign-reversed signal by being hyperpolarized by glutamate. The glutamate analog 2-amino-4-phosphonobutyric acid (L-AP4 or APB), an agonist to group III metabotropic glutamate receptors, was first discovered as an agonist for ON-bipolar cells [2,3]. Intracellular electrophysiological recordings demonstrated that APB selectively blocks the light response of ON-bipolar cells in the mudpuppy [3] and rabbit [4] retina, mimicking glutamate release in darkness. Subsequent studies identified the metabotropic glutamate receptor 6 (mGluR6) as the receptor mediating the ON-response. In mammals this receptor is exclusively expressed on the dendrites of ON-bipolar cells [5], where it interacts with the effector G protein Goα [6,7]. Consistently, genetic inactivation of mGluR6 in mice blocks the ON-response [8]. In humans, mutations in the mGluR6 gene (GRM6) have been linked to congenital stationary night blindness, characterized in the electroretinogram by the absence of an ON response [9,10].

Upon glutamate binding, these APB-sensitive receptors close cation channels, causing the cells to hyperpolarize [11]. Recently, at least one of these channels has been identified as the transient receptor potential channel M1 (TrpM1) [12,13,14].

In the present study we report the identification of two *mglur6* paralogs in the zebrafish genome. The true identity of the two *mglur6* orthologs were confirmed by sequence alignment, genomic structure, and phylogenetic analysis. Subsequent expression studies identified *mglur6* and *gnao* (the gene coding for Goα) expression in the inner nuclear layer, and more surprisingly, strong expression in ganglion cells in both, larval and adult retinas. We confirmed this unexpected finding by immunohistochemistry using

a paralog specific peptide antibody against mGluR6b. These data suggest the exciting and unexpected possibility that sign reversing synapses are also present in the inner retina, in addition to the well described role in the outer retina. Indeed, morpholino antisense based knockdown of mGluR6b leads to a reduction in the ON response recorded in the electroretinogram, consistent with findings in other organisms. Additionally, we also found expression in confined brain regions, suggesting a novel, so far unappreciated, role of mGluR6 signaling in retinal ganglion cells and other parts of the brain.

Results and Discussion

Molecular cloning and identification of zebrafish metabotropic glutamate receptor type 6

The high sequence homology between class III metabotropic glutamate receptors (*mglur4*, *mglur6*, *mglur7* and *mglur8*) makes it a challenging task to unequivocally identify the true zebrafish *mglur6* ortholog. We identified and manually annotated six unique sequences in the zebrafish genome that clearly belong to class III metabotropic glutamate receptors. On the protein level the identity between these sequences ranged from 71 to 89% (Table 1). In order to assign these sequences to the various members of the subgroup, we performed a phylogenetic analysis using these sequences with the published sequences of the mouse and human group III orthologs (Figure 1A). In this way we identified one zebrafish *mglur4* and *mglur7* ortholog each, while *mglur6* and *mglur8* have two paralogous genes per mammalian ortholog. These paralogs reside on different chromosomes and are likely remnant of the teleost specific genome duplication event [26,27]. We gained further support for the correct assignment of *mglur6* sequences by comparing the genomic structure of the class III genes. Interestingly, with the exception of *mglur6*, the length of exon 8 is 936 bp in all class III *mglur* genes. However, in *mglur6* this exon is split into two exons. The length of these two split exons add up to yield the conserved length of exon 8 (Figure 1B). Hence this exonal split likely predates the origin of vertebrates about 500 million years ago.

Embryonic and adult gene expression of zebrafish *mglur6a* and *mglur6b*

Surprisingly, both *mglur6* paralogs revealed a predominant expression in the ganglion cell layer (GCL) in larval (Figure 2A3, B3) as well as in adult fish (Figure 2A4, B4). Moreover, both larval and adult retinas, expressed small amounts of *mglur6a* and *-6b* RNA in the proximal inner nuclear layer (INL) close to the inner plexiform layer (IPL) (arrow, Figure 2A3, A4, B3, B4). An additional expression in the medial INL is visible in retinas stained with the *mglur6b* riboprobe (arrowhead, Figure 2B3, B4), however, *mglur6a* expression in this layer seems to be restricted to adult fish (arrowhead, Figure 2A4).

In order to additionally confirm these results and localize the encoded protein, we raised paralog specific polyclonal antibodies against mGluR6b. We detected mGluR6b immunoreactivity in the outer plexiform layer and in both ON-and OFF-layer of the IPL. Additionally, single cells adjacent to the IPL in both INL and GCL were labeled with the mGluR6b antibody (Figure 3A). In the adult retina we found a similar expression with the exception that we did not see labeled cells in the GCL (Figure 3B). In order to confirm the postsynaptic localization of mGluR6b protein in the OPL, we co-stained adult retinal sections with antibodies against mGluR6b and the presynaptic marker SV2 (Figure 3C). Finally, we performed a fluorescent *in situ* hybridization on sections with PKCalpha immunolabeled ON-bipolar cells, to additionally confirm the expression of *mglur6b* in ON-bipolar cells (Figure 3D).

These results contrast with most studies in other vertebrates that find mGluR6 exclusively expressed in ON-bipolar cells [5,28,29]. However, few studies report *mglur6* expression in juvenile and regenerating rat retinal ganglion cells [30]. Recently, the expression of mGluR6 mRNA in some human ganglion cells has been reported [31].

There is good physiological evidence that the ON-response of the rod pathway [32,33] and to a lesser extent also the cone ON-pathway [33,34] is mediated at least partially by mGluR6 signaling in the zebrafish.

In order to demonstrate a role of mGluR6b in mediating the cone ON-response, we downregulated mGluR6b by morpholino antisense injections. We found a concentration dependent reduction of the ERG b-wave, confirming a role of mGluR6b in mediating the cone ON-response, since at this stage (5 dpf) most if not all of the visual response is cone mediated. We verified the efficiency of our knockdown by showing a concomitant loss of immunohistochemical staining (Figure S1). Since we recorded a small b-wave at the highest non-toxic concentrations where all mGluR6b protein staining was abolished, we suggest that at least one other glutamate receptor system may be involved in the cone ON response in the zebrafish. The mGluR6a paralog may mediate this remaining ON response, but we deem it more likely that a mGluR6 independent pathway accounts for part of the ON response.

At least in lower vertebrates there is good evidence that the cone ON- response is predominantly mediated by an excitatory amino acid transporter (EAAT) mediated mechanism [33,35,36].

The strong expression of both *mglur6* paralogs in the ganglion cell layer during larval and adult stages implies an additional function of mGluR6 signaling cascade in this cell layer. In order to find supportive evidence for this unexpected result, we cloned the downstream effector G protein Goα subunit, which is part of the mGluR6 signaling cascade [6,7]. We identified the two zebrafish paralogs *gnaoa* and *gnaob* whose expression pattern in the retina is very similar to the *mglur6* paralogs. The retinal location of *gnaoa* in larval and adult zebrafish (Figure 2C3, C4) is similar to the expression of *mglur6a*, whereas *gnaob* is located in the medial INL already in larval fish (Figure 2D3) – comparable to *mglur6b*. Like the *mglur6* paralogs, both *gnao* paralogs were expressed in retinal ganglion cells (Figure 2C3, C4, D3, D4). These results are interesting in the context of nyctalopin. This enigmatic protein is directly involved in the mGluR6 signaling cascade and likely interacts with both mGluR6 and TrpM1 protein [37]. Consistent with the presence of a functional mGluR6 signaling cascade, we found *nyctalopin* expression in larval and adult retinal ganglion cell layer ([38] and Edda Kastenhuber, personal communication). Interestingly a transgenic zebrafish line expressing yellow fluorescent protein under the control of about 1.5 kb upstream of the start codon of the *nyctalopin* gene lacks expression in ganglion cells [39]. Presumably regulatory regions needed for retinal ganglion cell expression are located farther away from the coding sequence.

Equally surprising, we found *mglur6* expression outside of the retina. The larval zebrafish brain shows *mglur6a* labeling in the habenula (Ha), medial and lateral tectum opticum (TeO, lTeO), midbrain (mb), mid-hindbrain boundary (mhb) and in a bilateral nucleus of the medulla oblongata (MO, Figure 2A1, A2). *mglur6b* expression in the larval brain is confined to the olfactory bulb (OB, Figure 2B1, B2) and a part of the diencephalon (di, Figure 2B1, B2). These results point to the exciting possibility of more widespread use of mGluR6 signaling, potentially in sign reversing synapses, not only in the inner retina but also in the central

Table 1. Pairwise alignment of protein sequences of human (hs), and zebrafish (dr) class III mGluRs.

mGluR4_dr	mGluR6_hs	mGluR6a_dr	mGluR6b_dr	mGluR7_hs	mGluR7_dr	mGluR8_hs	mGluR8a_dr	mGluR8b_dr	
81 (90)	**71** (83)	**72** (85)	**73** (85)	**71** (85)	**70** (85)	**77** (87)	**74** (85)	**75** (85)	**mGluR4_hs**
	69 (83)	**72** (85)	**72** (84)	**70** (83)	**71** (84)	**76** (85)	**74** (85)	**74** (85)	**mGluR4_dr**
		75 (86)	**76** (87)	**68** (83)	**69** (83)	**72** (83)	**71** (83)	**71** (83)	**mGluR6_hs**
			87 (95)	**73** (88)	**73** (87)	**75** (87)	**74** (86)	**73** (87)	**mGluR6a_dr**
				73 (87)	**73** (86)	**74** (86)	**73** (86)	**73** (86)	**mGluR6b_dr**
					83 (91)	**76** (87)	**73** (86)	**73** (86)	**mGluR7_hs**
						74 (85)	**73** (86)	**71** (85)	**mGluR7_dr**
							85 (92)	**83** (92)	**mGluR8_hs**
								89 (94)	**mGluR8a_dr**

The percentage of identical amino acids between sequences is given in bold numbers, whereas the percentage of conserved amino acids is given in parenthesis. Conservation between orthologs is emboldened.

doi:10.1371/journal.pone.0035256.t001

nervous system in general. This hypothesis is substantiated by the expression of Gαo in these brain regions.

In future experiments, it will be important to follow up these findings in the mammalian brain, where so far there are only two reports on the expression of *mglur6* outside of the retina [40,41].

In conclusion, we have identified two paralogous *mglur6* genes in the zebrafish genome. Apart from expression in the inner nuclear layer of the retina, we found strong expression in retinal ganglion cells and in other parts of the brain, suggesting a more widespread use of the mGluR6 signaling cascade in the central nervous system.

Materials and Methods

Fish Maintenance and breeding

Fish were maintained and bred as previously described [15] and kept under a 14 h/10 h light/dark cycle. The wild-type strain used for all studies was WIK. Embryos were raised at 28°C in E3 medium and staged according to development in days post fertilization (dpf). All examinations were performed in accordance with the ARVO Statement for the Use of Animals in Ophthalmic and Vision Research and were approved by the local authorities (Veterinäramt Zürich TV4206).

Cloning of *mglur6* and *gnao* paralogs

Total mRNA was isolated using the QIAShredder and the RNeasy kit (Qiagen, Hombrechtikon, Switzerland) from about 50 larvae at 5 days post-fertilization (dpf) and reversed transcribed to single strand cDNA using oligo-dT primer (First Strand Kit; Stratagene, La Jolla, CA). Polymerase chain reaction (PCR) was performed with Taq polymerase (Taq Gold; Applied Biosystems, Switzerland) using sequence specific oligonucleotide primers. Amplified DNA pieces were subcloned into TOPO pCRII vectors (Invitrogen, Basel, Switzerland) and sequenced.

Annotation of *mglur* cDNAs

As gene predictions within GeneBank are produced by automated processes which have been shown to contain numerous errors, mGluR cDNA sequences used in this study were manually annotated. Sequences were identified and annotated using combined information from expressed sequence tags and genome databases (GeneBank, http://www.ncbi.nlm.nih.gov; Ensembl, http://www.ensembl.org/index.html; version 50/51, 2008). Human and mouse sequences were used as initial query (for more details on sequence annotation see [16]).

Phylogenetic tree analysis

The EditSeq software (Lasergene; DNASTAR, Madison, WI, USA) was used to translate the coding sequences of *mglur* genes into amino acid sequences and the obtained protein sequences were used to generate a combined sequence file in FASTA format. Sequence alignment and phylogenetic analysis was performed on the Phylogeny.fr platform ([17]; http://www.phylogeny.fr/version2_cgi/phylogeny.cgi). Sequences were aligned using muscle (v3.7; [18]) configured for highest accuracy (muscle with default settings). After alignment, ambiguous regions (i.e. containing gaps and/or being poorly aligned) were removed with Gblocks (v0.91b; [19]). The phylogenetic tree was reconstructed by the maximum likelihood method [20], 2003) using the WAG amino acid replacement matrix [21] implemented in the PhyML program (v3.0). The approximate likelihood ratio test (aLRT; [22]) was used to judge branch reliability. Graphical representation and editing of the phylogenetic tree was done using TreeDyn (v198.3) and the obtained svg files were colored using the CorelDraw program.

Whole mount and transverse cross sections *in situ* hybridization

Sequence-confirmed cDNA clones were used as templates for *in vitro* transcription to produce RNA probes for DIG (digoxigenin labeled) *in situ* hybridization (Roche Diagnostics, Rotkreuz, Switzerland). The used riboprobes spanned the following regions (base pairs counted from the ATG): *mglur6a*: 1345–2425, *mglur6b*: −10–1676, *gnaoa*: 410–1335 or 2221 and *gnaob*: 191–1192 or 193–2059. Sense and antisense RNA probes were synthesized by Sp6 and T7 RNA polymerase (Roche). RNA probes were hydrolyzed to yield fragments of about 300–500 nucleotides in length. Whole-mount *in situ* hybridization was performed on 3 µM PTU (1-phenyl-2-thiourea, Sigma, St. Louis, MO, USA) - treated WIK wild-type larvae. They were collected at 5 dpf, anesthetized on ice, and immediately fixed in 4% paraformaldehyde (PFA) in phosphate buffered saline (PBS, freshly prepared, pH 7.4) over night at 4°C. Whole mount *in situ* hybridization was performed according to Thisse and Thisse [23] with minor modifications: 5-day-old fish were treated with proteinase K (10 µg/ml) for 75 min. From day two on TNT (100 mM Tris HCl pH 7.5, 150 mM NaCl, 0.5% Tween 20) was used for all

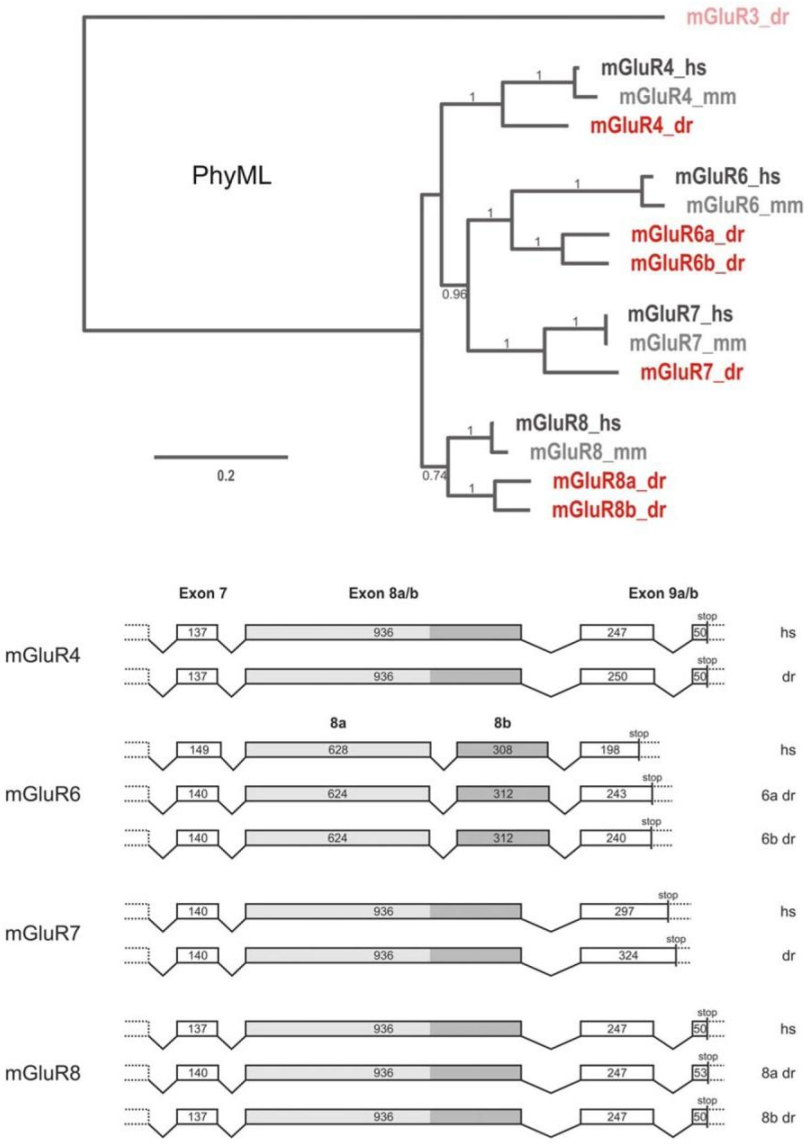

Figure 1. Phylogenetic Reconstruction of mGluR class III genes. *mGluR* sequences of class III metapotropic glutamate receptors of the following species were used in phylogenetic reconstructions (hs = *Homo sapiens*; mm = *Mus musculus* and dr = *Danio rerio*). Sequences were aligned using MUSCLE. A conserved stretch of 746 amino acids determined by the program Gblocks was used for phylogenetic reconstruction. The phylogenetic tree was build using the maximum likelihood method with the WAG amino acid replacement matrix. LRT values above 0.5 are shown. While zebrafish *mglurs* are shown in dark red, mouse *mGluRs* are given in light gray and human mGluRs in dark gray. The genomic organization of mGluR6 differs from other class III *mGluRs*. Analysis of the last exons within the *class III mGluRs* reveals an exon split and a reduced coding sequence length in mGluR6. While the first 7 exons within the class III mGluR subfamily are highly conserved in length, the 936 bp exon 8 found in mGluR4, mGluR7 and mGluR8 is split in mGluR6 (628 bp+308 bp). Moreover the sequence length following the split exons is significantly reduced. Human and zebrafish sequence identity is indicated.
doi:10.1371/journal.pone.0035256.g001

washing steps instead of PBT (PBS, 0.1% Tween 20). AP-conjugated anti-DIG antibodies (Roche) were diluted 1:5000 in blocking solution (Roche) in TNT. The staining was stopped with PBT and the larvae were postfixed in 4% PFA in PBS ON at 4°C. Subsequently, larvae were mounted on an adapted glass slide in 100% glycerol (Sigma) and imaged with an Olympus BX61 microscope using a color camera (ColorView IIIu, Soft Imaging System, Olympus). For obtaining cross sections of adult eyes, the eyecups were dissected and, similar to larval fish, fixed over night in 4% PFA at 4°C. After washing twice with PBT for 5 min at RT, the eyes were placed in 30% sucrose and incubated ON at 4°C. Subsequently, the eyecups were embedded in cryomatrix (Tissue Tek O.C.T., Sakura, Zoeterwonde, NL), fast frozen with liquid N_2 and stored at −80°C until further use. 16 µm thick transverse sections were cut using a Microm microtome (HM 550), collected on glass slides, dried at 37°C

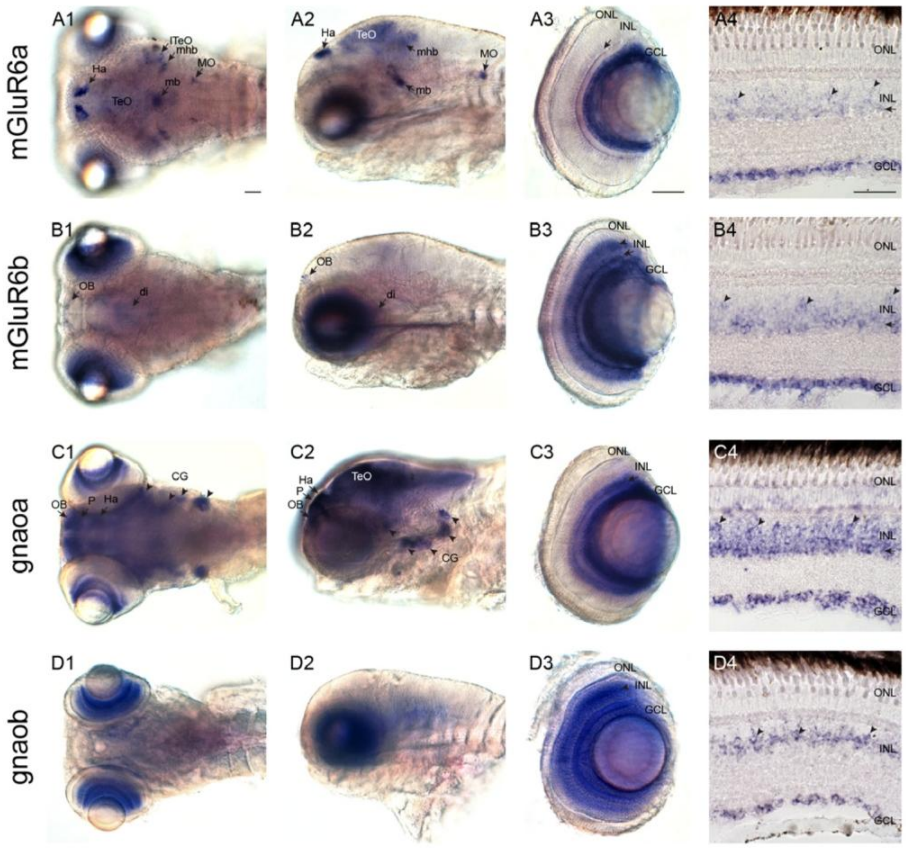

Figure 2. RNA expression of zebrafish *mglur6 and gnao* paralogs. RNA expression of *mglur6a* (A1–A4), *mglur6b* (B1–B4), *gnaoa* (C1–C4) and *gnaob* (D1–D4) in dorsal (1) and lateral (2) views and in isolated eyes (3) of a 5 dpf zebrafish, as well as in adult retinal cross-sections (4). **A1, A2:** Expression of *mglur6a* is visible in the habenula (Ha), the medial (TeO) and lateral (lTeO) tectum opticum, the midbrain (mb), a part of the mid-hindbrain boundary (mhb) and a bilateral nucleus of the medulla oblongata (MO). **A3:** In an eye separated from a whole mount stained larva *mglur6a* is expressed in the proximal inner nuclear layer (INL, arrow) and the ganglion cell layer (GCL). **A4:** Additional to the cellular expression in the proximal INL (arrows) and the GCL, *mglur6a* labels cells in the medial INL (arrowheads) in adult. **B1, B2:** *mglur6b* reveals a staining in the olfactory bulb (OB) and a weak labeling of a part of the diencephalon (di). **B3:** The isolated eye shows, *mglur6b* expression in the medial INL (arrowhead), the proximal INL (arrow) and the GCL. **B4:** The adult retinal cross section shows the same localization for *mglur6b* as the larval fish, however, the staining in the medial INL is restricted to a subset of cells (arrowheads). **C1, C2:** *gnaoa* is expressed in the olfactory bulb (OB), the pallium (P), the habenula (Ha), the tectum opticum (TeO) and in all cranial ganglia (CG, arrowheads). **C3:** The retina reveals *gnaoa* labeling in the proximal INL (arrow) and the GCL. **C4:** Similar to the larval retina, *gnaoa* labels the proximal INL (arrow) and the GCL in the adult retina. Additionally, *gnaoa* stains weakly a subset of cells in the medial INL (arrowheads). **D1, D2:** *gnaob* shows no expression in the brain. **D3:** The expression of *gnaob* in the larval fish eye is restricted to the medial INL (arrow) and the GCL. **D4:** Similar to the larval eye, in adult retinal cross-sections *gnaob* is located in cells of the medial INL and the GCL. All scale bars = 40 μm. Scale bar in A1 applies to all whole mount images, scale bar in A3 applies to A3, B3, C3 and D3, scale bar in A4 applies to A4, B4, C4 and D4.
doi:10.1371/journal.pone.0035256.g002

for 30 min and stored at −80°C until using them for *in situ* hybridization. *In situ* hybridization was done as described above for larval fish, but proteinase K permeabilization time was reduced to 2.5 min and PBT was used for the washing steps and to dissolve the blocking reagent on day 2. Finally, slides were cover-slipped with Kaiser's glycerol gelatine (Merck KGaA, Darmstadt, Germany) and images were taken with the bright field modus of a light microscope (Olympus BX61). For fluorescent *in situ* hybridization on adult eye sections, an incubation step in 1% H_2O_2 in PBT for 20 min prior to the blocking step was included to quench endogenous peroxidase activity. To detect the probe a 1:400 dilution of anti-DIG-POD antibody (Roche) was used. The next day, the slides were washed several times with PBT and incubated for 1 h in the dark at RT with the tyramide working solution (Invitrogen, TSA Kit *41, Alexa 555). For the subsequent immunostaining, slides were kept in darkness. After three additional washing steps in PBT, slides were treated as previously described [24] but blocking solution was applied for 1 h at RT. For the labeling of ON-bipolar cells we used the mouse anti-PCKalpha (MC5) antibody (Novus Biologicals, NB200-586; 1:500).

Generation of antibodies

For immunization, a peptide specific for mGluR6b has been chosen. Rabbits were immunized with the peptide **QKS**SD**KQNGETK**V**EPDRSQ** (889–905; amino acids in bold represent sequence identity with zebrafish mGluR6a). The mGluR6b antibody was affinitypurified against the respective peptide by Eurogentec (Eurogentec S.A., Seraing, Belgium).

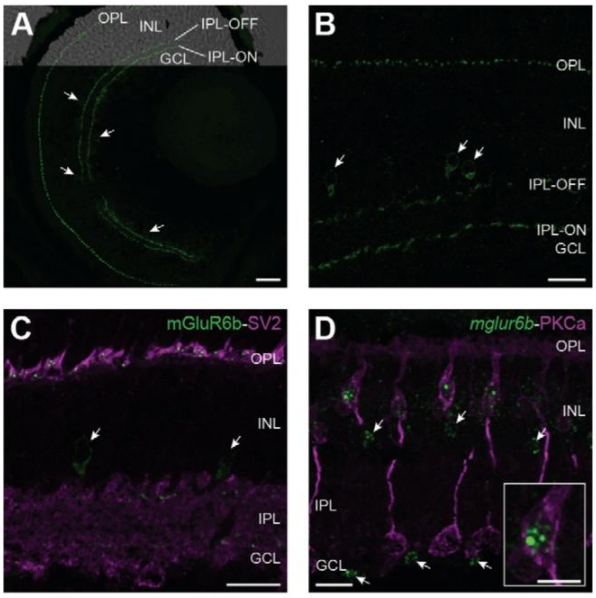

Figure 3. Subcellular localization of mGluR6b in the zebrafish retina. Z-projections of confocal image stacks of immunohistochemically labeled larval and adult retinal cross-sections. **A:** A larval retina at 5 dpf stained with the mGluR6b antibody shows labeling in the outer plexiform layer (OPL) and in an ON- and an OFF-layer of the inner plexiform layer (IPL). In addition, single cells adjacent to the IPL in the INL and the GCL (arrowheads) express mGluR6b as well. Scale bar = 20 μm. **B:** In the adult zebrafish retina, mGluR6b stains similar structures as in the larval retina with the exception that we could only detect labeled cells in the inner part of the INL (arrowhead) but not in the GCL. Scale bar = 15 μm. **C:** A doublelabeling of mGluR6b (green) and SV2 (magenta) in an adult retinal cross-section reveals the postsynaptic localization of mGluR6b in the OPL. Again, an mGluR6b expression in single cells of the proximal IPL is detected (arrows). Scale bar = 15 μm. **D:** Fluorescent *in situ* hybridization of *mglur6b* (green) combined with an immunohistochemical labeling of ON-bipolar cells by PKCalpha (magenta) confirms the localization of mGluR6b in ON-bipolar cells of the INL. Scale bar = 15 μm. Arrows point to cells of the proximal INL and the GCL expressing *mglur6b*. The insert shows a close up of an ON-bipolar cell body and its fluorescent *mglur6b* signal in the cytosol. Scale bar = 5 μm.
doi:10.1371/journal.pone.0035256.g003

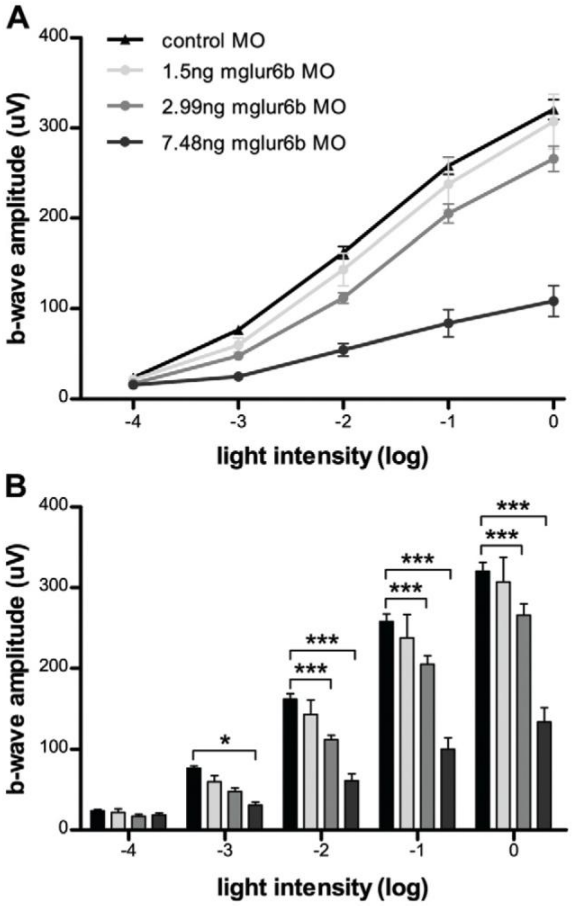

Figure 4. Electroretinogram recordings of *mglur6b*-depleted zebrafish larvae. The downregulation of mGluR6b leads to a dose dependent decrease of the ERG b-wave in 5 day old zebrafish larvae indicating a diminished ON-response. **A:** Plotted b-wave amplitudes at different light intensities. Control Morpholino (MO) injected larvae of different concentrations showed no significant differences in b-wave amplitude, neither among each other nor in comparison to uninjected wild type larvae (data not shown). Therefore, recordings of all control MO larvae (n = 46) were taken together to build one curve. Injection of *mglur6b* MO leads to a dose dependent depletion of the b-wave (1.5 ng *mglur6b* MO: n = 14; 2.99 ng MO: n = 24; 7.48 ng MO: n = 13). All data points represent the means ± SEM. **B:** Significance of the b-wave amplitude reduction was calculated using a 2-way ANOVA (* = $p<0.1$; ** = $p<0.01$; *** = $p<0.001$).
doi:10.1371/journal.pone.0035256.g004

Immunohistochemistry

Immunohistological staining was performed as previously described [24], however, blocking solution was only applied for 1 h at RT.

To increase specificity, the rabbit anti-mGluR6b antibody was cross-absorbed against the respective mGluR6a epitope using CNBr-activated sepharose (4B, GE Healthcare, Little Chalfont, UK) and the increased specificity was tested on dot-blots (Figure S2). The final concentration of the cross-absorbed rabbit anti-mGluR6b antibody on the sections was 1:150. Doublelabelings were performed with mouse anti-synaptic vesicle 2 (SV2; 1:100; DSHB, Iowa, USA). Pictures were taken with a Leica confocal microscope (Leica SP5, Leica Microsystems GmbH, Wetzlar, Germany). Confocal z-stacks were analyzed by using Imaris (Bitplane, Zürich, Switzerland).

Targeted gene knockdown (Morpholino)

The specific downregulation of *mglur6b* was accomplished by the injection of an antisense morpholino oligonucleotide (MOs; Gene Tools, Philomath, Oregon, USA) designed against the translational start site (5′-TGTGATGTCATAGTTGCTGGCATTC-3′). As a control, a standard MO (5′-CCTCTTACCTCAGTTACAATTTATA-3′) was used. Prior to use, both MOs were dissolved in ddH_20 to a stock concentration of 2 mM and stored at −20°C. To obtain a working solution, MOs were diluted in PBS pH 7.4 containing 0.2% phenol red to the desired concentration. Embryos were injected in the one-cell stage with the given concentrations (see Figure 4).

Electroretinogram

Electroretinogram (ERG) recordings were performed as previously described [25]. Before the recordings, larvae were dark adapted for at least 30 min. Stimuli of 100 ms with an interstimulus interval of 5 s were applied to elicit a response.

The light stimulus intensity was 6800 lux or 72 W/m^2 (for log 0). The measurement series started with the lowest light intensity (log −4).

Statistical analysis was performed in GraphPad Prism 5 (GraphPad Software, La Jolla, CA, USA).

Supporting Information

Figure S1 mGluR6b expression in the *mglur6b*-depleted zebrafish retina at 5 dpf. Immunohistochemical analysis using the mGluR6b antibody confirms the downregulation of mGluR6b in the 5 dpf zebrafish retina. **A:** mGluR6b expression in a non-injected sibling. **B:** Injection of 2.5 ng *mglur6b* MO leads to an incomplete downregulation of the mGluR6b protein since a faint staining in the plexiform layers is still visible. **C:** 6.7 ng mglur6b antisense-RNA lead to a complete knockdown of the mGluR6b protein in 5 dpf zebrafish retinas. Scale bar (applies for all images A–C) = 20 µm.
(TIF)

Figure S2 Cross-absorbance of the mGluR6b antibody. **A:** Immunohistochemistry image of a cross section through a 5 day old larval retina stained with the original mGluR6b antibody (1:200). **B:** Confocal image of a larval retina at 5 dpf stained with the cross-absorbed mGluR6b antibody (1:150). For further description see Figure 3. Scale bar in B = 20 µm (applies for A and B). **C:** Dot-blot analysis showing the increased specificity of the cross-absorbed mGluR6b antibody. 1 µg of mGluR6a (6a) and mGluR6b (6b) epitopes were pipetted on nitrocellulose membranes (0.45 µm; Bio-Rad, Reinach, Switzerland) and incubated with the non cross-absorbed and the cross-absorbed antibodies. Following cross-absorbing the epitope of the mGluR6a is not recognized anymore.
(TIF)

Acknowledgments

We thank Kara Dannenhauer for excellent fish care.

Author Contributions

Conceived and designed the experiments: SCFN. Performed the experiments: MFH YYH. Analyzed the data: MFH MG YYH SCFN. Contributed reagents/materials/analysis tools: MG SCFN. Wrote the paper: SCFN.

References

1. DeVries SH (2000) Bipolar cells use kainate and AMPA receptors to filter visual information into separate channels. Neuron 28: 847–856.
2. Shiells RA, Falk G, Naghshineh S (1981) Action of glutamate and aspartate analogues on rod horizontal and bipolar cells. Nature 294: 592–594.
3. Slaughter MM, Miller RF (1981) 2-amino-4-phosphonobutyric acid: a new pharmacological tool for retina research. Science 211: 182–185.
4. Massey SC, Redburn DA, Crawford ML (1983) The effects of 2-amino-4-phosphonobutyric acid (APB) on the ERG and ganglion cell discharge of rabbit retina. Vision Res 23: 1607–1613.
5. Nomura A, Shigemoto R, Nakamura Y, Okamoto N, Mizuno N, et al. (1994) Developmentally regulated postsynaptic localization of a metabotropic glutamate receptor in rat rod bipolar cells. Cell 77: 361–369.
6. Dhingra A, Lyubarsky A, Jiang M, Pugh EN, Jr., Birnbaumer L, et al. (2000) The light response of ON bipolar neurons requires G[alpha]o. J Neurosci 20: 9053–9058.
7. Nawy S (1999) The metabotropic receptor mGluR6 may signal through G(o), but not phosphodiesterase, in retinal bipolar cells. J Neurosci 19: 2938–2944.
8. Masu M, Iwakabe H, Tagawa Y, Miyoshi T, Yamashita M, et al. (1995) Specific deficit of the ON response in visual transmission by targeted disruption of the mGluR6 gene. Cell 80: 757–765.
9. Dryja TP, McGee TL, Berson EL, Fishman GA, Sandberg MA, et al. (2005) Night blindness and abnormal cone electroretinogram ON responses in patients with mutations in the GRM6 gene encoding mGluR6. Proc Natl Acad Sci U S A 102: 4884–4889.
10. Zeitz C, van Genderen M, Neidhardt J, Luhmann UF, Hoeben F, et al. (2005) Mutations in GRM6 cause autosomal recessive congenital stationary night blindness with a distinctive scotopic 15-Hz flicker electroretinogram. Invest Ophthalmol Vis Sci 46: 4328–4335.
11. Nawy S, Jahr CE (1990) Suppression by glutamate of cGMP-activated conductance in retinal bipolar cells. Nature 346: 269–271.
12. Koike C, Obara T, Uriu Y, Numata T, Sanuki R, et al. (2010) TRPM1 is a component of the retinal ON bipolar cell transduction channel in the mGluR6 cascade. Proc Natl Acad Sci U S A 107: 332–337.
13. Morgans CW, Zhang J, Jeffrey BG, Nelson SM, Burke NS, et al. (2009) TRPM1 is required for the depolarizing light response in retinal ON-bipolar cells. Proc Natl Acad Sci U S A 106: 19174–19178.
14. Shen Y, Heimel JA, Kamermans M, Peachey NS, Gregg RG, et al. (2009) A transient receptor potential-like channel mediates synaptic transmission in rod bipolar cells. J Neurosci 29: 6088–6093.
15. Mullins MC, Hammerschmidt M, Haffter P, Nusslein-Volhard C (1994) Large-scale mutagenesis in the zebrafish: in search of genes controlling development in a vertebrate. Curr Biol 4: 189–202.
16. Gesemann M, Lesslauer A, Maurer CM, Schonthaler HB, Neuhauss SC (2010) Phylogenetic analysis of the vertebrate excitatory/neutral amino acid transporter (SLC1/EAAT) family reveals lineage specific subfamilies. BMC Evol Biol 10: 117.
17. Dereeper A, Guignon V, Blanc G, Audic S, Buffet S, et al. (2008) Phylogeny.fr: robust phylogenetic analysis for the non-specialist. Nucleic Acids Res 36: W465–469.
18. Edgar RC (2004) MUSCLE: a multiple sequence alignment method with reduced time and space complexity. BMC Bioinformatics 5: 113.
19. Castresana J (2000) Selection of conserved blocks from multiple alignments for their use in phylogenetic analysis. Mol Biol Evol 17: 540–552.
20. Guindon S, Gascuel O (2003) A simple, fast, and accurate algorithm to estimate large phylogenies by maximum likelihood. Syst Biol 52: 696–704.
21. Whelan S, Goldman N (2001) A general empirical model of protein evolution derived from multiple protein families using a maximum-likelihood approach. Mol Biol Evol 18: 691–699.
22. Anisimova M, Gascuel O (2006) Approximate likelihood-ratio test for branches: A fast, accurate, and powerful alternative. Syst Biol 55: 539–552.
23. Thisse C, Thisse B (2008) High-resolution in situ hybridization to whole-mount zebrafish embryos. Nat Protoc 3: 59–69.
24. Fleisch VC, Schonthaler HB, von Lintig J, Neuhauss SC (2008) Subfunctionalization of a retinoid-binding protein provides evidence for two parallel visual cycles in the cone-dominant zebrafish retina. J Neurosci 28: 8208–8216.
25. Makhankov YV, Rinner O, Neuhauss SC (2004) An inexpensive device for non-invasive electroretinography in small aquatic vertebrates. J Neurosci Methods 135: 205–210.
26. Meyer A, Van de Peer Y (2005) From 2R to 3R: evidence for a fish-specific genome duplication (FSGD). Bioessays 27: 937–945.
27. Taylor JS, Braasch I, Frickey T, Meyer A, Van de Peer Y (2003) Genome duplication, a trait shared by 22000 species of ray-finned fish. Genome Res 13: 382–390.
28. Morgans CW, Brown RL, Duvoisin RM (2010) TRPM1: the endpoint of the mGluR6 signal transduction cascade in retinal ON-bipolar cells. Bioessays 32: 609–614.
29. Nakajima Y, Iwakabe H, Akazawa C, Nawa H, Shigemoto R, et al. (1993) Molecular characterization of a novel retinal metabotropic glutamate receptor mGluR6 with a high agonist selectivity for L-2-amino-4-phosphonobutyrate. J Biol Chem 268: 11868–11873.
30. Tehrani A, Wheeler-Schilling TH, Guenther E (2000) Coexpression patterns of mGLuR mRNAs in rat retinal ganglion cells: a single-cell RT-PCR study. Invest Ophthalmol Vis Sci 41: 314–319.
31. Klooster J, Blokker J, Ten Brink JB, Unmehopa U, Fluiter K, et al. (2011) Ultrastructural Localization and Expression of TRPM1 in the Human Retina. Invest Ophthalmol Vis Sci 52: 8356–8362.
32. Wong KY, Adolph AR, Dowling JE (2005) Retinal bipolar cell input mechanisms in giant danio. I. Electroretinographic analysis. J Neurophysiol 93: 84–93.
33. Wong KY, Cohen ED, Dowling JE (2005) Retinal bipolar cell input mechanisms in giant danio. II. Patch-clamp analysis of on bipolar cells. J Neurophysiol 93: 94–107.
34. Saszik S, Alexander A, Lawrence T, Bilotta J (2002) APB differentially affects the cone contributions to the zebrafish ERG. Vis Neurosci 19: 521–529.
35. Grant GB, Dowling JE (1995) A glutamate-activated chloride current in cone-driven ON bipolar cells of the white perch retina. J Neurosci 15: 3852–3862.
36. Wong KY, Gray J, Hayward CJ, Adolph AR, Dowling JE (2004) Glutamatergic mechanisms in the outer retina of larval zebrafish: analysis of electroretinogram b- and d-waves using a novel preparation. Zebrafish 1: 121–131.
37. Cao Y, Posokhova E, Martemyanov KA (2011) TRPM1 Forms Complexes with Nyctalopin In Vivo and Accumulates in Postsynaptic Compartment of ON-Bipolar Neurons in mGluR6-Dependent Manner. J Neurosci 31: 11521–11526.

Supporting Information

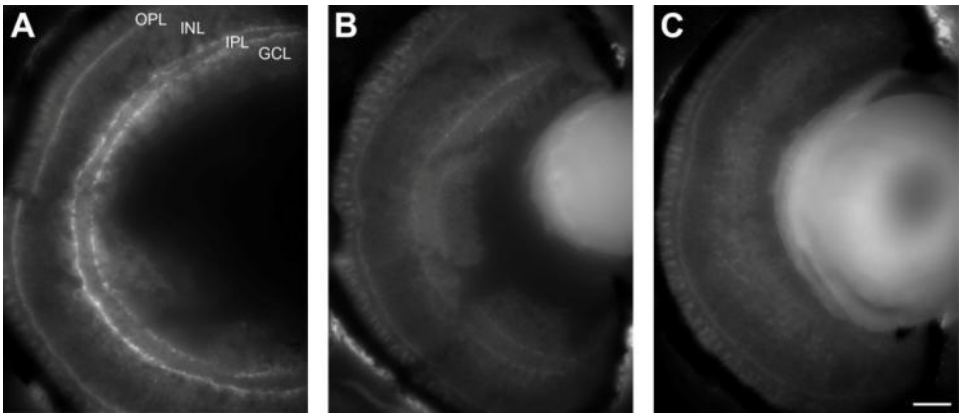

Figure S1: mGluR6 expression in the mglur6b-depleted zebrafish retina at 5 dpf
Immunohistochemical analysis using the mGluR6b antibody confirms the downregulation of mGluR6b in the 5 dpf zebrafish retina. ***A:*** *mGluR6b expression in a non-injected sibling.* ***B:*** *Injection of 2.5 ng mglur6b MO leads to an incomplete downregulation of the mGluR6b protein since a faint staining in the plexiform layers is still visible.* ***C:*** *6.7 ng mglur6b antisense-RNA lead to a complete knockdown of the mGluR6b protein in 5 dpf zebrafish retinas. Scale bar (applies for all images A-C) = 20 µm.*

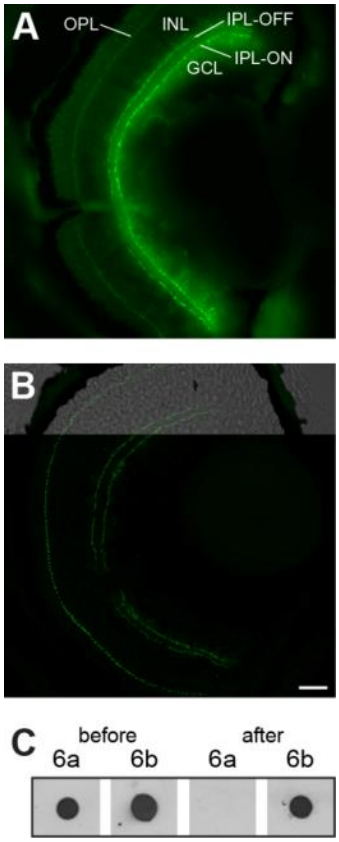

Figure S2: Cross-absorbance of the mGluR6b antibody
A: *Immunohistochemistry image of a cross section through a five-day-old larval retina stained with the original mGluR6b antibody (1:200).* ***B:*** *Confocal image of a larval retina at 5 dpf stained with the cross-absorbed mGluR6b antibody (1:150). For further description see Figure 3. Scale bar in B = 20 µm (applies for A and B).* ***C:*** *Dot-blot analysis showing the increased specificity of the cross-absorbed mGluR6b antibody. 1 µg of mGluR6a (6a) and mGluR6b (6b) epitopes were pipetted on nitrocellulose membranes (0.45 µm; Bio-Rad, Reinach, Switzerland) and incubated with the non cross-absorbed and the cross-absorbed antibodies. Following cross-absorbing the epitope of the mGluR6a is not recognized anymore.*

Chapter 4

Generation of the Zebrafish ON-Response

Marion F. Haug[1], Edda Kastenhuber[1], Colette M. Maurer[1†], Stephan C. F. Neuhauss[1]

[1]Institute of Molecular Life Sciences, University of Zurich, Winterthurerstrasse 190, 8057 Zurich, Switzerland

[†]present address: Max Planck Institute for Medical Research, Jahnstrasse 19, 69120 Heidelberg, Germany

Report on an ongoing research project

Personal contribution:

performing of all experiments, preparation of figures, writing of the manuscript

4.1 Abstract

In the retina two different pathways mediate the sense of light increments and light decrements and thereby build the basis for contrast vision. Since glutamate is the sole neurotransmitter used in the first visual synapse, these ON- and OFF-pathways need two opposed glutamate receptors to fulfill their function. The ON-pathway is mediated via the inhibitory metabotropic glutamate receptor 6 (mGluR6) expressed on dendrites of bipolar cells. Its intracellular second messenger cascade is gated via a G-protein and closes a constitutively open cation channel (TRPM1) which finally hyperpolarizes the ON-bipolar cell when light decreases. Pharmacological and electrophysiological investigations in lower vertebrates suggest the involvement of excitatory glutamate transporters (EAATs) in ON-signaling. These are able to hyperpolarize ON-bipolar cells via a chloride conductance. Yet, the exact contributions of mGluR6 and EAATs to the ON-response are unknown. It is hypothesized that short wavelength cones and rods mainly elicit the mGluR6 pathway. In our study we use the vertebrate model zebrafish to shine more light on mGluR6 and EAAT mediated ON-signaling. First, we investigate the mGluR6 signaling pathway and found that all members of the transduction cascade are present in ON-bipolar cells. Hence, the mGluR6 pathway seems to be conserved in zebrafish. Analysis of mGluR6a in larval and adult zebrafish showed protein localization in the outer plexiform layer of adults as well as the inner retina in both larvae and adults. Investigation of photoreceptor terminals with the zebrafish specific mGluR6a and -6b antibodies revealed that both paralogs are expressed in rod photoreceptor terminals. Moreover, mGluR6b-positive dendrites contact all cone subtypes and mGluR6a expression was found at least in doublecone terminals. This suggests that the different ON-responses measured for short and long wavelengths originate from other effects such as different glutamate affinity rather than a different distribution of mGluR6s.

EAAT7 was found to be expressed on bipolar cell dendrites and its downregulation leads to a diminished photopic ERG ON-response in zebrafish, similar to the downregulation of mGluR6b. Here, we show that the knock down of both proteins, EAAT7 and mGluR6b, significantly reduces the ON-response even more compared to the single knock downs. The persisting small b-wave suggests the involvement of other receptors in the zebrafish cone ON-signaling.

In summary, this study contributes to the understanding of zebrafish ON-signaling. It helps to unravel the relative contributions of both mGluR6 paralogs and EAATs to the ON-response but also shows the complexity of retinal signaling at the first visual synapse.

4.2 Introduction

The vertical visual stream through the retina is divided into an ON- and OFF- pathways already in the outer plexiform layer (OPL), responding to light increments or decrements, respectively. Two distinct glutamate receptor subtypes present at bipolar cell dendrites mediate these opposing responses. A light decrease results in an increased glutamate release from photoreceptors which leads to the opening of AMPA/kainate types of ionotropic glutamate receptors that depolarize the following OFF-bipolar cell (Saito & Kaneko, 1983). On the other hand, an increase in glutamate also turns on the inhibitory glutamate receptor 6- (mGluR6-) pathway (Larison & Bremiller, 1990). After glutamate binding to mGluR6, intracellular G-protein signaling leads to the closure of the transient receptor potential channel TRPM1 (Shen *et al.*, 2009; Morgans *et al.*, 2009). A G_o class of G-protein interacts with the channel (Weng *et al.*, 1997; Dhingra *et al.*, 2002), however, whether interaction occurs via the $G\alpha_o$ or $G\beta\gamma$ subunit is still unclear (Koike *et al.*, 2010; Shen *et al.*, 2012; Tummala *et al.*, 2012). Besides that, nyctalopin (NYX), a cell-surface leucine-rich proteoglycan, is proposed to place mGluR6 and the TRPM1 channel to its correct position in the membrane (Cao *et al.*, 2011; Pearring *et al.*, 2011). Mice lacking any of the above mentioned members involved in the signaling cascade show no ERG b-wave reflecting their essential involvment in generating the ON-response (Masu *et al.*, 1995; Dhingra *et al.*, 2002; Shen *et al.*, 2009; Morgans *et al.*, 2009; Gregg *et al.*, 2003). In humans, mutations in these genes manifest in congenital stationary night blindness (CSNB) (Bech-Hansen *et al.*, 2000; Zeitz *et al.*, 2005; Dryja *et al.*, 2005; van Genderen *et al.*, 2009; Audo *et al.*, 2009).

Due to its cone-dominated larval retina and the ease of conducting loss-of-function studies followed by visual performance testing (Nasevicius & Ekker, 2000; Seeliger *et al.*, 2002; Neuhauss, 2003; Fleisch & Neuhauss, 2006), the zebrafish emerged during the last decade as a very attractive model in vision research. In a recent study we identified two mGluR6 paralogs in zebrafish of which at least one, mGluR6b, is participating in photopic ON-signaling (Huang *et al.*, 2012). Although it is generally believed that the mGluR6 pathway mediates the full retinal ON-response, data from lower vertebrates suggest an involvement of glutamate transporters (excitatory amino acid transporters, EAATs) that enable sign inversion via an increase in chloride conductance (Nawy & Copenhagen, 1987; Grant & Dowling, 1995, 1996; Wong *et al.*, 2004; Wong *et al.*, 2005a; Wong *et al.*, 2005b; Wong & Dowling, 2005). Some studies support the hypothesis that mGluR6 mostly mediates scotopic ON-responses whereas EAATs fulfill their main task in the cone mediated ON-signaling (Nawy & Copenhagen, 1987; Grant & Dowling, 1995, 1996; Wong *et al.*, 2005a) but other findings clearly show that a fundamental part of the photopic ON-response in lower vertebrates involves mGluR6 (Saszik *et al.*, 2002; Nelson & Singla, 2009; Huang *et al.*, 2012). This hypothesis is supported by the notion that blocking of the photopic ERG b-wave has the largest effect in the UV- and blue-light range (Saszik *et al.*, 2002; Nelson & Singla, 2009). Taken together, it is hypothesized that the ON-signal of short wavelength cones is predominantly mediated by mGluR6 and long wavelength cones contact ON-bipolar cells which mainly express a glutamate transporter. Moreover, rod ON-signals are likely to fully rely on mGluR6 signaling. In this case the ON-response generated by long wavelengths should be majorly mediated via EAATs. A recent study in our lab found EAAT7 to be located in the postsynaptic outer plexiform layer (OPL) and depletion leads to a reduced photopic ON-response (Maurer, 2010) similar to mGluR6b (Huang *et al.*, 2012). However, we still do not know to what extend mGluR6s and/or EAATs contribute

to the zebrafish ON-response. In our study we make use of the cone dominant retina of larval zebrafish for investigating the involvement of the mGluR6- and the EAAT-pathway to the photopic ON-response.

Before we directly addressed this question, we investigated the members of the mGluR6 signaling cascade and find that they all colocalize in ON-bipolar cells of adult zebrafish, suggesting a conservation of the signaling pathway in zebrafish. This validates the zebrafish as model in vision research and enables, combined with the available pharmacological and genetic tools, a thorough analysis of the vertebrate ON-pathway. Next we localized mGluR6 protein in photoreceptor terminals to find an explanation for the larger contribution of short wavelength cones to the metabotropic ON-response. Our results reveal that all photoreceptors including rods contact mGluR6-positive bipolar cells. This result suggests that the larger effect of UV- and blue-cones to the metabotropic ON-response is not mediated via photoreceptors contacting different receptor subtypes. Hence, other mechanisms such as a different amount or location of receptors on the dendrites or different glutamate affinity are more likely explanations. By depleting both mGluR6b and EAAT7 in larval fish we found a significant decrease in b-wave amplitude compared to the single knock downs, however, a small remaining b-wave was still visible. This suggests that both mGluR6b and EAAT7 are involved in the generation of the zebrafish ON-response but at least one other so far unknown protein is participating as well. This might be mGluR6a, the second mGluR6 paralog, or one of the other zebrafish EAATs, most likely one of the EAAT5 paralogs.

4.3 Material and Methods

4.3.1 Fish maintenance and breeding

Zebrafish (*Danio rerio*) were kept under standard conditions at a 14h/10h light/dark cycle at 28°C. Embryos were raised at 28 °C in E3 medium (5 mM NaCl, 0.17 mM KCl, 0.33 mM $CaCl_2$, 0.33 mM $MgSO_4$, 0.01% methylen blue) and staged according to development in days post fertilization (dpf). Wild-type fish of the strain "WIK" were used in this study. All examinations were performed in accordance with the ARVO Statement for the Use of Animals in Ophthalmic and Vision Research and were approved by the local authorities (Veterinäramt Zürich TV4206).

4.3.2 *In situ* hybridization

4.3.2.1 Probe preparation

Cloning of the *mglur6* and *gnao* genes into the pcRII vector (Invitrogen, Zug, Switzerland) is described elsewhere (Huang *et al.*, 2012). Additionally, plasmids containing the *trpm1a*, *trpm1b* or *nyx* gene were generated using the following primers: *trpm1a fwd* 5'-GCAGGAGAAATGGTCGGT-3', *rev* 5'-GGGCGAAGGAAATGATGT-3'*; trpm1b fwd* 5'-AGAGGGCATGGATTGAAAGG-3', *rev* 5'-GGTTTGGTAGGGTCGTGT-3' and *rev* 5'-TCACACACCACCACAGGCA-3'; *nyx fwd* 5'-GCACATGCACTCAGGAGAAG-3', *rev* 5'-CGATTCTCTTGCAAGTTGAGG-3' and *fwd* 5'-GGCTTGCACACGCTCCT-3', *rev* 5'-AGTCTGAGAAGCACCGAACA-3'. Plasmids were linearized for T7 and Sp6 *in vitro* transcription and column purified (Macherey-Nagel, Oensingen, Switzerland). DIG- and DNP-labeled probes were generated using kits (DIG-RNA labeling kit; Roche, Basel, Switzerland and DNP-11-UTP, NEL555; Perkin

Elmer, Waltham, MA, USA). Transcripts longer than 1 kb were hydrolyzed to obtain fragments of approximately 300 - 500 nucleotides of length. As working probes a mixture of non-hydrolyzed (2 ng/ul) and hydrolyzed (1 ng/ul) probe were used.

4.3.2.2 Fluorescent *in situ* hybridization (FISH)

For the first three days of the double-FISH we used a protocol described elsewhere for single-FISH (Huang *et al.*, 2012). In our double-FISH, the DIG-antibody and the tyramide-Alexa488 working solution (TSA kit #12; Molecular Probes, Life Technologies, Zug, Switzerland) were used first. After the first staining step, the staining solution was washed away with PBT and the sections were again incubated in 1% H_2O_2 in PBT to inactivate the peroxidase activity of the first antibody. Since we always used the DNP-11-UTP ribonucleotides as second antisense probe, a 1:200 dilution of the HRP-conjugated anti-DNP antibody (TSA Plus DNP System, NEL747A; Perkin Elmer) was applied ON at 4°C after a second round of blocking. The next day, all sections were washed again 5 times for 10 min in PBT before performing the second staining step similar to the first one using a different Alexa-conjugated tyramide (Alexa555 or Alexa568; Molecular Probes). Subsequently, the slides were washed 3 times for 10 min in PBT and coverslipped with Kaiser's glycerol gelatine (Merck KGaA, Darmstadt, Germany). Images were taken with a confocal microscope (CLSM Leica SP 5; Leica Microsystems GmbH, Wetzlar, Germany) and Z-stacks of 2-3 images were produced in Imaris (X64; Bitplane, Zurich, Switzerland). Finally, all images were processed and arranged with Adobe Photoshop and Illustrator CS5.

4.3.3 Generation of antibodies

An mGluR6a-specific peptide was chosen for immunization. Guinea pigs (Eurogentec S.A., Seraing, Belgium) were immunized with the peptide **C**KSINE**KQNGETK**I**EPDR**T**Q** (874-893, amino acids in bold represent sequence identity with zebrafish mGluR6b) that recognizes the C-terminus of mGluR6a. The final bleeds were affinity purified against the respective peptide by Eurogenetec. To increase specificity, the mGluR6a antibody was cross-absorbed against the respective mGluR6b-epitope using CNBr-activated sepharose (4B; GE Healthcare, Little Chalfont, UK). Specificity was tested on dot-blots (Supplemental Figure 1).

4.3.4 Immunohistochemistry

Immunohistochemical labeling of adult zebrafish retinal slices was performed as previously described (Fleisch *et al.*, 2008) with the difference that blocking solution was applied for 1 hour. Besides the wild-type fish "WIK" transgenic lines with GFP-labeled photoreceptor subtypes were used (Takechi *et al.*, 2003; Takechi *et al.*, 2008; Tsujimura *et al.*, 2007). The final concentration of the cross-absorbed mGluR6a antibody was 1:100. The mGluR6b antibody was used as described elsewhere (Huang *et al.*, 2012). Additionally, specific doublecone labeling was performed using the Zpr1 antibody at a concentration of 1:250 (Larison & Bremiller, 1990). The immunoreactions were visualized by using the appropriate fluorescently labeled secondary antibody (Alexa Fluor 488 anti-mouse 1:1000 in PBS, Alexa Fluor 568 anti-rabbit or anti-guinea pig 1:500 in PBS, all from Molecular Probes). Labeling of GFP-positive cells was increased with a chicken-anti GFP-antibody (1:700, A20162; Invitrogen) in combination with Alexa Fluor 488 (1:1000; Molecular Probes). Slides were imaged by confocal microsco-

py (CLSM Leica SP 5), z-stacks were viewed and processed in Imaris (Bitplane) and images were arranged in Adobe photoshop and illustrator CS5.

4.3.5 Targeted gene knock down using Morpholino

Downregulations of mGluR6b and EAAT7 were accomplished as previously described (Huang *et al.*, 2012; Maurer, 2010). For the knock down of EAAT7 an antisense morpholino oligonucleotide (MO) designed against the translational start site was used (5'-AAATGTTTATTCGTCATGTTATCTG-3') and the knock down was confirmed by western blot (data not shown). Additionally, a standard control-MO was used (5'-CCTCTTACCTCAGTTACAATTTATA-3'). All morpholinos were purchased from Gene Tools (Philomath, Oregon, USA). Prior to use, the stock solutions of the MOs were heated at 65°C for 5 min before dilution in ddH_2O containing 0.2% phenol red. Embryos were injected in the one-cell stage with either the *mglur6b*, the *eaat7* or a combination of both MOs. Injections were performed as described (Westerfield, 2000) by using a manual micromanipulator and a pressure pump (both Eppendorf, Schönenbuch, Basel).

4.3.6 Electroretinogram measurements

ERG measurements were performed as previously described (Makhankov *et al.*, 2004). Briefly, after dark adaptation for at least 30 min, larvae were set on a sponge soaked with blank E3 medium (5 mM NaCl, 0.17 mM KCl, 0.33 mM $CaCl_2$, 0.33 mM $MgSO_4$). While the reference electrode was placed beneath the fish, a recording electrode with a tip diameter of 25 to 30 µm filled with blank E3 was placed in the middle of the cornea. Stimuli of 100 ms with an interstimulus interval of 5 sec were applied, starting with the lowest light intensity (log 0 corresponds to 6800 lux or 72 W/m²). Statistical analysis was performed in GraphPad Prism 5 (GraphPad Software, La Jolla, CA, USA).

4.4 Results

4.4.1 Colocalization of *mglur6* pathway genes in adult zebrafish

Recently, we have shown that one mGluR6 paralog, mGluR6b, is located in ON-bipolar cell dendrites and that its downregulation leads to a diminished ON-response in larval zebrafish (Huang *et al.*, 2012), a similar effect as has been described in mammals (Masu *et al.*, 1995). Up to now it is unknown whether the same molecules as in mammals are involved in the zebrafish mGluR6 mediated ON-signaling. We performed a double-fluorescent *in situ* hybridization (FISH) study on adult zebrafish retinal slices with molecules described to be involved in the mammalian mGluR6 pathway. Since they all have been described to be expressed in the INL we investigated the colocalization of both *mglur6* and *trpm1* paralogs, *nyx* as well as one of the $G\alpha_o$s (*gnaob*) (Huang *et al.*, 2012; Bahadori *et al.*, 2006; Kastenhuber *et al.*, 2012). Our data reveal a colocalization of *mglur6a* with *mglur6b*, *gnaob*, and *trpm1a* (Fig. 1A-C, arrowheads) and of *trpm1a* with *mglur6b* and *nyx* (Fig. 1D,E, arrowheads). The two *trpm1* paralogs seem not to colocalize in ON-bipolar cells. While *trpm1a* riboprobes clearly stain cell bodies in the medial INL, *trpm1b* expression was rather found around the *trpm1a*-positive cells or in the proximal INL (Fig. 1F).

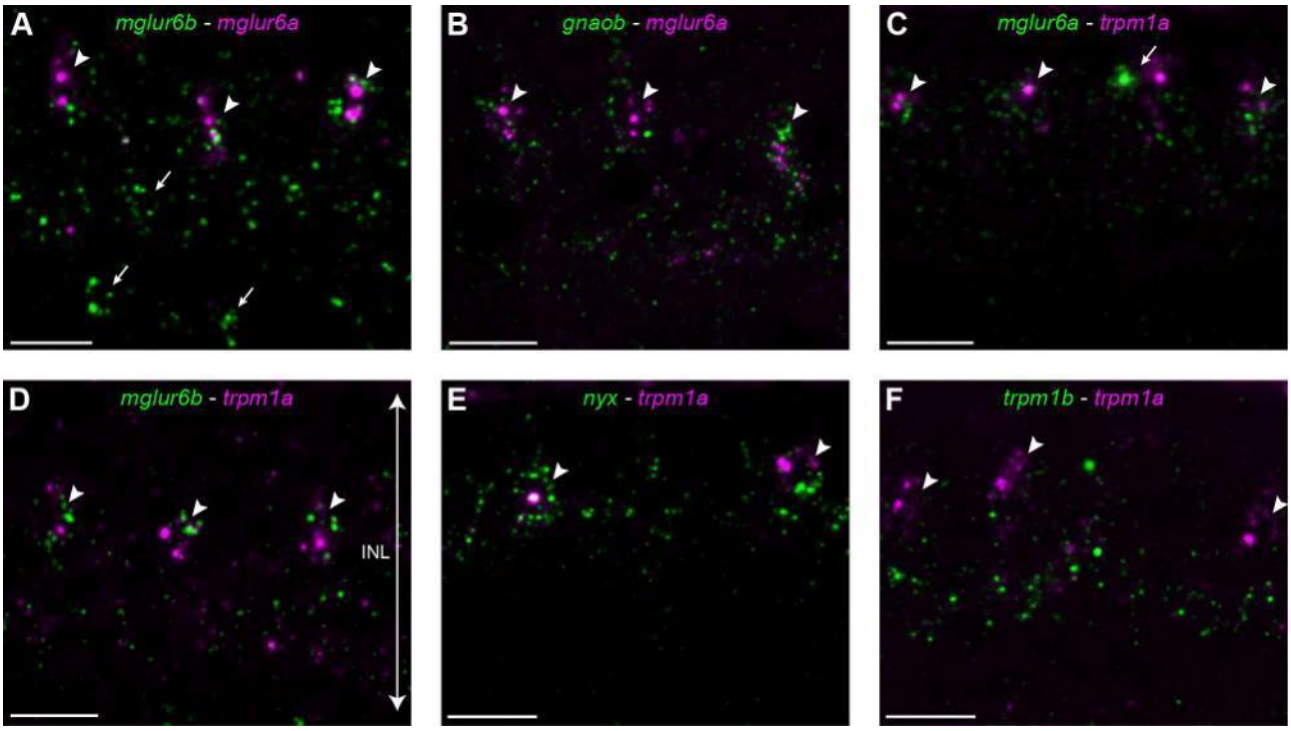

Figure 1: Colocalization of mglur6 pathway genes labeled by fluorescent in situ hybridization.
A-F: *Z-stacks of 2-3 images of adult zebrafish retinal slices taken with a confocal microscope.* ***A:*** *The arrowheads point to bipolar cell soma where mglur6b in green and mglur6a in magenta colocalize. While mglur6a labeling is restricted to the medial INL, the mglur6b riboprobe additionally labels cell bodies in the proximal INL (arrows).* ***B:*** *The α-subunit of the G-protein (gnaob) in green is located in the same ON-bipolar cells as mglur6a in magenta (arrowheads).* ***C:*** *mglur6a (green) colocalizes with trpm1a in ON-bipolar cells (arrowheads), however, for some cell bodies it is not distinguishable whether exactly the same soma or two different cell bodies next to each other are labeled (arrow).* ***D:*** *The mglur6b riboprobe in green is expressed in the same cells where trpm1a (magenta) is located (arrowheads).* ***E:*** *The cation channel trpm1a in magenta colocalizes with nyx in green in the medial INL (arrowheads).* ***F:*** *Both trpm1 channels are expressed in the INL. While trpm1a in magenta clearly labels ON-bipolar cell soma (arrowheads), trpm1b (green) is only marginally expressed in the medial INL but rather labels structures in the proximal INL. All images reveal the whole inner nuclear layer (INL) as depicted in D. Scale bars = 10 µm.*

4.4.2 Analysis of photoreceptor-to-ON-bipolar cell contacts

The effect of a group III mGluR blocker on the ERG is largest in the short wavelength range which suggests that UV- and blue-cones primarily use mGluR6 to generate their ON-response and long wavelength cones rely mainly on EAATs (Saszik *et al.*, 2002). This mechanism could be mediated via different photoreceptors that are in contact with ON-bipolar cells expressing either mGluR6s or EAATs on their dendrites. To answer this question we investigated which photoreceptor subtypes contain mGluR6-positive labeling within their synapses. Both mGluR6 paralogs are located in the outer plexiform layer (OPL) of adult fish where bipolar cell dendrites are located (Fig. 2B; Huang *et al.*, 2012). Larval fish however seem not to express mGluR6a in the OPL but rather reveal a confuse labeling in cells around the inner plexiform layer (IPL, Fig. 2A). In adults an additional expression is found in the ganglion cell layer (GCL) and in an ON- and an OFF-layer of the IPL. Labeling in photoreceptor cell bodies (ONL) is unspecific.

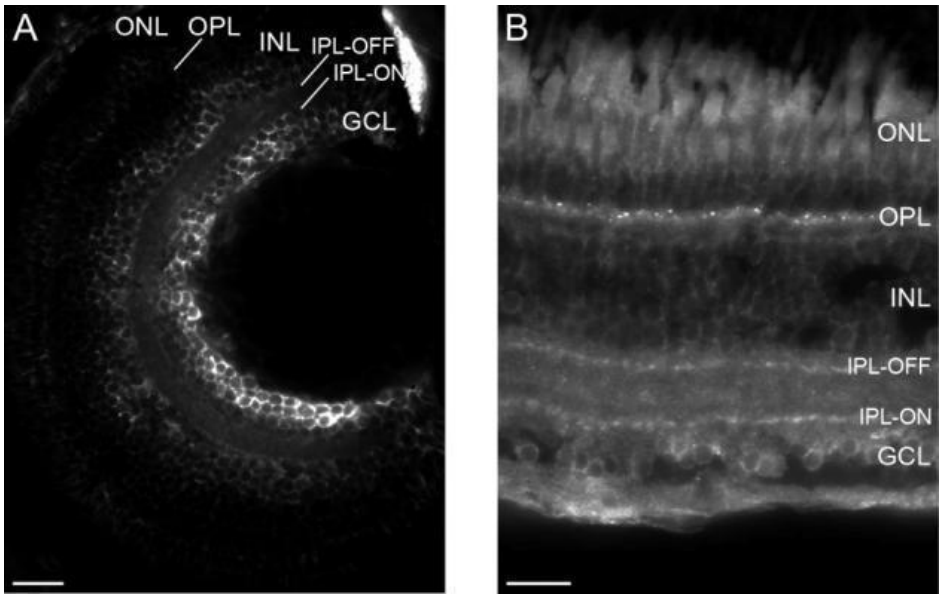

Figure 2: Retinal expression of mGluR6a in larval and adult zebrafish.
Immunohistochemical labeling of mGluR6a on larval (A) and adult (B) retinal cross-sections. ***A:*** *The mGluR6a-specific antibody is expressed in cells of the proximal INL and the GCL in five-day-old zebrafish larvae.* ***B:*** *Expression of mGluR6a in the adult retina. A punctuated expression is seen in the OPL as well as in the ON- and the OFF-layer of the IPL. mGluR6a is also weakly expressed in cells of the GCL. The expression in the ONL was found to be an unspecific background labeling of the photoreceptors. GCL: ganglion cell layer; INL: inner nuclear layer; IPL-OFF: off-layer of the inner plexiform layer; IPL-ON: on-layer of the inner plexiform layer; ONL: outer nuclear layer; OPL: outer plexiform layer. Scale bars = 20 µm.*

We raised zebrafish specific mGluR6a and -6b antibodies and performed doublelabelings with the Zpr1 antibody as a marker for doublecones. Additionally we performed immunolabelings on retinal sections of transgenic fish that express GFP under a number of different opsin promoters (Takechi et al., 2003; Takechi et al., 2008; Tsujimura et al., 2007). By taking confocal images of the OPL where photoreceptors contact bipolar cells we were able to detect mGluR6-positive synaptic spherules or pedicles. Our analysis reveals that all SWS1 (UV-cones) (Fig. 3G), all SWS2 (blue-cones) (Fig. 3H), and all RH2-2 (green-cones) (Fig. 3I) show mGluR6b labeling within their synapses. When zooming through the Z-stacks, every single synaptic terminal appears to be in contact with a postsynaptic mGluR6b. Additionally, a double labeling with Zpr1, a marker for red-green doublecones, reveals that already at larval stage all doublecones maintain mGluR6b within their spherules (Fig. 3C). Moreover, all rods of larval and adult zebrafish contain mGluR6a- and -6b-positive bipolar cell dendrites in their pedicles (Fig. 3A,B,D,E). For mGluR6a we have only investigated double labeling with Zpr1 and found, similar to mGluR6b, that these cones contact mGluR6a-positive ON-bipolar cell dendrites as well. When applying both mGluR6 antibodies we find that they colocalize at some spots but not at others in the OPL (Fig. 3J). However, the different localization of mGluR6a and -6b does not automatically imply the localization in different cells, since we cannot assign individual dendrites to a specific bipolar cell.

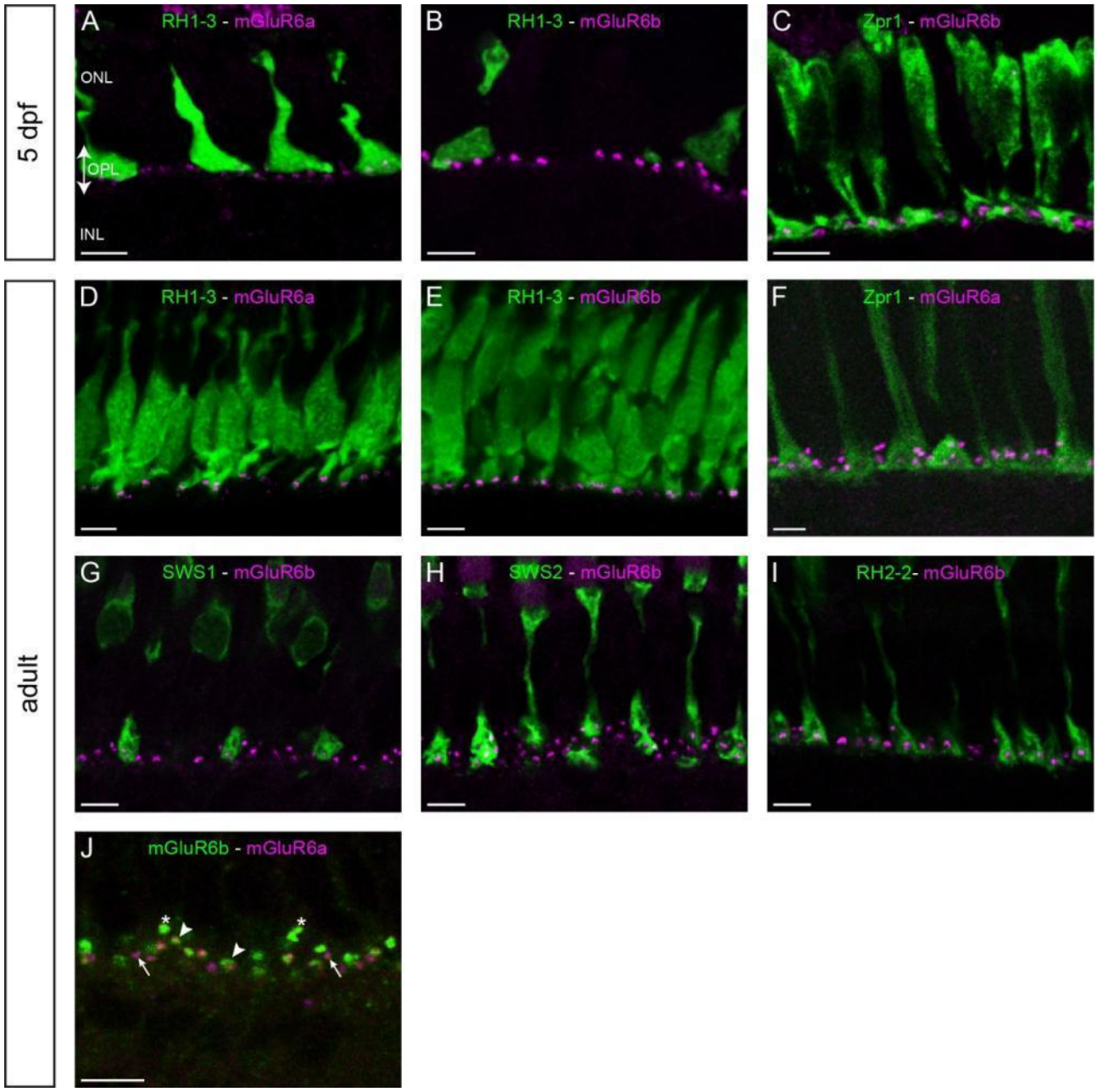

Figure 3: All photoreceptor terminals contact mGluR6a- and/or mGluR6b-positive cells.
A-J: *Z-stacks taken with a confocal microscope of five-day-old (A-C) and adult (D-J) zebrafish retinal slices.* ***A,B:*** *RH1-3 transgenic zebrafish larvae expressing GFP in their rods show that all rods contact mGluR6a- (A) and mGluR6b- (B) positive bipolar cells.* ***C:*** *A double-labeling with the red-green doublecone marker Zpr1 in five-day-old fish reveals mGluR6b staining in each synaptic terminal.* ***D,E:*** *Similar to the larvae, all rod pedicles of adult fish show mGluR6a (D) and mGluR6b (E) labeling.* ***F:*** *All red-green doublecones (green) show mGluR6a expression around and within their synapses.* ***G-I:*** *In adult fish mGluR6b-positive labeling is found in pedicles of UV- (G), blue- (H), and green- (I) cones labeled with GFP.* ***J:*** *Double-labeling with mGluR6a (magenta) and mGluR6b (green) antibody shows that they colocalize in some dendrites (arrowheads) while others only seem to express mGluR6a (arrows) or mGluR6b (asterisks). Whether these dendrites are actually from different bipolar cells cannot be said with this labeling alone. As depicted in A, all images show a close-up of the outer plexiform layer (arrow, OPL) with the outer nuclear layer (ONL) and the inner plexiform layer (INL) around. Scale bars = 5 µm.*

4.4.3 Contribution of mGluR6b and EAAT7 to the zebrafish ON-bipolar cell signal

Several studies conducted in lower vertebrates propose the involvement of EAATs in ON-signaling (Nawy & Copenhagen, 1987; Grant & Dowling, 1995, 1996; Wong *et al.*, 2004; Wong *et al.*, 2005a; Wong *et al.*, 2005b; Wong & Dowling, 2005). A phylogenetic analysis has shown that the zebrafish possess 13 different EAATs (Gesemann *et al.*, 2010). The transcripts of one of them, *eaat7*, were found to be expressed in the inner nuclear layer, suggesting functional relevance for EAAT7 in the ON-signaling. To ascertain this, we used a morpholino-based gene knock down followed by electroretinogram measurements at 5 dpf. Concentrations for a full downregulation have been investigated in earlier studies by immunohistochemistry on mGluR6b-depleted larvae (Huang *et al.*, 2012) or by western blot in the case of EAAT7 (Maurer, 2010). As previously shown the downregulation of both mGluR6b or EAAT7 led to a large reduction in b-wave amplitude (Huang *et al.*, 2012; Maurer, 2010). Depletion of both proteins affected the b-wave in a dose dependent manner. A larger reduction in the b-wave amplitude was found at the highest concentration as compared to the single knock downs (Fig. 3B). This suggests that both mGluR6b and EAAT7 work in parallel to generate the cone ON-response in zebrafish. However, due to the remaining small b-wave in double-morphant fish there must be an additional molecule involved.

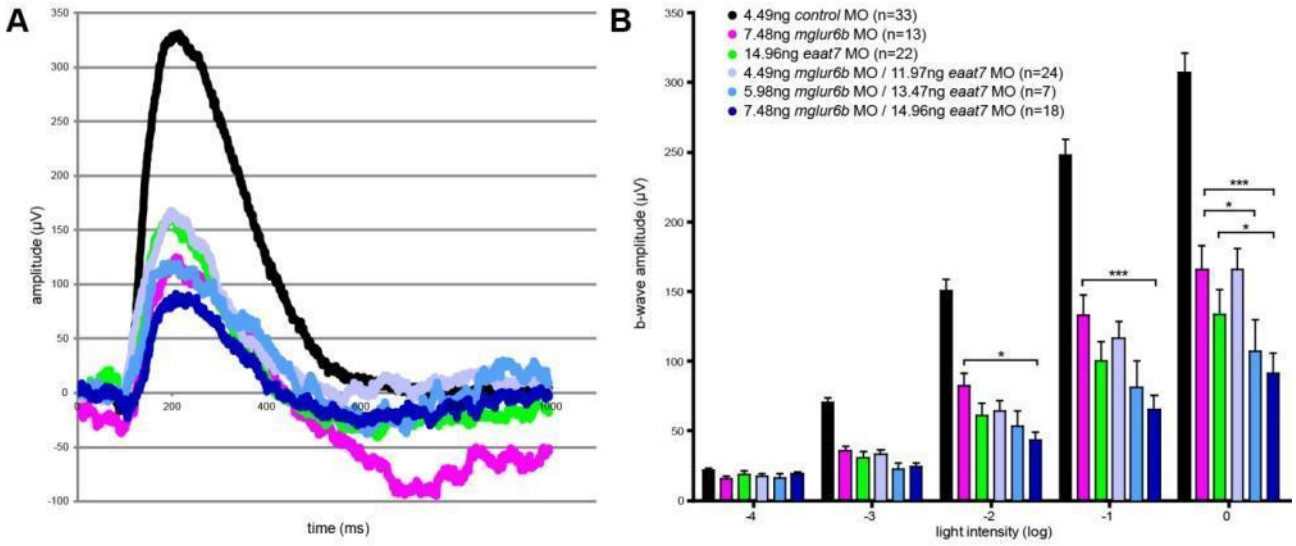

Figure 4: Electroretinogram recordings of mGluR6b and EAAT7 depleted zebrafish larvae.
A: *Representative ERG measurements of control, single and double morphants at the highest light intensity (log 0) showing the a-wave elicited by photoreceptor and the larger b-wave representing the ON-response.* ***B:*** *Plotted b-wave amplitudes. The single injected morphants show a clear reduction in b-wave amplitude (pink and green) compared to the control morphants (black). When injecting both morpholinos, a dose dependent decrease (light blue < blue < dark blue) in the b-wave amplitude is observed. The highest dose of the combined injection of mglur6b and eaat7 morpholinos (dark blue) leads to a significantly lower b-wave compared to the single injection of either mglur6b (pink) or eaat7 (green). For statistical analysis a two-way ANOVA was used. Statistically significant values are only shown between the single and double morphant b-wave amplitudes (p<0.5=*, p<0.01=**, p<0.001=***).*

4.5 Discussion

Glutamate is the main neurotransmitter used by photoreceptor cells of the vertebrate retina. By studying its receptors one can gain insight into glutamatergic processes at the photoreceptor terminal and increase the understanding of synaptic mechanism in the retina. In our study we addressed the question of how ON-responses are generated in the zebrafish retina. We not only investigated the mGluR6 mediated ON-signaling but enlarged our study to the excitatory amino acid transporters (EAATs) suggested to be involved in ON-signaling (Grant & Dowling, 1995, 1996).

4.5.1 Conservation of the mGluR6-signaling pathway

The metabotropic glutamate receptor 6 (mGluR6) has been identified more than two decades ago and its involvement in ON-signaling of mammals is thoroughly studied (Masu *et al.*, 1995; Zeitz *et al.*, 2005; Vardi *et al.*, 2000; Vardi & Morigiwa, 1997). Recent publications uncovered downstream molecules participating in mGluR6 mediated ON-signaling. TRPM1 was identified as the cation channel whose closure leads to the hyperpolarization when light is turned off (Shen *et al.*, 2009; Morgans *et al.*, 2009), while the function of NYX is not completely understood (Cao *et al.*, 2011; Pearring *et al.*, 2011). A whole genome duplication event early in the teleost lineage led to the duplication and subsequent retention of many genes in zebrafish (Force *et al.*, 1999; Ohno, 1999; Postlethwait, 2007). It is therefore common to find two zebrafish orthologs for a given mammalian gene. In a recent study, we have shown that two mGluR6 and Goα paralogs exist (Huang *et al.*, 2012). Since both transcripts of *mglur6* and *gnaob* (gnao is the gene encoding Goα) are expressed in the INL we investigated the colocalization of these and other molecules involved in the mGluR6 pathway. By double-fluorescent *in situ* hybridization we found that *mglur6a*, *mglur6b*, *gnaob*, *trpm1a* and *nyx* are found inside the same cells of the medial inner nuclear layer (INL). A confirmation that the fluorescently labeled precipitates indeed stain ON-bipolar cell bodies of the INL is given by the fact that *mglur6b* is located within PKCα-positive cell bodies (Huang *et al.*, 2012). This suggests that the whole mGluR6-signaling pathway is conserved from fish to humans. The zebrafish is already widely used in vision research but will gain even more importance if general molecular pathways are conserved. These can be thoroughly studied in this lower vertebrate with the additional possibility of loss-of-function analysis for instance by morpholino injections, or targeted gene ablation (reviewed in Renninger *et al.*, 2011) followed by behavioral analysis using electroretinogram (Seeliger *et al.*, 2002), optokinetic- or optomotor responses (Fleisch & Neuhauss, 2006; Emran *et al.*, 2008).

4.5.2 Wavelength specificity of mGluR6 mediated ON-signaling

It is generally accepted that the generation of ON-responses in lower vertebrates involves beside the mGluR6 pathway, glutamate transporters. Multiple studies suggest that these mainly mediate the photopic ON-response whereas the rod-derived signal to ON-bipolar cells is mediated via mGluR6 (Grant & Dowling, 1995, 1996; Wong *et al.*, 2005a; Wong *et al.*, 2005b; Wong & Dowling, 2005; Wong *et al.*, 2004). In contradiction to that it has been shown that application of APB that blocks group III mGluRs mainly affects the short wavelength input to the ERG b-wave (Saszik *et al.*, 2002). This was confirmed by the study of Nelson and Singla who found highest metabotropic contribution in the UV- and blue range when isolating single elements of the photopic ERG in adult

zebrafish (Nelson & Singla, 2009). So far it is unknown how these different ON-responses are generated and why there might be such a difference. Our recent study showed a clear involvement of mGluR6b to the cone-mediated ON-signaling of larval zebrafish (Huang *et al.*, 2012). However, we used white light stimuli and were therefore not able to investigate the influence of monochromatic light on mGluR6b mediated ON-signaling. We investigated the role of mGluR6 signaling for the cone ON-responses by examining cone-to-mGluR6-positive bipolar cell contacts. A reasonable explanation for the results gained by electrophysiology would be if UV- and blue-cones show an increased number of mGluR6-positive synapses compared to the long wavelength cone types. With the help of transgenic fish expressing GFP in their UV-, blue- or green-cones (Takechi *et al.*, 2003; Takechi *et al.*, 2008; Tsujimura *et al.*, 2007) as well as Zpr1 as a marker for doublecones (Larison & Bremiller, 1990) we found that all cone synapses contact mGluR6-positive ON-bipolar cells. Moreover, all rods contain mGluR6a and -6b expression within their synapses. Although we did not investigate mGluR6a expression in transgenic fish, the overlapping expression of both paralogs in ON-bipolar cells and the fact that mGluR6a is found in doublecone synapses suggests that there will most likely be no difference and both mGluR6 paralogs contact all cone subtypes. This holds possibly also true for larval fish, as all their doublecones express at least mGluR6b within their synapses. At first glance this contradicts the above mentioned hypothesis of mGluR6 mediating mainly short wavelength photopic responses. Although our result is based on morphology and does not imply functional relevance there are several other possibilities to accomplish differences in spectral signaling. Our method does not allow counting for abundance or investigating the exact location of the receptors on the bipolar cell dendrites. The rate of receptors found on dendrites that contact certain photoreceptor types certainly influences ON-signaling. Moreover, a different absolute number of bipolar cells per photoreceptor would also influence ON-responses. Another explanation could be a difference in glutamate affinity of one or the other receptor. Moreover, until now we do not know whether all photoreceptors contact EAAT-positive bipolar cells. We might only find a difference there, with only doublecones expressing EAATs in their synaptic terminals, which would explain the results of the other studies.

MGluR6b is located in every PKCα positive ON-bipolar cell and it seems that the *mglur6* transcripts colocalize (Fig. 1A and Huang *et al.*, 2012). The double labeling suggests distinct locations for mGluR6a and -6b, however, we did not counterstain ON-bipolar cells in this image and are therefore not able to distinguish different bipolar cell dendrites. In zebrafish six different ON-bipolar cell subtypes as well as four different mixed-type bipolar cells that send their dendrites into the ON- and the OFF-layer of the IPL have been identified (reviewed in Connaughton, 2011). Often PKCα is used as a marker for ON-bipolar cells although it labels not all but only a subtype of ON-bipolar cells which resemble mixed-type bipolar cells of goldfish (Connaughton *et al.*, 2004). In order to reach a firm conclusion about mGluR6 expression in specific bipolar cells different markers need to be employed. So far, few transgenic zebrafish lines expressing GFP in some bipolar cells have been developed (Vitorino *et al.*, 2009; Zhao *et al.*, 2009). However, subtype-specific markers are needed for a thorough analysis. Recently it was found that ON- and mixed-type bipolar cells contact all combinations of photoreceptors and in most cases more than one subtype (Li *et al.*, 2011). This makes it difficult to find the individual contribution of each pathway to the ON-pathway and it is therefore advisable to focus on a specific receptor or bipolar cell subtype when investigating morphology. Another question that emerges is why zebrafish need such a large variety of different bipolar cells when they still contact a variety of cone subtypes? The zebrafish is a diurnal animal and the spectral composition of the light input changes during the day. This markedly affects the behavior, as has

been demonstrated by the strong influence of colored light on cichlid fish (Pauers *et al.*, 2012). A system that enables the distinction of slight changes in the light spectrum could help guiding such and other behavioral tasks from dawn to dusk. By electrophysiological recordings scientists were able to distinguish between the contributions of different receptors to the b-wave so only a combination of morphological analysis and ERG will help uncovering the mysteries about ON-signaling. With a further investigation using spectral ERG in mGluR6-deficient fish larvae we hope to contribute to resolve this fascinating story.

4.5.3 Contribution of mGluR6s and EAATs to the zebrafish cone ON-response

In mammals it is generally believed that mGluR6 mediates the full scotopic and photopic ON-response (Dryja *et al.*, 2005; Masu *et al.*, 1995) whereas studies in lower vertebrates suggest the involvement of EAATs in ON-signaling (Grant & Dowling, 1995, 1996; Wong *et al.*, 2004; Wong *et al.*, 2005a; Wong *et al.*, 2005b; Wong & Dowling, 2005). In an earlier work of our laboratory the phylogeny of EAATs has been thoroughly analyzed (Gesemann *et al.*, 2010). The zebrafish possess 13 different EAATs, of which some of them originated from the additional whole genome duplication events and other from tandem duplication. EAAT7 was found to be expressed in the postsynaptic OPL where ON-bipolar cell dendrites are located and depletion affects the ERG ON-response (Maurer, 2010) similar to mGluR6b (Huang *et al.*, 2012). If only these two receptors mediate the zebrafish cone ON-response, we would expect that the b-wave is fully diminished after downregulation of both. After a morpholino-based double knock down, we found that the ON-response is affected in a dose dependent manner and is significantly smaller when depleting both molecules compared to the single knock downs. To our surprise the b-wave of double morphant larvae was still measurable, even at lower light intensities. An incomplete knock down may only lead to a partial loss of the protein since the MO is injected into 1-cell staged zebrafish eggs and dilutes out over the course of the fish's development. These residual proteins could generate the remaining b-wave. However, the complete knock down of the single molecules was confirmed by immunohistochemistry and western blot, respectively, and in this study similar concentrations were used for double knock downs. Therefore, we hypothesize that at least one additional molecule is involved in the generation of the cone ON-response of larval zebrafish. The second mGluR6 paralog, mGluR6a, would be a candidate for fulfilling such a task. A preliminary ERG study showed no significant reduction of the b-wave in mGluR6a-depleted larvae, however, downregulation could not be confirmed so far. Another possibility is the involvement of one of the EAAT5 paralogs, as EAAT5 is known to have a particularly prominent chloride conductance needed for ON-bipolar cell hyperpolarization (Arriza *et al.*, 1997) and is expressed in the INL of the mammalian retina (Pow & Barnett, 2000; Wersinger *et al.*, 2006). This qualifies this glutamate transporter as a perfect candidate for mediating ON-signaling. In addition, a preliminary study performed on adult zebrafish retinal slices showed a colocalization of EAAT5b with mGluR6b, supporting this hypothesis. So far EAAT-involvement in mammalian ON-signaling had been neglected by most scientists. Only few studies consider this possibility to explain their results (Hecht & Shlaer, 1948; Jacobs, 1990; Stockman *et al.*, 1991; Tse *et al.*, 2012). There might be a considerable difference in generating the cone mediated ON-response in fish and mammals which could explain the attitude of these scientists. EAAT7 that fulfills a major task of the transporter mediated ON-response in fish, is only found in lower vertebrates (Gesemann *et al.*, 2010). Moreover, there is only one EAAT5 paralog in mammals and it does not necessarily possess the same function as in fish. However, a recent investigation in mice revealed

hints for EAAT5 involvement in direct ON-signaling (Tse *et al.*, 2012) which will hopefully convince the field about EAAT-contribution to the ON-response. Unlike humans, fish, amphibians and reptiles have the standard vertebrate repertoire of four cone types (Robinson *et al.*, 1993; Sherry *et al.*, 1998; Loew *et al.*, 1996). They might need the additional EAAT7 for UV-mediated ON-responses. Thus, expression analysis of zebrafish EAATs on photoreceptor synapses will be very interesting but remains to be determined. A further idea that has to be considered is that EAATs do not necessarily have to be located on bipolar cell dendrites to participate in the ON-response. EAATs on horizontal or photoreceptor terminals or on Muller glia cells located around the bipolar cell dendrite can influence ON-signaling via re-uptake of glutamate, thereby decreasing the b-wave amplitude. An investigation of EAAT2 paralogs in zebrafish has already shown their distinct effects on ERG b-waves (Maurer, 2010) and recently a similar result was obtained in mice (Tse *et al.*, 2012).

So far we are not able to distinguish the different contributions of each receptor or transporter to the photopic ON-response. We might get an answer to this question by downregulating mGluR6b, EAAT5b, and EAAT7 in the same fish followed by ERG analysis. The complete reduction of the b-wave would support the hypothesis that mGluR6a is not involved in the photopic ON-response, although this would not exclude an involvement of mGlu6a in rod-mediated ON-signaling.

4.5.4 Conclusion

In this study we assessed the involvement mGluR6 and glutamate transporters in the zebrafish ON-response. A colocalization study shows that the whole mGluR6-signaling pathway is conserved in zebrafish. Therefore, the zebrafish is a veritable vertebrate model for studying visual ON-signal transduction pathways. We found that mGluR6-positive ON-bipolar cells are contacting all photoreceptor terminals, suggesting the involvement of mGluR6 paralogs in all cone- and rod-mediated ON-responses independent on the spectrum. This stands in contradiction to electrophysiological results showing a larger input of mGluR6 to short wavelength signals but suggests that such differences are generated via other mechanisms. Further, we demonstrate that both mGluR6b and EAAT7 are involved in the larval zebrafish cone ON-response. The remaining ON-signal is most likely due to the involvement of an additional EAAT, probably EAAT5b. It will be highly interesting to combine morphological analysis of the OPL with monochromatic ERG analysis to decipher the input of each single molecule to the zebrafish ON-response.

4.6 Outlook

The role of NYX in the ON-response is not clearly understood but recent publications suggest an involvement in transport of mGluR6 to the membrane. To further elucidate the interaction of NYX with other mGluR6 pathway members we will use the recently developed DuoLink Assay which helps us identifying protein-protein interaction within pathway members.

To complete the study, we will confirm the downregulation of mGluR6a by immunohistochemistry or western blot. This would show that the ERG measurements performed in mGluR6a depleted larvae hold true and this protein is not involved in cone ON-signaling.

Next, the morphological analyses of photoreceptor to bipolar cell contacts need to be confirmed. Furthermore, the transgenic line for the red cone can be added to this study. This in combination with ERG responses to monochromatic stimuli of different wavelengths in mGluR6 depleted larvae will give us more insight into the spectral input to mGluR6 mediated ON-signaling. Such a study can surely be combined with pharmacological tools such as the EAAT-blocker TBOA or the group III mGluR antagonist APB. It would help differentiating between transporter mediated and mGluR6 mediated ON-responses.

We just started with the analysis of EAAT5b but the preliminary results are already promising and suggest involvement in ON-signaling. Hence, in a second study it would make sense to assess photoreceptor to EAAT5b-positive ON-bipolar cell contacts, deplete the protein by morpholino knock down, and measure spectral ERGs. Finally, we hope to draw a complete picture of the complex cone ON-responses of larval zebrafish, thus shine more light on synaptic visual transmission.

We found that both mGluR6 paralogs are expressed in the retinal ganglion cell layer. The mRNA and protein expression pattern suggests a postsynaptic localization in this layer. So far no other study found a hint for a sign inversing synapse mediated via mGluR6 in retinal ganglion cells. We would like to shine more light on our finding of mGluR6 in the GCL by patch clamping mGluR6 positive retinal ganglion cells. To help differentiating these cells we already started to generate transgenic zebrafish lines with GFP-labeled cells expressing mGluR6a or -6b using the Tol2 system (Amsterdam *et al.*, 1995; Kawakami & Shima, 1999; Stuart *et al.*, 1988).

4.7 Supplemental Information

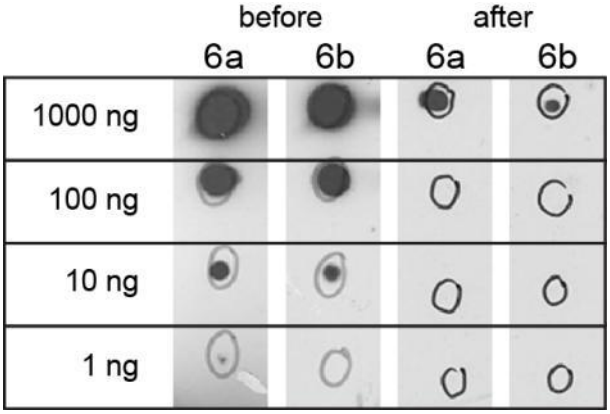

Supplemental Figure 1: Cross-absorbance of the mGluR6a antibody.
Dot-blot analysis showing the increased specificity of the cross-absorbed mGluR6a antibody. 1000 ng of mGluR6a (6a) and mGluR6b (6b) epitopes were pipetted onto nitrocellulose membranes (0.45 µm; Bio-Rad, Reinach, Switzerland). After cross-absorbing the mGluR6a antibody against the respective mGluR6b epitope, either the original (1:1000, before) or the cross-absorbed (1:500, after) mGluR6a antibody was applied.

4.8 References

Amsterdam, A., Lin, S. & Hopkins, N. (1995) *The Aequorea victoria green fluorescent protein can be used as a reporter in live zebrafish embryos. Dev. Biol.*, 171, 123–129.

Arriza, J.L., Eliasof, S., Kavanaugh, M.P. & Amara, S.G. (1997) *Excitatory amino acid transporter 5, a retinal glutamate transporter coupled to a chloride conductance. Proc. Natl. Acad. Sci. U.S.A.*, 94, 4155–4160.

Audo, I., Bujakowska, K., Orhan, E., Poloschek, C.M., Defoort-Dhellemmes, S., (…), Bhattacharya, S.S. & Zeitz, C. (2012) Whole-exome sequencing identifies mutations in GPR179 leading to autosomal-recessive complete congenital stationary night blindness. Am. J. Hum. Genet., 90, 321–330.

Bahadori, R., Biehlmaier, O., Zeitz, C., Labhart, T., Makhankov, Y.V., Forster, U., Gesemann, M., Berger, W. & Neuhauss, S.C.F. (2006) *Nyctalopin is essential for synaptic transmission in the cone dominated zebrafish retina. Eur. J. Neurosci.*, 24, 1664–1674.

Bech-Hansen, N.T., Naylor, M.J., Maybaum, T.A., Sparkes, R.L., Koop, B., Birch, D.G., Bergen, A.A., Prinsen, C.F., Polomeno, R.C., Gal, A., Drack, A.V., Musarella, M.A., Jacobson, S.G., Young, R.S. & Weleber, R.G. (2000) *Mutations in NYX, encoding the leucine-rich proteoglycan nyctalopin, cause X-linked complete congenital stationary night blindness. Nat. Genet.*, 26, 319–323.

Cao, Y., Posokhova, E. & Martemyanov, K.A. (2011) *TRPM1 forms complexes with nyctalopin in vivo and accumulates in postsynaptic compartment of ON-bipolar neurons in mGluR6-dependent manner. J. Neurosci.*, 31, 11521–11526.

Connaughton, V.P. (2011) *Bipolar cells in the zebrafish retina. Vis. Neurosci.*, 28, 77–93.

Connaughton, V.P., Graham, D. & Nelson, R. (2004) *Identification and morphological classification of horizontal, bipolar, and amacrine cells within the zebrafish retina. J. Comp. Neurol.*, 477, 371–385.

Dhingra, A., Jiang, M., Wang, T.-L., Lyubarsky, A., Savchenko, A., Bar-Yehuda, T., Sterling, P., Birnbaumer, L. & Vardi, N. (2002) *Light response of retinal ON bipolar cells requires a specific splice variant of Galpha(o). J. Neurosci.*, 22, 4878–4884.

Dryja, T.P., McGee, T.L., Berson, E.L., Fishman, G.A., Sandberg, M.A., Alexander, K.R., Derlacki, D.J. & Rajagopalan, A.S. (2005) *Night blindness and abnormal cone electroretinogram ON responses in patients with mutations in the GRM6 gene encoding mGluR6. Proc. Natl. Acad. Sci. U.S.A.*, 102, 4884–4889.

Emran, F., Rihel, J. & Dowling, J.E. (2008) *A behavioral assay to measure responsiveness of zebrafish to changes in light intensities. J Vis Exp*.

Fleisch, V.C. & Neuhauss, S.C.F. (2006) *Visual behavior in zebrafish. Zebrafish*, 3, 191–201.

Fleisch, V.C., Schonthaler, H.B., Lintig, J. von & Neuhauss, S.C.F. (2008) *Subfunctionalization of a retinoid-binding protein provides evidence for two parallel visual cycles in the cone-dominant zebrafish retina. J. Neurosci.*, 28, 8208–8216.

Force, A., Lynch, M., Pickett, F.B., Amores, A., Yan, Y.L. & Postlethwait, J. (1999) *Preservation of duplicate genes by complementary, degenerative mutations. Genetics*, 151, 1531–1545.

Gesemann, M., Lesslauer, A., Maurer, C.M., Schönthaler, H.B. & Neuhauss, S.C.F. (2010) *Phylogenetic analysis of the vertebrate excitatory/neutral amino acid transporter (SLC1/EAAT) family reveals lineage specific subfamilies. BMC Evol. Biol*, 10, 117.

Grant, G.B. & Dowling, J.E. (1995) *A glutamate-activated chloride current in cone-driven ON bipolar cells of the white perch retina. J Neurosci*, 15, 3852–3862.

Grant, G.B. & Dowling, J.E. (1996) *On bipolar cell responses in the teleost retina are generated by two distinct mechanisms. J Neurophysiol*, 76, 3842–3849.

Gregg, R.G., Mukhopadhyay, S., Candille, S.I., Ball, S.L., Pardue, M.T., McCall, M.A. & Peachey, N.S. (2003) *Identification of the gene and the mutation responsible for the mouse nob phenotype. Invest. Ophthalmol. Vis. Sci.*, 44, 378–384.

Hecht, S. & Shlaer, S. (1948) *The visual functions of the complete colorblind. J. Gen. Physiol.*, 31, 459–472.

Huang, Y.-Y., Haug, M.F., Gesemann, M. & Neuhauss, S.C.F. (2012) *Novel expression patterns of metabotropic glutamate receptor 6 in the zebrafish nervous system. PLoS ONE*, 7, e35256.

Jacobs, G.H. (1990) *Duplicity theory and ground squirrels: linkages between photoreceptors and visual function. Vis. Neurosci.*, 5, 311–318.

Kastenhuber, E., Staeuble A., Gesemann M., Niklaus S., Haug M.F. & Neuhauss S.C. (2012) *Characterization of TRPM and TRPC Channels in the Zebrafish Retina*, ARVO Abstract Nr. 4311.

Kawakami, K. & Shima, A. (1999) *Identification of the Tol2 transposase of the medaka fish Oryzias latipes that catalyzes excision of a nonautonomous Tol2 element in zebrafish Danio rerio. Gene*, 240, 239–244.

Koike, C., Numata, T., Ueda, H., Mori, Y. & Furukawa, T. (2010) *TRPM1: a vertebrate TRP channel responsible for retinal ON bipolar function. Cell Calcium*, 48, 95–101.

Larison, K.D. & Bremiller, R. (1990) *Early onset of phenotype and cell patterning in the embryonic zebrafish retina. Development*, 109, 567–576.

Li, Y., Tsujimura, T., Kawamura, S. & Dowling, J. (2011) *Bipolar Cell-Photoreceptor Connections in the Zebrafish Retina*, ARVO Abstract Nr. 2573.

Loew, E.R., Govardovskii, V.I., Röhlich, P. & Szél, A. (1996) *Microspectrophotometric and immunocytochemical identification of ultraviolet photoreceptors in geckos. Vis. Neurosci.*, 13, 247–256.

Makhankov, Y.V., Rinner, O. & Neuhauss, S.C.F. (2004) *An inexpensive device for non-invasive electroretinography in small aquatic vertebrates. J. Neurosci. Methods*, 135, 205–210.

Masu, M., Iwakabe, H., Tagawa, Y., Miyoshi, T., Yamashita, M., Fukuda, Y., Sasaki, H., Hiroi, K., Nakamura, Y., Shigemoto, R. & et al. (1995) *Specific deficit of the ON response in visual transmission by targeted disruption of the mGluR6 gene. Cell*, 80, 757–765.

Maurer, C.M. (2010) *Aspects of retinal signaling and visual behavior in the zebrafish*, Ph.D. Thesis, University of Zurich, Switzerland.

Morgans, C.W., Zhang, J., Jeffrey, B.G., Nelson, S.M., Burke, N.S., Duvoisin, R.M. & Brown, R.L. (2009) *TRPM1 is required for the depolarizing light response in retinal ON-bipolar cells. Proc. Natl. Acad. Sci. U.S.A.*, 106, 19174–19178.

Nasevicius, A. & Ekker, S.C. (2000) *Effective targeted gene 'knockdown' in zebrafish. Nat. Genet.*, 26, 216–220.

Nawy, S. & Copenhagen, D.R. (1987) *Multiple classes of glutamate receptor on depolarizing bipolar cells in retina. Nature*, 325, 56–58.

Nelson, R.F. & Singla, N. (2009) *A spectral model for signal elements isolated from zebrafish photopic electroretinogram. Vis. Neurosci.*, 26, 349–363.

Neuhauss, S.C.F. (2003) *Behavioral genetic approaches to visual system development and function in zebrafish. J. Neurobiol.*, 54, 148–160.

Ohno, S. (1999) *Gene duplication and the uniqueness of vertebrate genomes circa 1970-1999. Semin Cell Dev Biol*, 10, 517–522.

Pauers, M.J., Kuchenbecker, J.A., Neitz, M. & Neitz, J. (2012) *Changes in the colour of light cue circadian activity. Animal behaviour*, 83, 1143–1151.

Pearring, J.N., Bojang, P., Shen, Y., Koike, C., Furukawa, T., Nawy, S. & Gregg, R.G. (2011) *A role for nyctalopin, a small leucine-rich repeat protein, in localizing the TRP melastatin 1 channel to retinal depolarizing bipolar cell dendrites. J. Neurosci.*, 31, 10060–10066.

Postlethwait, J.H. (2007) *The zebrafish genome in context: ohnologs gone missing. J Exp Zoolog B Mol Dev Evol*, 308, 563–577.

Pow, D.V. & Barnett, N.L. (2000) *Developmental expression of excitatory amino acid transporter 5: a photoreceptor and bipolar cell glutamate transporter in rat retina. Neurosci. Lett.*, 280, 21–24.

Renninger, S.L., Schonthaler, H.B., Neuhauss, S.C.F. & Dahm, R. (2011) *Investigating the genetics of visual processing, function and behaviour in zebrafish. Neurogenetics*, 12, 97–116.

Robinson, J., Schmitt, E.A., Hárosi, F.I., Reece, R.J. & Dowling, J.E. (1993) *Zebrafish ultraviolet visual pigment: absorption spectrum, sequence, and localization. Proc. Natl. Acad. Sci. U.S.A.*, 90, 6009–6012.

Saito, T. & Kaneko, A. (1983) *Ionic mechanisms underlying the responses of off-center bipolar cells in the carp retina. I. Studies on responses evoked by light. J. Gen. Physiol.*, 81, 589–601.

Saszik, S., Alexander, A., Lawrence, T. & Bilotta, J. (2002) *APB differentially affects the cone contributions to the zebrafish ERG. Vis. Neurosci.*, 19, 521–529.

Seeliger, M.W., Rilk, A. & Neuhauss, S.C.F. (2002) *Ganzfeld ERG in zebrafish larvae. Doc Ophthalmol*, 104, 57–68.

Shen, Y., Heimel, J.A., Kamermans, M., Peachey, N.S., Gregg, R.G. & Nawy, S. (2009) *A transient receptor potential-like channel mediates synaptic transmission in rod bipolar cells. J. Neurosci.*, 29, 6088–6093.

Shen, Y., Rampino, M.A.F., Carroll, R.C. & Nawy, S. (2012) *G-protein-mediated inhibition of the Trp channel TRPM1 requires the Gβγ dimer. Proc. Natl. Acad. Sci. U.S.A.*, 109, 8752–8757.

Sherry, D.M., Bui, D.D. & Degrip, W.J. (1998) *Identification and distribution of photoreceptor subtypes in the neotenic tiger salamander retina. Vis. Neurosci.*, 15, 1175–1187.

Stockman, A., Sharpe, L.T., Zrenner, E. & Nordby, K. (1991) *Slow and fast pathways in the human rod visual system: electrophysiology and psychophysics. J Opt Soc Am A*, 8, 1657–1665.

Stuart, G.W., McMurray, J.V. & Westerfield, M. (1988) *Replication, integration and stable germ-line transmission of foreign sequences injected into early zebrafish embryos. Development*, 103, 403–412.

Takechi, M., Hamaoka, T. & Kawamura, S. (2003) *Fluorescence visualization of ultraviolet-sensitive cone photoreceptor development in living zebrafish. FEBS Lett.*, 553, 90–94.

Takechi, M., Seno, S. & Kawamura, S. (2008) *Identification of cis-acting elements repressing blue opsin expression in zebrafish UV cones and pineal cells. J. Biol. Chem.*, 283, 31625–31632.

Tse, D.Y., Chung, I. & Wu, S.M. (2012) *Effects Of Glutamate Transporters On Bipolar Cell Responses In Dark-adapted Living Mice*, ARVO Abstract Nr. 3160.

Tsujimura, T., Chinen, A. & Kawamura, S. (2007) *Identification of a locus control region for quadruplicated green-sensitive opsin genes in zebrafish. Proc. Natl. Acad. Sci. U.S.A.*, 104, 12813–12818.

Tummala, S., Fina, M., Dhingra, A. & Vardi, N. (2012) *Gαo1 is Required for the Proper Expression of mGluR6 Transduction Elements in ON-Bipolar Cells*, ARVO Abstract Nr. 4314.

van Genderen, M.M., Bijveld, M.M.C., Claassen, Y.B., Florijn, R.J., Pearring, J.N., Meire, F.M., McCall, M.A., Riemslag, F.C.C., Gregg, R.G., Bergen, A.A.B. & Kamermans, M. (2009) *Mutations in TRPM1 are a common cause of complete congenital stationary night blindness. Am. J. Hum. Genet.*, 85, 730–736.

Vardi, N. & Morigiwa, K. (1997) *ON cone bipolar cells in rat express the metabotropic receptor mGluR6. Vis Neurosci*, 14, 789–794.

Vardi, N., Duvoisin, R., Wu, G. & Sterling, P. (2000) *Localization of mGluR6 to dendrites of ON bipolar cells in primate retina. J Comp Neurol*, 423, 402–412.

Vitorino, M., Jusuf, P.R., Maurus, D., Kimura, Y., Higashijima, S.-I. & Harris, W.A. (2009) *Vsx2 in the zebrafish retina: restricted lineages through derepression. Neural Dev*, 4, 14.

Weng, K., Lu, C., Daggett, L.P., Kuhn, R., Flor, P.J., Johnson, E.C. & Robinson, P.R. (1997) *Functional coupling of a human retinal metabotropic glutamate receptor (hmGluR6) to bovine rod transducin and rat Go in an in vitro reconstitution system. J. Biol. Chem.*, 272, 33100–33104.

Wersinger, E., Schwab, Y., Sahel, J.A., Rendon, A., Pow, D.V., Picaud, S. & Roux, M.J. (2006) *The glutamate transporter EAAT5 works as a presynaptic receptor in mouse rod bipolar cells. J Physiol*, 577, 221–234. Available at: http://www.ncbi.nlm.nih.gov/entrez/query.fcgi?cmd=Retrieve&db=PubMed&dopt=Citation&list_uids=16973698.

Westerfield, M. (2000) *The zebrafish book. A guide for the laboratory use of zebrafish (Danio rerio). 4th ed., Univ. of Oregon Press, Eugene.*

Wong, K.Y. & Dowling, J.E. (2005) *Retinal bipolar cell input mechanisms in giant danio. III. ON-OFF bipolar cells and their color-opponent mechanisms. J. Neurophysiol.*, 94, 265–272.

Wong, K.Y., Adolph, A.R. & Dowling, J.E. (2005a) *Retinal bipolar cell input mechanisms in giant danio. I. Electroretinographic analysis. J Neurophysiol*, 93, 84–93.

Wong, K.Y., Cohen, E.D. & Dowling, J.E. (2005b) *Retinal bipolar cell input mechanisms in giant danio. II. Patch-clamp analysis of on bipolar cells. J Neurophysiol*, 93, 94–107.

Wong, K.Y., Gray, J., Hayward, C.J.C., Adolph, A.R. & Dowling, J.E. (2004) *Glutamatergic mechanisms in the outer retina of larval zebrafish: analysis of electroretinogram b- and d-waves using a novel preparation. Zebrafish*, 1, 121–131.

Zeitz, C., van Genderen, M., Neidhardt, J., Luhmann, U.F.O., Hoeben, F., Forster, U., Wycisk, K., Mátyás, G., Hoyng, C.B., Riemslag, F., Meire, F., Cremers, F.P.M. & Berger, W. (2005) *Mutations in GRM6 cause autosomal recessive congenital stationary night blindness with a distinctive scotopic 15-Hz flicker electroretinogram. Invest. Ophthalmol. Vis. Sci.*, 46, 4328–4335.

Zhao, X.-F., Ellingsen, S. & Fjose, A. (2009) *Labelling and targeted ablation of specific bipolar cell types in the zebrafish retina. BMC Neurosci*, 10, 107.

Chapter 5

Molecular Dissection of the Circadian Rhythm found in Zebrafish Visual Sensitivity

Marion F. Haug, Edda Kastenhuber, Stephan C. F. Neuhauss

Institute of Molecular Biology, Winterthurerstrasse 190, 8057 Zurich, Switzerland

Report on an ongoing research project

Personal contribution:

preparation of i*n situ* hybridization probes for *mglur6* paralogs and *gnaob*, performing of i*n situ* hybridization experiments (together with EK), preparation of all figures, writing of the manuscript

5.1 Abstract

Many aspects of retinal signaling are under circadian control. This includes visual sensitivity which has been shown to be highest at dusk and lowest in the morning. The molecular mechanism underlying this phenomenon is unknown. In zebrafish ERG b-waves were found to be significantly higher in the evening, thus reflecting the higher visual sensitivity. Since b-waves are generated by the retinal ON-signal, circadian regulation of the ON-pathway might regulate the difference in sensitivity. ON-responses in zebrafish involve bipolar cell hyperpolarization in darkness via the metabotropic glutamate receptor 6 (mGluR6) and possibly glutamate transporters (EAATs). Here, we investigate the circadian regulation of the mGluR6 pathway genes. We find that both *mglur6* paralogs show an increased expression in ON-bipolar cells in the evening, while expression in other layers remains constant. Moreover, *nyctalopin*, known to be of importance for a functional mGluR6 pathway, shows a high expression in ON-bipolar cells in the morning in larvae. In contrast to that, *nyx* is highly expressed in these cells in adult retinal section which may reflects a developmental regulation of this gene. Besides that, *trpm1a* seems to be under circadian control in the photoreceptors, since we only find a staining in this layer in the morning. The effect of this different expression on visual sensitivity is so far unknown but localization of the TRPM1a protein will hopefully shine more light on that.

Our expression study suggests that higher visual sensitivity in the evening is mediated via a more sensitive ON-pathway. Further studies will include functional analysis of the mGluR6 mediated ON-pathway in wild-type and morphant zebrafish larvae.

5.2 Introduction

The visual system is adapted to function over a very broad light range. Additionally, the system needs to be sensitive to daily changes of light in order to react properly upon visual stimuli perceived throughout the 24 hours of a day. Some mechanisms such as translocation of retinal signaling proteins are light-dependent (reviewed in Calvert *et al.*, 2006) but others rely on a working circadian clock that maintains their daily rhythm. The circadian clock composed of two transcriptional feedback loops is constantly ticking and controls these circadian rhythms. Although the clock works endogenously, it is entrained to the environment by so called Zeitgebers of which the day-night shift of light is the most crucial one. Several mechanisms within the retina are mediated by a circadian clock, mostly driven by rhythmic melatonin and dopamine expression (Li & Dowling, 2000; Ribelayga *et al.*, 2002, 2004). Amongst them the ERG b-wave as well as visual sensitivity determined by behavior were found to be highest at dusk adjusting the visual system to darkness (Bassi & Powers, 1987; Li & Dowling, 1998; Lavoie *et al.*, 2010). The mechanism by which visual sensitivity can be adjusted on the molecular level is so far unknown. As the b-wave reflects ON-bipolar cell activity (Stockton & Slaughter, 1989), ON-signaling pathways are the first candidates to generate such differences in visual sensitivity. In zebrafish it has been shown that ON-responses are generated via the inhibitory metabotropic glutamate receptor mGluR6 as well as glutamate transporters (Chapter 4, (Huang *et al.*, 2012; Maurer, 2010). Here, we focus on the mGluR6 mediated ON-signaling and try to elucidate its role in circadian changes of visual sensitivity in zebrafish.

In a detailed expression analysis we found that *mglur6* paralogs are expressed in a circadian manner: they show higher expression in ON-bipolar cells of larval and adult fish in the evening while expression in other layers such as the GCL did not differ throughout 24 hours. Further analysis of the genes involved in the mGluR6-signaling pathway showed that expression of *gnaob* and both *trpm1* paralogs does not change much throughout a day in ON-bipolar cells but *trpm1a* additionally stains photoreceptors in the morning in adult fish. Nyctalopin seems to be differently regulated in larval and in adult tissue: in larvae, *nyx* shows high expression in bipolar cells after light onset but low expression in the evening and in the adult fish it is exactly the other way round, similar to the *mglur6* paralogs. Since similar results were obtained under constant dark conditions we assume that expression is circadian regulated. Our results strongly suggest that higher expression of ON-pathway molecules might lead to increased visual sensitivity. The possibly differential role of NYX in larvae and adults as well as the increased expression of TRPM1a in photoreceptors at dawn in adults needs further investigations.

5.3 Material and Methods

5.3.1 Fish maintenance and breeding

Adult fish were kept under standard conditions at a 14h/10h light/dark cycle at 28°C. For this study only fish of the wild-type strain “WIK” were used. Embryos were raised at 28 °C in E3 medium and staged according to development in days post fertilization (dpf). All experiments were performed in accordance with the ARVO State-

ment for the Use of Animals in Ophthalmic and Vision Research and were approved by the local authorities (Veterinäramt Zürich TV4206).

5.3.2 Whole mount and transverse cross-section *in situ* hybridization

Cloning of zebrafish specific mGluR6 pathway genes, probe preparation, whole mount and slide *in situ* hybridization as well as imaging and image processing were performed as described elsewhere (Chapter 4; Huang *et al.*, 2012). 16-day-old fish were treated like adult fish and retinal sections of the same thickness were produced (16 µm). To ensure similar treatment of am and pm tissue, larvae from different time points were kept in the same tube throughout the experiment. Adult retinal am and pm sections were collected on the same slide. For DD experiments zebrafish embryos were placed and kept in constant darkness from around 10 hours after fertilization on. Adult fish were placed in constant darkness for 4 days prior to fixation. Care was taken to euthanize the fish at the correct time points. Larvae or eyecups fixed during dark hours or for DD experiments were handled under dim red light and fixed in darkness.

5.4 Results

5.4.1 Circadian expression of *mglur6* paralogs

The mRNA expression of *mglur6* paralogs in zebrafish ON-bipolar cells has already been described (Huang *et al.*, 2012), however without focusing on a specific time point of the day. We find clear differences when distinguishing between tissue of larval and adult fish fixed in the morning at 9 am one hour after light onset (corresponds to Zeitgeber time 1) or at 9 pm one hour prior to light offset (corresponds to Zeitgeber time 13). While *mglur6a* shows a similar expression in the GCL and proximal INL of larval and adult fish throughout the day, expression in ON-bipolar cells is variable (Fig. 1A-D). Zebrafish larvae express *mglur6a* in ON-bipolar cells very marginally and only in the evening (Fig. 1D) whereas in adult fish expression in this cells is much stronger but also mainly observed in the evening (Fig. 1B,C). For *mglur6b* the difference was even more apparent. To our surprise, expression in ON-bipolar cells was highly increased and was much more defined at 9 pm in larval and adult retinas (Fig. 1E-H) compared to 9am. As we found similar varying expression patterns in fish kept in constant darkness from shortly after fertilization on or for 4 days in the case of adults (data not shown), we hypothesize that the rhythmic gene expression underlies a circadian rhythm and is not just induced by light. Altogether, these results strongly support our hypothesis of mGluR6 signaling being involved in the circadian regulation of visual sensitivity. The small difference in *mglur6a* expression in the medial INL of larval fish compared to the adults even suggests different regulation throughout development, maybe due to the later incorporation of rods (Branchek & Bremiller, 1984).

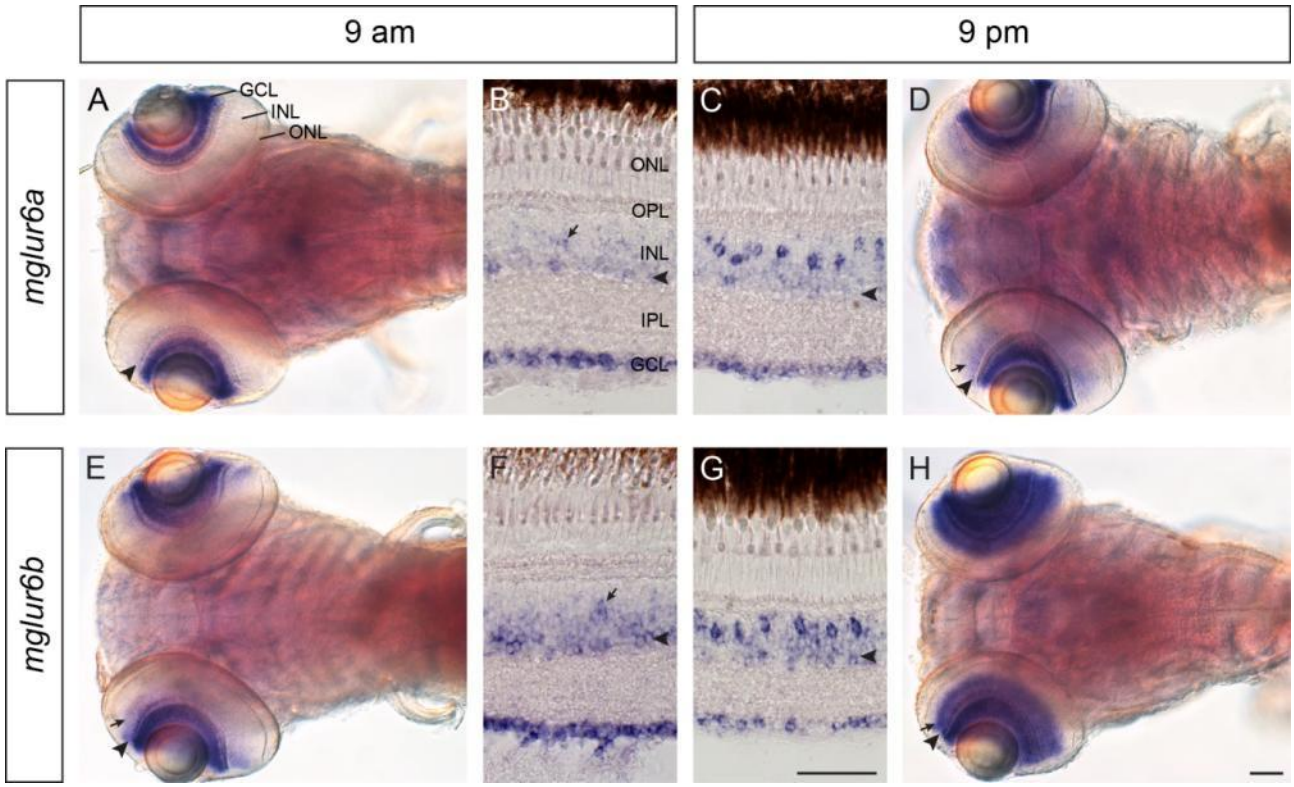

Figure 1: Circadian expression of mglur6 paralogs in the zebrafish retina.
A-D: *Expression of mglur6a in five-day-old larvae (A,D) and in adult retinal slices (B,C) at 9 am and 9 pm.* ***A:*** *Shortly after light onset at 9 am mglur6a is strongly expressed in the GCL of zebrafish larvae. Additionally, a weak expression in the proximal part of the INL is found (arrowhead).* ***B:*** *Similar to the larvae, expression in the adult retina is weak in the proximal INL (arrowhead) but strong in the GCL at 9 am. Some mglur6a-positive ON-bipolar cells are also found (arrow).* ***C:*** *At 9 pm mglur6a expression seems similar in the proximal INL (arrow) and the GCL of adult fish compared to 9 am. A surprising strong mglur6a expression was found in ON-bipolar cells in the medial INL at 9 pm.* ***D:*** *While the mglur6a mRNA is expressed in a similar way in the proximal INL (arrowhead) and the GCL in larvae at dawn and dusk, we find an additional weak expression in the ON-bipolar cells (arrow) at 9 pm.* ***E-H:*** *Expression of mglur6b at 5 dpf (E,H) and in adult retinal cross-sections (F,G) at 9 am and 9 pm.* ***E:*** *The mglur6b riboprobe is predominantly located in the GCL of larval fish but also very faintly in the proximal (arrowhead) and medial (arrow) INL, mostly at the periphery of the retina, at 9 am.* ***F:*** *Similar to larvae, in adult retinal slices mglur6b expression is strong in the GCL. Additionally, mglur6b stains the proximal INL (arrowhead) as well as some ON-bipolar cell bodies (arrow).* ***G:*** *While mglur6b expression in the proximal INL (arrowhead) and the GCL is of similar strength as at 9 am, expression in ON-bipolar cells of adult fish is highly increased at 9 pm.* ***H:*** *In larval zebrafish mglur6b expression in the medial INL is much stronger at 9 pm (arrow) whereas expression in the GCL is similar to 9 am. The proximal IPL (arrowhead) shows a higher mglur6b expression as well, however, the medial and the proximal INL are not fully distinguishable anymore.*
GCL, ganglion cell layer; INL, inner nuclear layer; IPL, inner plexiform layer; ONL, outer nuclear layer; OPL, outer plexiform layer. Scale bar in G (applies to B,C,F,G) = 50 µm, scale bar in H (applies to A,D,E,H) = 20 µm.

5.4.2 Expression of *trpm1a* and *nyx* depends on developmental stage and time of the day

After we found a strong circadian oscillating expression pattern for *mglur6b* in ON-bipolar cells we investigated the other known members of this pathway. Besides the two mGluR6 paralogs, an intracellular G-protein (*gnaob*), nyctalopin (*nyx*), and the two TRPM1 paralogs (*trpm1a* and *-1b*) have shown to be co-expressed in ON-bipolar cells of the zebrafish retina (Chapter 4). While we found unchanged expression domains at both time points for *gnaob* and *trpm1b* (data not shown), we detected a different expression in larval and adult fish using the *trpm1a*

and *nyx* riboprobes. Because this might be due to the later incorporation of rods into the zebrafish retina (Branchek & Bremiller, 1984) we expanded our study to 16- and 67-day-old fish. We found that *trpm1a* has a constant expression pattern in ON-bipolar cells (Fig. 2A-H) but is additionally expressed in photoreceptors in the morning, at least in adult retinal slices (Fig. 2C,D). On the other hand *nyx* seems to be completely differentially regulated in larval and adult zebrafish. In larvae, *nyx* is highly expressed in ON-bipolar cells at 9 am but only faintly before light offset (Fig. 2I,M) while in adults it is the other way round: low expression in the morning and high expression in the evening (Fig. 2L,P). This pattern seems to change gradually during development. While *nyx* expression at 16 dpf seems still lower in the evening (Fig. 2JN), expression in the evening is slightly higher at 67 dpf (Fig. 2KO). In DD experiments similar results were found (data not shown). Our data suggest that besides mGluR6b NYX might also contribute to the circadian variability in visual sensitivity. The opposing but gradually changing expression of *nyx* in larval and adult ON-bipolar cells points towards a different function throughout development, maybe due to the later incorporation of rods into the retina. Oscillating *trpm1a* expression in photoreceptors possibly does not directly interfere with the mGluR6 mediated ON-pathway.

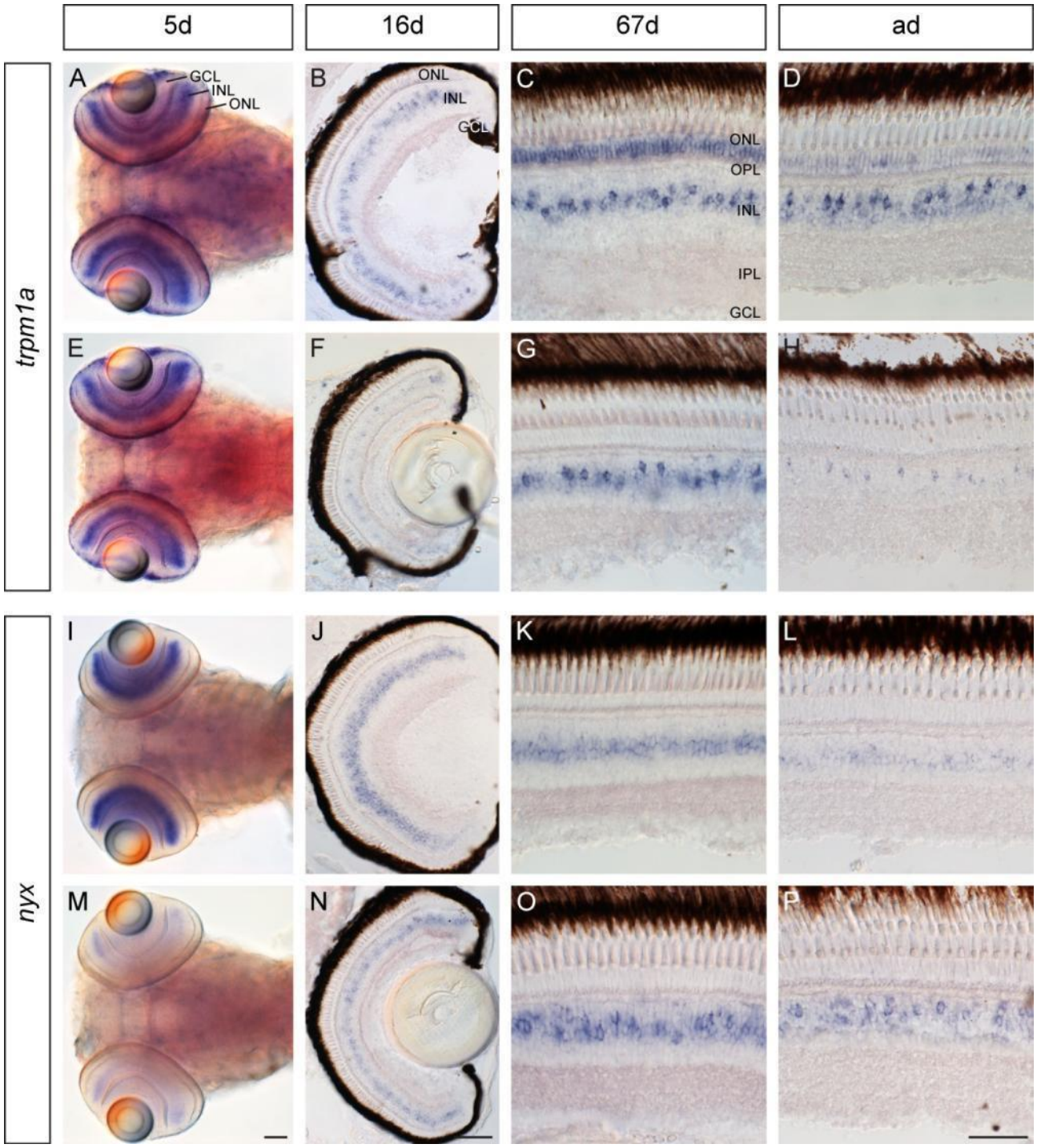

Figure 2: Circadian expression of trpm1a and nyx in the developing fish retina.
A-H: *Expression of trpm1a in 5 (A,E), 16- (B,F), and 67- (C,G) day-old fish as well as in adults (ad, D,H) at 9 am (A-D) and 9 pm (E-H).* ***A,E:*** *The trpm1a riboprobe is expressed in the INL, the ONL and cells around the lens in five-day-old fish at 9 am (A) and 9 pm (E).* ***B,F:*** *At 16 dpf trpm1a expression in the ON-bipolar cells is still stronger in the morning (B) compared to the afternoon (F).* ***C,G:*** *67-day-old fish show a similar labeling of ON-bipolar cells in the INL at 9 am (C) and 9 pm (G). In addition, trpm1a is highly expressed in photoreceptors in the ONL in the morning (C) but not in the evening (G).* ***D,H:*** *Although weaker, the different tprm1a expression in photoreceptors is also visible in adult fish. Moreover, staining of ON-bipolar cell bodies seems weaker at 9 pm (H).* ***I-P:*** *Expression of nyx in five- (I,M), 16- (J,N), and 67- (K,O) day-old fish as well as in adults (ad, L,P) at 9 am (I-L) and 9 pm (M-P).* ***I,M:*** *At 5 dpf nyx is highly expressed in the INL in the morning (I) but only very weakly in the evening (M).* ***J,N:*** *Expression at 16 dpf in the INL is somewhat stronger at 9 am (J), however, it seems more defined to cell bodies at 9 pm (N).* ***K,O:*** *In 67-day-old fish*

expression of nyx has changed and is higher and more defined in the ONL at 9 pm (O) compared to 9 am (K). ***L,P:*** *In adult retinal slices nyx expression in ON-bipolar cells is very weak in the morning (L) but stronger in the evening (P).*
GCL, ganglion cell layer; INL, inner nuclear layer; IPL, inner plexiform layer; ONL, outer nuclear layer; OPL, outer plexiform layer. All scale bars = 50 µm, whereas M applies to A,E,I,M; N applies to B,F,J,N; and P applies to C,D,G,H,K,L,O,P.

5.5 Discussion

A circadian clock oscillates in a more or less 24 hour rhythm and influences many physiological aspects such as hormone release and daily metabolism. It is entrained by external cues, mostly light, to 24 hours, but keeps its rhythm in the absence of such cues (reviewed in Sahar & Sassone-Corsi, 2012). In teleosts, visual sensitivity has shown to be mediated by a circadian clock (Bassi & Powers, 1987; Li & Dowling, 1998). In zebrafish ERG b-waves were found to be highest and the threshold to evoke an ERG b-wave was found to be lowest in the evening (Li & Dowling, 1998). Moreover, the difference in visual sensitivity is mediated by a variation in retinal dopamine levels (Li & Dowling, 2000) that mediate many circadian driven aspects of the retina (reviewed in Witkovsky, 2004). How dopamine exactly mediates this difference in visual sensitivity is unknown. Since ERG b-waves depend on a functional ON-pathway, we hypothesize that molecular differences in the ON-pathway will lead to this difference in visual sensitivity. In our study we also use the zebrafish as a model. Due to its ease in care, the raising availability of reversed genetic tools and its fast developing eye the zebrafish is nowadays a widely used model in vision research and could help us bringing more light into retinal circadian rhythms.

5.5.1 Does circadian oscillation of mGluR6 signaling mediate visual sensitivity changes?

By investigating several members of the mGluR6 pathway on the transcriptional level in larval and adult zebrafish we found that the expression of *mglur6a* and *-6b* is considerably higher in ON-bipolar cell in the evening. We additionally performed a 24 hour analysis concentrating on the time points of light transitions and did similar experiments in DD (data not shown). These results supported our previous data and confirmed the circadian regulation of the oscillating expression. Although the results are only based on mRNA expression they support the idea of a more active ON-pathway at dusk. This would lead to a faster ON-response and generate larger b-wave amplitudes, hence, it would lower the threshold for visual sensitivity as found in zebrafish (Li & Dowling, 1998, 2000).

For *mglur6a* we found a marginal expression in the INL in larvae only in tissue fixed at 9 pm. Whether this small difference in expression could lead to a variation in visual sensitivity between dusk and dawn is not known. The fish used for functional analysis in previous studies were all between 8 and 14 months old (Bassi & Powers, 1987; Li & Dowling, 1998, 2000) and we do not know whether a similar result can be found in larvae. In adult fish we observe a similar variation in *mglur6a* expression in ON-bipolar cells as for *mglur6b*. This implies that mGluR6a is also involved in directing different visual sensitivity, at least in adult fish. Overall, *mglur6a* expression is much stronger in adult ON-bipolar cells at dusk which points to a developmental regulation of gene expression. For mGluR6b we have previously described the involvement in the zebrafish photopic ON-response. So far we did not detect any effect in the ERG b-wave when depleting the mGluR6a protein, however, we also could not confirm the downregulation (data not shown). One reason why we cannot detect any involvement in

photopic ON-responses of mGluR6a might be because it is only mediating rod-derived ON-signals. Rods only start to integrate into the retina at later time points (Branchek & Bremiller, 1984). For that reason the need for a high *mglur6a* expression might not be given in five-day-old fish. However, at later stages, when rods are mature and functional, *mglur6a* expression is useful and expected. We found already at 16 dpf when rods have started to integrate into the retina (Branchek & Bremiller, 1984) high *mglur6a* expression in ON-bipolar cells (data not shown). Due to this result, we see our hypothesis confirmed and believe that *mglur6a* expression is under developmental control. Moreover, it also supports the idea of mGluR6a only mediating scotopic ON-reponses.

5.5.2 Developmental regulation of nyctalopin

While we did not find a different expression for *gnaob* and both *trpm1* paralogs in ON-bipolar cells throughout a day, *nyx* showed a very interesting result. In larvae its expression in the INL is high at dawn whereas in adults it is reversed and we found high expression in ON-bipolar cells at dusk. This expression seems to change gradually during development since at 16 dpf expression in the morning is still slightly higher but in 67-day-old fish expression in the evening is more pronounced. Rod photoreceptors start to integrate into the retina at later stages and are assumed to become functional at around 15 dpf but ERG responses appear still not adult-like at day 29 (Branchek & Bremiller, 1984; Branchek, 1984; Bilotta *et al.*, 2001). If NYX plays different roles in rod and cone visual pathways we would expect a change in expression at around 15 dpf and a stable and adult-like expression at later stages. The gradual changing *nyx* expression is consistent with the development of rod functions. Although scotopic ERG waveforms of fish up to an age of 29 still do not resemble the adult pattern (Bilotta *et al.*, 2001), we believe that the retina should behave adult-like at 67 dpf. However, at that time point we still see a different *nyx* expression compared to adult retinas. Hence, the rod system likely plays a role in regulating *nyx* expression, however, other factors are probably involved as well. The role of NYX in the ON-response of the retina is still incompletely understood. Recent studies propose the involvement of this cell-surface leucine-rich proteoglycan in the transport of mGluR6 and TRPM1 to the membrane (Cao *et al.*, 2011; Pearring *et al.*, 2011). Different NYX expression might therefore influence aggregation or disaggregation of mGluR6 signaling molecules, thereby generating higher or lower thresholds for ON-responses as seen in fish (Bassi & Powers, 1987; Li & Dowling, 1998) or humans (Lavoie *et al.*, 2010).

5.5.3 Rhythmic expression of *trpm1a* in photoreceptors

The transient receptor potential family of cation channels are involved in many sensory tasks (Damann *et al.*, 2008) and therefore it was not surprising to find TRPM1 to be the effector channel of the mGluR6 pathway (Morgans *et al.*, 2009). While *trpm1a* expression in ON-bipolar cells is not under circadian control, the photoreceptors only express this channel in the morning. This suggests that TRPM1a is not involved in mediating visual sensitivity differences within the mGluR6 pathway but it is likely involved in other circadian aspects of vision. As TRPM1 expression was also occasionally found in rod spherules of the human retina (Klooster *et al.*, 2011) a similar function might be present in mammals. It would be of great interest to know the exact time point of fixation of the human retina used for this study. We do not know which pathway leads to the opening or closure of TRPM1a in photoreceptors, which makes it hard to suggest a function. It might be possible to elucidate a role for

this channel in photoreceptors by measuring ERG a-waves at different time points, however, this would need to be accomplished in adult retinas.

To sum up, our study shows the circadian regulation of *mglur6b* and *nyx* in ON-bipolar cells and hence suggests that circadian regulation of visual sensitivity is guided by a variable activity of the mGluR6 pathway. Moreover, the additional finding of *trpm1a* being only expressed in photoreceptors in the morning and the differential expression of *nyx* in larval and adult fish shows the importance of the time point of tissue fixation for expression studies. Many physiological aspects are guided by circadian rhythms and a lot of symptoms can only be cured if medicals are given at the right physiological condition of the patient (reviewed in Sewlall *et al.*, 2010; Ohdo, 2010). During the last decade research focused more and more on this aspect, however, too often circadian regulation is neglected when doing basic research.

Altogether, this study will bring more insight into retinal ON-signaling as well as the understanding of circadian regulation of visual sensitivity.

5.6 Outlook

So far our mRNA expression study including the DD experiments clearly has shown circadian regulation of genes involved in the mGluR6 pathway; but we will continue this study with further experiments. Additionally, we will reverse the light-dark cycle before analyzing fish by *in situ* hybridization to show that circadian expression is not due to any other environmental factors than light. Moreover, as *in situ* hybridization is not quantitative we plan to confirm our results by qRT-PCR. Since expression changes only in distinctive cells we will have to dissect adult retinal layers, which might not be possible in larval fish. As currently transgenic lines are developed in our lab, they could be used for dissecting GFP-positive bipolar cells using FACS. However, most of the mGluR6 pathway members are also expressed in other retinal layers, which complicated the dissection of only bipolar cells by fluorescence in these lines. If we are lucky the promoter or parts of it will only drive expression for the *mglur6* pathway genes in bipolar cells but not in other retinal cells.

So far, we have only focused on mRNA expression but it is of crucial importance to prove circadian regulation at the protein level. Our lab developed zebrafish specific antibodies against both mGluR6 and TRPM1 paralogs as well as NYX. With these we hope to find similar results on the protein level.

To show the functional impact, we will measure thresholds to evoke ON-responses after light onset and before light offset with the visual motor response setup (VMR; Emran *et al.*, 2008) already established in the Neuhauss' lab. Here we might encounter the difficulty of non-ocular photoreception that interferes with normal vision (Fernandes *et al.*, 2012). Due to that we will add threshold measurements of ERG b-waves as was already done in other studies (Li & Dowling, 1998, 2000). However, these studies only used fish between 8 and 14 months where they nicely could show differences in visual sensitivity between am and pm. Although we find a clear difference in expression for *mglur6b* we do not know whether we find similar results on the behavioral level in larval fish. All these studies will include the use of morphant fish where we will be able to see the effects of a missing protein onto the sensitivity of the ON-pathway. A recently developed new technique for gene targeting by transcrip-

tion activator-like effector nucleases (TALENs) (Huang *et al.*, 2011) even enables functional analysis at later developmental stages.

As mentioned in the introduction dopamine was found to regulate a lot of circadian processes in the retina, including visual sensitivity in zebrafish (Li & Dowling, 2000). To study the effect of dopamine depletion on the mGluR6 pathway we could use two approaches. Either via ablation of dopaminergic cells in the retina by injection of 6-hydroxy-dopamine as was already done in zebrafish in the study mentioned above or by using the m1060 mutant that lacks the dopamine synthesizing enzyme tyrosin hydroxylase in the retina but not in other neurons (Löhr, 2009). By including these fish we could study the effect of dopamine depletion on circadian rhythmicity of mGluR6 pathway genes and their functional implications in VMR and ERG studies.

This study can be enlarged to dissect the establishment of these cycles at early larval stages, analyzing the involvement of typical clock genes in the transcriptional regulation of mGluR6 pathway genes, or checking for the circadian regulation of excitatory amino acid transporters (EAATs) known to be involved in ON-signaling (Chapter 4; Grant & Dowling, 1995, 1996; Wersinger *et al.*, 2006). It shows the broad potential and implication of our study and the importance of continuation.

5.7 References

Bassi, C.J. & Powers, M.K. (1987) Circadian rhythm in goldfish visual sensitivity. Invest. Ophthalmol. Vis. Sci., 28, 1811–1815.

Bilotta, J., Saszik, S. & Sutherland, S.E. (2001) Rod contributions to the electroretinogram of the dark-adapted developing zebrafish. Dev. Dyn., 222, 564–570.

Branchek, T. (1984) The development of photoreceptors in the zebrafish, brachydanio rerio. II. Function. J. Comp. Neurol, 224, 116–122.

Branchek, T. & Bremiller, R. (1984) The development of photoreceptors in the zebrafish, Brachydanio rerio. I. Structure. J Comp Neurol, 224, 107–115.

Calvert, P.D., Strissel, K.J., Schiesser, W.E., Pugh, E.N. & Arshavsky, V.Y. (2006) Light-driven translocation of signaling proteins in vertebrate photoreceptors. Trends Cell Biol., 16, 560–568.

Cao, Y., Posokhova, E. & Martemyanov, K.A. (2011) TRPM1 forms complexes with nyctalopin in vivo and accumulates in postsynaptic compartment of ON-bipolar neurons in mGluR6-dependent manner. J. Neurosci., 31, 11521–11526.

Damann, N., Voets, T. & Nilius, B. (2008) TRPs in our senses. Curr. Biol., 18, R880-9.

Emran, F., Rihel, J. & Dowling, J.E. (2008) A behavioral assay to measure responsiveness of zebrafish to changes in light intensities. J Vis Exp.

Fernandes, A.M; Fero K.; Arrenberg, A.B; Bergeron, S.A; Driever, W.; Burgess, H.A (2012) Deep brain photoreceptors control light seeking behavior in zebrafish larvae. Current Biology. In press.

Grant, G.B. & Dowling, J.E. (1995) A glutamate-activated chloride current in cone-driven ON bipolar cells of the white perch retina. J Neurosci, 15, 3852–3862.

Grant, G.B. & Dowling, J.E. (1996) On bipolar cell responses in the teleost retina are generated by two distinct mechanisms. J Neurophysiol, 76, 3842–3849.

Huang, P., an Xiao, Zhou, M., Zhu, Z., Lin, S. & Zhang, B. (2011) Heritable gene targeting in zebrafish using customized TALENs. Nat. Biotechnol., 29, 699–700.

Huang, Y.-Y., Haug, M.F., Gesemann, M. & Neuhauss, S.C.F. (2012) Novel expression patterns of metabotropic glutamate receptor 6 in the zebrafish nervous system. PLoS ONE, 7, e35256.

Klooster, J., Blokker, J., Brink, J.B. ten, Unmehopa, U., Fluiter, K., Bergen, A.A.B. & Kamermans, M. (2011) Ultrastructural localization and expression of TRPM1 in the human retina. Invest. Ophthalmol. Vis. Sci., 52, 8356–8362.

Lavoie, J., Gagné, A.-M., Lavoie, M.-P., Sasseville, A., Charron, M.-C. & Hébert, M. (2010) Circadian variation in the electroretinogram and the presence of central melatonin. Doc Ophthalmol, 120, 265–272.

Li, L. & Dowling, J.E. (1998) Zebrafish visual sensitivity is regulated by a circadian clock. Vis. Neurosci., 15, 851–857.

Li, L. & Dowling, J.E. (2000) Effects of dopamine depletion on visual sensitivity of zebrafish. J. Neurosci., 20, 1893–1903.

Löhr, H. (2009) A genetic screen for mutations affecting development of catecholaminergic systems in zebrafish reveals a novel role for the transcription factors Arnt2 and Sim1, Ph.D. Thesis, Albert-Ludwigs-Universität, Freiburg im Breisgau, Germany.

Maurer, C.M. (2010) Aspects of retinal signaling and visual behavior in the zebrafish, Ph.D. Thesis, University of Zurich, Switzerland.

Morgans, C.W., Zhang, J., Jeffrey, B.G., Nelson, S.M., Burke, N.S., Duvoisin, R.M. & Brown, R.L. (2009) TRPM1 is required for the depolarizing light response in retinal ON-bipolar cells. Proc. Natl. Acad. Sci. U.S.A., 106, 19174–19178.

Ohdo, S. (2010) Chronotherapeutic strategy: Rhythm monitoring, manipulation and disruption. Adv. Drug Deliv. Rev., 62, 859–875.

Pearring, J.N., Bojang, P., Shen, Y., Koike, C., Furukawa, T., Nawy, S. & Gregg, R.G. (2011) A role for nyctalopin, a small leucine-rich repeat protein, in localizing the TRP melastatin 1 channel to retinal depolarizing bipolar cell dendrites. J. Neurosci., 31, 10060–10066.

Ribelayga, C., Wang, Y. & Mangel, S.C. (2002) Dopamine mediates circadian clock regulation of rod and cone input to fish retinal horizontal cells. J. Physiol. (Lond.), 544, 801–816.

Ribelayga, C., Wang, Y. & Mangel, S.C. (2004) A circadian clock in the fish retina regulates dopamine release via activation of melatonin receptors. J. Physiol. (Lond.), 554, 467–482.

Sahar, S. & Sassone-Corsi, P. (2012) Regulation of metabolism: the circadian clock dictates the time. Trends Endocrinol. Metab., 23, 1–8.

Sewlall, S., Pillay, V., Danckwerts, M.P., Choonara, Y.E., Ndesendo, V.M.K. & Du Toit, L.C. (2010) A timely review of state-of-the-art chronopharmaceuticals synchronized with biological rhythms. Curr Drug Deliv, 7, 370–388.

Stockton, R.A. & Slaughter, M.M. (1989) B-wave of the electroretinogram. A reflection of ON bipolar cell activity. J. Gen. Physiol., 93, 101–122.

Wersinger, E., Schwab, Y., Sahel, J.-A., Rendon, A., Pow, D.V., Picaud, S. & Roux, M.J. (2006) The glutamate transporter EAAT5 works as a presynaptic receptor in mouse rod bipolar cells. J. Physiol. (Lond.), 577, 221–234.

Witkovsky, P. (2004) Dopamine and retinal function. Doc Ophthalmol, 108, 17–40.

Chapter 6

The Cryptochrome Family: Comparative Phylogeny and Expression in larval Zebrafish

Matthias Gesemann*, Marion F. Haug*, Viktor Lazovic, Stephan C. F. Neuhauss

Institute of Molecular Biology, Winterthurerstrasse 190, 8057 Zurich, Switzerland

*these authors contributed equally to this work

Report on an ongoing research project

Personal contribution:

project idea, expression study (together with VL), preparation of all figures except figure 1, writing of the manuscript

6.1 Abstract

The cryptochrome (Cry) family of blue-light receptors are descendants of CPD photolyases, although most of their members lost their photolyases activity. Crys are involved in the regulation of the circadian clock from plants to animals, however different mechanisms have been observed. While the *Drosophila*-type Crys act directly in a light-dependent way on the negative feedback loop that generates rhythmic gene expression, mammalian Crys do not depend on light but are rather involved in a transcriptional-translational feedback loop that mediates oscillating gene expression. All zebrafish *crys* were described to show oscillating expression patterns but specific expression that could indicate a function in circadian entrainment have not been found.

The inclusion of cryptochrome sequences from several species ranging from insects up to humans allowed us to draw a complete phylogenetic tree. This analysis revealed misinterpretations in earlier studies forcing us to renaming certain zebrafish cryptochromes according to phylogenetic relationship. Expression studies performed with gene paralogs help identifying evolutionary events such as neo- or subfunctionalization. Since all mammalian-type zebrafish *crys* are expressed in similar regions of larval fish, we hypothesize that function amongst them did not split. Further synteny analysis and comparative expression will shine more light on the interesting evolutionary events within the cryptochrome family.

6.2 Introduction

Cryptochromes (Crys), as the name already implies, were first described as the "cryptic" blue-light photoreceptors in plants that control aspects of growth and development such as seedling growth and flowering time (reviewed in Lin, 2000). Only in the 1990s the gene was cloned and identified as a UV- and blue-light absorbing flavoprotein with a close relationship to DNA photolyases (Ahmad & Cashmore, 1993). While photolyases possess the ability to repair UV-induced DNA damage, cryptochromes have lost or reduced this function (Malhotra *et al.*, 1995, reviewed in Sancar, 2003). Until now, cryptochromes have been described in bacteria, plants and animals where they are involved in a variety of light responses, most importantly circadian activity regulation (reviewed in Chaves *et al.*, 2011). The family is divided into two major groups: the plant cryptochromes and the animal cryptochromes. The latter can either be directly light-sensitive (*Drosophila*-type), or light-irresponsive and possess the ability to inhibit CLOCK:BMAL1 mediated transcription (mammalian-type). In some species another cryptochrome, CryDASH, that does not fit in any of the groups, is described (Brudler *et al.*, 2003; Hitomi *et al.*, 2000; Daiyasu *et al.*, 2004). It possesses the ability of photorepair and might be an intermediate between photolyases and cryptochromes. While mammals only feature the two mammalian-type cryptochromes Cry1 and Cry2 (Hsu *et al.*, 1996), some species such as monarch butterflies (Zhu *et al.*, 2008), zebrafish (Kobayashi *et al.*, 2000) or chicken (Ozturk *et al.*, 2009) maintain different types of cryptochromes within their genome. Amongst all animals, the zebrafish harbors the largest already described cryptochrome family with 7 members and a still active photolyase (Kobayashi *et al.*, 2000; Tamai *et al.*, 2004; Daiyasu *et al.*, 2004). An additional whole genome duplication event that happened about 350 Million years ago at the base of the teleost lineage had possibly led to this increase in gene number (Amores *et al.*, 1998; Vandepoele *et al.*, 2004). Such large-scale genomic events are not uncommon in evolution and likely build the basis of species radiation (Aury *et al.*, 2006; reviewed in Ohno, 1999 and Volff, 2005). Duplication of a gene leads to a redundant gene copy with identical functions, which minimizes the selective pressure to maintain both copies. Still, based on different approaches and data sets between 12 and 24% of duplicated genes were found to be retained in the genome (Postlethwait *et al.*, 2000; Lynch *et al.*, 2001; Jaillon *et al.*, 2004; Woods *et al.*, 2005; Brunet *et al.*, 2006; Kassahn *et al.*, 2009). Force and colleagues proposed in their duplication-degeneration-complementation (DDC) model the scenario of subfunctionalization that could explain this surprisingly high number: if each gene retains at least one ancestral function, the urge for both copies to become fixed in the genome raises (Force *et al.*, 1999). They additionally describe neofunctionalization, in which one paralog acquires a novel function through mutations within its regulatory elements and/or the structural gene, while the second copy renders the ancestral function. Due to their particular position regarding evolutionary events, the rising interest in zebrafish as a model organism, and the already sequenced genome, zebrafish are an attractive vertebrate model to study phylogenetic events. To shine more light on cryptochrome evolution and their possible functions, we investigated the phylogenetic relationship of cryptochromes in zebrafish and various species. Since we found misinterpretations of earlier phylogeny we renamed specific cryptochromes according to their phylogeny. The two zebrafish cryptochrome paralogs 1 and 3 (formerly named Cry2) both likely arose from a whole genome duplication event rather than tandem duplication. A rearrangement of the tree helped identifying the so far unknown zebrafish ortholog for the mammalian Cry2. In addition, an mRNA expression study in larval zebrafish revealed a broad distribution of the *cryptochromes -1*, *-3*, and *-4* in

the central nervous system (CNS). The two *cry1* and *-3* paralogs are both expressed in similar areas, which led us to the conclusion that the function seems not to have split amongst the two paralogs. Interestingly, *cryDASH* is expressed in the ciliary marginal zone around the lens. A synteny analysis as well as further investigation of expression including other species related to zebrafish is necessary to shine more light on cryptochrome evolution and function.

6.3 Material and Methods

6.3.1 Fish maintenance and breeding

Adult fish were kept under standard conditions at a 14h/10h light/dark cycle at 28°C. For this study only fish of the wild-type strain "Tü" were used (Haffter *et al.*, 1996). Embryos were raised at 28 °C in E3 medium (5mM NaCl, 0.17mM KCl, 0.33mM $CaCl_2$, and 0.33mM $MgSO_4$) and staged according to development in days post fertilization (dpf). All examinations were performed in accordance with the ARVO Statement for the Use of Animals in Ophthalmic and Vision Research and were approved by the local authorities (Veterinäramt Zürich TV4206).

6.3.2 Annotation of *cryptochrome* sequences

The sequences of all 8 zebrafish *cryptochromes* have been previously determined (Kobayashi *et al.*, 2000) and were confirmed in our lab by re-annotations, cloning from zebrafish cDNA and subsequent sequencing.

6.3.3 Phylogenetic tree analysis

Cryptochrome sequences for the different species used were identified using the zebrafish and human *cryptochrome* sequences as templates for Blast searches. Cry amino acid sequences were aligned using MUSCLE v3.7 configured for highest accuracy (MUSCLE with default settings). After alignment, ambiguous regions (i.e. containing gaps and/or being poorly aligned) were removed with Gblocks v0.91b. Remaining homologous sequences were reverse translated into nucleic acids and phylogenetic trees were reconstructed using the maximum likelihood method implemented in the PhyML program v3.0. The gamma shape parameter was estimated directly from the data. Branch reliability was assessed by the approximate likelihood-ratio test (aLRT, SH-like). Graphical representations of the phylogenetic trees were obtained using TreeDyn v198.3 and edited in Coral draw (Coral Corporation).

6.3.4 Cloning of zebrafish *cryptochromes*

Sequences of the previously described zebrafish *crys* were downloaded from zfin (http://zfin.org) and various primers for PCR amplification were ordered (Sigma-Aldrich, Buchs SG, Switzerland). Amplified fragments were sequenced were purified using the NucleoSpin Extract II kit (Macherey-Nagel, Oensingen, Switzerland) and subsequently cloned into a pCRII vector (pCRII TOPO TA-cloning kit; Invitrogen, Life Technologies, Zug, Switzerland). 6 µl of ligated plasmid DNA were added to 50 µl of bacterial suspension (OneShot TOP10; Invitrogen), left on ice for 20 min before being incubated for 40 sec at 42°C and again placed on ice for 2 min. 500 µl pre-warmed,

sterile 25% LB-medium (Luria Broth Base; Invitrogen) was added and the cell suspension was incubated for 1 h at 37°C in a gently shaking incubator. Afterwards, the cells were collected by centrifugation (8000 rpm for 3 min). The supernatant was discarded, the cells re-suspended and plated onto pre-warmed agar plates containing ampicillin (0.1 mg/ml), IPTG (0.71 µg/ml; Roche, Basel, Switzerland), and X-Gal (48 µg/ml; Roche). The plates were incubated over night at 37°C. The next day, colonies were picked using a sterile pipette tip, transferred to a snap-cap containing 5 ml of 25% LB-medium with ampicillin (0.1 mg/ml), and incubated over night in a shaking incubator at 37°C. Plasmid DNA was isolated and purified with the NucleoSpin Plasmid kit (Macherey-Nagel), concentration was measured using a NanoDrop (ND-1000; Witec AG, Litau, Switzerland). Subsequently, plasmids were sequenced in house.

6.3.5 *In situ* hybridization

6.3.5.1 Probe preparation

The primers used for probe preparation are listed in table 1. Plasmids were linearized for T7 and Sp6 *in vitro* transcription and purified on a column (Macherey-Nagel). The probes were DIG-labeled using a kit (DIG-RNA labeling kit; Roche). Transcripts were hydrolyzed to obtain fragments of approximately 300 - 500 nucleotides of length. As working probes a mixture of non-hydrolyzed (2 ng/ul) and hydrolyzed (1 ng/ul) probe were used.

Gene	Primer	5' to 3'	Gene	Primer	5' to 3'
cry1a	1a_dr_0359s	F: CAGGCGTGGAGGTGATAG	*cry2*	2_dr_1073s	F: GACATGCAGTAGCCTGTTTC
	1a_dr_0979as	R: AAGCCTCTGGGTTTTTATC		2_dr_1832as	R: TTGCAATCGGTGAAAACAC
cry1b	1b_dr_-0028s	F: CAGAAGGGGCTGCAATAC	*cry4*	4_dr_0778s	F: CGAACCTTCTACCACAGACTC
	1b_dr_0819as	R: TGGACAGTCCCTCTGTTTC		4_dr_1090as	R: CTCCGCGAGTCAGAAAAC
cry3a	3a_dr_1078s	F: GCTGTTGCATGTTTCCTC	*cry5*	5_dr_0838s	F: GATCCTCCGGTTTCTCTG
	3a_dr_1976as	R: TCAACTGTGCCATGTTTTG		5_dr_1526as	R: ATGGATGGACTCGCTTTG
cry3b	3b_dr_1171s	F: GCGGACTGGAGTGTGAAC	*cryDASH*	DASH_dr_-0013s	F: GCCGGTCTTCATGATGTC
	3b_dr_1963as	R: GGGAAGTTATAACACATTTAGC		DASH_dr_1613as	R: GATGCTGCAGTGTCACTTG

Table 1: Primer pairs used for riboprobe preparation.
Numbers within primer names indicate the position of the primer from the ATG on.

6.3.5.2 Whole mount *in situ* hybridization

Embryos used for ISH were treated with 0.2 mM PTU (1-phenyl-2-thiourea; Sigma-Aldrich) to prevent melanization of skin melanocytes and the retinal pigment epithelium. Embryos for the DD control were placed into complete darkness at 6 hpf. At the 5th dpf embryos were fixed in 4% paraformaldehyde (PFA; Sigma-Aldrich) in phosphate buffered saline, pH 7.4 (PBS) at the appropriate time point (7 am, 11 am , 7 pm, 11 pm) overnight (ON) at 4°C. Embryos kept in darkness were fixed under dim red light. The next day, the embryos were washed twice in PBS containing 1% Tween (PBT), dehydrated in a graded series of PBT:MeOH mixtures (3:1; 1:1; 1:3), and stored in 100% MeOH at -20°C until further use.

In situ hybridization and imaging was performed as previously described (Huang *et al.*, 2012). Images were processed and arranged with Adobe Photoshop and Illustrator.

6.4 Results

6.4.1 Cryptochrome phylogeny

We investigated the cryptochrome phylogenetic relationship in a variety of species ranging from chordates to mammals. For alignment reasons CryDASHs were excluded and the tree was rooted with the *Drosophila* CryX2. Overall, the zebrafish appears to possess the largest number of cryptochrome representatives. All vertebrates feature the two mammalian-type cryptochromes Cry1 and Cry2, however, the teleost orthologs built a separate group within those two branches. While the sea lamprey, the ancestor of all vertebrates, possesses one gene copy of a Cry1/3 ortholog, all species retained the Cry1s in their genome after a whole genome duplication event and only the teleost fish still possess a Cry3 ortholog. Amongst them, the zebrafish is the only member which retained both paralogs. Insects such as the flour beetle possess one Cry that falls into the family tree and that seems closer related to the animal Cry1, -2 and -3s. Only birds, lizards and the zebrafish possess a Cry4 and only lower vertebrates such as the lizard, the frog and teleost fish retain a Cry5 copy within their genome.

Fig. 1: The cryptochrome phylogeny.
Zebrafish possess the largest cryptochrome family amongst the investigated animals. Zebrafish cry genes are highlighted in dark red and other teleost cry genes are highlighted in light red.
The phylogenetic tree was built using using the Maximum-likelyhood method and the scale bar corresponds to 30% nucleotide exchanges.
ac: Anolis carolinensis; am: Apis mellifera; bomt: Bombyx mori; cf: Canis familiaris; dm: Drosophila melanogaster; dn: Dasypus novemcinctus; ga: Gasterosteus aculeatus; gg: Gallus gallus; hs: Homo sapiens; md: Monodelphis domestica; mg: Meleagris gallopavo; mm: Mus musculus; oa: Ornithorhynchus anatinus; ol: Oryzias latipes; pm: Petromyzon marinus; tc: Tribolium castaneum; tg: Taeniopygia guttata; tr: Takifugu rubripe; xt: Xenopus tropicalis.

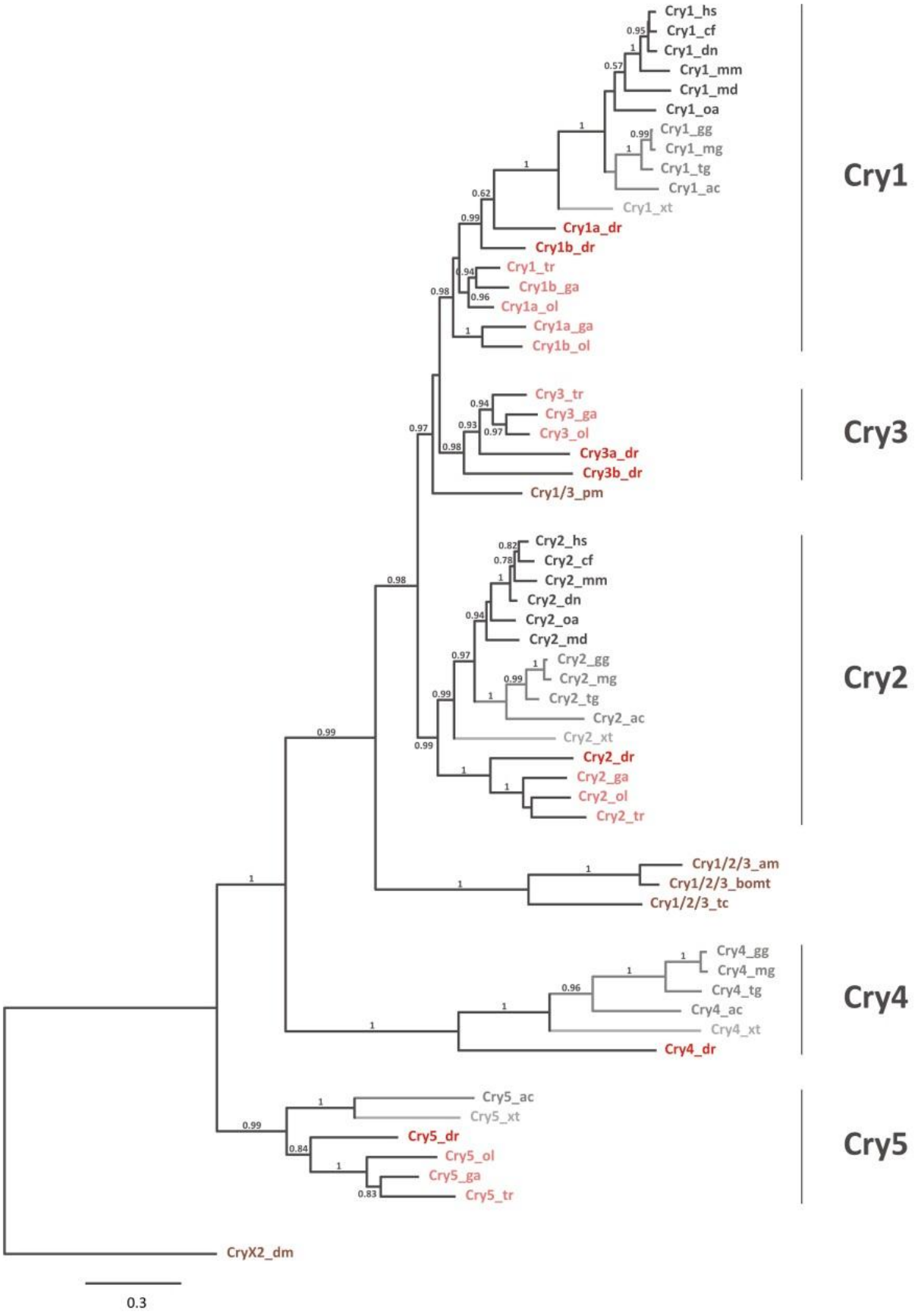
Cry1_hs
Cry1_cf
Cry1_dn
Cry1_mm
Cry1_md
Cry1_oa
Cry1_gg
Cry1_mg
Cry1_tg
Cry1_ac
Cry1_xt
Cry1a_dr
Cry1b_dr
Cry1_tr
Cry1b_ga
Cry1a_ol
Cry1a_ga
Cry1b_ol
Cry1
Cry3_tr
Cry3_ga
Cry3_ol
Cry3a_dr
Cry3b_dr
Cry1/3_pm
Cry3
Cry2_hs
Cry2_cf
Cry2_mm
Cry2_dn
Cry2_oa
Cry2_md
Cry2_gg
Cry2_mg
Cry2_tg
Cry2_ac
Cry2_xt
Cry2_dr
Cry2_ga
Cry2_ol
Cry2_tr
Cry2
Cry1/2/3_am
Cry1/2/3_bomt
Cry1/2/3_tc
Cry4_gg
Cry4_mg
Cry4_tg
Cry4_ac
Cry4_xt
Cry4_dr
Cry4
Cry5_ac
Cry5_xt
Cry5_dr
Cry5_ol
Cry5_ga
Cry5_tr
Cry5
CryX2_dm
0.3

6.4.2 Expression of *cryptochromes* in zebrafish embryos

The sparse knowledge about overall *cryptochrome* expression led us to perform an *in situ* hybridization analysis on five-day-old zebrafish embryos.

Both *cry1* paralogs are located in the same areas of the zebrafish central nervous system (CNS). Expression was detected in the ganglion cell layer (GCL), the proximal part of the inner nuclear layer (INL), the ear (arrowheads in Fig. 2A,C), and in broad regions of the central nervous system corresponding to the tegmentum (T) and the medulla oblongata (MO) (Fig. 2). Overall expression of *cry1b* seemed less pronounced.

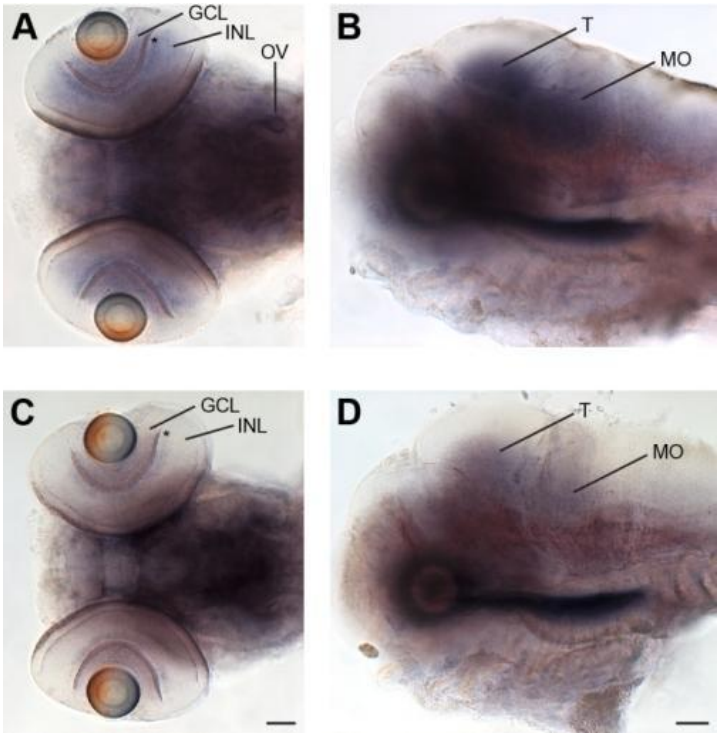

Fig. 2: Expression of cry1 paralogs in 5 dpf zebrafish embryos.
A,B: *Cry1a expression in a dorsal (A) and lateral (B) view. The cry1a riboprobe is expressed in the proximal inner nuclear layer (INL; asterisk) and the ganglion cell layer (GCL) of the retina. A staining is also visible in the otic vesicle (OV). While the dorsal view reveals broad expression in the CNS, the lateral view shows most specific labeling in the tegmentum (T) and the medulla oblongata (MO).* ***C,D:*** *cry1b expression in a dorsal (C) and lateral (D) view. Similar to its paralog, cry1b is located in the GCL, the proximal INL (asterisk) and in similar regions of the CNS (ear = arrow in C; T, MO in D). Positive labeling for both cry1 paralogs in the oesophagus (arrows in B and D) were also seen in sense probes (data not shown). The scale bars in C and D correspond to image A and B, respectively. Scale bars = 50 µm.*

The *cry3a* riboprobe strongly labels the ear (arrowhead Fig. 3A,C) and a broad part of the CNS including the optic tectum, the tegmentum and the medulla oblongata (Fig. 3C). Moreover, weak *cry3a* expression was detected in all retinal layers, however, the labeling seemed most pronounced in the proximal INL (Fig. 3B). The *cry3b* RNA is located throughout the whole INL. Labeling of other parts of the embryos was found to be unspecific as no difference between the sense and the antisense probe could be detected (data not shown).

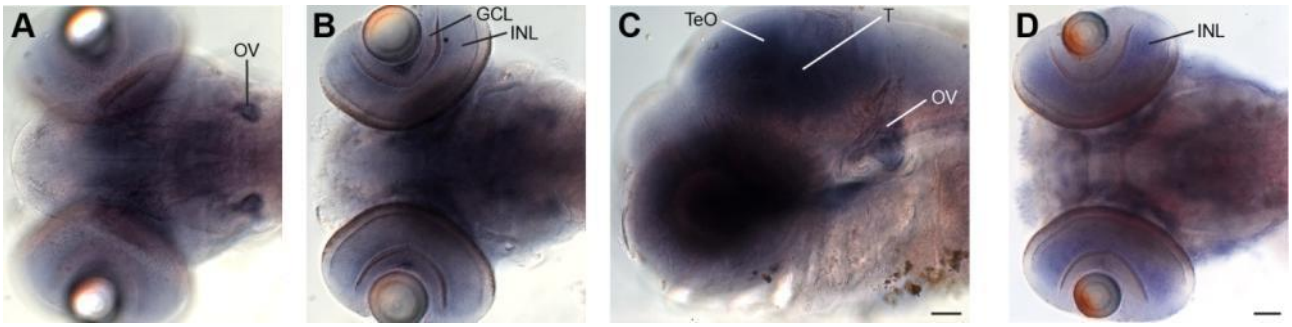

Fig. 3: Expression of cry3 paralogs in 5 dpf zebrafish embryos.
A-C: *Expression of cry3a in dorsal (A,B) and lateral (C) view. The riboprobe of cry3a significantly labels the otic vesicle (OV) and the proximal part of the inner nuclear layer (INL; asterisk) (B), although weak expression is seen throughout all retinal layers (B).The lateral view (C) depicts cry3a expression in the optic tectum (TeO), the tegmentum (T) and the medulla oblongata (MO).* ***D:*** *Expression of cry3b in a dorsal view. Highest labeling of the cry3b riboprobe is found throughout the INL of the retina. The scale bar in D corresponds to the images A and B as well. Scale bars = 50 µm.*

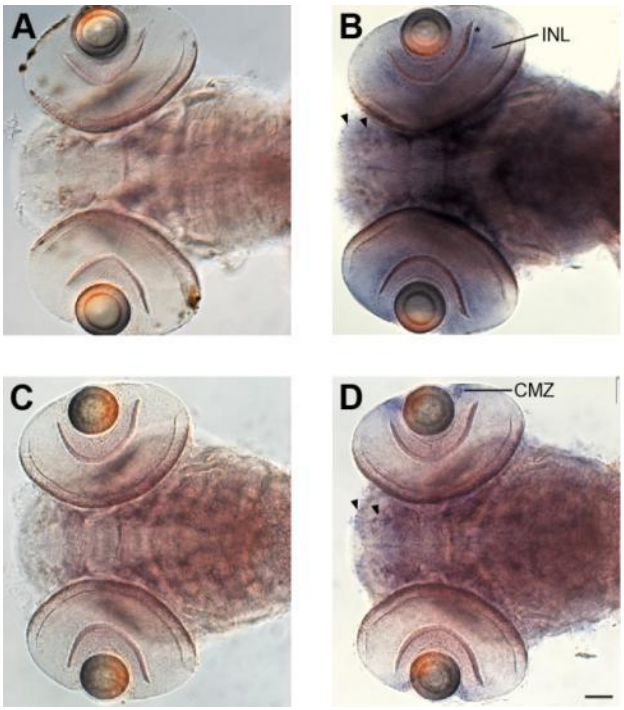

Fig. 4: Expression of cry2, -4, -5, and –DASH in 5 dpf zebrafish embryos.
A: *Expression of the cry2 riboprobe in a dorsal view reveals no expression in a five-day-old fish.* ***B:*** *Dorsal view of an embryo stained with the cry4 riboprobe. The cry4 RNA is weakly expressed in the INL and the GCL but shows a more prominent labeling in the proximal INL (asterisk). Weak expression is also seen throughout the CNS but most prominently in the olfactory epithelium (arrowheads)* ***C:*** *Expression of cry5 in a dorsal view. Application of the cry5 riboprobe does not label any structure in the embryo.* ***D:*** *Dorsal view of cryDASH expression. The cryDASH mRNA is located in few cells of the olfactory epithelium and bulb (arrowheads). Strongest labeling is seen in the ciliary marginal zone (CMZ) in close proximity to the lens. The scale bar in D corresponds to all images A-D. Scale bar = 50 µm.*

We were not able to locate the *cry2* (Fig. 4A) or *cry5* (Fig. 4C) mRNA in five-day-old zebrafish embryos. *Cry4* is weakly expressed in all inner layers of the retina but shows higher expression in the proximal INL (Fig. 4B). Moreover, the *cry4* labeling is weakly detected throughout the CNS. *CryDASH* is located in a few cells of the olfactory epithelium and bulb (arrowheads, Fig. 4D). Most interesting is the *cryDASH* expression around the lens in the ciliary marginal zone (CMZ) of the retina.

6.5 Discussion

A phylogenetic tree shows the evolutionary relationship genes within a family. This helps identifying possible gene functions in different species. Ray-finned fish, amongst them the zebrafish, went through a third round of whole genome duplication after the lineage branched off from the other vertebrates (Ohno, 1999; Christoffels *et al.*, 2004; Postlethwait, 2007). Such events have a huge impact on the evolution of species and it is assumed that this additional whole genome duplication provided the basis for the large radiation of teleost species (Hoegg *et al.*, 2004). Cryptochromes, UV- and blue light receptors of plants and animals, are discussed to have a variety of functions, especially in circadian entrainment (reviewed in Chaves *et al.*, 2011). In zebrafish eight cryptochromes have been described of which two appear to be duplicated gene paralogs (Kobayashi *et al.*, 2000). Until now, cryptochrome phylogeny remained inconsistent. For the mammalian Cry2 no zebrafish ortholog was detected but four zebrafish orthologs were found to segregate with the mammalian Cry1 (Kobayashi *et al.*, 2000; Lin & Todo, 2005). Moreover, phylogenetic trees usually only focused on mammals, fish and plants, or bacteria but did not include any other vertebrate species. We analyzed the phylogeny of the cryptochrome family thoroughly by including different species throughout the animal kingdom. To gain more knowledge about evolutionary events of paralogous genes such as sub- or neofunctionalization (Force *et al.*, 1999) we additionally investigated the expression pattern of the *cryptochrome* family in five-day-old zebrafish larvae by RNA expression analysis.

6.5.1 A thorough phylogenetic analysis uncovers earlier misinterpretations

The presence of cryptochromes is not restricted to the animal kingdom as they can also be found in archaea, bacteria and plants (reviewed in Chaves *et al.*, 2011). In accordance to the publication of Kobayashi and colleagues (Kobayashi *et al.*, 2000) we found 8 zebrafish cryptochromes of which two of them seem to be duplicated. Whether a duplicated gene originates from whole genome duplication rather than tandem duplication can only be determined by analysis of neighboring chromosomal structures in animals that possess one or two orthologs of the same gene. However, the fact that the duplicated genes are all located on different chromosomes already suggests duplication by a whole genome duplication event. Interestingly, we found misinterpretations in earlier publications that we could correct by relying on better sequenced genomes and better tools for analysis. Our analysis suggests a realignment of former cryptochrome phylogeny. According to the results, the zebrafish Cry2 paralogs are closer related with mammalian Cry1s, and Cry3 groups with the mammalian Cry2s. For the benefit of clarity renaming was performed: the zebrafish Cry3 was renamed Cry2, and the zebrafish Cry2 paralogs are now called Cry3a and Cry3b. Moreover, we renamed the zebrafish photolyase z(6-4)phr to Cry5, since, although it has kept its ability to repair UV-induced DNA damage (Kobayashi *et al.*, 2000; Tamai *et al.*, 2004), its sequence homology clearly places it into the cryptochrome family. During the following sections we only used the adapted nomenclature, even though in some cited publications still old names have been used.

6.5.2 Does relationship implicate similar function?

It is obvious that the two *cryptochromes* still present in the mammalian genome represent members of two different subfamilies. Cry1 and -2 in mammals are known to be involved in the core clock of the circadian feedback loop (Kume *et al.*, 1999). Both zebrafish Cry1 paralogs are also able to inhibit CLOCK:BMAL1-mediated transcrip-

tion (Kobayashi *et al.*, 2000). However, in addition Cry1a is described to act as the peripheral light-sensing molecule for the cell-autonomous circadian clocks in zebrafish (Tamai *et al.*, 2007), a function which has been lost during evolution of higher vertebrates. Such a function is supported by the broad mRNA expression found for *cry1a* in the brain. The ancestral function of the gene may have been light-dependent, however, the thick skull of mammals may have led to a dislocation of Cry function from serving as peripheral clock towards acting as light-independent core clock component. As the *cry1b* expression profile (see Chapter 7) points towards another, more light-independent function, it may fulfill a similar function as the mammalian Cry1/2s. In mammals, Cry1 is expressed strongest in the suprachiasmatic nucleus (SCN) (van der Spek *et al.*, 1996), the structure where the core clock is located, and in the retinal ganglion cell layer and inner nuclear layer (Miyamoto & Sancar, 1998). Surprisingly, we were not able to detect higher expression levels of a *cry1* paralog in photoreceptive brain structures such as the pineal gland (Cahill, 1996). Possibly, the zebrafish does not possess a core clock similar to higher vertebrates. The fact that the lack of ventral brain structures where SCN cells would be located barely influences circadian gene expression in other tissues supports that notion (Noche *et al.*, 2011).

All teleost Cry2s build a separate group within the Cry2 branch. As the zebrafish Cry2 was found to belong to the *Drosophila*-type Crys (Kobayashi *et al.*, 2000), teleost Cry2s might all bear other biochemical features than the mammalian Cry2s, implicating a different function. Here, it would be interesting to know more about the features of the Cry2s of the intermediate species armadillo (*dn*), opossum (*md*), and platypus (*oa*), and birds (*gg*, *gm*, *tg*), which build separate groups but are closer related to the mammalian Cry2s. One possible task where Cry2 might be involved is the synchronization of feeding time to the circadian clock. Recently, it has been described that the time of food uptake not only influences gene expression in peripheral tissues of goldfish but also in the brain (Feliciano *et al.*, 2011). Feliciano and colleagues also show that gene expression of Cry2 (termed Cry3 in that study) but not Cry1 and -3 (termed Cry2) oscillates according to food uptake in the optic tectum but still highest and most robust expression was found in the liver. The *in situ* hybridization analysis showed no *cry2* mRNA in the liver or in any other tissue of the larval zebrafish. However, the study mentioned above used qRT-PCR and we might get other results with this technique as well. Some retinal layers of adult fish express *cry2* (see Chapter 7), which demonstrated that the riboprobe itself is functional. A thorough analysis that includes younger fish stages or other time points might reveal additional results. Another possible function for Cry2 could be a light-dependent magnetosensation. The role of cryptochromes in magnetoreception has already been investigated in *Drosophila* (Kassahn *et al.*, 2009; Woods *et al.*, 2005) and birds (Ritz *et al.*, 2000). While migratory birds might use a cryptochrome for compass navigation (reviewed in Liedvogel & Mouritsen, 2010) a functional implication for this feature in other vertebrates and insects has not been found. However, one of the zebrafish cryptochromes might still be magnetosensitive.

While mammals only possess the Cry1 and -2s, other cryptochromes are still present lower vertebrates. These additional cryptochromes may fulfill crucial roles in these species but are apparently not relevant for humans. One interesting exception are the Cry3s. These build an additional branch within the Cry1 lineage but are only present in teleost fish. Surprisingly, the sea lamprey, a common ancestor to all vertebrates, possesses only one *cry1/3* gene. However, following the vertebrate specific genome duplication, all vertebrates must have possessed once a *cry3* ortholog but only the teleost fish retained it within its genome. Even more surprising is the fact that

amongst the teleost fish the zebrafish retained both Cry3 paralogs after the third whole genome duplication event at the base of the teleost lineage. The only teleost known until now to have retained both Cry3 copies as well is the Somalian cavefish. It lives in perpetual darkness, thus has degenerated eyes, and was recently described to possess a food-entrainable infradian clock that runs over about two days (Cavallari *et al.*, 2011). Due to the close evolutionary distance, zebrafish and cavefish showed the same pattern of *cry* retention and the cavefish was excluded from the tree. The zebrafish Cry3s have been described as mammalian-type cryptochromes, being able to inhibit CLOCK:BMAL1 mediated transcription (Kobayashi *et al.*, 2000). Their broad expression as well as their similar expression profiles as the mammalian Cry1 and -2 (see also Chapter 7) lead to the assumption that Cry3s could be clock components as well, maybe fulfilling similar roles in the peripheral clock. However, they are possibly not involved in light-induced entrainment, since the Somalian cavefish still possess both copies as well.

Also birds have one additional cryptochrome, the Cry4, compared to mammals. Why they did not lose this more distant Cry cannot be infered by phylogeny alone. Interesting is the fact that besides birds also lizards and the zebrafish were found to have retained this gene in their genomes. While the zebrafish *cry4* is only very distantly related to the other *cry4s*, we did not find even distantly related *cry4s* in any other tested fish. Initial speculations that this gene is accumulating mutations and will be inactivated soon are contradicted by the fact that the expression throughout the CNS and in inner retinal layers of larval zebrafish is robust, suggesting specific function in zebrafish. Moreover, regulation of the zebrafish *cry4* in the retina seems to be light-dependent (Chapter 7; Kobayashi *et al.*, 2000). This might be a hint for a specific function only in the retina, maybe even in light-input to the central clock or a separate clock located within the retina. However, since in chicken *cry4* expression oscillates differently in different tissues (Kubo *et al.*, 2006), it may has different tissue-dependent functions.

The zebrafish was found to have retained *cry5* or *(6-4)photolyase* (*(6-4)phr*) including its ability to repair UV-damaged DNA strands within its genome (Kobayashi *et al.*, 2000; Tamai *et al.*, 2004). The phylogenetic tree shows that only amphibians, reptiles and fish kept a copy of the *cry5* gene and *in vitro* functionality was also found in frog and snake cell lines (Selby & Sancar, 2006). This gene was lost in higher vertebrates during evolution, possibly before the amniotes branched off. Although we have no proof for that it seems plausible since with the origin of development protected by an egg shell the advantage of having an UV-induced DNA repair mechanisms decreases and releases this gene from selective pressure.

Besides Cry5, CryDASH has also been found to possess a weak remaining photolyase activity, although of the CPD- and not of the (6-4)-type (Daiyasu *et al.*, 2004; Selby & Sancar, 2006; Zikihara *et al.*, 2008). In larval zebrafish *cryDASH* is located around the lens where the ciliary marginal zone (CMZ) is located. This area harbors stem cells which are incorporated into the retina throughout life (Raymond *et al.*, 2006; reviewed in Otteson & Hitchcock, 2003). The CryDASHs ability to repair damaged DNA could help retinal stem cells minimizing their mutation rate. This could happen in a light-dependent way since CryDASH is a *Drosophila*-type Cry (Kobayashi *et al.*, 2000) having biophysical properties suggesting involvement of electron transfer (Zikihara *et al.*, 2008). Besides expression in the CMZ we also located the *cryDASH* mRNA in cells of the olfactory system. Which function it might have in these specific cells remains unknown. CryDASH stands for *Drosophila*, *Arabidopsis*, *Synechocystis* and *Homo*, although it is neither present in fruit flies nor humans it is meant to represent the relationship of

cryptochromes across all areas of life. Because this name is already so well established, we do not consider renaming CryDASH but due to its distant relation to other cryptochromes we excluded this member from the phylogenetic tree.

Some insects such as the monarch butterfly (*Danaus plexippus*) harbor two Cry subfamilies: a *Drosophila*-type Cry1 involved in light-sensitive circadian entrainment and a light-independent mammalian-like Cry2 that represses CLOCK:CYCLE mediated transcription (CYCLE is the insects BMAL1) (Yuan *et al.*, 2007; Zhu *et al.*, 2008). Hence most insects retained only one *cry* in the genome. *Drosophila* kept Cry1, whereas in honeybees (*am*), humblebees (*bomt*), and flour beetles (*tc*) it is Cry2 (Yuan *et al.*, 2007). As our phylogenetic tree includes only the aforementioned insects that harbor Cry2, the insect Crys group closer to the branches of the mammalian-type Cry1 and -2s.

In conclusion a thorough comparative phylogenetic analysis of such a complex gene family is necessary to unravel evolutionary relationships. Mistakes in phylogenetic lineages likely lead to misinterpretations of possible functions. Although final evidence of gene function can only be drawn after functional analysis, expression pattern comparison of gene orthologs provides first information. Considering the high number of cryptochromes in zebrafish, it is very reasonable to assume that they have specific functions and are not solely redundant. The DDC model of Force and colleague nicely explains the high amount of duplicated genes still found in modern genomes of for example teleosts (Force *et al.*, 1999). To identify events such as neo- or subfunctionalization a comparison of the expression pattern of paralogous genes is necessary. Although the mRNA expression analysis of *crys* in larval fish gave hints about possible functions, it did not provide enough information for final conclusions about evolutionary events.

6.6 Outlook

A more thorough expression analysis that includes other larval zebrafish stages will be done in order to get more insight into evolutionary events of gene paralogs. Since our results so far are only preliminary more work has to be done also including other species related to zebrafish into the study. Expression analysis of specific *crys* in the medaka (*Oryzias latipes*), which is also included in the phylogenetic tree, may provide us with information about evolutionary events such as sub-functionalization. Here it would be interesting to look first for *cry3* which is duplicated in zebrafish but not in medaka.

In addition, for a thorough phylogeny more animals need to be incorporated into the tree. Here the monarch butterfly (*Danaus plexippus*) that possesses two cryptochromes with different functions, or the elephant shark (*Callorhinchus milii*), a chordate that branched off before the teleost specific whole genome duplication, could provide further insight.

CryDASH has only been mentioned in the discussion but was not included in the phylogenetic analysis. There has been a lot of discussion about CryDASH function, however, a phylogenetic analysis is not available. A separate tree including CryDASHs from various species could possibly raise the interest in this study.

To finally conclude about evolutionary events on the chromosomal level, a comparison of neighboring genomic regions is necessary. Shared synteny between orthologous genes supports their functional relationship and ancestral non-functional gene parts give hint to evolutionary events. With such an analysis one might detects remnants of a lost *cry3* or *-5* in the mammalian genome. Besides that, a sequence comparison of the functional and conserved regions within each *cry* could give us more insight into each Crys function.

6.7 References

Ahmad, M. & Cashmore, A.R. (1993) HY4 gene of A. thaliana encodes a protein with characteristics of a blue-light photoreceptor. Nature, 366, 162–166.

Amores, A., Force, A., Yan, Y.L., Joly, L., Amemiya, C., Fritz, A., Ho, R.K., Langeland, J., Prince, V., Wang, Y.L., Westerfield, M., Ekker, M. & Postlethwait, J.H. (1998) Zebrafish hox clusters and vertebrate genome evolution. Science, 282, 1711–1714.

Aury, J.-M., Jaillon, O., Duret, L., Noel, B., Jubin, C., Porcel, B.M., Ségurens, B., et. al. (2006) Global trends of whole-genome duplications revealed by the ciliate Paramecium tetraurelia. Nature, 444, 171–178.

Brudler, R., Hitomi, K., Daiyasu, H., Toh, H., Kucho, K.-i., Ishiura, M., Kanehisa, M., Roberts, V.A., Todo, T., Tainer, J.A. & Getzoff, E.D. (2003) Identification of a new cryptochrome class. Structure, function, and evolution. Mol. Cell, 11, 59–67.

Brunet, F.G., Roest Crollius, H., Paris, M., Aury, J.-M., Gibert, P., Jaillon, O., Laudet, V. & Robinson-Rechavi, M. (2006) Gene loss and evolutionary rates following whole-genome duplication in teleost fishes. Mol. Biol. Evol., 23, 1808–1816.

Cahill, G.M. (1996) Circadian regulation of melatonin production in cultured zebrafish pineal and retina. Brain Res., 708, 177–181.

Cavallari, N., Frigato, E., Vallone, D., Fröhlich, N., Lopez-Olmeda, J.F., Foà, A., Berti, R., Sánchez-Vázquez, F.J., Bertolucci, C. & Foulkes, N.S. (2011) A blind circadian clock in cavefish reveals that opsins mediate peripheral clock photoreception. PLoS Biol., 9, e1001142.

Chaves, I., Pokorny, R., Byrdin, M., Hoang, N., Ritz, T., Brettel, K., Essen, L.-O., van der Horst, G.T.J., Batschauer, A. & Ahmad, M. (2011) The cryptochromes: blue light photoreceptors in plants and animals. Annu Rev Plant Biol, 62, 335–364.

Christoffels, A., Koh, E.G.L., Chia, J.-M., Brenner, S., Aparicio, S. & Venkatesh, B. (2004) Fugu genome analysis provides evidence for a whole-genome duplication early during the evolution of ray-finned fishes. Mol. Biol. Evol., 21, 1146–1151.

Daiyasu, H., Ishikawa, T., Kuma, K.-i., Iwai, S., Todo, T. & Toh, H. (2004) Identification of cryptochrome DASH from vertebrates. Genes Cells, 9, 479–495.

Feliciano, A., Vivas, Y., Pedro, N. de, Delgado, M.J., Velarde, E. & Isorna, E. (2011) Feeding time synchronizes clock gene rhythmic expression in brain and liver of goldfish (Carassius auratus). J. Biol. Rhythms, 26, 24–33.

Force, A., Lynch, M., Pickett, F.B., Amores, A., Yan, Y.L. & Postlethwait, J. (1999) Preservation of duplicate genes by complementary, degenerative mutations. Genetics, 151, 1531–1545.

Haffter, P., Granato, M., Brand, M., Mullins, M.C., Hammerschmidt, M., Kane, D.A., Odenthal, J., van Eeden, F.J., Jiang, Y.J., Heisenberg, C.P., Kelsh, R.N., Furutani-Seiki, M., Vogelsang, E., Beuchle, D., Schach, U., Fabian, C. & Nüsslein-Volhard, C. (1996) The identification of genes with unique and essential functions in the development of the zebrafish, Danio rerio. Development, 123, 1–36.

Hitomi, K., Okamoto, K., Daiyasu, H., Miyashita, H., Iwai, S., Toh, H., Ishiura, M. & Todo, T. (2000) Bacterial cryptochrome and photolyase: characterization of two photolyase-like genes of Synechocystis sp. PCC6803. Nucleic Acids Res., 28, 2353–2362.

Hoegg, S., Brinkmann, H., Taylor, J.S. & Meyer, A. (2004) Phylogenetic timing of the fish-specific genome duplication correlates with the diversification of teleost fish. J. Mol. Evol., 59, 190–203.

Hsu, D.S., Zhao, X., Zhao, S., Kazantsev, A., Wang, R.P., Todo, T., Wei, Y.F. & Sancar, A. (1996) Putative human blue-light photoreceptors hCRY1 and hCRY2 are flavoproteins. Biochemistry, 35, 13871–13877.

Huang, Y.-Y., Haug, M.F., Gesemann, M. & Neuhauss, S.C.F. (2012) Novel expression patterns of metabotropic glutamate receptor 6 in the zebrafish nervous system. PLoS ONE, 7, e35256.

Jaillon, O., Aury, J.-M., Brunet, F., Petit, J.-L., Stange-Thomann, N., Mauceli, E., et. al. (2004) Genome duplication in the teleost fish Tetraodon nigroviridis reveals the early vertebrate proto-karyotype. Nature, 431, 946–957.

Kassahn, K.S., Dang, V.T., Wilkins, S.J., Perkins, A.C. & Ragan, M.A. (2009) Evolution of gene function and regulatory control after whole-genome duplication: comparative analyses in vertebrates. Genome Res., 19, 1404–1418.

Kobayashi, Y., Ishikawa, T., Hirayama, J., Daiyasu, H., Kanai, S., Toh, H., Fukuda, I., Tsujimura, T., Terada, N., Kamei, Y., Yuba, S., Iwai, S. & Todo, T. (2000) Molecular analysis of zebrafish photolyase/cryptochrome family: two types of cryptochromes present in zebrafish. Genes Cells, 5, 725–738.

Kubo, Y., Akiyama, M., Fukada, Y. & Okano, T. (2006) Molecular cloning, mRNA expression, and immunocytochemical localization of a putative blue-light photoreceptor CRY4 in the chicken pineal gland. J. Neurochem., 97, 1155–1165.

Kume, K., Zylka, M.J., Sriram, S., Shearman, L.P., Weaver, D.R., Jin, X., Maywood, E.S., Hastings, M.H. & Reppert, S.M. (1999) mCRY1 and mCRY2 are essential components of the negative limb of the circadian clock feedback loop. Cell, 98, 193–205.

Liedvogel, M. & Mouritsen, H. (2010) Cryptochromes--a potential magnetoreceptor: what do we know and what do we want to know? J R Soc Interface, 7 Suppl 2, S147-62.

Lin, C. (2000) Plant blue-light receptors. Trends Plant Sci., 5, 337–342.

Lin, C. & Todo, T. (2005) The cryptochromes. Genome Biol., 6, 220.

Lynch, M., O'Hely, M., Walsh, B. & Force, A. (2001) The probability of preservation of a newly arisen gene duplicate. Genetics, 159, 1789–1804.

Malhotra, K., Kim, S.T., Batschauer, A., Dawut, L. & Sancar, A. (1995) Putative blue-light photoreceptors from Arabidopsis thaliana and Sinapis alba with a high degree of sequence homology to DNA photolyase contain the two photolyase cofactors but lack DNA repair activity. Biochemistry, 34, 6892–6899.

Miyamoto, Y. & Sancar, A. (1998) Vitamin B2-based blue-light photoreceptors in the retinohypothalamic tract as the photoactive pigments for setting the circadian clock in mammals. Proc. Natl. Acad. Sci. U.S.A., 95, 6097–6102.

Noche, R.R., Lu, P.-N., Goldstein-Kral, L., Glasgow, E. & Liang, J.O. (2011) Circadian rhythms in the pineal organ persist in zebrafish larvae that lack ventral brain. BMC Neurosci, 12, 7.

Ohno, S. (1999) Gene duplication and the uniqueness of vertebrate genomes circa 1970-1999. Semin. Cell Dev. Biol., 10, 517–522.

Otteson, D.C. & Hitchcock, P.F. (2003) Stem cells in the teleost retina: persistent neurogenesis and injury-induced regeneration. Vision Res., 43, 927–936.

Ozturk, N., Selby, C.P., Song, S.-H., Ye, R., Tan, C., Kao, Y.-T., Zhong, D. & Sancar, A. (2009) Comparative photochemistry of animal type 1 and type 4 cryptochromes. Biochemistry, 48, 8585–8593.

Postlethwait, J.H. (2007) The zebrafish genome in context: ohnologs gone missing. J. Exp. Zool. B Mol. Dev. Evol., 308, 563–577.

Postlethwait, J.H., Woods, I.G., Ngo-Hazelett, P., Yan, Y.L., Kelly, P.D., Chu, F., Huang, H., Hill-Force, A. & Talbot, W.S. (2000) Zebrafish comparative genomics and the origins of vertebrate chromosomes. Genome Res., 10, 1890–1902.

Raymond, P.A., Barthel, L.K., Bernardos, R.L. & Perkowski, J.J. (2006) Molecular characterization of retinal stem cells and their niches in adult zebrafish. BMC Dev. Biol., 6, 36.

Ritz, T., Adem, S. & Schulten, K. (2000) A model for photoreceptor-based magnetoreception in birds. Biophys. J., 78, 707–718.

Sancar, A. (2003) Structure and function of DNA photolyase and cryptochrome blue-light photoreceptors. Chem. Rev., 103, 2203–2237.

Selby, C.P. & Sancar, A. (2006) A cryptochrome/photolyase class of enzymes with single-stranded DNA-specific photolyase activity. Proc. Natl. Acad. Sci. U.S.A., 103, 17696–17700.

Tamai, T.K., Vardhanabhuti, V., Foulkes, N.S. & Whitmore, D. (2004) Early embryonic light detection improves survival. Curr. Biol., 14, R104-5.

Tamai, T.K., Young, L.C. & Whitmore, D. (2007) Light signaling to the zebrafish circadian clock by Cryptochrome 1a. Proc. Natl. Acad. Sci. U.S.A., 104, 14712–14717.

van der Spek, P.J., Kobayashi, K., Bootsma, D., Takao, M., Eker, A.P. & Yasui, A. (1996) Cloning, tissue expression, and mapping of a human photolyase homolog with similarity to plant blue-light receptors. Genomics, 37, 177–182.

Vandepoele, K., Vos, W. de, Taylor, J.S., Meyer, A. & van de Peer, Y. (2004) Major events in the genome evolution of vertebrates: paranome age and size differ considerably between ray-finned fishes and land vertebrates. Proc. Natl. Acad. Sci. U.S.A., 101, 1638–1643.

Volff, J.-N. (2005) Genome evolution and biodiversity in teleost fish. Heredity (Edinb), 94, 280–294.

Woods, I.G., Wilson, C., Friedlander, B., Chang, P., Reyes, D.K., Nix, R., Kelly, P.D., Chu, F., Postlethwait, J.H. & Talbot, W.S. (2005) The zebrafish gene map defines ancestral vertebrate chromosomes. Genome Res., 15, 1307–1314.

Yuan, Q., Metterville, D., Briscoe, A.D. & Reppert, S.M. (2007) Insect cryptochromes: gene duplication and loss define diverse ways to construct insect circadian clocks. Mol. Biol. Evol., 24, 948–955.

Zhu, H., Sauman, I., Yuan, Q., Casselman, A., Emery-Le, M., Emery, P. & Reppert, S.M. (2008) Cryptochromes define a novel circadian clock mechanism in monarch butterflies that may underlie sun compass navigation. PLoS Biol., 6, e4.

Zikihara, K., Ishikawa, T., Todo, T. & Tokutomi, S. (2008) Involvement of electron transfer in the photoreaction of zebrafish Cryptochrome-DASH. Photochem. Photobiol., 84, 1016–1023.

Chapter 7

Circadian Expression of Cryptochromes in Zebrafish Retina

Marion F. Haug, Viktor Lazovic, Stephan C. F. Neuhauss

Institute of Molecular Biology, Winterthurerstrasse 190, 8057 Zurich, Switzerland

Report on an ongoing research project

Personal contribution:

project idea, expression and qRT-PCR study (together with VL), preparation of all figures, writing of the manuscript

7.1 Abstract

Light emitted by the sun is the most important cue that entrains physiological processes to a 24 hour rhythm, enabling living beings to adjust their behavior to the environment. Due to their thick skull, mammals must process information about light-dark cycles via the retina to the central nervous system. Specific retinal ganglion cells expressing melanopsin absorb light and send this information via the retinohypothalmic tract to the brain, thereby providing non-visual information. Although in recent years melanopsin emerged as the major photopigment for non-visual photoreception, the knock down of cryptochromes (Crys) in mice affected circadian behavior. This suggests that Crys might be involved in the generation or processing of non-visual information as well.

Cryptochromes are descendants of DNA photolyases and absorb light in the UV- and blue range. The family consists of two major subtypes: mammalian-type and *Drosophila*-type Crys. They both regulate circadian oscillation, although not in a similar fashion. While the light-dependent *Drosophila*-type Crys function as circadian photoreceptor that entrains the clock, mammalian-type Crys act as light-independent repressor of CLOCK-BMAL1 components of the circadian clock. Since non-visual photoreception in mammals was found to be located in the eye, we expect any Cry involved in this process to be expressed in an oscillating manner in the retina. In this study we investigate the expression of all zebrafish *crys* in the adult retina by qRT-PCR analysis and *in situ* hybridization. We found a cyclic gene expression for all *crys* in the adult retina and overall, expression levels at different time points overlap with qRT-PCR results. However, we could not convincingly observe layer-specific oscillation. To focus our further analysis on a specific zebrafish Cry a layer-specific qRT-PCR analysis is necessary. The broad distribution of all *crys* in the zebrafish retina suggests other functions besides the involvement in non-visual phototransduction. Their biochemical properties would enable them to even act directly as light sensor and contribute to visual processes.

7.2 Introduction

Our physiology and behavior is strongly influenced by internal daily rhythms maintained by a central pacemaker in the suprachiasmatic nucleus (SCN) of the hypothalamus. The cycle of these circadian rhythms is around 24 hours (*circa diem* = approximately a day) under constant conditions but set to 24 hours by external Zeitgeber cues. Nearly all peripheral cells of mammals possess their own circadian oscillator, however, the central pacemaker synchronizes them to the outside world. Since this "master clock" is located under the skull in the deep brain, information has to find a way to reach this part of the body (reviewed in Dibner *et al.*, 2010).

The steady cycling of light intensities on earth is the major external cue that entrains the central pacemaker. As already first experiments from Jürgen Aschoff showed, light guides a number of crucial physiological processes (reviewed in Daan & Gwinner, 1998). But even in the absence of rods and cones light-mediated non-visual processes such as circadian entrainment to light-dark cycles (Ebihara & Tsuji, 1980; Freedman *et al.*, 1999), pupillary light responses (Lucas *et al.*, 2001), and photic suppression of melatonin synthesis in the pineal gland (Lucas *et al.*, 1999) still take place. Considering that only enucleation leads to a loss of these processes in mammals (Foster *et al.*, 1991; Nelson & Zucker, 1981; Czeisler *et al.*, 1995; Freedman *et al.*, 1999), the retina must be the sole source of non-visual photoreception. Mice lacking melanopsin, an opsin variant with bound retinol located in intrinsically photosensitive retinal ganglion cells (ipRGCs) that project to the SCN (Leak & Moore, 1997; Provencio *et al.*, 2000; Gooley *et al.*, 2001; Berson *et al.*, 2002), show impaired phase shifting of light/dark cycles (Panda *et al.*, 2002). The additional removal of rods and cones in these mutants completely abolished circadian entrainment and other non-visual photoreception (Hattar *et al.*, 2003; Panda *et al.*, 2003). Here, the cryptochromes (Crys) come into play. Vitamin A depletion should lead to impaired non-visual photoresponses, however, in mice lacking retinol only the additional elimination of cryptochromes reduced phototransduction to the SCN and non-visual photoreception (Thompson *et al.*, 2001; Thompson *et al.*, 2004).

Cryptochromes, closely related to DNA photolyases (Kanai *et al.*, 1997), are UV- and blue-light receptors known to be involved in a variety of light responses (reviewed in Chaves *et al.*, 2011). First evidence that they could be involved in circadian rhythmicity was demonstrated by plant scientists who showed an influence of both cryptochrome variants on circadian entrainment (Guo *et al.*, 1998; Somers *et al.*, 1998). Unlike in *Drosophila*, where cryptochromes act as circadian photoreceptor (Emery *et al.*, 1998; Stanewsky *et al.*, 1998), mammalian cryptochromes regulate transcription of crucial clock genes in the negative limb of the feedback loop of the circadian clock (Kume *et al.*, 1999; Shearman *et al.*, 2000). Different studies already assessed the impact of cryptochromes on non-visual photoreception. Mice deficient for both cryptochromes show a totally arrhythmic behavior in constant darkness but retain photic regulation of clock genes in the SCN (Okamura *et al.*, 1999; Vitaterna *et al.*, 1999), and show normal pupillary light responses (van Gelder *et al.*, 2003). Additional depletion of photoreceptors led to the loss of practically all behavioral photoresponses (Selby *et al.*, 2000; van Gelder *et al.*, 2002, 2003). Therefore, besides their function in the feedback loop of the central clock, cryptochromes seem to be involved in non-visual photoreception. This notion is supported by the presence of both mammalian cryptochromes in the inner retina, where circadian photoreception takes place (Miyamoto & Sancar, 1998; Thompson *et al.*, 2003).

Our study aimed to find evidence for an involvement of a certain zebrafish cryptochrome in circadian photoreception. The transparent tissue of *Drosophila* and zebrafish allows each cell to maintain a directly light-responsive, autonomous circadian clock (Emery *et al.*, 1998; Plautz *et al.*, 1997; Whitmore *et al.*, 2000). Cry1a was found to play a crucial role in light entrainment of peripheral clocks in zebrafish (Tamai *et al.*, 2007). These results show that the organization of the circadian system in fish and in insects seems to be distinct from the one of higher vertebrates. Nevertheless, as the zebrafish harbors *Drosophila*-type and mammalian-type Crys, it could serve as a model to study light perception of the circadian system via the retina. In zebrafish, 8 cryptochromes have been described so far (Kobayashi *et al.*, 2000; Daiyasu *et al.*, 2004). Except for *cryDASH* zebrafish *cry* mRNA levels were shown to oscillate in different tissues. mRNA expression in the ganglion cell layer of the retina was reported, however, further description of cryptochrome expression in the zebrafish retina is not available (Kobayashi *et al.*, 2000). Our study focuses on zebrafish *cry* expression in the retina to detect oscillating expression patterns in distinct retinal layers, which would be an indication for an involvement in circadian processes. The qRT-PCR analysis showed cyclic transcript expressions for all zebrafish *crys* in adult retinal tissue, however, it only tells us about overall *cry* expression levels. In order to detect layer specific cyclic expressions, sections were taken from adult eyecups fixed at four different time point throughout 24 hours. Cyclic gene expression is seen as a hint for an involvement in circadian signaling processes and supports a further analysis of these genes. Expression patterns obtained by *in situ* hybridization analysis revealed a broad distribution of all *crys* in the retina. In most cases the overall expression matched the results obtained by qRT-PCR, although the oscillation pattern was not always consistent in each retinal sublayer. Most prominent circadian expression profiles were found for the *cry1* paralogs and *cry2* in the INL, and in the *cry3* paralogs and *cry4* throughout the retina. *In situ* hybridization results were not quantitative enough to detect any zebrafish *cry* gene that has a constant expression in one layer but a cyclic expression in another. In summary, the study reveals a very broad and circadian abundance of all *cryptochromes* in the zebrafish retina. This result even could lead to the idea that cryptochromes are involved in visual processes. The question whether they could actually be involved in non-visual responses to light, is it directly as light sensor or indirectly via melanopsin signaling remains open.

Note that in this manuscript the adapted names of zebrafish cryptochromes according to Chapter 6 in this thesis were used.

7.3 Material and Methods

7.3.1 Fish maintenance and breeding

Adult fish were kept under standard conditions at a 14h/10h light/dark cycle at 28°C. For this study only fish of the wild-type strain “Tü” were used (Haffter *et al.*, 1996). Embryos were raised at 28 °C in E3 medium (5mM NaCl, 0.17mM KCl, 0.33mM $CaCl_2$, and 0.33mM $MgSO_4$) and staged according to development in days post fertilization (dpf). All experiments were performed in accordance with the ARVO Statement for the Use of Animals in Ophthalmic and Vision Research and were approved by the local authorities (Veterinäramt Zürich TV4206).

7.3.2 *In situ* hybridization

7.3.2.1 Probe preparation

Cloning of zebrafish *cryptochrome* genes into pCRII vector is described elsewhere (see Chapter 6). The primers (Sigma-Aldrich, Buchs SG, Switzerland) used for probe preparation are listed in table 1. Plasmids containing the correct *cryptochrome* sequences were linearized for T7 and Sp6 *in vitro* transcription and purified on a column (Macherey-Nagel, Oensingen, Switzerland). The probes were DIG-labeled using a kit (DIG-RNA labeling kit; Roche, Basel, Switzerland). Transcripts were hydrolyzed to obtain fragments of approximately 300 - 500 nucleotides of length. As working probes a mixture of non-hydrolyzed (2 ng/ul) and hydrolyzed (1 ng/ul) probe were used.

7.3.2.2 Slide *in situ* hybridization

Adult zebrafish were euthanized with tricaine (MS-222; Sigma-Aldrich) in iced water at the appropriate time point. Eyecups were removed and fixed ON at 4°C in 4% paraformaldehyde (PFA; Sigma-Aldrich) in phosphate buffered saline, pH 7.4 (PBS). For the DD control, fish were placed into complete darkness for 3.5 to 4 days before scarification. The further protocol is described elsewhere (Huang *et al.*, 2012).

In situ hybridization and imaging was performed as previously described (Huang *et al.*, 2012). Images were processed and arranged with Adobe Photoshop and Illustrator CS5.

7.3.3 Quantitative real-time PCR (qRT-PCR)

After removing the eyecups of the fish at the appropriate time point (Zeitgeber times 3, 7, 11, 15, 19, 23), the tissue was collected in RLT buffer (Quiagen, Hombrechtikon, Switzerland), pounded with the pistil, and homogenized with a sonificator (Sonopuls HD2070; Bandelin Electronic, Berlin, Germany). Fish were euthanized in darkness and eyecups were removed under dim red light when the tissue was collected during the dark period. RNA was extracted with the NucleoSpin RNA II Kit (Macherey-Nagel) and RNA concentration was measured with a NanoDrop (ND-1000; Witec AG, Litau, Switzerland). Reverse transcription was performed with 400 ng RNA and the Superscript II kit (Invitrogen, Life Technologies, Zug, Switzerland). qRT-PCR was performed in a transcriptor (Applied Biosystems Prism SDS 7900HT; Life Technologies) using the MESA Green Kit (Eurogentec, Seraing, Belgium). Primer pairs (Sigma-Aldrich) used for qRT-PCR were specifically designed to incorporate an intron to avoid unspecific amplification of genomic DNA (Tab. 1).

As a reference, the genes *rpl-13α* (ribosomal protein L-13a), *ef1α* (elongation factor 1 alpha), and *prkcα* (protein kinase C alpha) were selected (Tang *et al.*, 2007). The highest expression was given 100% and lower expression was set relative to this total. The values are means +/- standard deviations and were averaged from three independent samples. Analysis was completed in Microsoft Excel and graphs were arranged in Microsoft Excel and Adobe Illustrator CS5.

Gene	*In situ* probe preparation		qRT-PCR	
	Primer	5' to 3'	Primer	5' to 3'
cry1a	1a_dr_0359s	F: CAGGCGTGGAGGTGATAG	1a_dr_0359s	F: CAGGCGTGGAGGTGATAG
	1a_dr_0979as	R: AAGCCTCTGGGTTTTTATC	1a_dr_0461as	R: TGGAAGCGCTTATACGTG
cry1b	1b_dr_-0028s	F: CAGAAGGGGCTGCAATAC	1b_dr_0738s	F: ACACCGGTCAGTGATGATC
	1b_dr_0819as	R: TGGACAGTCCCTCTGTTTC	1b_dr_0819as	R: TGGACAGTCCCTCTGTTTC
cry3a	3a_dr_1078s	F: GCTGTTGCATGTTTCCTC	3a_dr_1078s	F: GCTGTTGCATGTTTCCTC
	3a_dr_1976as	R: TCAACTGTGCCATGTTTTG	3a_dr_1169as	R: CAGTCTGCATCCAAATAGAAG
cry3b	3b_dr_1171s	F: GCGGACTGGAGTGTGAAC	3b_dr_0632s	F: CCGGTGGAGAATCAGAAG
	3b_dr_1963as	R: GGGAAGTTATAACACATTTAGC	3b_dr_0722as	R: TTCGGTCGCTCAAAGTTC
cry2	2_dr_1073s	F: GACATGCAGTAGCCTGTTTC	2_dr_1073s	F: GACATGCAGTAGCCTGTTTC
	2_dr_1832as	R: TTGCAATCGGTGAAAACAC	2_dr_1163as	R: CGCATCCAACAGCAACTC
cry4	4_dr_0778s	F: CGAACCTTCTACCACAGACTC	4_dr_0778s	F: CGAACCTTCTACCACAGACTC
	4_dr_1090as	R: CTCCGCGAGTCAGAAAAC	4_dr_0890as	R: AGCGACGGTGTAGAAGAAC
cry5	5_dr_0838s	F: GATCCTCCGGTTTCTCTG	5_dr_0495s	F: ACCCATTCCTGCTCCAAC
	5_dr_1526as	R: ATGGATGGACTCGCTTTG	5_dr_0600as	R: CAGTCCAAGATCCTCAAGAG
cryDASH	DASH_dr_-0013s	F: GCCGGTCTTCATGATGTC	DASH_dr_0532s	F: ACTCCAGAACAGGTGAAATC
	DASH_dr_1613as	R: GATGCTGCAGTGTCACTTG	DASH_dr_0640s	R: GGAAGGCAGAACGACAGTC
Rpl-13a		-	Rpl13a_dr_0251s	F: GGACTGTAAGAGGTATGCTTC
			Rpl13a_dr_0330as	R: GATGCCATCAAACACCTTC
EF1 α		-	EF1a_dr_0607s	F: GAGGCCAGCTCAAACATG
			EF1a_dr_0698as	R: TCAAGGGCATCAAGAAGAG
prkcα		-	prkca_dr_0363s	F: GGACTCATACACCAAGGAATG
			prkca_dr_0440as	R: GCTTGGCACATTCATCAC

Table 1: Primer pairs used for riboprobe preparation and qRT-PCR analyses.
Numbers within primer names indicate the position of the primer from the ATG on.

7.4 Results

7.4.1 All *cryptochrome* transcripts are expressed in a circadian manner in the adult zebrafish retina

Both *cryptochrome 1* paralogs are most abundant during the morning hours after the light is turned on (Fig. 1). The cyclic expression of *cry1a* peaks at Zeitgeber time (ZT) 3 and declines steadily over the next hours until it reaches a dip at ZT 19 in the early morning. After that, a steep increase in transcript expression until ZT 3 is visible (Fig. 1A'). The *in situ* hybridization analysis shows a broad expression of *cry1a* in all retinal layers (Fig. 1A-D). While the strongest expression intensity was seen at ZT 3 (Fig. 1B), expression, at least in the ONL and INL, appears to be lowest at ZT 15 (Fig. 1D). Expression in the GCL is visible at all time points and seems more or less constant. The *cry1b* riboprobe is expressed in all retinal layers (Fig. 1E-H), although this paralog shows an oscillating pattern in the GCL with the highest expression at ZT 23 (Fig. 1E). Expression in the ONL and INL seems stable and is only reduced at ZT 15 (Fig. 1D). Total transcript abundance is oscillating with both a trough and a peak during the dark hours and decrease in expression during the light hours (Fig. 1E').

Figure 1: Circadian RNA expression pattern of cryptochrome 1 paralogs in adult zebrafish retinas.
A-H: *Expression of cry1a (A-D) and -1b (E-H) revealed by in situ hybridization on radial sections through the adult zebrafish retina at different time points.* ***A',E':*** *qRT-PCR analysis showing circadian expression of cry1a (A') and cry1b (E') transcripts in retinal tissue. cry1a is weakly expressed in the photoreceptors (ONL), and in the GCL. A stronger expression, especially in the morning hours, is visible in the INL. cry1a expression level measured by qRT-PCR increases already during the late night, peaks at ZT (Zeitgeber time) 3 or 11 am, and decreases again until it reaches the base level early in the morning at ZT 19 (A').*
cry1b is expressed throughout the retina from the ONL to the GCL (E-H). Expression is strongest at ZT 23 or 7 am (E) and decreases steadily over the next three time points. qRT-PCR reveals a peak in transcript expression at ZT 23 followed by a decrease until ZT 7, where the level remains at around 40% until it decreases again after ZT 15 (E'). Similar to cry1a, the expression level of cry1b ascends before the light is turned on.
The qRT-PCR values were averaged from three independent samples. Grey and white shading in qRT-PCR graphs represent night (lights off) and day (lights on), respectively. On the x-axis the time in daytime and ZT is given. GCL: ganglion cell layer; INL: inner nuclear layer; IPL; inner plexiform layer; ONL: outer nuclear layer; OPL: outer plexiform layer. Scale bar in H (applies to all images A-H) = 20 μm.

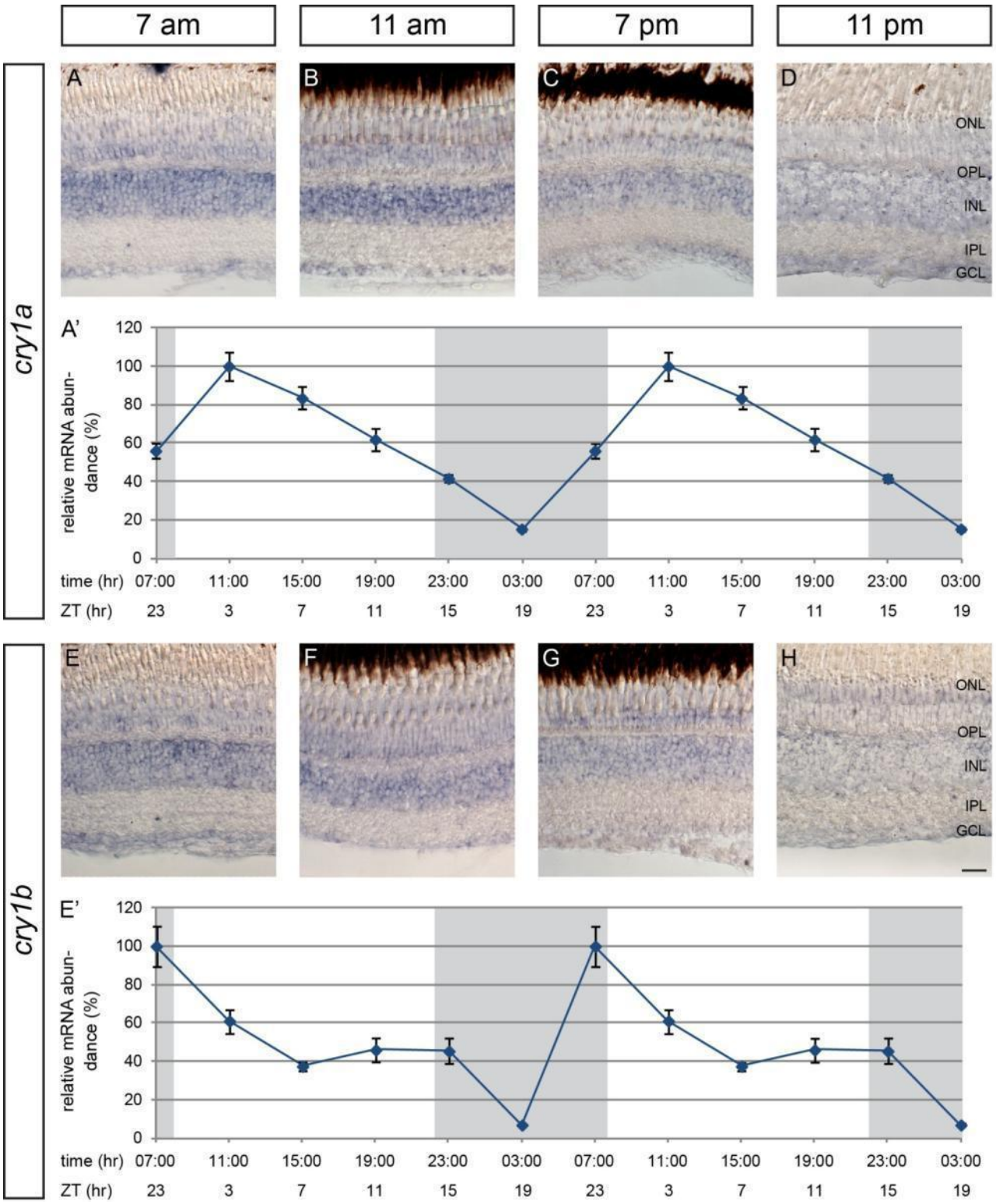
7 am
11 am
7 pm
11 pm
cry1a
A
B
C
D
ONL
OPL
INL
IPL
GCL
A'
relative mRNA abun-dance (%)
120
100
80
60
40
20
0
time (hr) 07:00 11:00 15:00 19:00 23:00 03:00 07:00 11:00 15:00 19:00 23:00 03:00
ZT (hr) 23 3 7 11 15 19 23 3 7 11 15 19
cry1b
E
F
G
H
ONL
OPL
INL
IPL
GCL
E'
relative mRNA abun-dance (%)
120
100
80
60
40
20
0
time (hr) 07:00 11:00 15:00 19:00 23:00 03:00 07:00 11:00 15:00 19:00 23:00 03:00
ZT (hr) 23 3 7 11 15 19 23 3 7 11 15 19

Cry3a and *-3b*, reveal both a prominent expression in the evening shortly after light offset (Fig. 2A-H). While *cry3a* RNA expression appears cyclic in the ONL with a peak at ZT 15 (Fig. 2D), expression in the INL increases during the light hours (Fig. 2A-C) until it remains constant from ZT 23 on, and expression in the GCL seems most intense at ZT 23 (Fig. 2C). The overall transcript expression measured by qRT-PCR resembles *cry3a* expression in the ONL: it steady increases during the day, peaks at ZT 15, and decreases again during the dark hours (Fig. 2A'). For its paralog *cry3b* a similar pattern was found with a steady increase during the day and a decrease after light offset (Fig. 2E'). The riboprobe of *cry3b* stains all retinal layers in a circadian manner (Fig. 2E-H). The oscillating expression in the GCL is similar to the qRT-PCR result with an increase in intensity during the day (Fig. 2E-H). Expression in the ONL is very weak at ZT 3 (Fig. 2F), increases until ZT 11 (Fig. 2G), and remains stable during later time points (Fig. 2H). The INL (mostly horizontal cells, see arrowheads Fig. 2H) reveals the most intense staining of *cry3b* in the evening and at the beginning of the night (Fig. 2G,H), whereas expression in the morning is low (Fig. 2E,F).

Figure 2: Circadian transcript expression of cryptochrome 3 paralogs in adult zebrafish retinas.
A-H: *In situ hybridization using cry3a (A-D) and -3b (E-H) riboprobes on radial sections of the adult zebrafish retina at different time points.* ***A',E':*** *qRT-PCR analysis showing circadian expression of cry3a (A') and cry3b (E') transcripts in retinal tissue. Overall, expression of cry3a increases during the day in all retinal layers containing cell somata (ONL, INL, GCL). Especially expression in photoreceptors (ONL) is strongly circadian and peaks at Zeitgeber time (ZT) 15 shortly after the light is turned off (D). A prominent staining in horizontal cell in the evening is visible (arrowheads in D). qRT-PCR results show that the abundance of cry3a transcripts increases after light onset and is highest at ZT 15, before it decreases again during the night (A').*
A similar in situ hybridization result as cry3a reveals cry3b with an increase in expression in all retinal layers during the day (E-H). Also expression in horizontal cells is seen but only at ZT 15 (arrowheads in H). Overall expression at ZT 11 (G) and 15 (H) appear to be of similar intensity. The qRT-PCR graph is comparable to cry3a as well: a steady increase of transcript expression from dawn throughout the day, and a decrease soon after the light is turned off (E').
The qRT-PCR values were averaged from three independent samples. Grey and white shading in qRT-PCR graphs represent night (lights off) and day (lights on), respectively. On the x-axis the time in daytime and ZT is given. GCL: ganglion cell layer; INL: inner nuclear layer; IPL; inner plexiform layer; ONL: outer nuclear layer; OPL: outer plexiform layer. Scale bar in H (applies to all images A-H) = 20 µm.

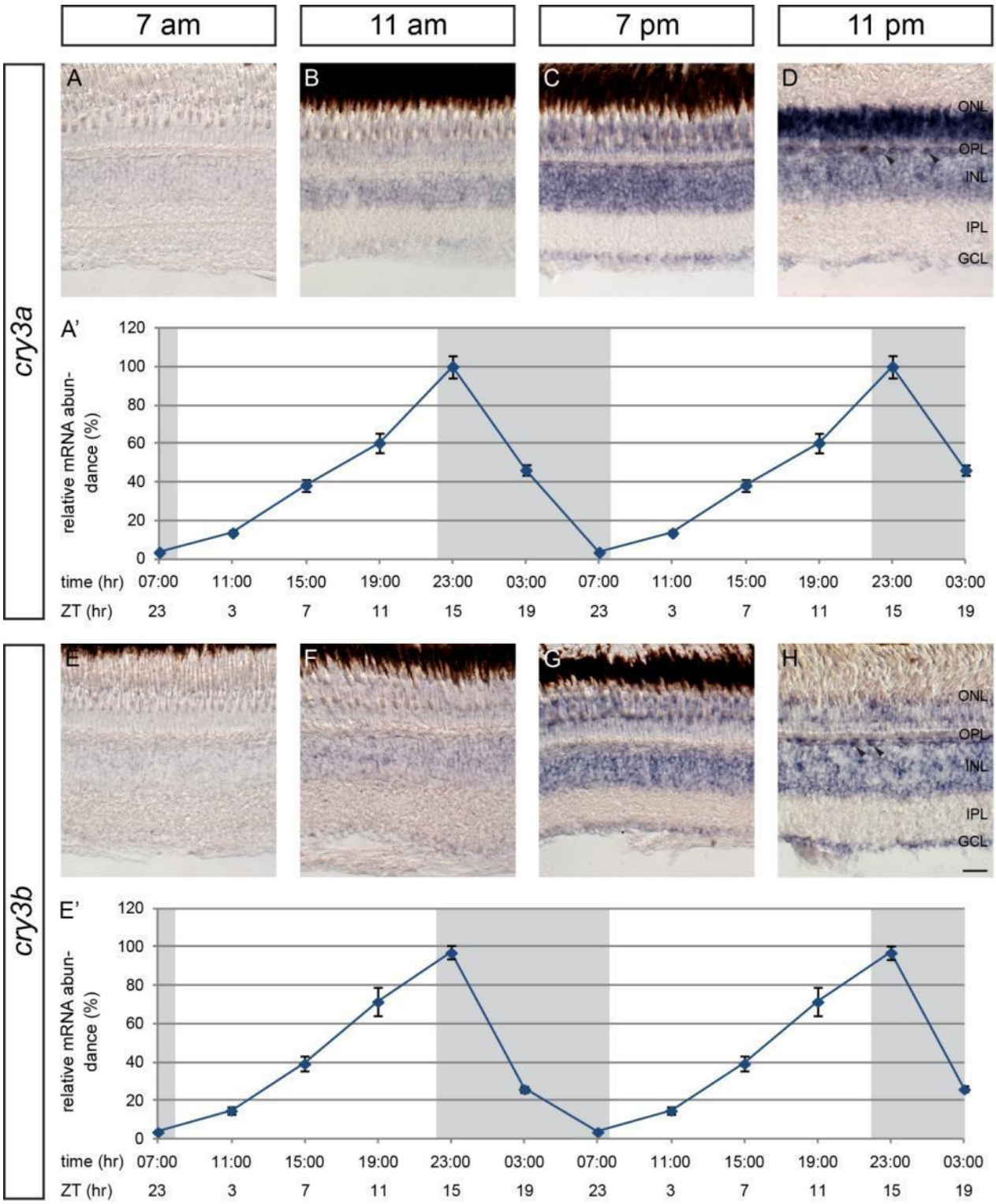
7 am
11 am
7 pm
11 pm
cry3a
A
B
C
D
ONL
OPL
INL
IPL
GCL
A'
relative mRNA abun-dance (%)
120
100
80
60
40
20
0
time (hr) 07:00 11:00 15:00 19:00 23:00 03:00 07:00 11:00 15:00 19:00 23:00 03:00
ZT (hr) 23 3 7 11 15 19 23 3 7 11 15 19
cry3b
E
F
G
H
ONL
OPL
INL
IPL
GCL
E'
relative mRNA abun-dance (%)
120
100
80
60
40
20
0
time (hr) 07:00 11:00 15:00 19:00 23:00 03:00 07:00 11:00 15:00 19:00 23:00 03:00
ZT (hr) 23 3 7 11 15 19 23 3 7 11 15 19

Transcript abundance of *cry2* peaks at ZT 23 before light onset, declines constantly and reaches its base level in the evening between ZT 11 and 15 around light offset (Fig. 3A'). Similar to that the most intense *in situ* hybridization staining was detected at ZT 23 in the ONL and INL (Fig. 3A,B). Expression in these layers are nearly vanished at ZT 11 (Fig. 3C) but appears a bit higher again at ZT 15 (Fig. 3D). In the GCL *cry2* mRNA reveals the highest expression at ZT 3 (Fig. 3B) but was not detected in the evening (Fig. 3C,D).

The zebrafish *cry4* qRT-PCR analysis reveals a steady increase in transcript abundance after ZT 23 with a peak at ZT 15. During the night the quantity of mRNA diminishes and reaches a trough around ZT 23 (Fig. 3E'). *In situ* hybridization revealed overlapping results: *cry4* expression is nearly invisible at ZT 23 (Fig. 3E), and increases in intensity in all layers during the next time points (Fig. 3F-H).

The circadian expression profile of *cry5* shows a sharp peak after light onset before returning back to base level and remaining low until the next light on period (Fig. 4A'). Although overall expression of *cry5* in adult retinal slices is low, it appears highest at ZT 3 in all retinal layers (Fig. 3B). Additional staining at other time points is only seen in the INL (Fig. 4A,C,D).

Overall transcript abundance of *cryDASH* is highest but fluctuating at ZT 3, has a trough at ZT 11, and increases during the dark hours (Fig. 4E'). *cryDASH* is weakly expressed in all retinal layers during in the morning (Fig. 4E,F) and at the beginning of the dark period (Fig. 4H) but not at ZT 11 (Fig. 4G).

Figure 3: Circadian RNA expression of cryptochrome 2 and -4 in adult zebrafish retinas.
A-H: *RNA expression shown by in situ hybridization of adult retinal sections using the cry2 (A-D), and the cry4 (E-H) riboprobe.* ***A',E':*** *qRT-PCR analysis showing circadian expression of cry2 (A') and cry4 (E') transcripts in retinal tissue. cry2 is highly expressed in the ONL, INL, and GCL at 7 am (A). While the intensity of the staining in the INL seems to drop from Zeitgeber time (ZT) 23 to 3 around light onset, the expression in photoreceptors and the GCL seems stable (A,B). Later on during day the expression of cry2 decreases in all layers (C,D). cry2 transcript expression peaks at ZT 23, steadily decreases during the day, reaches a base level at ZT 11 and increases again during the night after ZT 15 (A').*
The zebrafish cry4 shows no expression at ZT 23 (E). From 4 hours later on the cry4 riboprobe stains all retinal layers (F-H). Moreover, expression in photoreceptors (ONL) and the GCL seem to increase between ZT 3 (F) and 15 (H). The amount of cry4 mRNA transcripts in adult eyes increases after the light is turned on, peaks at ZT 15 shortly after light offset, and falls back to the base level during the night (E').
The qRT-PCR values were averaged from three independent samples. Grey and white shading in qRT-PCR graphs represent night (lights off) and day (lights on), respectively. On the x-axis the time in daytime and ZT is given. GCL: ganglion cell layer; INL: inner nuclear layer; IPL; inner plexiform layer; ONL: outer nuclear layer; OPL: outer plexiform layer. Scale bar in H (applies to all images A-H) = 20 µm.

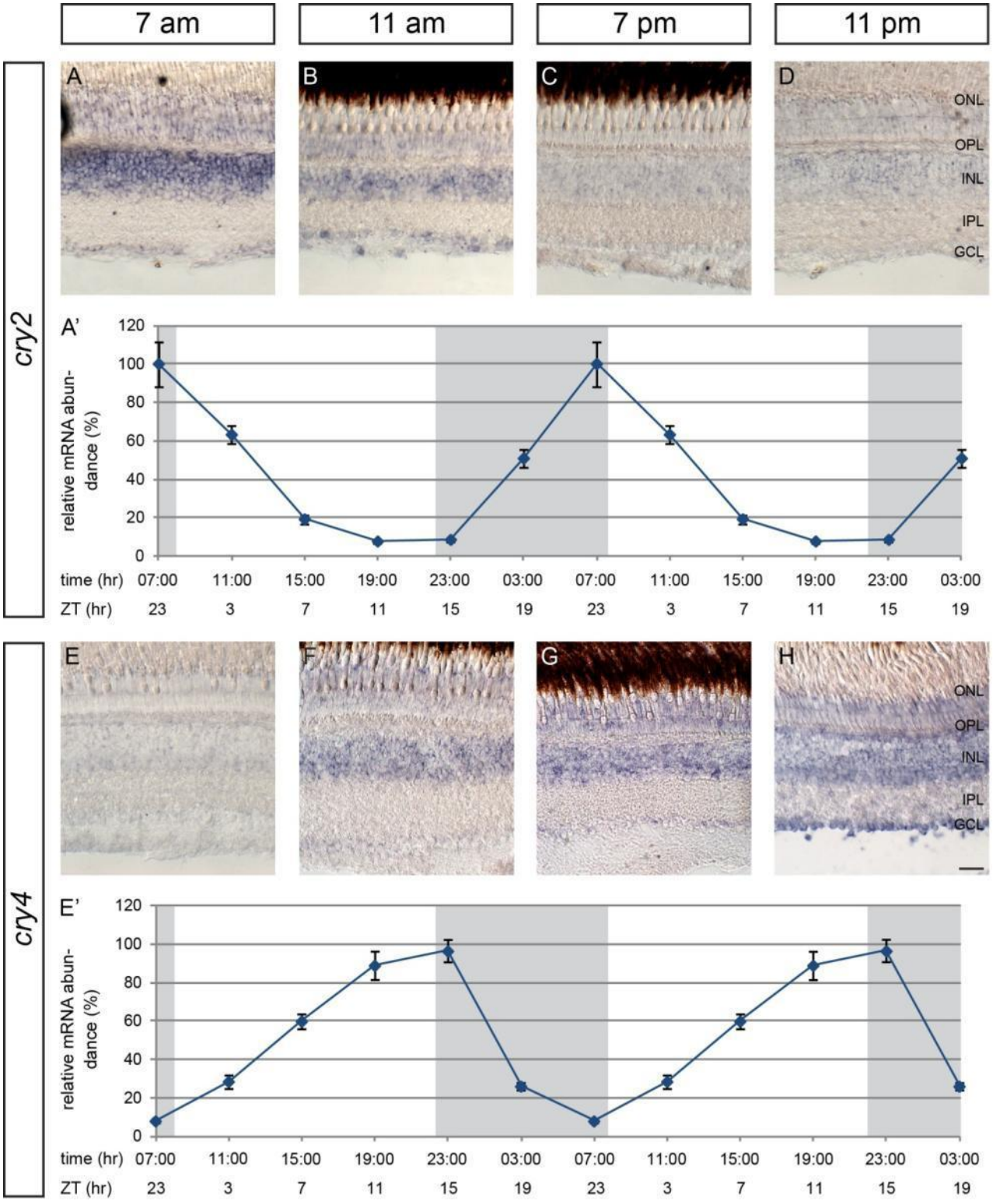
7 am
11 am
7 pm
11 pm
cry2
A
B
C
D
ONL
OPL
INL
IPL
GCL
A'
relative mRNA abun-dance (%)
120
100
80
60
40
20
0
time (hr) 07:00 11:00 15:00 19:00 23:00 03:00 07:00 11:00 15:00 19:00 23:00 03:00
ZT (hr) 23 3 7 11 15 19 23 3 7 11 15 19
cry4
E
F
G
H
ONL
OPL
INL
IPL
GCL
E'
relative mRNA abun-dance (%)
120
100
80
60
40
20
0
time (hr) 07:00 11:00 15:00 19:00 23:00 03:00 07:00 11:00 15:00 19:00 23:00 03:00
ZT (hr) 23 3 7 11 15 19 23 3 7 11 15 19

Figure 4: Circadian expression of cryptochrome 5 (6-4 phr) and –DASH in adult zebrafish retinas.
A-H: *In situ hybridizations on radial sections trough the adult retina with the cry5 (A-D) and the cryDASH (E-F) antisense RNA probe.* ***A',E':*** *qRT-PCR analysis showing circadian expression of cry5 (A') and cryDASH (E') transcripts in retinal tissue. Expression of cry5 is only visible in the INL at Zeitgeber time (ZT) 23 (A). Later on after the light is turned on the cry5 riboprobe reveals a broader expression and additionally stains cells in the ONL and the GCL (B). However, at ZT 11 (C) and 15 (D) the cry5 expression level is again very low and restricted to the INL. Transcript levels of cry5 in adult eyecups increase after light onset, reach a peak at ZT 3, decline again until a base level is reached at ZT 11 and remain low until the next day (A').*
cryDASH is expressed in the INL and the GCL in all sections (E,F,H) but not at ZT 11 (G). Additional weak expression is visible in the ONL in sections from tissue fixed in the morning (E,F). The qRT-PCR reveals a peak in cryDASH transcript levels at ZT 3 and a trough at ZT 11 (E'). The high standard deviation at ZT 3 suggests large fluctuation in mean values at this time point.
The qRT-PCR values were averaged from three independent samples. Grey and white shading in qRT-PCR graphs represent night (lights off) and day (lights on), respectively. On the x-axis the time in daytime and ZT is given. GCL: ganglion cell layer; INL: inner nuclear layer; IPL; inner plexiform layer; ONL: outer nuclear layer; OPL: outer plexiform layer. Scale bar in H (applies to all images A-H) = 20 µm.

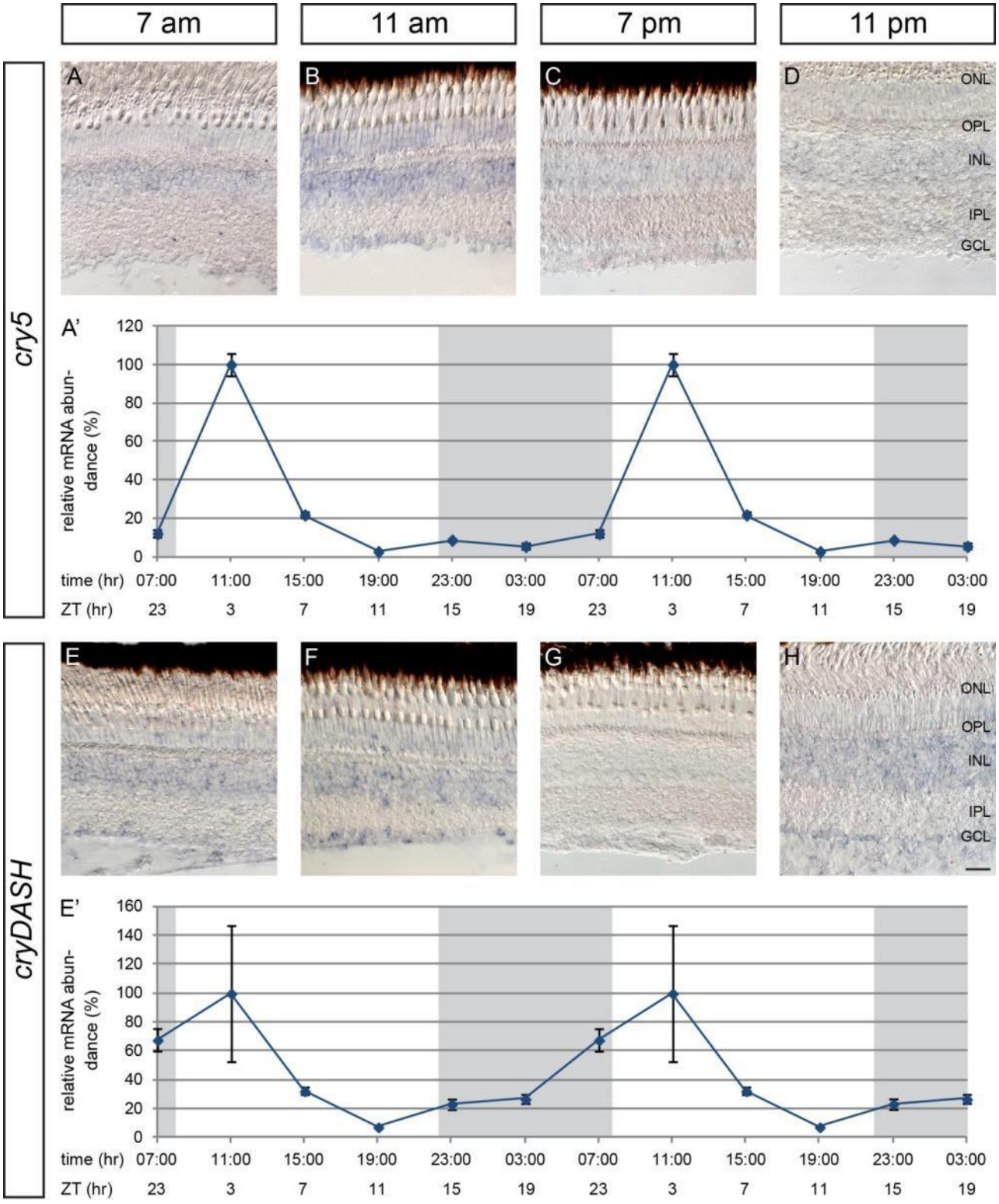
7 am
11 am
7 pm
11 pm
cry5
A
B
C
D
ONL
OPL
INL
IPL
GCL
A'
relative mRNA abun-dance (%)
120
100
80
60
40
20
0
time (hr) 07:00 11:00 15:00 19:00 23:00 03:00 07:00 11:00 15:00 19:00 23:00 03:00
ZT (hr) 23 3 7 11 15 19 23 3 7 11 15 19
cryDASH
E
F
G
H
ONL
OPL
INL
IPL
GCL
E'
relative mRNA abun-dance (%)
160
140
120
100
80
60
40
20
0
time (hr) 07:00 11:00 15:00 19:00 23:00 03:00 07:00 11:00 15:00 19:00 23:00 03:00
ZT (hr) 23 3 7 11 15 19 23 3 7 11 15 19

7.5 Discussion

Cryptochromes possess two chromophore binding domains (MTHF and FAD) that serve as receptors for UV- and blue light (reviewed in Chaves *et al.*, 2011). After their initial description in plants (Ahmad & Cashmore, 1993) and the discovery of them mediating light-dependent developmental processes (Guo *et al.*, 1998; Somers *et al.*, 1998), they were soon after found to be involved in circadian processes of insects (Emery *et al.*, 1998) and vertebrates (Miyamoto & Sancar, 1998). Mice with outer retinal degeneration lacking cryptochromes show impaired circadian entrainment, and if both genes are lost the animals behave totally arrhythmic (van der Horst *et al.*, 1999; Vitaterna *et al.*, 1999). Since in mammals visual information travels only via the retina to higher brain regions where the central pacemaker is located (Foster *et al.*, 1991; Nelson & Zucker, 1981), a signaling pathway that reacts to light but is independent of visual photoreception must be present. Both mammalian Crys are present in the retinal ganglion cell layer (Miyamoto & Sancar, 1998; Thompson *et al.*, 2003) where non-visual photoreception originates (Berson *et al.*, 2002; Leak & Moore, 1997). This makes them a reasonably good candidate for being involved in non-image forming vision, either acting directly as the light sensing molecule or within the signaling pathway to higher brain regions. However, during the last decade melanopsin was found to constitute the main input to the central clock (Hattar *et al.*, 2003; Owens *et al.*, 2012) and it seems unlikely that another receptor is participating in circadian photoreception. But the question whether a cryptochrome could be involved in circadian signaling pathways to the brain remains open.

7.5.1 Possible roles of cryptochromes

Over the past years the zebrafish (*Danio rerio*) has emerged as a fruitful model for a variety of scientific research fields. The cryptochrome family has already been studied in zebrafish (e.g. Ishikawa *et al.*, 2002; Kobayashi *et al.*, 2000; Tamai *et al.*, 2007), however, knowledge about their specific expression in the retina is lacking. We investigated circadian expression patterns of zebrafish *crys* in various retinal layers in order to find evidence for an involvement in non-visual processes. While mammalian Crys have been shown to act light-independently within the negative transcriptional feedback loop of the central clock where they inhibit CLOCK-BMAL1-mediated transcription (Griffin *et al.*, 1999; Kume *et al.*, 1999; Shearman *et al.*, 2000), the *Drosophila* cryptochrome functions instead as a light-dependent suppressor of PER-TIM-mediated inhibition of transcription (Ceriani *et al.*, 1999). This separates cryptochromes into two subgroups dependent on their ability to inhibit CLOCK-BMAL1-mediated transcription. The zebrafish Cry1 and -3 paralogs belong to the mammalian-type Crys, whereas Cry2, -4, and -5 are grouped as *Drosophila*-type Crys (Daiyasu *et al.*, 2004; Kobayashi *et al.*, 2000). CryDASH is not grouped together with the former groups and forms a third group. If certain Crys are involved in similar processes it would not be surprising to find similar oscillation and expression patterns for *crys* within the same group. Phylogeny of the cryptochrome family shows that the Cry1 paralogs are the closest relatives of the mammalian Cry1. In the rat retina *cry1* shows the highest transcript expression at Zeitgeber 2 (around 10 am) and stays more or less stable at a lower level between 6 and 18 hours after light onset (Kamphuis *et al.*, 2005). While the zebrafish *cry1a* peaks at ZT 3 and has a trough in the dark phase (Fig. 1A'), its paralog shows both a trough and a peak in the dark phase and decreases during the light phase (Fig. 1E'). Although Cry1a and -1b are classified as mammalian-type Crys and on first sight their expression profiles are similar to the pattern of *cry1* in nocturnal rats (Kamphuis *et*

al., 2005), the circadian pattern of zebrafish *cry1a* show an almost perfect match to the circadian expression in diurnal chicken *cry1* and *Drosophila cry* (Emery *et al.*, 1998; Kubo *et al.*, 2006). This suggests similar functions for those orthologs. In some insects, Cry acts as the circadian photoreceptor itself to entrain clocks present in every cell throughout the body (Plautz *et al.*, 1997; Emery *et al.*, 1998). A few years ago, the Whitmore lab described a similar ability of zebrafish peripheral cells: they sense light and entrain cell-autonomously to light-dark cycles over the directly light-inducible Cry1a (Whitmore *et al.*, 2000; Tamai *et al.*, 2007). Since the transcription starts to increase during the night, the cycling of *cry1a* has to be at least partially under autoregulatory control. The broad and cyclic expression of the *cry1a* riboprobe (Fig. 1A-D) is consistent with the idea of the molecule being involved in light input to cell-autonomous circadian clocks.

Although the oscillation patterns of *cry1* paralogs differ, *cry1b* transcript abundance also increases before the light phase (Fig. 1E'). The *cry1b* riboprobe is found in all retinal layers from shortly before light onset at ZT 23 on and is only visibly reduced at ZT 15 (Fig. 1E-H). The expression pattern of *cry1b* in zebrafish described by Kobayashi and colleagues via Northern blot and RNase protection assays (Kobayashi *et al.*, 2000) shows a second peak around Zeitgeber 13. This discrepancy to our result can be explained by the different tissues analyzed: while they used brain and eye preparations, we focused specifically on the eye. However, the expression levels of *cry1* in rat retinas resemble our results for *cry1b* (Kamphuis *et al.*, 2005). Since Cry1a is thought to act as a peripheral clock component, the ancestral functions of the gene may have split with Cry1b is being exclusively involved in the feedback loop of the core clock similar to the mammalian Cry1.

Cry3s are descendants of a lost *cry1* homolog and are only retained in the genomes of teleost fish (see Chapter 6). Their oscillation pattern is closely matched with a steady increase after light onset and a decrease during the night (Fig. 2A',E'). In this case light input or a secondary pathway acting over light may trigger transcript level increase and an auto controlled degradation their decrease during the night. Both paralogs reveal a broad expression in all retinal layers (Fig. 2A-H). While c*ry3a* expression is oscillating strongest in the photoreceptor layer, *cry3b* shows the strongest pattern in the GCL. Prominent is the labeling of horizontal cells for both paralogs (arrowheads in Fig. 2D,H). Since Cry3a and -3b are described as mammalian-type Crys, and their circadian profile matches the mammalian Crys (Preitner *et al.*, 2002), a function as a circadian clock component is possible. However, as the Somalian cave fish (*Phreatichthys andruzzii*) that has degenerated eyes still retained both copies of this gene (www.uniprot.org) similar to the zebrafish another light-independent function in peripheral tissues is also expected.

The oscillation pattern of the zebrafish *cry2* is clearly distinct from its rodent orthologs: while in zebrafish *cry2* transcript abundance increases during the night and decreases during the day (Fig. 3A'), the rodent's *cry2s* behave the other way round (Preitner *et al.*, 2002; Kamphuis *et al.*, 2005). Surprisingly, studies involving human cells show a tendency to decrease *cry2* expression during the day and increase it during the night, similar to zebrafish (Kusanagi *et al.*, 2008; Yang *et al.*, 2011). In chicken and goldfish *cry2* expression levels were measured in various tissues and a similar oscillation pattern to the zebrafish retina was found in the retina but not elsewhere for these species (Kubo *et al.*, 2006; Velarde *et al.*, 2009). Although the zebrafish Cry2 groups with the mammalian Cry2s (see Chapter 6), it belongs to the *Drosophila*-type Crys. However, signaling may not only occur over inhibition of CLOCK:BMAL1-mediated transcription. If the physiological role of this cryptochrome depends

on activity rhythms and is therefore similar in diurnal and nocturnal animals, the zebrafish and the human Cry2 might still have similar functions. Moreover, the different oscillation patterns found in the examined tissues of chicken do not suggest identical function all over the body. A light-dependent inhibition of expression could explain the decrease in retinal *cry2*-levels during the light-phase and their increase during darkness (Fig. 3A'). While direct light-dependent degradation has not been detected in any of the biochemically tested properties of vertebrate cryptochromes, it was found to be present in *Drosophila* (Sathyanarayanan *et al.*, 2008; Ozturk *et al.*, 2009). Besides that, another also light-dependent function for Cry2 in magnetoreception was recently described (Gegear *et al.*, 2008; Yoshii *et al.*, 2009; Foley *et al.*, 2011). While in migratory birds the sensation of the magnetic field seems a useful source of compass navigation (Ritz *et al.*, 2000), it is currently unknown which role it may has in other animals or whether it is actually even present. For fish like zebrafish that more or less permanently stay in the same habitat during their life (Engeszer *et al.*, 2007), magnetoreception does not seem to be of big importance and might – if functional – just be an evolutionary relict.

Knowledge about cryptochrome 4 is scarce, since it belongs to the *Drosophila*-type Crys and is only present in birds, fish, and lizards (Chapter 6; Kobayashi *et al.*, 2000). In the zebrafish retina *cry4* shows a steady increase in expression during light hours and a decrease during dark hours (Fig. 3E'), which suggests a light-dependent regulation of expression. The chicken pineal gland reveals a similar oscillation pattern for *cry4*, whereas in the retina the decline already starts before the light is turned off (Kubo *et al.*, 2006). In addition, in other tissues of chicken, *cry4* shows either a different expression pattern or does not oscillate at all, which suggests that *cry4* has not a crucial function within the circadian clock. On the molecular level, *cry4* still possess the ability of blue-light absorption (Kubo *et al.*, 2006; Ozturk *et al.*, 2009). Whether this cryptochrome still uses this ability *in vivo* has not been shown so far. The light-dependent increase in *cry4*-transcript levels is discussed to act as so called "time taker". A molecule with a similar function was found by McWatters and colleagues in *Arabidopsis* (McWatters *et al.*, 2000). Why it is only present in lower vertebrates and what function it may confine is still elusive.

While mammalian Crys have lost their ancestral ability of light-dependent repair of UV-induced DNA damage, Cry5 has maintained this function (Kobayashi *et al.*, 2000). The detected spike-like peak around midday in transcript expression seems a plausible response to the increasing UV-light (Fig. 4A'). A small raise in expression level is already seen at ZT 23 (Fig. 1A,A'), which may be a preceding reaction to light onset. Although expression in the retina is broad, overall level appears low compared to other family members. A stronger expression might be triggered by the application of higher doses of UV-light when actual damage is induced. Cry5 function in zebrafish has been shown to have a strong impact on embryonic survival (Tamai *et al.*, 2004) and a photorepair system seems to be present in fish (Dong *et al.*, 2007). However, a direct link between Cry5 repair activity and zebrafish viability has not been shown so far. A preliminary experiment performed in our lab revealed slightly increased apoptotic rates in zebrafish fins upon downregulation of Cry5, suggesting an *in vivo* DNA repair activity (data not shown).

CryDASH has only been found in bacteria, plants, fish, and frogs (Hitomi *et al.*, 2000; Kleine *et al.*, 2003; Daiyasu *et al.*, 2004). Weak photorepair activity was detected in CryDASH of bacteria, zebrafish, and *Xenopus* (Hitomi *et al.*, 2000; Daiyasu *et al.*, 2004) but not in plants. Although with a high fluctuation at 11 am (Fig. 4E'), zebrafish *cryDASH* reveals an oscillating expression in the retina. Similar to *cry5*, overall expression is low (Fig. 4E-H) but

peaks at ZT 3. This could as well be a reaction to DNA damage. So far no other function than DNA repair is discussed for CryDASH in vertebrates and an involvement in circadian photoreception seems unlikely.

We did not expect to find such a broad expression for each *cryptochrome* in the zebrafish retina. Therefore, a function in non-visual photoreception cannot be clearly assigned to an individual family member. However, the evident oscillating expression of each *cry* in the zebrafish eye suggests involvements in circadian processes, whether it is the above mentioned non-visual photoreception or other processes remains open.

7.5.2 Peripheral and central clocks

Although a circadian clock is present in the majority of cells throughout the mammalian body (Balsalobre *et al.*, 1998; Reppert & Weaver, 2002; Nagoshi *et al.*, 2004), a central organizer is needed to synchronize them in a hierarchical manner (reviewed in Dibner *et al.*, 2010). Rhythmic variations in melatonin blood level for example are driven by a light-dependent input from the central clock to the pineal gland, and convey one of the major outputs of the circadian clock (reviewed in Pevet & Challet, 2011). In lower vertebrates such as fish (Samejima *et al.*, 1997; Ekström & Meissl, 1997), reptiles (Menaker & Wisner, 1983), and birds (Okano & Fukada, 2001), the pineal gland and the deep brain were found to contain photoresponsive cells themselves which do not need input from a higher brain center. Moreover, as mentioned above, peripheral cells in zebrafish are directly entrainable by light and possess a cell autonomous circadian clock (Whitmore *et al.*, 2000). The organization of the circadian system seems to differ between mammalian and non-mammalian vertebrates, in so far as in the latter a hierarchical organisator is not needed. Therefore, the retina cannot be seen as the sole source of circadian photoreception. This further raises the question whether it is reasonable to quest for molecules involved in circadian processes within the eye in a non-mammalian vertebrate. Grasping an evolutionary perspective, nature may has invented retinal input to the circadian system only once and the mechanism might be conserved between lower and higher vertebrates. In mammals, the master clock in the SCN fully relies on light input from melanopsin and photoreceptors (Hattar *et al.*, 2003). Only recently it was found that zebrafish possess five different melanopsin subtypes of which two of them are present in the adult retina (Davies *et al.*, 2011). Whether they mediate similar functions as in mammals is currently unknown. Already known is that melanopsin is not involved in light-input to peripheral pacemakers. Its expression is mainly restricted to the central nervous system in zebrafish (Balsalobre *et al.*, 1998; Matos-Cruz *et al.*, 2011) and molecules that are involved in such a function need to be present in a variety of tissues. In zebrafish, Cry1a was found to be the molecule guiding the light signal to peripheral oscillators (Tamai *et al.*, 2007). The signaling pathway trough which Cry1a acts on the clock components is not fully understood but seems to involve other clock proteins such as CLOCK and BMAL (Tamai *et al.*, 2007). Other cryptochromes are possibly involved within that signaling pathway (Cermakian *et al.*, 2002) and might adopt the function of the clock component that Cry1/2 have in mammals. In some insects both a *Drosophila*-type and mammalian-type cryptochromes were found (e.g. monarch butterfly in Zhu *et al.*, 2008). This provides evidence that an ancestral clock might has used both types of cryptochromes, one as a light sensor and the other as transcriptional regulator. During evolution Cry function may have changed from the photoreceptive molecule to a core clock component independent of light.

To sum up, although expression levels vary, the *in situ* hybridization results clearly show that all *cryptochromes* are broadly expressed throughout all retinal layers and exhibit circadian transcript oscillation in the retina. We could not find a *cry* clearly oscillating only in a distinct retinal layer. However, our study provides a general overview of *cryptochrome* expression in zebrafish in a tissue relevant not only for visual light input. Non-visual photoreception clearly involves Cryptochromes, as has already been shown by Tamai and colleagues (Tamai *et al.*, 2004). This function accomplished in peripheral cells might be similar in retinal cells, however, the retina has not been investigated so far. Besides that, the broad expression of *crys* in the zebrafish retina suggests other functions such as magnetoreception or DNA damage repair. They might even contribute to visual input or, since they are activated by UV- and blue light, participate in light adaptation processes in the low light range.

7.6 Outlook

Whether oscillation of a certain *cryptochrome* is circadian regulated or only induced by light can only be shown with the evaluation of expression patterns under constant conditions. In future experiments, we will study expression for each *cry* under DD conditions. Preliminary experiments of *cry2* and *cry4* expression in retinas from adult zebrafish kept in constant darkness for four days do not show any differences to the LD results which suggests circadian regulation of retinal *cry* expression. Besides that, it has been shown that feeding can alter circadian expression of genes in zebrafish (Sanchez & Sanchez-Vazquez, 2009; Feliciano *et al.*, 2011). However, our preliminary results show that feeding has no significant influence on *cryptochrome* expression in the adult retina (data not shown).

We aimed to see oscillation patterns of *crys* within a retinal layer. qRT-PCR was performed on whole adult zebrafish eyecups. Therefore, we were not able to distinguish between cyclic expressions in different retinal layers. Cutting only one retinal layer or a single cell from one layer with a laser and perform qRT-PCR on that tissue would solve this problem. Whether this works for zebrafish retinal layers has to be investigated, but would certainly help us finding specific oscillation patterns. We already investigated layer-specific transcript oscillation by *in situ* hybridization. However, this technique is not quantitative but only shows mRNA expression at a specific location. Although our results show rhythmic expression of *crys* in zebrafish retinal layers, it cannot be significantly proven. Here, a fluorescent *in situ* hybridization (FISH) could help since fluorescence intensity could be measured over a region of interest and set in relation to a base level.

So far, our results did not help us much to find a certain cryptochrome which might has a function in retinal circadian light-uptake and where we can focus our research on. However, after our broad phylogenetic approach it might be more fruitful to quest for the function of zebrafish cryptochromes that have not been previously investigated and are expected to have specific roles, maybe even in visual processes. Here, a morpholino knock down followed by behavioral analysis could be used. In addition, it would also be possible to test the impact of cryptochromes on circadian activity patterns using the visual motor response setup (Emran *et al.*, 2008). A quest for conserved regions that are known to be necessary for specific biochemical functions (binding of a chromophore, binding to DNA for repair, etc.) could be done with *cryptochrome* sequences from different species. This might give us further knowledge about in what kind of physiological processes zebrafish

cryptochromes are involved. Moreover, from tomato it is known that cryptochromes are able to regulate each other's expression (Facella *et al.*, 2006). A yeast-two-hybrid approach could validate interactions within cryptochromes and between cryptochromes and other proteins. This should shine more light on the circuits that control circadian behavior in zebrafish and would also allow us to focus on more specific properties of cryptochromes.

While working with oscillating mRNA expression one has to keep in mind that mRNA expression does not necessarily reflect protein expression levels. Translation to proteins and functional impact is delayed. Preitner *et al.* have shown that the phase between transcription and translation into a protein is about 2 hours (Preitner *et al.*, 2002). However, not only protein turnover but also protein decay strongly influences protein levels. To date, nothing is known about the turnover of cryptochromes which makes speculations about protein level oscillations impossible. Only the development of zebrafish-specific cryptochrome antibodies could help.

7.7 References

Ahmad, M. & Cashmore, A.R. (1993) HY4 gene of A. thaliana encodes a protein with characteristics of a blue-light photoreceptor. Nature, 366, 162–166.

Balsalobre, A., Damiola, F. & Schibler, U. (1998) A serum shock induces circadian gene expression in mammalian tissue culture cells. Cell, 93, 929–937.

Berson, D.M., Dunn, F.A. & Takao, M. (2002) Phototransduction by retinal ganglion cells that set the circadian clock. Science, 295, 1070–1073.

Ceriani, M.F., Darlington, T.K., Staknis, D., Más, P., Petti, A.A., Weitz, C.J. & Kay, S.A. (1999) Light-dependent sequestration of TIMELESS by CRYPTOCHROME. Science, 285, 553–556.

Cermakian, N., Pando, M.P., Thompson, C.L., Pinchak, A.B., Selby, C.P., Gutierrez, L., Wells, D.E., Cahill, G.M., Sancar, A. & Sassone-Corsi, P. (2002) Light induction of a vertebrate clock gene involves signaling through blue-light receptors and MAP kinases. Curr. Biol., 12, 844–848.

Chaves, I., Pokorny, R., Byrdin, M., Hoang, N., Ritz, T., Brettel, K., Essen, L.-O., van der Horst, G.T.J., Batschauer, A. & Ahmad, M. (2011) The cryptochromes: blue light photoreceptors in plants and animals. Annu Rev Plant Biol, 62, 335–364.

Czeisler, C.A., Shanahan, T.L., Klerman, E.B., Martens, H., Brotman, D.J., Emens, J.S., Klein, T. & Rizzo, J.F. (1995) Suppression of melatonin secretion in some blind patients by exposure to bright light. N. Engl. J. Med., 332, 6–11.

Daan, S. & Gwinner, E. (1998) Jürgen Aschoff (1913-98). Nature, 396, 418.

Daiyasu, H., Ishikawa, T., Kuma, K.-i., Iwai, S., Todo, T. & Toh, H. (2004) Identification of cryptochrome DASH from vertebrates. Genes Cells, 9, 479–495.

Davies, W.I.L., Zheng, L., Hughes, S., Tamai, T.K., Turton, M., Halford, S., Foster, R.G., Whitmore, D. & Hankins, M.W. (2011) Functional diversity of melanopsins and their global expression in the teleost retina. Cell. Mol. Life Sci., 68, 4115–4132.

Dibner, C., Schibler, U. & Albrecht, U. (2010) The mammalian circadian timing system: organization and coordination of central and peripheral clocks. Annu. Rev. Physiol., 72, 517–549.

Dong, Q., Svoboda, K., Tiersch, T.R. & Monroe, W.T. (2007) Photobiological effects of UVA and UVB light in zebrafish embryos: evidence for a competent photorepair system. J. Photochem. Photobiol. B, Biol., 88, 137–146.

Ebihara, S. & Tsuji, K. (1980) Entrainment of the circadian activity rhythm to the light cycle: effective light intensity for a Zeitgeber in the retinal degenerate C3H mouse and the normal C57BL mouse. Physiol. Behav., 24, 523–527.

Ekström, P. & Meissl, H. (1997) The pineal organ of teleost fishes. Reviews in Fish Biology and Fisheries, 7, 199–284.

Emery, P., So, W.V., Kaneko, M., Hall, J.C. & Rosbash, M. (1998) CRY, a Drosophila clock and light-regulated cryptochrome, is a major contributor to circadian rhythm resetting and photosensitivity. Cell, 95, 669–679.

Emran, F., Rihel, J. & Dowling, J.E. (2008) A behavioral assay to measure responsiveness of zebrafish to changes in light intensities. J Vis Exp.

Engeszer, R.E., Patterson, L.B., Rao, A.A. & Parichy, D.M. (2007) Zebrafish in The Wild: A Review of Natural History And New Notes from The Field. Zebrafish, 4, 21–40.

Facella, P., Lopez, L., Chiappetta, A., Bitonti, M.B., Giuliano, G. & Perrotta, G. (2006) CRY-DASH gene expression is under the control of the circadian clock machinery in tomato. FEBS Lett., 580, 4618–4624.

Feliciano, A., Vivas, Y., Pedro, N. de, Delgado, M.J., Velarde, E. & Isorna, E. (2011) Feeding time synchronizes clock gene rhythmic expression in brain and liver of goldfish (Carassius auratus). J. Biol. Rhythms, 26, 24–33.

Foley, L.E., Gegear, R.J. & Reppert, S.M. (2011) Human cryptochrome exhibits light-dependent magnetosensitivity. Nat Commun, 2, 356.

Foster, R.G., Provencio, I., Hudson, D., Fiske, S., Grip, W. de & Menaker, M. (1991) Circadian photoreception in the retinally degenerate mouse (rd/rd). J. Comp. Physiol. A, 169, 39–50.

Freedman, M.S., Lucas, R.J., Soni, B., Schantz, M. von, Muñoz, M., David-Gray, Z. & Foster, R. (1999) Regulation of mammalian circadian behavior by non-rod, non-cone, ocular photoreceptors. Science, 284, 502–504.

Gegear, R.J., Casselman, A., Waddell, S. & Reppert, S.M. (2008) Cryptochrome mediates light-dependent magnetosensitivity in Drosophila. Nature, 454, 1014–1018.

Gooley, J.J., Lu, J., Chou, T.C., Scammell, T.E. & Saper, C.B. (2001) Melanopsin in cells of origin of the retinohypothalamic tract. Nat. Neurosci., 4, 1165.

Griffin, E.A., Staknis, D. & Weitz, C.J. (1999) Light-independent role of CRY1 and CRY2 in the mammalian circadian clock. Science, 286, 768–771.

Guo, H., Yang, H., Mockler, T.C. & Lin, C. (1998) Regulation of flowering time by Arabidopsis photoreceptors. Science, 279, 1360–1363.

Haffter, P., Granato, M., Brand, M., Mullins, M.C., Hammerschmidt, M., Kane, D.A., Odenthal, J., van Eeden, F.J., Jiang, Y.J., Heisenberg, C.P., Kelsh, R.N., Furutani-Seiki, M., Vogelsang, E., Beuchle, D., Schach, U., Fabian, C. & Nüsslein-Volhard, C. (1996) The identification of genes with unique and essential functions in the development of the zebrafish, Danio rerio. Development, 123, 1–36.

Hattar, S., Lucas, R.J., Mrosovsky, N., Thompson, S., Douglas, R.H., Hankins, M.W., Lem, J., Biel, M., Hofmann, F., Foster, R.G. & Yau, K.-W. (2003) Melanopsin and rod-cone photoreceptive systems account for all major accessory visual functions in mice. Nature, 424, 76–81.

Hitomi, K., Okamoto, K., Daiyasu, H., Miyashita, H., Iwai, S., Toh, H., Ishiura, M. & Todo, T. (2000) Bacterial cryptochrome and photolyase: characterization of two photolyase-like genes of Synechocystis sp. PCC6803. Nucleic Acids Res., 28, 2353–2362.

Huang, Y.-Y., Haug, M.F., Gesemann, M. & Neuhauss, S.C.F. (2012) Novel expression patterns of metabotropic glutamate receptor 6 in the zebrafish nervous system. PLoS ONE, 7, e35256.

Ishikawa, T., Hirayama, J., Kobayashi, Y. & Todo, T. (2002) Zebrafish CRY represses transcription mediated by CLOCK-BMAL heterodimer without inhibiting its binding to DNA. Genes Cells, 7, 1073–1086.

Kamphuis, W., Cailotto, C., Dijk, F., Bergen, A. & Buijs, R.M. (2005) Circadian expression of clock genes and clock-controlled genes in the rat retina. Biochem. Biophys. Res. Commun., 330, 18–26.

Kanai, S., Kikuno, R., Toh, H., Ryo, H. & Todo, T. (1997) Molecular evolution of the photolyase-blue-light photoreceptor family. J. Mol. Evol., 45, 535–548.

Kleine, T., Lockhart, P. & Batschauer, A. (2003) An Arabidopsis protein closely related to Synechocystis cryptochrome is targeted to organelles. Plant J., 35, 93–103.

Kobayashi, Y., Ishikawa, T., Hirayama, J., Daiyasu, H., Kanai, S., Toh, H., Fukuda, I., Tsujimura, T., Terada, N., Kamei, Y., Yuba, S., Iwai, S. & Todo, T. (2000) Molecular analysis of zebrafish photolyase/cryptochrome family: two types of cryptochromes present in zebrafish. Genes Cells, 5, 725–738.

Kubo, Y., Akiyama, M., Fukada, Y. & Okano, T. (2006) Molecular cloning, mRNA expression, and immunocytochemical localization of a putative blue-light photoreceptor CRY4 in the chicken pineal gland. J. Neurochem., 97, 1155–1165.

Kume, K., Zylka, M.J., Sriram, S., Shearman, L.P., Weaver, D.R., Jin, X., Maywood, E.S., Hastings, M.H. & Reppert, S.M. (1999) mCRY1 and mCRY2 are essential components of the negative limb of the circadian clock feedback loop. Cell, 98, 193–205.

Kusanagi, H., Hida, A., Satoh, K., Echizenya, M., Shimizu, T., Pendergast, J.S., Yamazaki, S. & Mishima, K. (2008) Expression profiles of 10 circadian clock genes in human peripheral blood mononuclear cells. Neurosci. Res., 61, 136–142.

Leak, R.K. & Moore, R.Y. (1997) Identification of retinal ganglion cells projecting to the lateral hypothalamic area of the rat. Brain Res., 770, 105–114.

Lucas, R.J., Douglas, R.H. & Foster, R.G. (2001) Characterization of an ocular photopigment capable of driving pupillary constriction in mice. Nat. Neurosci., 4, 621–626.

Lucas, R.J., Freedman, M.S., Muñoz, M., Garcia-Fernández, J.M. & Foster, R.G. (1999) Regulation of the mammalian pineal by non-rod, non-cone, ocular photoreceptors. Science, 284, 505–507.

Matos-Cruz, V., Blasic, J., Nickle, B., Robinson, P.R., Hattar, S. & Halpern, M.E. (2011) Unexpected diversity and photoperiod dependence of the zebrafish melanopsin system. PLoS ONE, 6, e25111.

McWatters, H.G., Bastow, R.M., Hall, A. & Millar, A.J. (2000) The ELF3 zeitnehmer regulates light signalling to the circadian clock. Nature, 408, 716–720.

Menaker, M. & Wisner, S. (1983) Temperature-compensated circadian clock in the pineal of Anolis. Proc. Natl. Acad. Sci. U.S.A., 80, 6119–6121.

Miyamoto, Y. & Sancar, A. (1998) Vitamin B2-based blue-light photoreceptors in the retinohypothalamic tract as the photoactive pigments for setting the circadian clock in mammals. Proc. Natl. Acad. Sci. U.S.A., 95, 6097–6102.

Nagoshi, E., Saini, C., Bauer, C., Laroche, T., Naef, F. & Schibler, U. (2004) Circadian gene expression in individual fibroblasts: cell-autonomous and self-sustained oscillators pass time to daughter cells. Cell, 119, 693–705.

Nelson, R.J. & Zucker, I. (1981) Absence of extraocular photoreception in diurnal and nocturnal rodents exposed to direct sunlight. Comparative Biochemistry and Physiology Part A: Physiology, 69, 145–148.

Okamura, H., Miyake, S., Sumi, Y., Yamaguchi, S., Yasui, A., Muijtjens, M., Hoeijmakers, J.H. & van der Horst, G.T. (1999) Photic induction of mPer1 and mPer2 in cry-deficient mice lacking a biological clock. Science, 286, 2531–2534.

Okano, T. & Fukada, Y. (2001) Photoreception and circadian clock system of the chicken pineal gland. Microsc. Res. Tech., 53, 72–80.

Owens, L., Buhr, E., Tu, D.C., Lamprecht, T.L., Lee, J. & van Gelder, R.N. (2012) Effect of circadian clock gene mutations on nonvisual photoreception in the mouse. Invest. Ophthalmol. Vis. Sci., 53, 454–460.

Ozturk, N., Selby, C.P., Song, S.-H., Ye, R., Tan, C., Kao, Y.-T., Zhong, D. & Sancar, A. (2009) Comparative photochemistry of animal type 1 and type 4 cryptochromes. Biochemistry, 48, 8585–8593.

Panda, S., Provencio, I., Tu, D.C., Pires, S.S., Rollag, M.D., Castrucci, A.M., Pletcher, M.T., Sato, T.K., Wiltshire, T., Andahazy, M., Kay, S.A., van Gelder, R.N. & Hogenesch, J.B. (2003) Melanopsin is required for non-image-forming photic responses in blind mice. Science, 301, 525–527.

Panda, S., Sato, T.K., Castrucci, A.M., Rollag, M.D., DeGrip, W.J., Hogenesch, J.B., Provencio, I. & Kay, S.A. (2002) Melanopsin (Opn4) requirement for normal light-induced circadian phase shifting. Science, 298, 2213–2216.

Pevet, P. & Challet, E. (2011) Melatonin: both master clock output and internal time-giver in the circadian clocks network. J. Physiol. Paris, 105, 170–182.

Plautz, J.D., Kaneko, M., Hall, J.C. & Kay, S.A. (1997) Independent photoreceptive circadian clocks throughout Drosophila. Science, 278, 1632–1635.

Preitner, N., Damiola, F., Lopez-Molina, L., Zakany, J., Duboule, D., Albrecht, U. & Schibler, U. (2002) The orphan nuclear receptor REV-ERBalpha controls circadian transcription within the positive limb of the mammalian circadian oscillator. Cell, 110, 251–260.

Provencio, I., Rodriguez, I.R., Jiang, G., Hayes, W.P., Moreira, E.F. & Rollag, M.D. (2000) A novel human opsin in the inner retina. J. Neurosci., 20, 600–605.

Reppert, S.M. & Weaver, D.R. (2002) Coordination of circadian timing in mammals. Nature, 418, 935–941.

Ritz, T., Adem, S. & Schulten, K. (2000) A model for photoreceptor-based magnetoreception in birds. Biophys. J., 78, 707–718.

Samejima, M., Tamotsu, S., Uchida, K., Moriguchi, Y. & Morita, Y. (1997) Melatonin excretion rhythms in the cultured pineal organ of the lamprey, Lampetra japonica. Biol. Signals, 6, 241–246.

Sanchez, J.A. & Sanchez-Vazquez, F.J. (2009) Feeding entrainment of daily rhythms of locomotor activity and clock gene expression in zebrafish brain. Chronobiol. Int., 26, 1120–1135.

Sathyanarayanan, S., Zheng, X., Kumar, S., Chen, C.-H., Chen, D., Hay, B. & Sehgal, A. (2008) Identification of novel genes involved in light-dependent CRY degradation through a genome-wide RNAi screen. Genes Dev., 22, 1522–1533.

Selby, C.P., Thompson, C., Schmitz, T.M., van Gelder, R.N. & Sancar, A. (2000) Functional redundancy of cryptochromes and classical photoreceptors for nonvisual ocular photoreception in mice. Proc. Natl. Acad. Sci. U.S.A., 97, 14697–14702.

Shearman, L.P., Sriram, S., Weaver, D.R., Maywood, E.S., Chaves, I., Zheng, B., Kume, K., Lee, C.C., van der Horst, G.T., Hastings, M.H. & Reppert, S.M. (2000) Interacting molecular loops in the mammalian circadian clock. Science, 288, 1013–1019.

Somers, D.E., Devlin, P.F. & Kay, S.A. (1998) Phytochromes and cryptochromes in the entrainment of the Arabidopsis circadian clock. Science, 282, 1488–1490.

Stanewsky, R., Kaneko, M., Emery, P., Beretta, B., Wager-Smith, K., Kay, S.A., Rosbash, M. & Hall, J.C. (1998) The cryb mutation identifies cryptochrome as a circadian photoreceptor in Drosophila. Cell, 95, 681–692.

Tamai, T.K., Vardhanabhuti, V., Foulkes, N.S. & Whitmore, D. (2004) Early embryonic light detection improves survival. Curr. Biol., 14, R104-5.

Tamai, T.K., Young, L.C. & Whitmore, D. (2007) Light signaling to the zebrafish circadian clock by Cryptochrome 1a. Proc. Natl. Acad. Sci. U.S.A., 104, 14712–14717.

Tang, R., Dodd, A., Lai, D., McNabb, W.C. & Love, D.R. (2007) Validation of zebrafish (Danio rerio) reference genes for quantitative real-time RT-PCR normalization. Acta Biochim. Biophys. Sin. (Shanghai), 39, 384–390.

Thompson, C.L., Blaner, W.S., van Gelder, R.N., Lai, K., Quadro, L., Colantuoni, V., Gottesman, M.E. & Sancar, A. (2001) Preservation of light signaling to the suprachiasmatic nucleus in vitamin A-deficient mice. Proc. Natl. Acad. Sci. U.S.A., 98, 11708–11713.

Thompson, C.L., Bowes Rickman, C., Shaw, S.J., Ebright, J.N., Kelly, U., Sancar, A. & Rickman, D.W. (2003) Expression of the blue-light receptor cryptochrome in the human retina. Invest. Ophthalmol. Vis. Sci., 44, 4515–4521.

Thompson, C.L., Selby, C.P., van Gelder, R.N., Blaner, W.S., Lee, J., Quadro, L., Lai, K., Gottesman, M.E. & Sancar, A. (2004) Effect of vitamin A depletion on nonvisual phototransduction pathways in cryptochromeless mice. J. Biol. Rhythms, 19, 504–517.

van der Horst, G.T., Muijtjens, M., Kobayashi, K., Takano, R., Kanno, S., Takao, M., Wit, J. de, Verkerk, A., Eker, A.P., van Leenen, D., Buijs, R., Bootsma, D., Hoeijmakers, J.H. & Yasui, A. (1999) Mammalian Cry1 and Cry2 are essential for maintenance of circadian rhythms. Nature, 398, 627–630.

van Gelder, R.N., Gibler, T.M., Tu, D., Embry, K., Selby, C.P., Thompson, C.L. & Sancar, A. (2002) Pleiotropic effects of cryptochromes 1 and 2 on free-running and light-entrained murine circadian rhythms. J. Neurogenet., 16, 181–203.

van Gelder, R.N., Wee, R., Lee, J.A. & Tu, D.C. (2003) Reduced pupillary light responses in mice lacking cryptochromes. Science, 299, 222.

Velarde, E., Haque, R., Iuvone, P.M., Azpeleta, C., Alonso-Gómez, A.L. & Delgado, M.J. (2009) Circadian clock genes of goldfish, Carassius auratus: cDNA cloning and rhythmic expression of period and cryptochrome transcripts in retina, liver, and gut. J. Biol. Rhythms, 24, 104–113.

Vitaterna, M.H., Selby, C.P., Todo, T., Niwa, H., Thompson, C., Fruechte, E.M., Hitomi, K., Thresher, R.J., Ishikawa, T., Miyazaki, J., Takahashi, J.S. & Sancar, A. (1999) Differential regulation of mammalian period genes and circadian rhythmicity by cryptochromes 1 and 2. Proc. Natl. Acad. Sci. U.S.A., 96, 12114–12119.

Whitmore, D., Foulkes, N.S. & Sassone-Corsi, P. (2000) Light acts directly on organs and cells in culture to set the vertebrate circadian clock. Nature, 404, 87–91.

Yang, M.-Y., Yang, W.-C., Lin, P.-M., Hsu, J.-F., Hsiao, H.-H., Liu, Y.-C., Tsai, H.-J., Chang, C.-S. & Lin, S.-F. (2011) Altered expression of circadian clock genes in human chronic myeloid leukemia. J. Biol. Rhythms, 26, 136–148.

Yoshii, T., Ahmad, M. & Helfrich-Förster, C. (2009) Cryptochrome mediates light-dependent magnetosensitivity of Drosophila's circadian clock. PLoS Biol., 7,4.

Zhu, H., Sauman, I., Yuan, Q., Casselman, A., Emery-Le, M., Emery, P. & Reppert, S.M. (2008) Cryptochromes define a novel circadian clock mechanism in monarch butterflies that may underlie sun compass navigation. PLoS Biol., 6,1.

Chapter 8

Wavelength-dependent Aspects of Visual and Non-Visual Photo-reception in larval Zebrafish

Marion F. Haug*, Viktor Lazovic*, Stephan C. F. Neuhauss

Institute of Molecular Biology, Winterthurerstrasse 190, 8057 Zurich, Switzerland

*these authors contributed equally to this work

Report on an ongoing research project

Personal contribution:

VMR and qrtPCR experiments (together with VL), preparation of all figures, writing of the manuscript

8.1 Abstract

Mammals use their retina for both visual and non-visual photoreception. This complicates the study of non-visually guided behaviors such as circadian rhythmicity. In lower vertebrates extraocular photoreceptors located in peripheral tissues contribute to non-visual light perception. Melanopsin, ancient opsins such as TMT-opsin or VA-opsin as well as cryptochromes are photopigments expressed in such tissues and therefore discussed to be involved in such processes but it still remains open to what extent they influence circadian activity levels and non-visually guided light perception. As lower vertebrates possess cell-autonomous circadian clocks they bear the possibility to study circadian activity levels without the influence of eyes. To benefit from this we used wild-type and eyeless larval zebrafish to decipher the influence of eyes on activity levels. Moreover, using different spectral light enabled us to measure the wavelength dependency of visually and non-visually guided photopic behaviors, thereby gaining information about the photoreceptors involved in these tasks.

While eyeless fish did not show activity level differences between day and night, we found that these fish show a fast response upon dark to light transitions under white light or when omitting UV-light but not under red light, suggesting that the light-ON response is driven by an extraocular photoreceptor absorbing light in the blue to green range. OFF-responses are likely driven by a photopigment located within the eye, since such a behavior was never observed in eyeless mutant fish. Moreover, a large variety of photopigments are likely involved in these processes, since these responses could be elicited using different light spectra. After raising the fish in different light conditions a qRT-PCR analysis was performed. Fish raised only under red light showed a downregulation in some but not all *cryptochrome* mRNA levels. To what extend this influenced certain behaviors can only be shown by specific downregulation followed by behavioral testing. Although these results are only preliminary and further studies are needed for confirmation, they show the impact of light conditions on light-mediated behaviors of zebrafish and help us distinguishing the photoreceptive molecules involved in such tasks.

8.2 Introduction

In mammals the retina is exclusively involved in both visual and non-visual input to higher brain centers (Hattar *et al.*, 2003). Lower vertebrates however do not only rely on their eyes but additionally possess peripheral photoreceptors that perceive non-visual input. Information about irradiance gained by such extraretinal photoreceptors majorly influences daily or seasonal changing behaviors such as activity level (Garg & Sundararaj, 1986) or reproductivity (Kang *et al.*, 2010). It is well established that removing of the pineal gland or other deep brain structures in lower vertebrates such as birds, lizards or fish has various effects on circadian physiology and seasonal reproduction (Zimmerman & Menaker, 1979; Underwood & Menaker, 1976; Menaker & Keatts, 1968; Underwood, 1990). During the last decade photoreceptive cells have been discovered in both the pineal gland (Frigato *et al.*, 2006; Bailey & Cassone, 2005) and the deep brain (Halford *et al.*, 2009; Nakane *et al.*, 2010) of lower vertebrates. In mammals, melanopsin, a vitamin A based photopigment located in specific ganglion cells, is known to account primarily for non-visual photoreception (Hattar *et al.*, 2003). Melanopsin-containing cells have also been found in non-mammalian vertebrate retinas (Frigato *et al.*, 2006; Bailey & Cassone, 2005; Matos-Cruz *et al.*, 2011), however, due to extraocular photoreception non-image forming vision is far more complex in these animals. Opsins such as the vertebrate ancient (VA) opsin or the teleost multiple tissue (TMT) opsin have been discussed to be involved in circadian photoregulation since they absorb light at the behaviorally measured wavelength to mediate such processes and are expressed in photosensitive tissues (Davies *et al.*, 2010; Moutsaki *et al.*, 2003). Besides that, the family of cryptochromes (Crys) is also discussed to act as non-visual photopigment. Although not all cryptochromes are still directly photosensitive, they all possess chromophore binding domains that let them absorb light in the UV- and blue-light range (reviewed in Chaves *et al.*, 2011). Moreover, the light-responsive cryptochrome 1a has already been shown to mediate cell-autonomous circadian oscillation in zebrafish (Tamai *et al.*, 2007).

To date many studies describe extraocular photoreception including its visual pigments. However, it is still unclear to what extent they influence circadian activity levels. The zebrafish, a widely used model organism in science, is well suited for such studies. Its larvae develop relatively fast and show reliably measurable behaviors already shortly after hatching. Transparent body tissue enables light to penetrate the skin and thereby act directly on cells and organs. Due to an additional whole genome duplication followed by retainment of a large percentage of duplicated genes (Force *et al.*, 1999), the zebrafish possess one of the largest varieties of photosensitive molecules (for an overview, see Davies *et al.*, 2010). These are not only expressed in the retina but also in other photosensitive structures such as the pineal (Mano *et al.*, 1999; Tarttelin *et al.*, 2011) and other parts of the brain (Moutsaki *et al.*, 2003; Matos-Cruz *et al.*, 2011). Mammals lacking eyes experience circadian blindness (Freedman *et al.*, 1999). This complicates decipherment of circadian activity and photovisual responses. Since zebrafish possess cell-autonomous circadian clocks (Whitmore *et al.*, 2000) the eyes may be completely irrelevant for circadian rhythmicity. This can directly be tested in *chokh* mutants. Due to a mutation in the *rx3* homeodomain-containing transcription factor, which prevents the evagination of the immature optic cup from the brain, these mutants lack any visible eye (Loosli *et al.*, 2003). Hence, they are uniquely suited to study activity level and circadian expression profiles without the influence of any photoreceptive cell in the retina. Furthermore, an *in vivo* study on wavelength response of circadian photoreceptors is possible. Together, these experiments should give

us more insight into the wavelength dependent development of light-mediated behaviors of larval fish. Finally, by using narrow-band LEDs, we can also assess the spectral properties of the photopigment involved in these behaviors.

We measured activity levels between 3 and 5 dpf (days post fertilization) of wild-type and *chokh* mutant larval zebrafish. Since we observed no activity level changes in eyeless fish we suggest that circadian activity rhythms are dependent on light input through eyes. The startle response of larval zebrafish shown upon fast changes in illumination reflects protective behavior to flee an approaching predator, which enables measurements of light ON- and OFF-locomotor responses (Emran *et al.*, 2008). We found that blue and green light is necessary to elicit a robust startle response. While fish raised under red light lacked ON- but showed OFF-responses, we suppose that a short wavelength receptor such as the cryptochromes is involved in the light-input pathway of the ON-response. To our surprise *chokh* mutants showed a startle response when turning the lights on under all light conditions, suggesting that the startle-ON-response is robustly driven by an extraretinal photopigment. To shine more light on the influence of cryptochromes to these light-mediated processes, we performed a qRT-PCR study using wild-type fish and fish lacking eyes. We found a clear downregulation of some but not all *crys* when raising fish only under red light, which is not able to activate the blue light absorbing cryptochromes. Surprisingly, *cry4* and *-5* were upregulated in eyeless fish which raises the question of how cryptochrome expression is actually regulated.

8.3 Material and Methods

8.3.1 Fish maintenance

Adult fish were kept under standard conditions at a 14h/10h light/dark cycle at 28°C. All experiments were performed in accordance with the ARVO Statement for the Use of Animals in Ophthalmic and Vision Research and were approved by the local authorities (Veterinäramt Zürich TV4206).

8.3.2 Visual motor response (VMR)

8.3.2.1 VMR setup

Emran and colleagues developed a tracking setup to measure activity levels in fish larvae (Emran *et al.*, 2008). A similar setup was built in our lab by Kaspar Müller (Mueller, 2011; see Fig. 1 for an overview). The well plate was illuminated from below with an array of 36 infrared-emitting diodes (λ_{peak} = 880 nm) shielded by a diffuser. In addition to that, the array contained 36 UV- (λ_{peak} = 361 nm), blue- (λ_{peak} = 435 nm), cyan- (λ_{peak} = 500 nm), and red- (λ_{peak} = 630 nm) light emitting diodes (LEDs) each. Each color can be singly lit, and the brightness of each color can be controlled by a pulse-width modulator (PWM83; National Control Devices, Osceola, MO, USA) connected to the serial port of a computer. Brightness levels of the LEDs were measured in lux with a spectrometer (USB2000+XR1; Ocean Optics, Dunedin, FL, USA) and were 5 for UV only, 608 for red only, 1366 for red, green and blue together, and 1350 for the full spectrum. Larvae were monitored from above using an infrared sensitive CCD-camera (Pike F-032B; Allied Vision Technologies, Stadtroda, Germany) equipped with a zoom lens

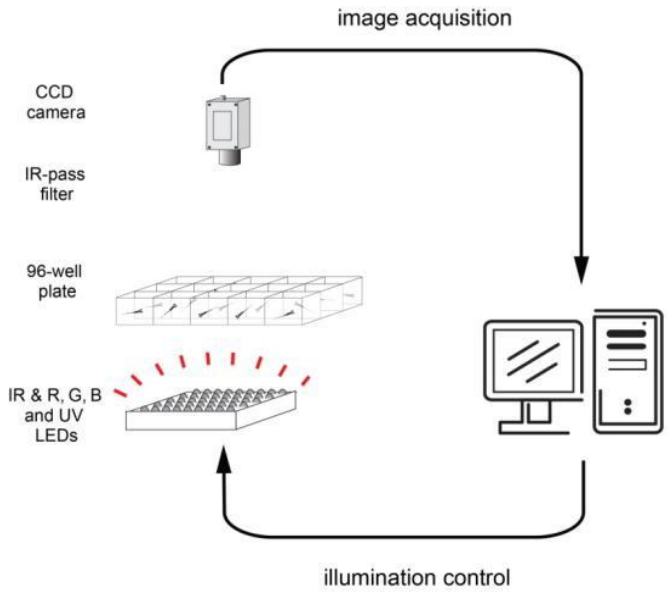

Figure 1: Overview of the VMR-setup.
Up to 48 larvae are placed in a well plate under the camera. A computer tracks and records their movements and controls illumination of the LEDs. Figure kindly provided by K. Müller.

(C6Z1218-FA; Pentax, Hamburg, Germany) fitted with an IR-pass filter (IF-093-SN1-49; Schneider-Kreuznach, Bad Kreuznach, Germany). Detection and tracking of individual larvae was done by a custom-made software based on LabView 7.1 and NI-IMAQ 3.7 (National Instruments). Swimming speed of each larva was calculated in real time at 20 frames per second, averaged over periods of 1 second, and written to disk every second. The startle response was separately analyzed for each light/dark transition. Activity levels of the larvae were averaged over 2 seconds and the highest activity in each condition was set as 1. All other activities were calculated as a percentage of this.

8.3.2.2 VMR experiments

Immediately after the lights were turned on in the morning (8 am) a male and a female fish were placed together in a breeding tank which had been set up the previous afternoon. Wild-type fish of the strain "Tü" (Haffter *et al.*, 1996) and *chokh* mutants (Loosli *et al.*, 2003) were used for these experiments. 45 to maximally 60 minutes later, the eggs were collected, cleaned and placed into the VMR room in a petri dish containing E3 (5mM NaCl, 0.17mM KCl, 0.33mM $CaCl_2$, and 0.33mM $MgSO_4$). The VMR room had a constant temperature of 28°C. Additionally, the light cycle was adjusted to 14h/10h light/dark and 8 am was set as Zeitgeber time (ZT) 0. The conditions used included a dark/dark cycle without any light, UV, blue, green, and red and each color separate or in combination. After two days, unhatched embryos were dechorionated under the appropriate light conditions. On the 3rd day of development the mutants, siblings or wild-type larvae were placed randomly into a 48-well plate (one larvae/well) (677 102; Greiner Bio-One, St. Gallen, Switzerland) containing E3 medium and recording for the next 50 hours started at ZT 3.5. After the recording was finished the larvae were immediately collected and sacrificed using ice-cold tricaine (MS-222; Sigma-Aldrich, Buchs SG, Switzerland) in E3. E3 was exchanged with RNA-later (Sigma-Aldrich) and the samples were fast frozen in liquid N2 for subsequent RNA collection for qRT-PCR analysis.

8.3.3 Quantitative real-time PCR (qRT-PCR)

Frozen tissue was thawed on ice and homogenized with a pistil and a sonificator (Sonopuls HD2070; Bandelin Electronic, Berlin, Germany). RNA was extracted with the NucleoSpin RNA II Kit (Macherey-Nagel) and RNA concentration was measured with a NanoDrop (ND-1000; Witec AG, Litau, Switzerland). Reverse transcription was performed with 400 ng RNA and the Superscript II kit (Invitrogen, Life Technologies, Zug, Switzerland). qRT-PCR

was performed in a transcriptor (Applied Biosystems Prism SDS 7900HT; Life Technologies) using the MESA Green Kit (Eurogentec, Seraing, Belgium). Primer pairs (Sigma-Aldrich) used for qRT-PCR were specifically designed to span an excised intron to avoid unspecific amplification of genomic DNA (Tab. 1). As a reference, the genes *Rpl-13α* (ribosomal protein L-13a), *EF1α* (elongation factor 1 alpha), and *prkcα* (protein kinase C alpha) were selected (Tang *et al.*, 2007). Cryptochrome expression in tissue from larvae raised under the whole light spectrum was taken as reference set (standard = 1). The values are means +/- standard deviations. Analysis was completed in Microsoft Excel and graphs were arranged in Microsoft Excel and Adobe Illustrator CS5.

Gene	Primer	5' to 3'
cry1a	1a_dr_0359s	F: CAGGCGTGGAGGTGATAG
	1a_dr_0461as	R: TGGAAGCGCTTATACGTG
cry1b	1b_dr_0738s	F: ACACCGGTCAGTGATGATC
	1b_dr_0819as	R: TGGACAGTCCCTCTGTTTC
cry3a	3a_dr_1078s	F: GCTGTTGCATGTTTCCTC
	3a_dr_1169as	R: CAGTCTGCATCCAAATAGAAG
cry3b	3b_dr_0632s	F: CCGGTGGAGAATCAGAAG
	3b_dr_0722as	R: TTCGGTCGCTCAAAGTTC
cry2	2_dr_1073s	F: GACATGCAGTAGCCTGTTTC
	2_dr_1163as	R: CGCATCCAACAGCAACTC
cry4	4_dr_0778s	F: CGAACCTTCTACCACAGACTC
	4_dr_0890as	R: AGCGACGGTGTAGAAGAAC
cry5	5_dr_0495s	F: ACCCATTCCTGCTCCAAC
	5_dr_0600as	R: CAGTCCAAGATCCTCAAGAG
cryDASH	DASH_dr_0532s	F: ACTCCAGAACAGGTGAAATC
	DASH_dr_0640s	R: GGAAGGCAGAACGACAGTC

Gene	Primer	5' to 3'
Rpl-13a	Rpl13a_dr_0251s	F: GGACTGTAAGAGGTATGCTTC
	Rpl13a_dr_0330as	R: GATGCCATCAAACACCTTC
EF1 α	EF1a_dr_0607s	F: GAGGCCAGCTCAAACATG
	EF1a_dr_0698as	R: TCAAGGGCATCAAGAAGAG
prkcα	prkca_dr_0363s	F: GGACTCATACACCAAGGAATG
	prkca_dr_0440as	R: GCTTGGCACATTCATCAC

Table 1: Primer pairs used for qRT-PCR analyses.
Numbers within primer names indicate the position of the primer from the ATG on.

8.4 Results

8.4.1 Activity levels of zebrafish larvae raised in different light conditions

The VMR can give information about the activity of the zebrafish larvae as well as their immediate reaction upon changes in illumination. In our first experiment we compared activity levels of wild-type larvae raised under complete darkness or under UV-light (Fig. 2), a spectrum that should activate cryptochromes which absorb light in this range. Fish raised in darkness show a medium level of activity and no obvious change between the subjective day or subjective night between the 3rd and the 5th day of development (Fig. 2A). In contrast to that, wild-type fish increased their swimming speed immediately after UV-light is turned on (time = 20.5 h and 44.5 h; Zeitgeber time (ZT) 0). This effect seems to increase with the age of the larvae. While no difference is seen directly upon lights-off (time = 10.5 h and 34.5h; ZT 14), overall activity seems decreased during dark hours.

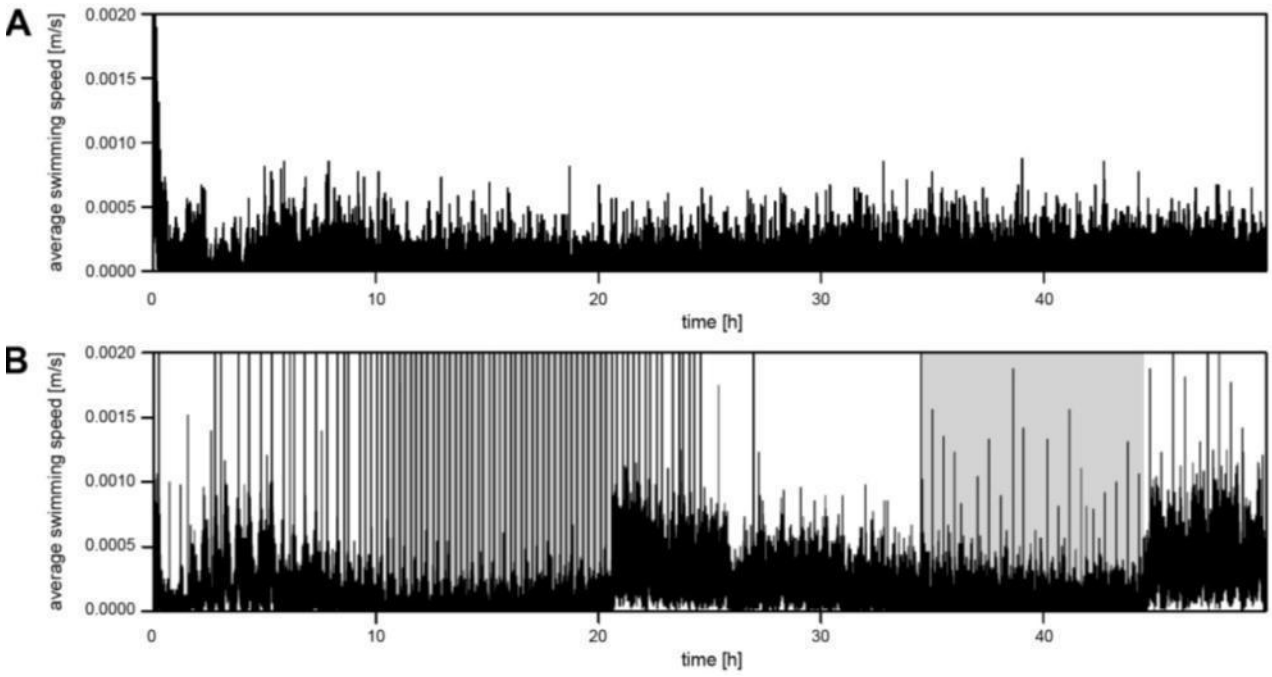

Figure 2: Average swimming speed of wild-type zebrafish larvae raised in complete darkness or under narrow-band UV- light.

Recordings were taken for 50 hours between 3 and 5 dpf. Swimming speed of each larvae was measured and averaged for each time point. A: Zebrafish larvae (n = 48) raised in darkness reveal a medium overall swimming speed. Changes between subjective day and night are not visible and spiking activity is low. B: Larvae raised under 14h UV-light/10h dark cycles (n = 48) clearly show an increase in swimming speed at the OFF-ON switch. The x-axis depicts the time in hours counted after the recording started (ZT 3.5) and lights-off periods are shaded in grey.

8.4.2 Behavior of zebrafish larvae raised under different light spectra

To access how larvae react towards raising in different light conditions and how these effects differ between wild-type and the eyeless *chokh* mutant we measured the larvae's locomotor activity between the 3rd and the 5th day of development for 50 hours. The startle response elicited each time when light conditions change rapidly is

an indicator of the function of the retinal ON- and OFF-system. To investigate development of ON- and OFF-responses and dependency of them on light conditions, each light/dark transition was analyzed individually.

When raised under white light, wild-type fish show an increased swimming speed during the day (Fig. 3A). Overall, a high spiking activity is observed and during the lights-on periods rhythmic phases of activity levels that last for about 15 to 20 minutes. At light/dark transitions the larvae reveal a sharp increase in activity throughout development (Fig. 3A1-4). *Chokh* mutants do not show differences between day and night (Fig. 3B), and no specific increase upon lights-off could be measured (Fig. 3B1,3). On the other hand, eyeless fish seem to react upon lights-on since they show a startle response to that change in illumination at both 4 and 5 dpf (Fig. 3B2,4). Omitting UV-light from otherwise white light causes an overall decrease in spiking activity in wild-type fish but still a slightly increased locomotor activity is observed during the lights-on periods (Fig. 4A). Startle responses at the time point of the light/dark transitions are clearly observed at all developmental stages (Fig. 4A1-4). Apparently, the activity levels of *chokh* mutants do not differ between day and night, however, a marginal increase in swimming speed upon lights-on at 4 dpf can be observed (Fig. 4B). Similar to the white light experiments, only unspecific increases in OFF-responses are seen in mutant fish at 3 dpf (Fig. 4B1). At 4 dpf the response is more prominent but does not resemble the curve of a normal OFF-response (Fig. 4B3). The lights-on responses at both 4 and 5 dpf seem a bit delayed but are clearly detectable (Fig. 4B2,4).

Although activity levels are generally lower, fish raised under red light still show visible differences in locomotor activity during day and night (Fig. 5A). While the startle response at the light/dark transition seems normal a gradual decrease in activity level is only observed at 4 dpf (Fig. 5B1,3). Moreover, the dark/light transition caused no startle response but only a slight increase in overall activity at 5 dpf (Fig. 5A2,4). Overall activity throughout the measurement stayed at base levels in *chokh* mutant larvae (Fig. 5B). Lights-on and lights-off do not cause any fast changes in activity levels (Fig. 5B1-4). The response seen in Figure 5B1 and B2 starts before the illumination is switched and therefore does not correspond to a startle response. At 4 dpf the mutant larvae show a late increase in overall locomotor activity (Fig. 5B3).

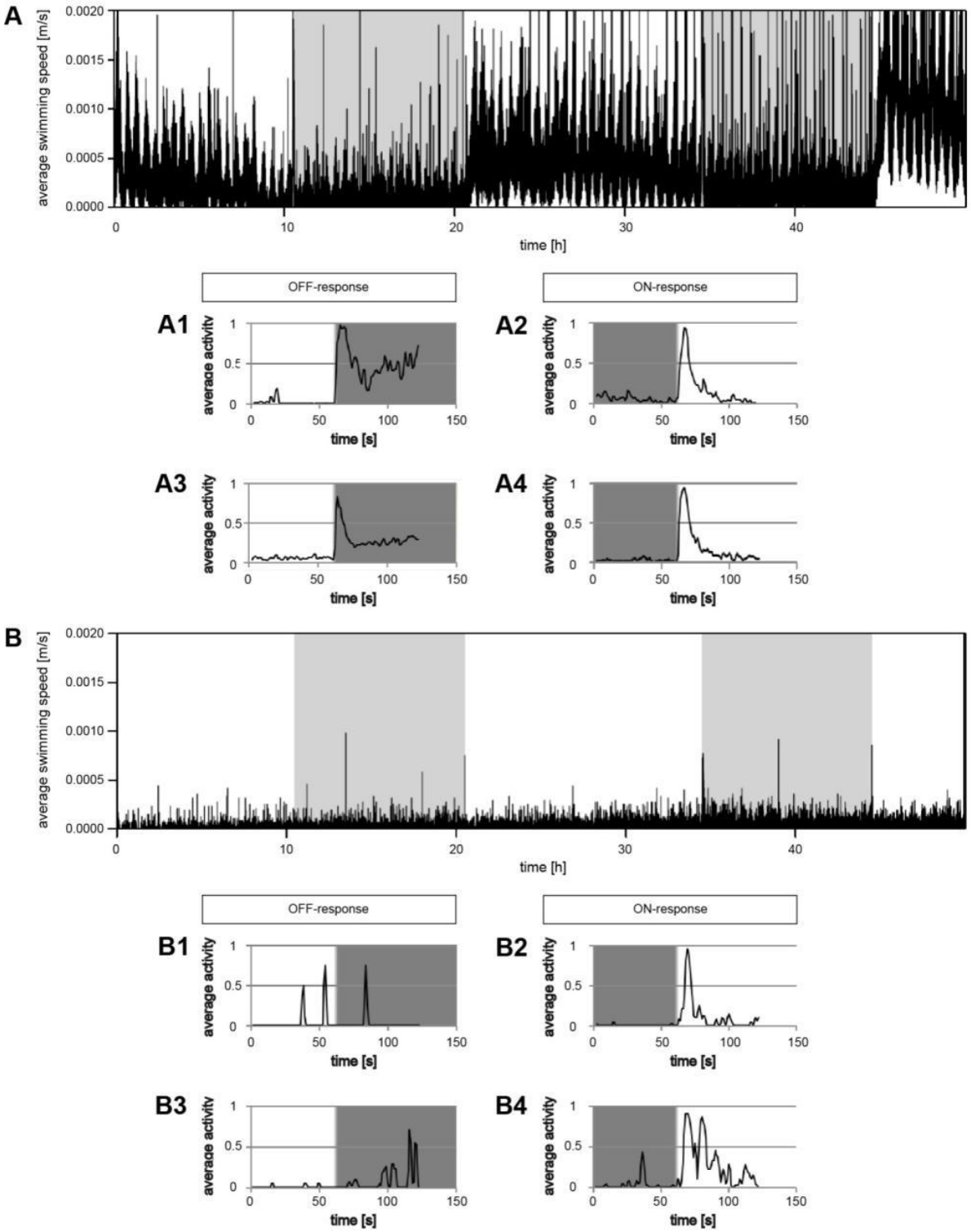

Figure 3: Activity levels of wild-type and chokh larvae raised under white light.
Recordings were taken for 50 hours between 3 and 5 dpf. ***A:*** *50 hour recording of wild-type zebrafish larvae (n = 48) reveal an increased swimming speed during lights-on periods. The x-axis depicts the time in hours counted after the recording started (ZT 3.5) and lights-off periods are shaded in grey.* ***A1-4:*** *Activity level measurements during 1 min before and 1 min after the ON-OFF switch (A1,3; corresponds to the light OFF-response) and the OFF-ON switch (A2,4; corresponds to the light ON-response) reveal a sharp increase in motor activity between the 3rd and the 4th (A1,2), and between the 4th and the 5th dpf (A3,4).* ***B:*** *50 hour recording of chokh mutants (n = 25) show no obvious difference in motor activity between lights-on (white) and lights-off (grey) periods.* ***B1,3:*** *Activity level measurements between 1 min before and 1 min after the ON-OFF switch (light OFF-response) show*

no specific increase in activity at 3 dpf (B1) and 4 dpf (B3). ***B2,4:*** *Activity level measurements 1 min before and 1 min after the light is turned on (ON-reponse) at 4 dpf (B2) and 5 dpf (B4) in the morning show an acceleration in swimming speed*

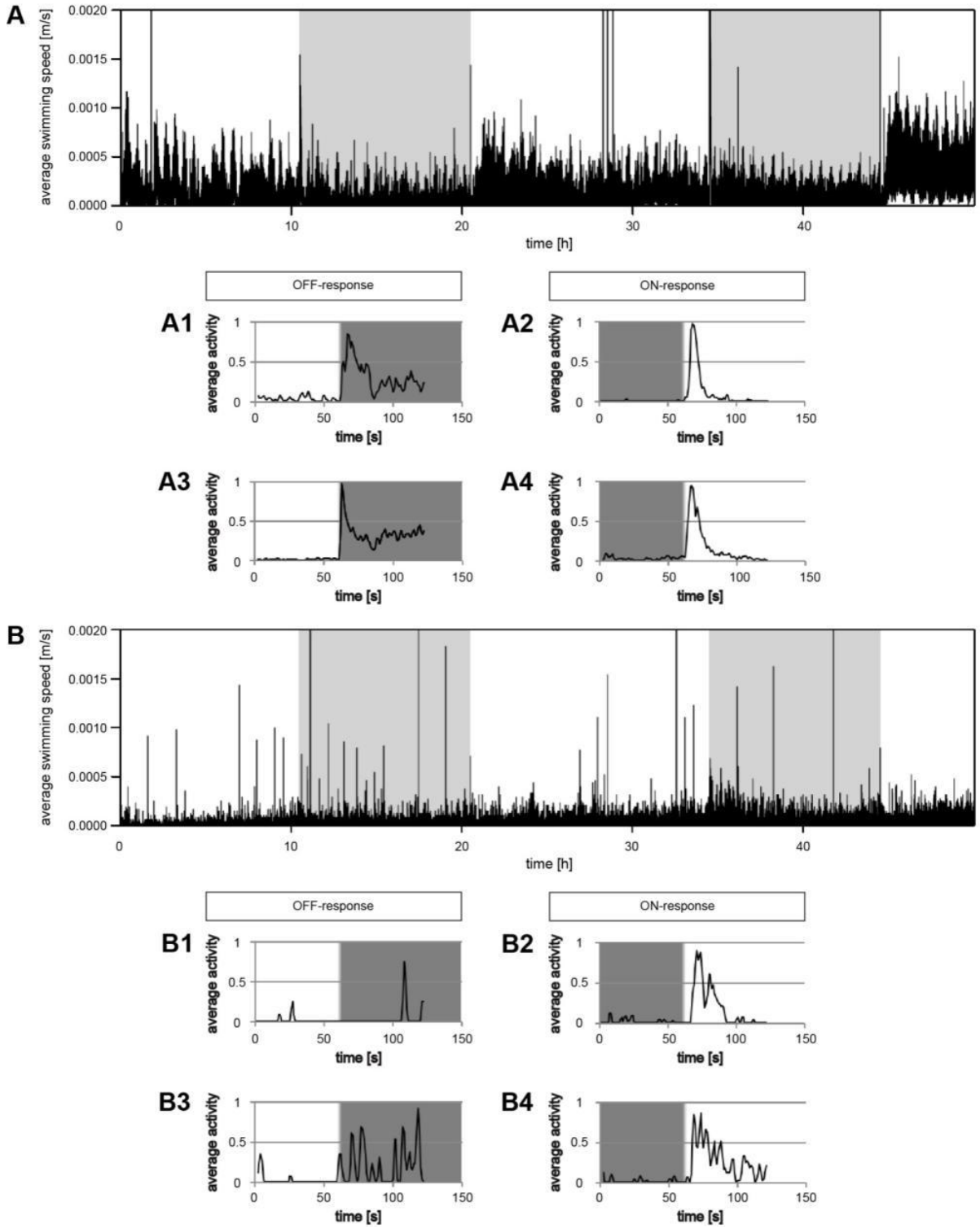

Figure 4: Activity levels of wild-type and chokh larvae raised without UV-light.

Recordings were taken for 50 hours between 3 and 5 dpf. ***A:*** *50 hour recording of wild-type zebrafish larvae (n = 48) reveal reveals a minor increase in locomotor activity during the lights-on periods. The x-axis depicts the time in hours counted after the recording started (ZT 3.5) and lights-off periods are shaded in grey.* ***A1-4:*** *Activity level measurements during 1 min before and 1 min after the ON-OFF switch (A1,3; corresponds to the light OFF-response) and the OFF-ON switch (A2,4; corresponds to the light ON-response) show increased locomotion shortly after changing the illumination.* ***B:*** *50 hour recording of chokh mutants (n =*

25). Lights-on periods are shown in white and lights-off periods in grey, respectively. Although a slight increase in swimming speed upon turning the light off at 4 dpf is visible, overall no obvious difference in motor activity between the different illuminations. ***B1,3:*** *Activity level measurements between 1 min before and 1 min after the ON-OFF switch (light OFF-response) show a late increase in activity at 3 dpf (B1) and an overall higher locomotor activity to light offset at 4 dpf (B3).* ***B2,4:*** *Activity level measurements 1 min before and 1 min after the light is turned on (ON-reponse) at 4 dpf (B2) and 5 dpf (B4) in the morning show a sharp increase in swimming speed more similar to the wild-type measurements than the OFF-reponses.*

Figure 5: Activity levels of wild-type and chokh larvae raised under narrow-band red light.
Recordings were taken for 50 hours between 3 and 5 dpf. ***A:*** *50 hour recording of wild-type zebrafish larvae (n = 48) reveal slightly increased swimming speeds in lights-on periods. The x-axis depicts the time in hours counted after the recording started (ZT 3.5) and lights-off periods are shaded in grey.* ***A1,3:*** *Although not clearly visible in A, activity level measurements during 1 min before and 1 min after the ON-OFF switch (corresponds to the light OFF-response) reveals clear light OFF-reactions of wild-type larvae at 3 (A1), and 4 (A3) dpf. The usually observed gradual decrease after increased activity upon light cessations is only visible at 4 dpf.* ***A2,4:*** *Activity level during 1 min before and 1 min after the OFF-ON switch (corresponds to the light ON-response). At 4 dpf (A2) wild-type larvae show no clear ON-response, however, at 5 dpf (A4) a late overall increase in activity level is visible after the light is turned ON.* ***B:*** *50 hour recording of chokh fish (n = 25) show no obvious increase in swimming speed in lights-on periods.* ***B1,3:*** *Activity level measurements between 1 min before and 1 min after the ON-OFF switch (light OFF-response) show no sharp increase in swimming speed. The amplitude at 3 dpf (B1) increases before the light/dark transition happens and does not show a startle response. At 4 dpf (B2) a late increase in overall activity is visible.* ***B2,4:*** *Activity level measurements 1 min before and 1 min after the light is turned on (ON-reponse) at 4 dpf (B2) and 5 dpf (B4) in the morning show no difference.*

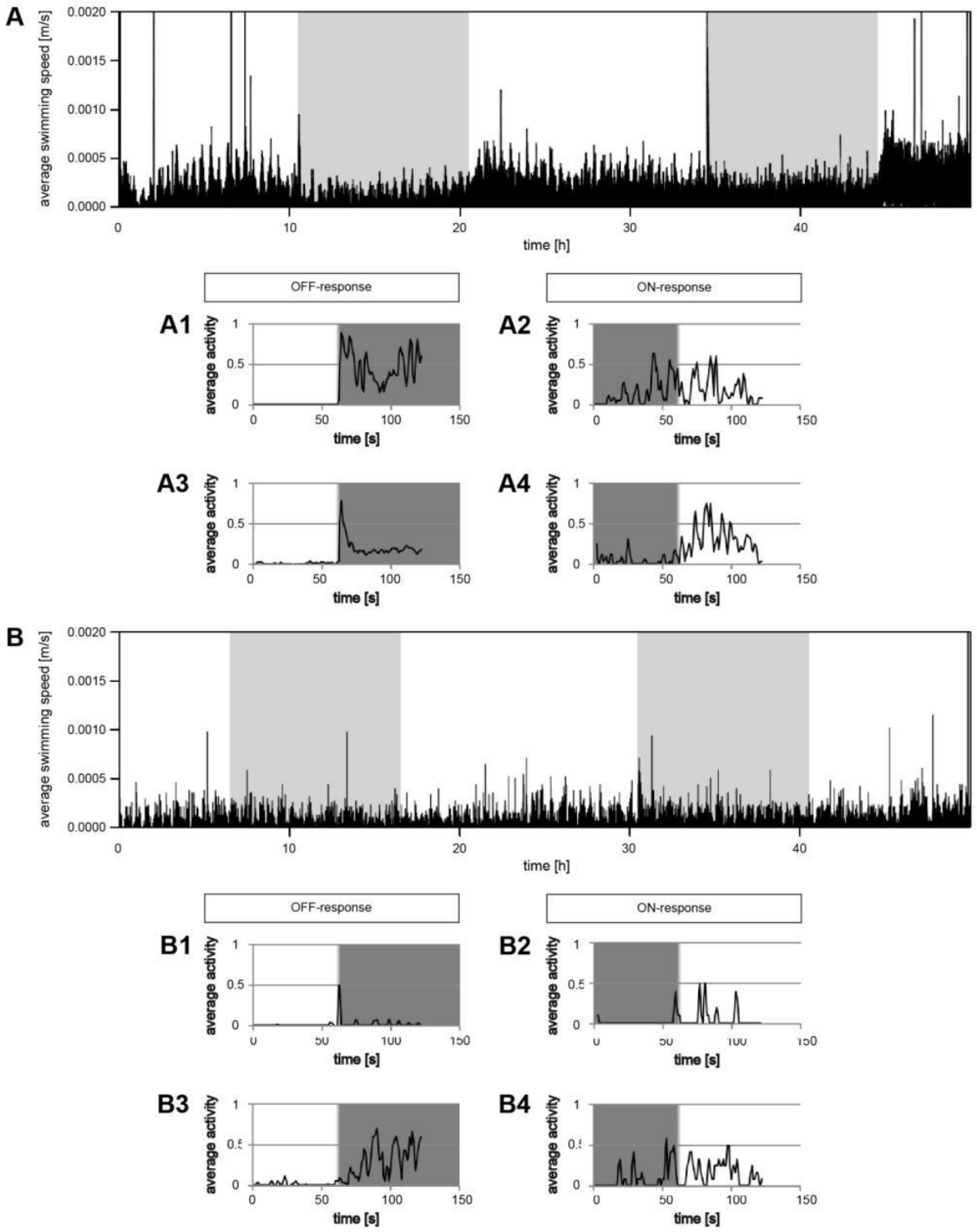

8.4.3 Influence of spectral rearing on *cryptochrome* mRNA levels

After raising the wild-type and mutant fish for five days under different light conditions, overall mRNA levels of cryptochromes were measured using qRT-PCR. With this experiment we aimed to suggest a dependence of *cry*

expression to wavelength and to detect differences between eyeless and wild-type fish. The broad-spectrum reared wild-type fish were used as a reference.

When raising wild-type larvae under red light only, they show clear decrease in expression of *cry1* and *cry3* paralogs as well as *cryDASH*. Overall *cry* expression in *chokh* mutants raised under red, green and blue light (Fig. 6 RGB chk) seems, besides some minor changes, similar to the reference set. Surprisingly, larger differences were found between mutants and wild-types raised under the broad-light spectrum. Here, especially the *cry1* and *-3* paralogs as well as *cryDASH* seem to be downregulated. When raised under red light, wild-types show majorly diminished cryptochrome levels, while mutants rather have a tendency to increase *cry* expression.

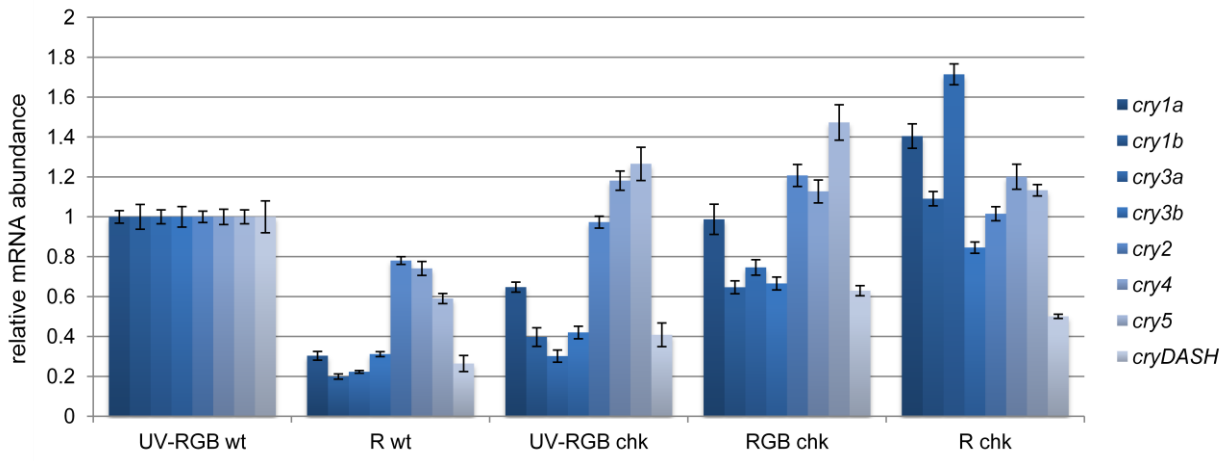

Fig. 6: Relative cryptochrome mRNA abundance in fish raised under different light conditions.
Wild-type zebrafish raised under the full light spectrum were used as a reference and set as standard 1. For each individual analysis 48 wild-type larvae and 25 chokh mutants were used. All cryptochromes were named according to Chapter 6 in this thesis. UV-RGB: full light spectrum; RGB: red, green and blue light; R: red light; chk: chokh mutant zebrafish; wt: wild-type zebrafish.

8.5 Discussion

The majority of an animal's daily behavior is adapted to their photic environment. In order to do so, information on ambient irradiance needs to be gathered by photosensitive molecules. Classical visual pathways are optimized to discriminate shapes, colors and motion within the visual field. Although this enables high temporal and spatial precision it is not suited to accurately encode irradiance. For that a measurement of the overall environmental luminance level is necessary. While lower vertebrates solved this problem by extraretinal photoreceptors located in various tissues such as the pineal gland (Bailey & Cassone, 2005), the brain (Halford *et al.*, 2009) or other organs (Whitmore *et al.*, 2000; Moutsaki *et al.*, 2003), mammals possess intrinsically photosensitive retinal ganglion cells containing melanopsin that fulfill this task (Hattar *et al.*, 2002). It is hypothesized that early mammals were forced to behave increasingly nocturnal due to the edacious archosaurs that hunted during the day. This "nocturnal bottleneck" may had caused the loss of extraretinal photoreceptors since they were not sensitive enough to function at twilight and during the night (Davies *et al.*, 2010).

The quest for circadian photoreceptors revealed a number of candidates, ranging from all the opsins (Magnoli *et al.*, 2012; Mano *et al.*, 1999) including melanopsin (Underwood, 1990; Frigato *et al.*, 2006) and more ancient

forms such as TMT- or VA-opsins (Moutsaki *et al.*, 2003; Halford *et al.*, 2009; Davies *et al.*, 2012). Cryptochromes have been discussed to participate in this task as well and were even found to mediate light input to the peripheral clock in zebrafish (Tamai *et al.*, 2007, 2007; Kubo *et al.*, 2006). The aim of this study is to shine light on wavelength dependent aspects of visual and non-visual photoreception measured via locomotor output in zebrafish larvae.

8.5.1 Activity levels of wild-type fish raised under different light conditions

Larval zebrafish show a sleep-like state during dark hours (Zhdanova *et al.*, 2001) and while their activity stays at base levels when reared in constant darkness, they show robust circadian behavior under LD-conditions (Prober *et al.*, 2006). As expected, we observe similar effects in our experiments. The wild-type larvae are much more active during the light phase, moreover, activity levels seems to increase with age as a much higher activity is seen in five-day-old fish compared to three-day-old larvae. When reared in constant darkness larvae show no circadian behavior but a basal activity level similar to the one LD-fish show in darkness. Cyclic expression of genes involved in the circadian feedback loop was already observed from the first day after fertilization on (Dekens & Whitmore, 2008), however, an entraining signal after 20 hpf is necessary to synchronize oscillating gene expression (Kazimi & Cahill, 1999; Hurd & Cahill, 2002; Dekens & Whitmore, 2008). In our experiment we placed the larvae into constant darkness within the first hour after fertilization, thereby preventing entrainment of the circadian clock. This possibly led to the basal overall activity level shown by larvae raised in constant darkness.

Activity level changes between day and night of wild-type larvae are highest when using white light. Already omitting UV-light decreases overall daily activity. They seem calmer and show less spiking activity. Interestingly, the change in activity level does not depend on brightness as this differs when illuminating different set of LEDs (see 8.3.2.1). A recent study in cichlid fish has shown that changes in light color but not intensity are crucial for circadian activity (Pauers *et al.*, 2012). This could explain why larvae raised solely with UV-light show a much clearer change in activity level between day and night than larvae raised under the much brighter red light.

In wild-type larvae regular periods of increased activity of about 20 minutes were found during day time. This effect is best seen in Figure 3A when the light is turned on after 44.5 hours of measurement. We found that this is not a behavioral effect but rather depended on air-conditioning that was turned on and off regularly. In later experiments when the air conditioning was turned off such phases were not observed anymore (K. Müller, personal communication).

8.5.2 Wavelength-dependent response of circadian photoreception

Larval zebrafish show robust circadian activity when raised under white light. Omitting UV-light or using narrow-band red or UV-LEDs only led to a reduced activity during light hours but did not affect circadian rhythmicity. This suggests that a large variety of photoreceptors is involved in mediating circadian photoreception. Moreover, most of the molecules discussed to be involved this task such as cryptochromes, TMT-opsin or other vitamin A derivates (reviewed in Peirson *et al.*, 2009) are not activated by the narrow-band red LEDs used in this study. In this case light must be sensed by one or both red-sensitive photopigments LWS1 and LWS2 present in

the zebrafish retina (Chinen *et al.*, 2003), or another, yet unknown photopigment present in either the eye or another photosensitive tissue that absorbs light in the red range.

To investigate extraretinal photoreception and their wavelength dependent input to circadian locomotor activity independent of visual opsin involvement, we used *chokh* mutants. These lack any visible eye due to a mutation in *rx3*, a transcription factor necessary for optic vesicle evagination from the forebrain (Loosli *et al.*, 2003; Kennedy *et al.*, 2004). We found that *chokh* mutants do not exhibit a circadian activity pattern under any light condition. Moreover, mutant larvae showed no age dependent increase in motor activity. This led us conclude that the eyes and its photoreceptive molecules are crucial for the generation of circadian activity. The independently developing rhythmic gene expression in the pineal gland and other peripheral cells (Kazimi & Cahill, 1999; Dekens *et al.*, 2003) seems not to be sufficient to generate rhythmic locomotor output. However, during the experiments we noticed some drawbacks for using this mutant in such studies. Throughout the measurements the activity level of *chokh* mutants was rather low, even lower than the level observed in wild-type fish during dark hours. Although the mutation does not affect swimming ability (Loosli *et al.*, 2003), we observed a decreased response to external stimuli compared to wild-type larvae. Besides that, although very weak, some illumination from standby lights of computer, camera, and other electronics always remains in the room. If this light is sufficient for the wild-type larvae to orientate themselves in the well plate and maintain an overall increased activity level compared to the eyeless larvae is hard to say. These observations of course challenge the readout of our experiments and have to be considered when working with this setup and *chokh* mutants. To complete this study and draw conclusions from the results behavioral abilities of *chokh* larvae need to be thoroughly tested.

At around 24 hpf the pineal gland differentiates and expresses first photoreceptor markers (Heisenberg *et al.*, 1996; Masai *et al.*, 1997; Wilson & Easter, 1991; Falcón *et al.*, 2003). This correlates well with the earliest developmental time where environmental cues are able to set the phase of behavioral rhythms (Kazimi & Cahill, 1999; Hurd & Cahill, 2002). The later differentiating retina (Larison & Bremiller, 1990; Raymond *et al.*, 1995) might account for the gradual increase in amplitude responses, however, other structures are believed to contribute to circadian entrainment as well. In zebrafish circadian locomotion still persisted after pinealectomy and enucleation (Hurd & Cahill, 2002) and in a recent publication a light seeking behavior triggered by photosensitive neurons in the preoptic area has been shown (Fernandes *et al.*, 2012). An involvement of deep brain photoreception in circadian behaviors was previously shown in many non-mammalian vertebrates (reviewed in Foster *et al.*, 1994; Davies *et al.*, 2010). However, which photopigments mediate such behaviors is still debated. The teleost multiple tissue (TMT) opsin is expressed in extensive parts of the fish, including the kidneys, liver, heart, and brain (Moutsaki *et al.*, 2003). A recent study on the eyeless Somalian cavefish, which lack single cell circadian entrainment by light, showed that by inserting a functional *tmt-opsin* into the genetic code, light-sensitivity can be regained. Somalian cavefish carry natural mutations in *tmt-opsin* and *opn4m2* (one of the melanopsin orthologs) which inhibits the light entrainability pathway (Cavallari *et al.*, 2011). This study seems to exclude other photopigments from the list of potential non-visual light sensors, however, the effect of different wavelengths on the induction of clock gene expression suggests that more than these two photopigments contribute to circadian entrainment (Cavallari *et al.*, 2011). In birds it is hypothesized that vertebrate ancient (VA) opsins present in the hypothalamus mediate photoperiodic behavior (Davies *et al.*, 2012; Halford *et al.*, 2009). Due to

the additional whole genome duplication in the teleost lineage (Ohno, 1999) the zebrafish possesses two VA-opsins which are both present in the retina and the brain (Kojima *et al.*, 2000; Kojima *et al.*, 2008). Whether they have a similar function as is discussed for birds is unknown. However, fish lacking the ventral brain still show robust photoentrainment, suggesting only a minor involvement of this tissue for the establishment of circadian rhythms (Noche *et al.*, 2011). In mammals, the visual photoreceptors as well as melanopsin containing intrinsic photosensitive retinal ganglion cells (ipRGCs) mediate non-visual light perception (Hattar *et al.*, 2003). A similar function has been suggested for melanopsin-positive cells in the pineal gland of chicken (Chaurasia *et al.*, 2005). Recently, two groups independently identified five melanopsins in zebrafish, although neither of them was expressed in the larval pineal gland but rather in other brain structures or throughout the retina (Matos-Cruz *et al.*, 2011; Davies *et al.*, 2011). Since due to its expression one of the melanopsin subtypes might be able to interact with photosensitive structures (Matos-Cruz *et al.*, 2011), and since expression in the adult zebrafish brain has not been shown so far, brain melanopsin contribution to circadian entrainment is still under discussion. The cryptochromes are another family of molecules discussed to be involved in non-visual photoreception. This group consists of two members in mammals which are both involved in the negative feedback loop of the circadian clock (Kume *et al.*, 1999; Shearman *et al.*, 2000). The zebrafish possess 8 cryptochromes with mostly unknown functions, however, they are expressed in photosensitive tissues (Kobayashi *et al.*, 2000). So far, a specific function was only designated for Cry1a that acts as light-sensor for cell-autonomous circadian regulation (Tamai *et al.*, 2007).

Recent studies suggest the involvement of several different photoreceptors in photic entrainment leading to a reliable representation of changing light levels (reviewed in, see Peirson *et al.*, 2009). This complicates the quest for extraretinal photoreceptors, since the spectral sensitivity for a specific non-visual photic behavior is possibly influenced by more than one photopigment. By using *chock* mutant fish in our study we aimed to get more insight into the biophysical properties of circadian activities. As they did not show circadian rhythmicity under any light condition the usefulness of this mutant has to be reconsidered. Another approach as using enucleated larvae might be a better solution. Nevertheless, due to the transparent body, the fast embryonic development, and the available genetic tools the zebrafish is a favorable model for investigating non-image forming photic behavior. This is represented by the growing number of laboratories that use zebrafish as their model organism.

8.5.3 Light ON- and OFF-responses

Fast light/dark or dark/light transitions lead to a sharp increase in activity levels of zebrafish larvae (Emran *et al.*, 2008). These so called “startle responses” represent light-ON and -OFF locomotor responses. To investigate dependency of ON- and OFF-responses on age and light conditions each transition was separately analyzed. Moreover, the use of eyeless *chokh* mutants enabled us to discriminate between retinal and non-retinal input to these responses.

It has already been shown that zebrafish larvae increase their motor activity to light increments and decrements during the day (Emran *et al.*, 2007; Prober *et al.*, 2006). Wild-type larvae raised under the full light spectrum as well as when omitting UV-light revealed a sharp increase in activity which gradually returned back to baseline in dark/light transitions or stayed above baseline in light/dark transitions, similar to the results of Emran and col-

leagues (Emran *et al.*, 2007). While under red light increased activity was observed upon lights-off, the gradual decrease only occurred at 4 dpf and instead of fast ON-responses a sluggish and delayed increase in activity was seen at 5 dpf. These results suggest that UV-light is not necessary for stable ON- and OFF-responses, however, red light is only able to drive a startle response upon light-off but not light-on. Therefore, light in the blue and green range is necessary for the generation of robust startle responses, especially for the dark/light transition. Whether the photopigments that mediate these responses are located in the retina is unclear. A VMR-investigation of eyeless *chokh* mutants revealed no ON- and OFF-responses (Emran *et al.*, 2007) which proposes that visual opsins mediate this behavior. However, we found clear and sharp increases in activity levels upon dark/light transitions of *chokh* mutants raised under white light or when omitting UV-light. We hypothesize therefore, that the startle response to a change in illumination from dark to bright can be robustly driven via a photosensitive molecule that absorbs light in the blue or green spectrum and is located extraretinally. Candidate photopigments that absorb light in this range are the cryptochromes, which are located in various peripheral tissues of zebrafish (Chapter 7; Kobayashi *et al.*, 2000). Although this theory needs to be further tested, it suggests that cryptochromes or other non-visual blue-green light receptors are indeed present in the periphery of the fish to sense a change in irradiation. The previous study that did not detect any response in *chokh* mutants only measured 30 minute intervals during the day (Emran *et al.*, 2007). It may be that such responses are only measurable with a longer dark adaptation than 30 minutes.

While *chokh* mutants show a delayed increase in activity upon lights-off at 4 dpf, we never observed any clear and sharp startle-OFF-response in these fish. Wild-type fish on the other hand showed fast increases in locomotion to light/dark transitions under all light conditions. This implicates that eyes are necessary for robust, fast OFF-responses, whereas the delayed increase in activity levels in *chokh* mutants is probably mediated via other extraocular photosensitive molecules that are present from the 4th day after fertilization. The fact that raising fish only under red light led to robust OFF-responses in wild-type fish suggests an involvement of a molecule absorbing light in the red range. However, so far we did not measure light/dark transitions when omitting red light and it is well possible that various photosensitive pigments contribute to the OFF-response.

8.5.4 Relative *cryptochrome* mRNA levels differences in larvae raised under various light conditions

Since cryptochromes absorb light in the UV- and blue range and are discussed to be involved in circadian locomotor behavior (reviewed in Chaves *et al.*, 2011) we used the fish reared under different light conditions to investigate the effect of spectral rearing on *cryptochrome* mRNA abundance. Omitting short-wavelength light could either lead to an increase in expression of photopigments absorbing light at this spectrum (e.g. UV-opsin or Crys) in order to compensate but it may also lead to a lower abundance of them, since they are not activated. Raising wild-type larvae only under red light clearly affects expression of both *cry1* and both *cry3* paralogs as well as *cryDASH* while the effect on *cry2*, *-4*, and *-5* mRNA levels is only minor. Whether this lower expression of *crys* could be the cause for the lacking ON-response in fish raised under the narrow-band red LEDs is only speculation and needs further confirmation, for instance by repeating the experiments after downregulating a specific cryptochrome. When raising eyeless mutants under red light *cry* mRNA levels seem much less affected and even upregulated in some cases. This raises the question how *cryptochrome* expression is regulated? Except for *cry2*

and *-5* we found that *cryptochromes* generally show a broad expression pattern in the central nervous system (Chapter 6 and 7). If they function as photopigment in extraretinal tissues regulation of expression is expected to be independent of the development of the visual system and therefore should be similar in wild-type and *chokh* fish. However, eyes seem to be crucial for normal *cryptochrome* expression.

Overall *cry* expression in *chokh* mutants raised under red, green and blue light seems, besides some minor changes, similar to the reference set. Surprisingly, larger differences were found between mutants and wild-types raised under white light. Here, especially the *cry1* and *-3* paralogs as well as *cryDASH* seem to be downregulated.

The photolyases-like Cry5 still possesses the ability to repair UV-induced DNA damages (Kobayashi *et al.*, 2000; Tamai *et al.*, 2004). Omitting UV-light should decrease DNA damage thereby leading to decreased *cry5* mRNA levels. While *cry5* expression was lower in wild-type fish reared under red light only, *chokh* mutants show an increased *cry5* level when using only red, green and blue light. This result is unexpected and raises again the question of *cryptochrome* level regulation. Since all these experiments were only accomplished once the data presented here has to be regarded as preliminary. At least two more trials are necessary to get reliable results to draw further conclusions. Moreover, some sets such as fish raised under UV-light are missing and would be necessary to complete the study.

8.5.5 Summary and conclusion

By deciphering visually guided behaviors in wild-type and eyeless larval zebrafish we could show that the eye is crucial for the generation of circadian activity rhythms. Moreover, entrainment of circadian rhythmicity seems independent on the light spectrum. This suggests the involvement of a variety of photopigments absorbing light in a broad range. Investigation of wavelength specificity to elicit startle responses in zebrafish larvae revealed that light in blue and green range is necessary for the generation of robust ON- and OFF-locomotor responses. As fast light-on responses were also observed in eyeless chokh mutants when omitting UV-light but not when using only red light, we hypothesize that the startle response to a change in illumination from dark to bright can be robustly driven via a photosensitive molecule that absorbs light in the blue and/or green light spectrum and is located extraretinally. Generating OFF-responses likely includes in addition a photopigment that absorbs light in the red range, since under red light wild-type larvae only showed OFF- but no ON-responses. This molecule is probably located in the eye, since *chokh* mutant fish never showed fast responses to light/dark transitions.

Although preliminary, our study shows with simple experiments the impact of spectral rearing on visually and non-visually guided behavior in larval zebrafish. Recently a study using skylight-mimicking light sources in fish revealed the influence of color on circadian activity rhythms (Pauers *et al.*, 2012). Their and our results depict the importance of light conditions while rearing animals in laboratories, especially when working in the field of circadian rhythmicity or vision research.

8.6 Outlook

Although our results are promising and provide new insights into the relation of photoreception and wavelength specific behavior of wild-type and *chokh* mutant zebrafish larvae, all experiments were only performed once. For reliable results and statistics at least three individual experiments should be performed with VMR-setup as well as with qRT-PCR. Until now we performed long VMR studies with the whole light spectrum, when omitting UV-light and under red light only but all other combinations and narrow-band experiments are missing. To improve this study all these experiments will have to be done including the following qRT-PCR for *cryptochrome* mRNA level analysis. If one of the *cryptochromes* shows an interesting up- or downregulation in fish reared under a specific light spectrum we consider a morpholino-based downregulation of the respective protein followed by a VMR-study.

As mentioned in the discussion section, the VMR experiments itself were biased due to the influence of air conditioning. We do not believe that this chanced the outcome of our experiments, however, for further analyses we will try to avoid influence of external stimuli by turning off the air conditioning. Additional recording of humidity, temperature and air pressure would ensure constant conditions but these were not further recorded throughout experiments. Since the larvae stay inside the VMR room from shortly after fertilization on, handling during dechorionation and transfer from petri dish to the well plate could also be improved. Although the room was not entered during the recordings, light entering the room trough opening of the door prior to the experiments or as emission from electronic devices may also had an effect. This can only be avoided by adding a second door or a thick curtain between door and setup.

Experiments could be also be biased since the mutant fish are generally less active and do not act similar to external stimuli as wild-type larvae. Moreover, we observed a spastic, continuous pectoral fin response. Although swimming ability was described as normal in these larvae (Loosli *et al.*, 2003), we do not know in which way this might affect their swimming speed and thereby also influences VMR measurements. Before pursuing this study behavioral abilities of *chokh* larvae need to be thoroughly tested.

8.7 Supplementary material

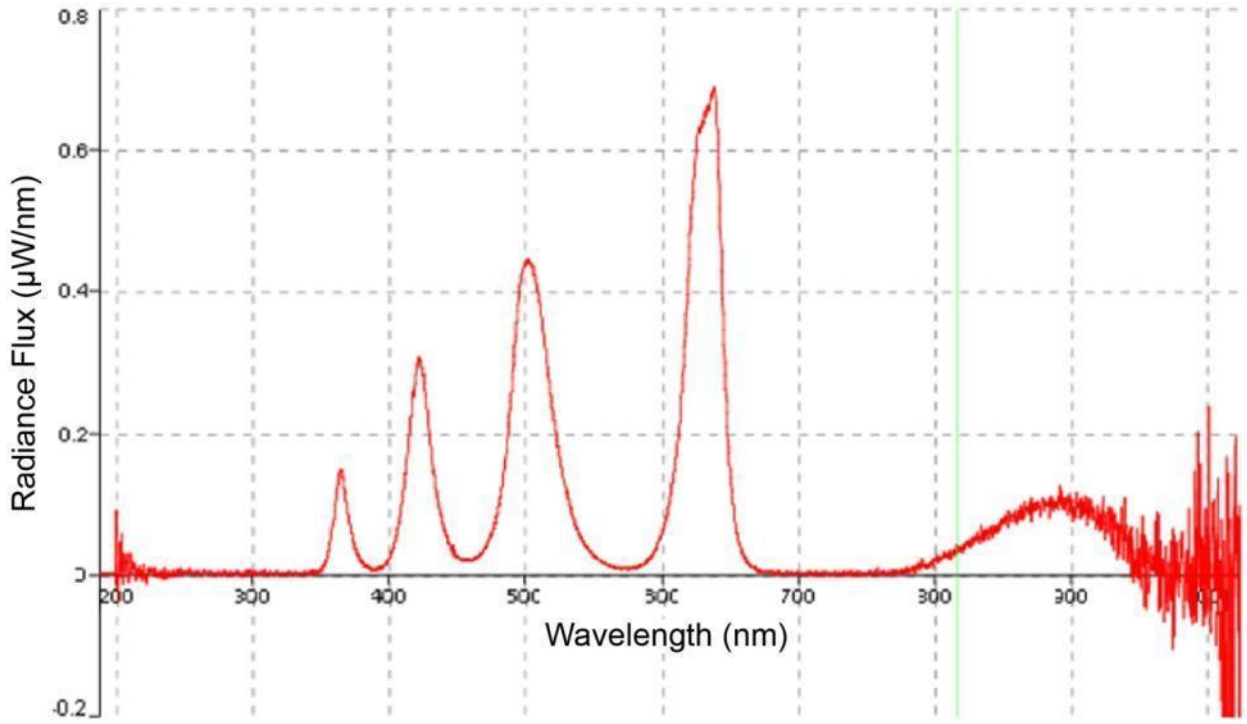

Supplementary Figure 1: Wavelength measure and irradiance profile of the LED used in the VMR setup.
The graph nicely shows the spectral properties of each individual LED source used for the VMR-measurements. The narrow amplitudes show that individual LEDs do not cross-activate other wavelengths. This reliably enables activation of small wavelength ranges. For the measurement a spectrometer (USB2000+XR1; Ocean Optics, Dunedin, FL, USA) was used.

8.8 References

Bailey, M.J. & Cassone, V.M. (2005) Melanopsin expression in the chick retina and pineal gland. Brain Res. Mol. Brain Res., 134, 345–348.

Cavallari, N., Frigato, E., Vallone, D., Fröhlich, N., Lopez-Olmeda, J.F., Foà, A., Berti, R., Sánchez-Vázquez, F.J., Bertolucci, C. & Foulkes, N.S. (2011) A blind circadian clock in cavefish reveals that opsins mediate peripheral clock photoreception. PLoS Biol., 9, e1001142.

Chaurasia, S.S., Rollag, M.D., Jiang, G., Hayes, W.P., Haque, R., Natesan, A., Zatz, M., Tosini, G., Liu, C., Korf, H.W., Iuvone, P.M. & Provencio, I. (2005) Molecular cloning, localization and circadian expression of chicken melanopsin (Opn4): differential regulation of expression in pineal and retinal cell types. J. Neurochem., 92, 158–170.

Chaves, I., Pokorny, R., Byrdin, M., Hoang, N., Ritz, T., Brettel, K., Essen, L.-O., van der Horst, G.T.J., Batschauer, A. & Ahmad, M. (2011) The cryptochromes: blue light photoreceptors in plants and animals. Annu Rev Plant Biol, 62, 335–364.

Chinen, A., Hamaoka, T., Yamada, Y. & Kawamura, S. (2003) Gene duplication and spectral diversification of cone visual pigments of zebrafish. Genetics, 163, 663–675.

Davies, W.I.L., Turton, M., Peirson, S.N., Follett, B.K., Halford, S., Garcia-Fernandez, J.M., Sharp, P.J., Hankins, M.W. & Foster, R.G. (2012) Vertebrate ancient opsin photopigment spectra and the avian photoperiodic response. Biol. Lett., 8, 291–294.

Davies, W.I.L., Zheng, L., Hughes, S., Tamai, T.K., Turton, M., Halford, S., Foster, R.G., Whitmore, D. & Hankins, M.W. (2011) Functional diversity of melanopsins and their global expression in the teleost retina. Cell. Mol. Life Sci., 68, 4115–4132.

Davies, W.L., Hankins, M.W. & Foster, R.G. (2010) Vertebrate ancient opsin and melanopsin: divergent irradiance detectors. Photochem. Photobiol. Sci., 9, 1444–1457.

Dekens, M.P.S. & Whitmore, D. (2008) Autonomous onset of the circadian clock in the zebrafish embryo. EMBO J., 27, 2757–2765.

Dekens, M.P.S., Santoriello, C., Vallone, D., Grassi, G., Whitmore, D. & Foulkes, N.S. (2003) Light regulates the cell cycle in zebrafish. Curr. Biol., 13, 2051–2057.

Emran, F., Rihel, J. & Dowling, J.E. (2008) A behavioral assay to measure responsiveness of zebrafish to changes in light intensities. J Vis Exp.

Emran, F., Rihel, J., Adolph, A.R., Wong, K.Y., Kraves, S. & Dowling, J.E. (2007) OFF ganglion cells cannot drive the optokinetic reflex in zebrafish. Proc. Natl. Acad. Sci. U.S.A., 104, 19126–19131.

Falcón, J., Gothilf, Y., Coon, S.L., Boeuf, G. & Klein, D.C. (2003) Genetic, temporal and developmental differences between melatonin rhythm generating systems in the teleost fish pineal organ and retina. J. Neuroendocrinol., 15, 378–382.

Fernandes, A.M; Fero K.; Arrenberg, A.B; Bergeron, S.A; Driever, W.; Burgess, H.A (2012) Deep brain photoreceptors control light seeking behavior in zebrafish larvae. Current Biology. In press.

Force, A., Lynch, M., Pickett, F.B., Amores, A., Yan, Y.L. & Postlethwait, J. (1999) Preservation of duplicate genes by complementary, degenerative mutations. Genetics, 151, 1531–1545.

Foster, R.G., Grace, M.S., Provencio, I., Degrip, W.J. & Garcia-Fernandez, J.M. (1994) Identification of vertebrate deep brain photoreceptors. Neurosci Biobehav Rev, 18, 541–546.

Freedman, M.S., Lucas, R.J., Soni, B., Schantz, M. von, Muñoz, M., David-Gray, Z. & Foster, R. (1999) Regulation of mammalian circadian behavior by non-rod, non-cone, ocular photoreceptors. Science, 284, 502–504.

Frigato, E., Vallone, D., Bertolucci, C. & Foulkes, N.S. (2006) Isolation and characterization of melanopsin and pinopsin expression within photoreceptive sites of reptiles. Naturwissenschaften, 93, 379–385.

Garg, S.K. & Sundararaj, B.I. (1986) Role of pineal in the regulation of some aspects of circadian rhythmicity in the catfish, Heteropneustes fossilis (Bloch). Chronobiologia, 13, 1–11.

Haffter, P., Granato, M., Brand, M., Mullins, M.C., Hammerschmidt, M., Kane, D.A., Odenthal, J., van Eeden, F.J., Jiang, Y.J., Heisenberg, C.P., Kelsh, R.N., Furutani-Seiki, M., Vogelsang, E., Beuchle, D., Schach, U., Fabian, C. & Nüsslein-Volhard, C. (1996) The identification of genes with unique and essential functions in the development of the zebrafish, Danio rerio. Development, 123, 1–36.

Halford, S., Pires, S.S., Turton, M., Zheng, L., González-Menéndez, I., Davies, W.L., Peirson, S.N., García-Fernández, J.M., Hankins, M.W. & Foster, R.G. (2009) VA opsin-based photoreceptors in the hypothalamus of birds. Curr. Biol., 19, 1396–1402.

Hattar, S., Liao, H.W., Takao, M., Berson, D.M. & Yau, K.W. (2002) Melanopsin-containing retinal ganglion cells: architecture, projections, and intrinsic photosensitivity. Science, 295, 1065–1070.

Hattar, S., Lucas, R.J., Mrosovsky, N., Thompson, S., Douglas, R.H., Hankins, M.W., Lem, J., Biel, M., Hofmann, F., Foster, R.G. & Yau, K.-W. (2003) Melanopsin and rod-cone photoreceptive systems account for all major accessory visual functions in mice. Nature, 424, 76–81.

Heisenberg, C.P., Brand, M., Jiang, Y.J., Warga, R.M., Beuchle, D., van Eeden, F.J., Furutani-Seiki, M., Granato, M., Haffter, P., Hammerschmidt, M., Kane, D.A., Kelsh, R.N., Mullins, M.C., Odenthal, J. & Nusslein-Volhard, C. (1996) Genes involved in forebrain development in the zebrafish, Danio rerio. Development, 123, 191–203.

Hurd, M.W. & Cahill, G.M. (2002) Entraining signals initiate behavioral circadian rhythmicity in larval zebrafish. J. Biol. Rhythms, 17, 307–314.

Kang, S.W., Leclerc, B., Kosonsiriluk, S., Mauro, L.J., Iwasawa, A. & El Halawani, M.E. (2010) Melanopsin expression in dopamine-melatonin neurons of the premammillary nucleus of the hypothalamus and seasonal reproduction in birds. Neuroscience, 170, 200–213.

Kazimi, N. & Cahill, G.M. (1999) Development of a circadian melatonin rhythm in embryonic zebrafish. Brain Res. Dev. Brain Res., 117, 47–52.

Kennedy, B.N., Stearns, G.W., Smyth, V.A., Ramamurthy, V., van Eeden, F., Ankoudinova, I., Raible, D., Hurley, J.B. & Brockerhoff, S.E. (2004) Zebrafish rx3 and mab21l2 are required during eye morphogenesis. Dev. Biol., 270, 336–349.

Kobayashi, Y., Ishikawa, T., Hirayama, J., Daiyasu, H., Kanai, S., Toh, H., Fukuda, I., Tsujimura, T., Terada, N., Kamei, Y., Yuba, S., Iwai, S. & Todo, T. (2000) Molecular analysis of zebrafish photolyase/cryptochrome family: two types of cryptochromes present in zebrafish. Genes Cells, 5, 725–738.

Kojima, D., Mano, H. & Fukada, Y. (2000) Vertebrate ancient-long opsin: a green-sensitive photoreceptive molecule present in zebrafish deep brain and retinal horizontal cells. J. Neurosci., 20, 2845–2851.

Kojima, D., Torii, M., Fukada, Y. & Dowling, J.E. (2008) Differential expression of duplicated VAL-opsin genes in the developing zebrafish. J. Neurochem., 104, 1364–1371.

Kubo, Y., Akiyama, M., Fukada, Y. & Okano, T. (2006) Molecular cloning, mRNA expression, and immunocytochemical localization of a putative blue-light photoreceptor CRY4 in the chicken pineal gland. J. Neurochem., 97, 1155–1165.

Kume, K., Zylka, M.J., Sriram, S., Shearman, L.P., Weaver, D.R., Jin, X., Maywood, E.S., Hastings, M.H. & Reppert, S.M. (1999) mCRY1 and mCRY2 are essential components of the negative limb of the circadian clock feedback loop. Cell, 98, 193–205.

Larison, K.D. & Bremiller, R. (1990) Early onset of phenotype and cell patterning in the embryonic zebrafish retina. Development, 109, 567–576.

Loosli, F., Staub, W., Finger-Baier, K.C., Ober, E.A., Verkade, H., Wittbrodt, J. & Baier, H. (2003) Loss of eyes in zebrafish caused by mutation of chokh/rx3. EMBO Rep., 4, 894–899.

Magnoli, D., Zichichi, R., Laurà, R., Guerrera, M.C., Campo, S., Carlos, F. de, Suárez, A.Á., Abbate, F., Ciriaco, E., Vega, J.A. & Germanà, A. (2012) Rhodopsin expression in the zebrafish pineal gland from larval to adult stage. Brain Res., 1442, 9–14.

Mano, H., Kojima, D. & Fukada, Y. (1999) Exo-rhodopsin: a novel rhodopsin expressed in the zebrafish pineal gland. Brain Res. Mol. Brain Res., 73, 110–118.

Masai, I., Heisenberg, C.P., Barth, K.A., Macdonald, R., Adamek, S. & Wilson, S.W. (1997) floating head and masterblind regulate neuronal patterning in the roof of the forebrain. Neuron, 18, 43–57.

Matos-Cruz, V., Blasic, J., Nickle, B., Robinson, P.R., Hattar, S. & Halpern, M.E. (2011) Unexpected diversity and photoperiod dependence of the zebrafish melanopsin system. PLoS ONE, 6, e25111.

Menaker, M. & Keatts, H. (1968) Extraretinal light perception in the sparrow. II. Photoperiodic stimulation of testis growth. Proc. Natl. Acad. Sci. U.S.A., 60, 146–151.

Moutsaki, P., Whitmore, D., Bellingham, J., Sakamoto, K., David-Gray, Z.K. & Foster, R.G. (2003) Teleost multiple tissue (tmt) opsin: a candidate photopigment regulating the peripheral clocks of zebrafish? Brain Res. Mol. Brain Res., 112, 135–145.

Mueller, K. (2011) Visual behavior of zebrafish. Ph.D. Thesis, Universtity of Zurich, Switzerland.

Nakane, Y., Ikegami, K., Ono, H., Yamamoto, N., Yoshida, S., Hirunagi, K., Ebihara, S., Kubo, Y. & Yoshimura, T. (2010) A mammalian neural tissue opsin (Opsin 5) is a deep brain photoreceptor in birds. Proc. Natl. Acad. Sci. U.S.A., 107, 15264–15268.

Noche, R.R., Lu, P.-N., Goldstein-Kral, L., Glasgow, E. & Liang, J.O. (2011) Circadian rhythms in the pineal organ persist in zebrafish larvae that lack ventral brain. BMC Neurosci, 12, 7.

Ohno, S. (1999) Gene duplication and the uniqueness of vertebrate genomes circa 1970-1999. Semin. Cell Dev. Biol., 10, 517–522.

Pauers, M.J., Kuchenbecker, J.A., Neitz, M. & Neitz, J. (2012) Changes in the colour of light cue circadian activity. Animal behaviour, 83, 1143–1151.

Peirson, S.N., Halford, S. & Foster, R.G. (2009) The evolution of irradiance detection: melanopsin and the non-visual opsins. Philos. Trans. R. Soc. Lond., B, Biol. Sci., 364, 2849–2865.

Prober, D.A., Rihel, J., Onah, A.A., Sung, R.-J. & Schier, A.F. (2006) Hypocretin/orexin overexpression induces an insomnia-like phenotype in zebrafish. J. Neurosci., 26, 13400–13410.

Raymond, P.A., Barthel, L.K. & Curran, G.A. (1995) Developmental patterning of rod and cone photoreceptors in embryonic zebrafish. J. Comp. Neurol., 359, 537–550.

Shearman, L.P., Sriram, S., Weaver, D.R., Maywood, E.S., Chaves, I., Zheng, B., Kume, K., Lee, C.C., van der Horst, G.T., Hastings, M.H. & Reppert, S.M. (2000) Interacting molecular loops in the mammalian circadian clock. Science, 288, 1013–1019.

Tamai, T.K., Vardhanabhuti, V., Foulkes, N.S. & Whitmore, D. (2004) Early embryonic light detection improves survival. Curr. Biol., 14, R104-5.

Tamai, T.K., Young, L.C. & Whitmore, D. (2007) Light signaling to the zebrafish circadian clock by Cryptochrome 1a. Proc. Natl. Acad. Sci. U.S.A., 104, 14712–14717.

Tang, R., Dodd, A., Lai, D., McNabb, W.C. & Love, D.R. (2007) Validation of zebrafish (Danio rerio) reference genes for quantitative real-time RT-PCR normalization. Acta Biochim. Biophys. Sin. (Shanghai), 39, 384–390.

Tarttelin, E.E., Fransen, M.P., Edwards, P.C., Hankins, M.W., Schertler, G.F.X., Vogel, R., Lucas, R.J. & Bellingham, J. (2011) Adaptation of pineal expressed teleost exo-rod opsin to non-image forming photoreception through enhanced Meta II decay. Cell. Mol. Life Sci., 68, 3713–3723.

Underwood, H. (1990) The pineal and melatonin: regulators of circadian function in lower vertebrates. Experientia, 46, 120–128.

Underwood, H. & Menaker, M. (1976) Extraretinal photoreception in lizards. Photophysiology, 23, 227–243.

Whitmore, D., Foulkes, N.S. & Sassone-Corsi, P. (2000) Light acts directly on organs and cells in culture to set the vertebrate circadian clock. Nature, 404, 87–91.

Wilson, S.W. & Easter, S.S. (1991) Stereotyped pathway selection by growth cones of early epiphysial neurons in the embryonic zebrafish. Development, 112, 723–746.

Zhdanova, I.V., Wang, S.Y., Leclair, O.U. & Danilova, N.P. (2001) Melatonin promotes sleep-like state in zebrafish. Brain Res., 903, 263–268.

Zimmerman, N.H. & Menaker, M. (1979) The pineal gland: a pacemaker within the circadian system of the house sparrow. Proc. Natl. Acad. Sci. U.S.A., 76, 999–1003.

Chapter 9

General Discussion and Conclusion

In the studies presented here we exploited the zebrafish as a model system in many ways to gain new insight into evolutionary processes, identifying new signaling mechanisms, and to elucidate vertebrate vision from different angles. By focusing on signal transmission in the first visual synapse, we aimed at enlightening the discussion about how retinal ON-signals are generated. In addition, the exploration of circadian regulation of visual sensitivity brings insight into basic regulatory mechanisms. Second, the study of how light reaches the circadian clocks is fundamental as circadian mechanisms regulate many physiological processes. Investigating the cryptochrome family of blue-light receptors had the goal of finding hints for an involvement in such signaling mechanisms. Besides that, zebrafish larvae were used to exploit visual and non-visual behavioral aspects. This part of the study had the objective to contribute to the basic understanding of light perception. The following paragraphs will summarize and discuss the presented results and consider perspectives for future research.

9.1 About the usefulness of phylogentic trees

The duplication of genes had a major impact on genome evolution. As tandem duplications result from unequeal crossing over, they usually lead to two genes that may remain under the control of the same regulatory elements and perform similar functions. Whole genome duplication (WGD) events on the other hand lead to the duplication of a full genome, creating tetraploid individuals in an otherwise diploid species. In plant genomes WGDs are fairly frequent and likely build the basis for rapid species formation (reviewed in Hegarty & Hiscock, 2008). Interestingly, such events are also possible in vertebrates. Even if polyploidy of vertebrates is generally incompatible with normal development and function the comparison of Hox-clusters, groups of clustered genes relevant for pattern formation, revealed two WGD events that likely happened around 500 Mya at the basis of the vertebrate lineage (Dryja *et al.*, 2005; Hoegg & Meyer, 2005). These increases in genetic material were possibly relevant for the evolutionary radiation of vertebrate species, as duplicated genes are released from selective pressure and can acquire new or subfunctions that finally lead to their retainment in the genome (Force *et al.*, 1999; Ohno, 1999). As teleost fish underwent an additional WGD event around 350 Mya, up to two paralogs can be found for one mammalian ortholog (Amores *et al.*, 1998; Vandepoele *et al.*, 2004). While this increased complexity might complicate the comparison of human and zebrafish genomes and the investigation of gene functions, it also yields many possibilities. The ancestral gene function might be split onto two paralogs, which could help to generate loss-of-function animals of an otherwise lethal gene. Moreover, tissue-specific regulatory elements could be identified by expression analysis of paralogous genes. Still, prerequisite for every study dealing with zebrafish genes is a thorough phylogenetic analysis. This has been done for the mGluR gene family, where we

investigated comparative phylogeny and expression. The high resemblance of zebrafish and mammalian expression found for both group I mGluR paralogs shows the suitability of this fish as a model organism. Our detailed description of brain regions where *mglur* genes are localized will serve as a reference-set, thereby paving the way for next studies dealing with mGluR function. A comparison of spatial and temporal expression patterns allows insight into the evolutionary mechanisms of sub- or neofunctionalization events (Force *et al.*, 1999). While this likely happened for *mglur1* and *mglur2* paralogs, expression of *mglur8a* and *-8b* is still similar and rather suggests genome dosage constraints. However, such questions can only be conclusively answered by studying and comparing their regulatory subunits among different species. Next generation sequencing will increase and specify the available genomic databases, thereby facilitating bioinformatic analyses.

How important the reconstruction of phylogenetic history can be is shown in Chapter 6, where we investigated the evolutionary relationship of cryptochromes. Previous studies mostly grouped the zebrafish Cry2 (previously named Cry3 or Cry3b) outside the lineage of the mammalian Crys, therefore no zebrafish ortholog for the mammalian Cry2 was found (Kobayashi *et al.*, 2000; Lin & Todo, 2005; Schröder *et al.*, 2003). Such misinterpretations likely happened because they only compared few species and did not include all zebrafish cryptochromes within the tree. However, as our comparative study involves species from insects to mammals, we found the zebrafish ortholog for the mammalian Cry2 and renamed it from Cry3 to Cry2 according to its relation. Interestingly, of the tested species only the zebrafish and the closely related cavefish retained these two paralogs which we renamed as *cry3a* and *-3b*, while other teleosts only possess one copy of this gene and all other vertebrates seem to have lost it. In addition, Cry4 is also only retained by zebrafish and its closes relatives but not by other teleosts, however, we also located this member in amphibians, reptiles and birds. Such observations raise the questions of the function of these specific genes? Since expression analysis showed robust mRNA expression of these genes, it is unlikely that they will be inactivated soon. A comparative expression analysis involving other species might show some hints for a specific function, however, before that is accomplished further *in silico* investigations that predict evolutionary events have to be exploited. First, other intermediate species such as the elephant shark (*Callorhinchus milii*), a chordate that branched off before the teleost specific whole genome duplication (Yu *et al.*, 2008), or the monarch butterfly (*Danaus plexippus*), an insect that retained both a *Drosophila*-type and a mammalian-type cryptochrome (Zhu *et al.*, 2008), have to be incorporated into the phylogenetic tree. Second, a synteny analysis, where the position and the flanking regions of genes on chromosomes amongst species are compared, would help understanding how genes evolved. When gene duplicates originate from large-scale evolutionary events, their chromosomal neighborhood should be conserved. If that is not the case the gene was likely duplicated by tandem duplication. In addition, such a study likely detects remnants of lost in the mammalian genome. In combination with molecular clock strategies determination of the evolutionary time point where for instance *cry3* was lost in the mammalian lineage could help identifying possible functions that are lost in one species but kept in others.

9.2 Dissecting retinal ON-signals

The separation of ON- and OFF-signals occurs at the bipolar cell dendrite, where either sign conserving ionotropic glutamate receptors or sign inversing metabotropic glutamate receptors are present. The metabo-

tropic glutamate receptor 6 (mGluR6) located on ON-bipolar cell dendrites was found to mediate ON-signaling (Masu *et al.*, 1995; Vardi *et al.*, 2000). During the past years a lot of research has been undertaken to discover the molecular mechanisms behind this signaling pathway. Only recently, the effector channel has been found to be the transient receptor potential channel M 1 (TRPM1) (Shen *et al.*, 2009; Morgans *et al.*, 2009). In addition, the cascade was found to involve nyctalopin (NYX) and the G protein-coupled receptors 158/179 (GPR158/179), molecules that are likely involved in compartmentalization of pathway members crucial for proper signaling (Cao *et al.*, 2011; Orlandi *et al.*, 2012). Removal of any of the involved molecules tested leads to a non-functional mGluR6 pathway manifested by loss of the ERG b-wave, and affects the organization of mGluR6 pathway molecules (Dryja *et al.*, 2005; Zeitz *et al.*, 2005; Audo *et al.*, 2012; Peachey *et al.*, 2012; Dhingra *et al.*, 2002; Gregg *et al.*, 2003; Bech-Hansen *et al.*, 2000; Morgans *et al.*, 2009; Shen *et al.*, 2009; Xu *et al.*, 2012; Tummala *et al.*, 2012; Neinstein A.G. *et al.*, 2012; Pearring *et al.*, 2011). As due to retrograde signaling postsynaptic reorganization likely affects the proper localization of presynaptic proteins (Neinstein A.G. *et al.*, 2012), photoreceptor integrity might also be affected. These results show the importance of understanding the full molecular mechanism of the mGluR6 pathway and all its interaction partners. Our research on the mGluR6 mediated ON-signaling in zebrafish adds to the understanding of this pathway. We found that the mGluR6 pathway is conserved in zebrafish, which bears the possibility of studying all pathway members as well as their interaction partners in this model system. Hence, one could employ the recently developed DuoLink Assay (from e.g. Olink Bioscience or Eurogenetec) for identification of protein-protein interactions. We are currently generating transgenic fish lines that express GFP under the *mglur6a* or *-6b*, *trpm1a* or *nyx* promoter using Tol2-based constructs (Amsterdam *et al.*, 1995; Kawakami & Shima, 1999; Stuart *et al.*, 1988). Patch clamping GFP-positive bipolar cells in the adult retina will increase our knowledge about the kinetics of the mGluR6 pathway. Moreover, as ERG recordings only exploit outer retinal functions, patch clamping of GFP-positive ganglion cells in mGluR6a or -6b transgenic lines will allow the investigation of mGluR6 function in the inner retina. A recent publication describes mGluR6 expression in human retinal ganglion cells (Klooster *et al.*, 2011), yet physiological evidence for a sign inversing synapse in the IPL has not been found. Transgenic zebrafish lines in combination with electrophysiological techniques will hopefully bring more light into mGluR6 function in the inner retina.

Patients with mutations in any member of the mGluR6 pathway suffer from congenital stationary night blindness (CSNB1) (Bech-Hansen *et al.*, 2000; Audo *et al.*, 2012; Zeitz *et al.*, 2005; van Genderen *et al.*, 2009). However, besides that these patients have normal photopic vision and visual acuity, indicating that the cone pathway might not be affected by these mutations. An idea about cone ON-mechanisms comes from studies conducted in lower vertebrates where it is hypothesized that chloride conductance of glutamate transporters (excitatory amino acid transportes, EAATs) mediates hyperpolarization in ON-bipolar cells during light decrease (Grant & Dowling, 1995, 1996; Wong *et al.*, 2005; Wong & Dowling, 2005; Wong *et al.*, 2004), however, mGluR6 is thought to contribute to photopic ON-signaling as well (Nelson & Singla, 2009; Saszik *et al.*, 2002). EAATs might drive photopic vision in patients lacking proper mGluR6 signaling, however, while EAATs are hypothesized to indirectly modulate ON- and OFF-signaling (Tse *et al.*, 2012; Wersinger *et al.*, 2006; Rowan *et al.*, 2010), a direct function of glutamate transporters in ON-signaling has never been found in mammals. Most research in ON-signaling has been conducted in rodents, model systems whose vision highly relies on rods. If mGluR6, as it has been hypothesized, is mainly mediating rod ON-responses, an involvement of EAATs was probably missed. As the larval

zebrafish retina is cone dominant and as its cones were found to be molecularly similar to human ones (Imanishi *et al.*, 2002; Rinner *et al.*, 2005; Vihtelic *et al.*, 1999), zebrafish suit perfectly for analyzing cone specific signaling. In line with other studies, our results show that at least mGluR6b is involved in cone ON-responses, however, only partially. Besides mGluR6b EAAT7 has been found to affect the ERG b-wave as well (Maurer, 2010) and a combined knockdown confirmed the involvement of both glutamate receptors/transporters in ON-signaling. However, EAAT7 is only present in lower vertebrates but not in mammals (Gesemann *et al.*, 2010), indicating that lower vertebrates might be a special case concerning the generation of the ON-response. The nocturnal bottleneck within the mammalian lineage (reviewed in Davies *et al.*, 2012) likely led to the extinction of an EAAT-based mechanism, as only scotopic vision was necessary. Later on, however, when cone vision became important again, they might have adapted the mGluR6-based rod system to mediate both rod and cone derived signals. Nevertheless, a recent study in mice found evidence for EAAT5 mediating direct ON-signaling (Tse *et al.*, 2012). Since after downregulation of both mGluR6b and EAAT7 in zebrafish, a small ERG b-wave remained, EAAT5 might be involved in zebrafish cone ON-responses as well. Consistent with that, preliminary results show EAAT5b expression in the postsynaptic OPL, the correct place for mediating ON-signaling. mGluR6a, the second mGluR6 paralog, is also present in ON-bipolar cells and colocalizes with *mglur6b*. However, as preliminary results have shown no influence in cone ON-responses after mGluR6a depletion, we hypothesize that mGluR6b, EAAT7 and likely EAAT5b fulfill the zebrafish cone ON-response.

Besides exploiting ON-signaling on the functional level, we aimed at shining light on the input pathway of each photoreceptor subtype to ON-responses. As spectral sensitivity of the metabotropic proportion of the photopic ON-response was found to be shifted towards shorter wavelengths (Nelson & Singla, 2009; Saszik *et al.*, 2002), we expected mGluR6-positive cells to solely or mostly have contact with UV- and blue-cones, however, at least mGluR6b-expressing cells seemingly have contact with all cone subtypes as well as rods. Therefore, the increased mGluR6 mediated ON-response to short wavelength stimuli is likely due to other effects, possibly a higher number of receptors on synapses contacting short wavelength cones. As ON-bipolar cell diversity in zebrafish is high (reviewed in Connaughton, 2011) and most of them contact more than one photoreceptor subtype (Li *et al.*, 2011), a simple estimation of the numbers of activated receptors by measuring Ca^{2+} or Na^{+} influx through TRPM1 channels would not help much. Dissection of the contribution of each receptor subtype to different spectral input is better done on the physiological level. Monochromatic ERG recordings in morphant fish combined with pharmacological tools to specifically block metabotropic or transporter mediated ON-signals might be helpful. While this would exploit zebrafish cone ON-responses, it does not add to the knowledge of scotopic ON-signaling. In zebrafish robust rod ERG responses can only be measured at later stages when rods are fully incorporated into the retina (Branchek, 1984; Branchek & Bremiller, 1984). However, Dowling's group was able to evoke small scotopic responses at 5 dpf in a zebrafish mutant that lacks cone function (Mills *et al.*, 2009). Using this mutant might help us gaining additional knowledge about rod ON-signaling in larval fish.

While a targeted gene knock down using morpholinos is very useful for studying early development, their main disadvantage is that they dilute over the process of growth. Therefore, measuring the contribution of a specific receptor to rod function at later stages would require the generation of a mutant fish line lacking one of the receptor subtypes. During recent years several new technologies have arisen to disrupt specific genes in zebrafish.

TILLING (targeting-induced local lesions in genomes) relies on random generation of mutations in the genome and requires subsequent screening of the F1 generation (reviewed in Moens *et al.*, 2008). Since this procedure can be automated, it allows large-scale approaches that led to the establishment of several zebrafish TILLING libraries all over the world with the goal to generate and distribute loss-of-function mutations in genes of interest to the zebrafish community. To specifically target sequences in the genome zinc finger nucleases (ZFNs; reviewed in Ekker, 2008) or the newly developed TALEN technology (transcription activator-like effect nuclease; reviewed in Clark *et al.*, 2011) can be used. The advantage of TALEN is the high predictability and specificity of its DNA binding domain, ceasing the need for screening or identifying a DNA binding domaine with the requisite specificity. Looking to the future, it is very likely that the TALEN technology will be a preferred technology for creating targeted knockout mutants in zebrafish and will play a major role in establishing a library of loss-of-function alleles.

The retinal network is very diverse and harbors a number of dynamic interaction pathways. Studying such networks adds not only to the knowledge of visual processing but also has a great impact on the understanding of neuronal networks in general. The understanding and modeling of networks relies on the basic knowledge about synaptic signaling mechanisms such as the one we have analyzed in this work. As vertebrates harbor a number of different bipolar cells (reviewed in Masland, 2001; Connaughton, 2011), future research has to concentrate on specific photoreceptor-to-bipolar cell networks. This is most efficiently done by combining different techniques such as the generation of transgenic lines in order to electrophysiologically investigate the functional properties of specific cell types or by using optogenetic tools that allow specific analyzation of neuronal circuits. As such tools are already available in zebrafish, and as it bears the advantage of a diurnal animal relying on cone vision, this model organism will be of great use for future research.

9.3 Circadian aspects of vision

A circadian clock is a molecular oscillator with a period of approximately 24 hours. Although self-sustained, it is entrained to environmental changes by external input such as light or temperature thereby enabling a living being to optimally adapt and anticipate its behavior. A circadian clock controls a number of daily or seasonal physiological changes such as hormone release, metabolic activity or breeding (reviewed in Sahar & Sassone-Corsi, 2012). To adapt the visual system in an optimal way to the changing environment, the retina harbors many crucial processes that are circadian driven. Melatonin and dopamine act in counterphase, with melatonin suppressing dopamine release from specific interplexiform cells at night and dopamine inhibiting melatonin production during the day (Cahill *et al.*, 1991; Doyle *et al.*, 2002). The increase of dopamine at dawn leads to various direct and indirect modulation in the vertebrate visual system, most of them crucial for switching vision from being rod-mediated to cone-mediated (reviewed in Witkovsky, 2004; Jackson *et al.*, 2012). Dopamine release generally alters rod-cone input to second order cells, thereby adapting the visual system to operate over the ~10 billion-fold change in ambient light intensity during a day. This is for instance achieved by enhancing electrical rod-cone coupling during the night, which allows cones to receive dim light signals from rods at night (Krizaj *et al.*, 1998; Ribelayga *et al.*, 2008). Also visual sensitivity has been found to underlie a circadian clock. Behavioral measurements in fish showed increased sensitivity at dusk (Bassi & Powers, 1987), and the threshold to evoke

ERG responses was reduced at dusk in both fish and humans (Lavoie *et al.*, 2010; Li & Dowling, 1998). As in ERG experiments the b-wave representing ON-signal was mainly affected, we investigated the molecules involved in retinal ON-signaling for a circadian regulation. To our surprise we found a substantially increased expression of both *mglur6* paralogs at dusk. As DD experiments confirmed the circadian control of this expression pattern, we hypothesize that at least a part of the molecular mechanism underlying higher visual sensitivity at dusk is driven by increased ON-signaling over mGluR6. As already mentioned in the outlook part of Chapter 5, transgenic fish lines could help in FACS sorting the cells expressing an mGluR6 paralog followed by qRT-PCR analysis. Like this we could show the increased expression of mGluR6 at dusk on a quantitative level. Since our hypothesis is only based on mRNA expression patterns, we will focus future research on finding functional relevance for the suggested mechanism. As measuring startle ON-responses in the VMR-setup might be influenced by light uptake over extraocular photoreceptive cells (Chapter 8; Fernandes *et al.*, 2012), we aim on measuring the threshold of ERG b-waves at dawn and dusk in wild-tpyes and in mGluR6-depleted fish larvae. Of course also here, mutant fish lacking mGluR6 completely generated by the TILLING or TALEN technology would be very helpful.

Not only *mglur6a* and *-6b* expression is regulated by a circadian clock, also *trpm1a* showed a very interesting changing expression pattern in the photoreceptor layer. Moreover, *Nyx*, whose function is still not completely understood, seems to be also developmentally and circadian regulated. In addition, preliminary results point towards circadian regulated gene expression of several EAATs (data not shown) that are possibly involved in ON-signaling. The large number of retinal genes that are regulated by a circadian clock shows the high impact of the circadian system on visual processes. However, most scientists do not consider the time of the day as important variable in experimental studies. Hence, as our results show, being aware of the circadian aspect could lead to surprising findings. Moreover, research about clock controlled visual processes conducted in zebrafish is possibly better comparable to humans, as they are both diurnal species in contrast to rodents.

9.4 How light acts on the circadian clock

Light is the major external factor to entrain circadian clocks. Some organisms such as *Drosophila* or zebrafish possess directly light-entrainable autonomous circadian clocks in nearly every cell (Emery *et al.*, 1998; Plautz *et al.*, 1997; Whitmore *et al.*, 2000). Although individual cells of mammals possess autonomous circadian clocks as well (Balsalobre *et al.*, 1998), they need to be synchronized by the central pacemaker located deep inside the brain in the suprachiasmatic nucleus (SCN). Photic input to the central pacemaker is mediated via the retina by non-image forming photoreceptors termed intrinsic photosensitive retinal ganglion cells (ipRGCs). These express the photopigment melanopsin and send their information directly via the retinohypothalamic tract to the SCN, where the release of neurotransmitters leads to the activation of several signaling pathways, evokes chromatin remodeling, and induces clock genes (reviewed in Hannibal & Fahrenkrug, 2006; Dibner *et al.*, 2010). It is generally suggested that ipRGCs and the visual photoreceptors rods and cones mediate photic input to the circadian clock, however, other factors are likely involved in modulating the amplitude of rhythmic behavioral output (Hattar *et al.*, 2003). Cryptochromes (Crys) are such other factors, as these UV- and blue-light absorbing photopigments have been found to influence circadian rhythmicity (van der Horst *et al.*, 1999; Vitaterna *et al.*, 1999; Selby *et al.*, 2000). Animals harbor two types of cryptochromes: the *Drosophila*-type Crys are light-

responsive and act as a direct photoreceptor of the circadian clock, whereas mammalian-type Crys are involved in the transcriptional-translational-feedback loop of the molecular oscillator (reviewed in Chaves *et al.*, 2011). As zebrafish possess both types of cryptochromes, they suit perfectly for studying the different functions of these within the circadian system. Moreover, the far more decentralized circadian system of zebrafish allows exploring circadian clock mechanisms independent of brain input. *In vitro* experiments have shown that photic input to cell-autonomous clocks is mediated via cryptochrome 1a (Tamai *et al.*, 2007; Whitmore *et al.*, 2000), however, whether other Crys are also involved in either direct photoentrainment or within the circadian feedback loops is not known.

The expression study we performed using adult retinal slices had the aim to show oscillating expression patterns of specific *cryptochromes*, as this could be a hint for an involvement in circadian processes. With a qRT-PCR analysis we confirmed that all eight zebrafish *crys* are expressed in an oscillating manner in the adult eye. *In situ* hybridization shows that some *crys* are strongly expressed throughout all retinal layers (e.g. *cry3a*), and others only marginally (e.g. *cry5*), however, rhythmic *cry* expressions matched the expression analysis performed by qRT-PCR analysis. As we could not convincingly observe layer-specific oscillation, we hypothesize that each zebrafish cryptochrome harbors a similar function throughout the retinal layers. We assume a function for the mammalian-type zebrafish Crys within the transcriptional-translational-feedback loop, as they have all been shown to be biochemically able to inhibit CLOCK:BMAL1-mediated transcription (Kobayashi *et al.*, 2000). Whether light could also directly adjust the cell-autonomous circadian clocks within the retina over Cry1a, as it has been shown in zebrafish cell lines (Tamai *et al.*, 2007), is currently unknown, as cell-lines derived from this tissue have never been tested. A recent study in cavefish discovered the teleost multiple tissue (TMT) opsin and melanopsin to serve as peripheral photoreceptor, however, they additionally predict the involvement of several other photopigments (Cavallari *et al.*, 2011). Therefore, future analysis that concentrates on a specific photopigment, be it one of the opsins or cryptochromes, has to validate the role of each of these in photoentrainment. Here, the VMR-experiments in combination with mRNA expression levels discussed in Chapter 8 might provide additional information. So far, our results are not specific enough to focus research about light-input to the circadian clock on one cryptochrome. Therefore, it might be worth concentrating on cryptochromes that likely have a more specific function in the retina such as CryDASH that shows an interesting expression in the ciliary margin zone or Cry5, which was shown to repair UV-damaged DNA (Kobayashi *et al.*, 2000; Tamai *et al.*, 2004).

The zebrafish cryptochromes 2, -4, and -5 are *Drosophila*-type Crys, however, an involvement for them in direct photic input mechanisms to the circadian clock similar to *Drosophila* has not been shown so far. Cry2 or -4 might be involved in light-dependent magnetosensation, as has been proposed for cryptochromes in insects and birds (Ritz *et al.*, 2000; Gegear *et al.*, 2008; Yoshii *et al.*, 2009). While such a mechanism makes perfect sense in animals that migrate over large distances, it barely helps the zebrafish to orient, since they usually do not leave their habitat throughout life (Engeszer *et al.*, 2007). Still, one group showed magnetic sensitivity in zebrafish (Shcherbakov *et al.*, 2005) and recently, the human Cry2 was found to be a possible light-dependent magnetosensor (Foley *et al.*, 2011), suggesting that this sense is probably more widespread than previously thought. Hence, the zebrafish could provide a useful tool for further investigations concerning cryptochrome involvement in light-dependent magnetosensation.

9.5 Visual and non-visual aspects of light perception

Featuring different photoreceptors offers the opportunity to perceive light input over a broad range which likely makes the system more reliable and adaptive towards external changes. It has already been shown that a variety of non-visual photopigments located within the retina or in peripheral tissues such as neuropsin or vertebrate ancient (VA) opsin are involved in photic responses of animals (Kojima *et al.*, 2000; Tarttelin *et al.*, 2003; Kojima *et al.*, 2008; Halford *et al.*, 2009; Ohuchi *et al.*, 2012, reviewed in Guido *et al.*, 2010). The differentiation between visual and non-visual light perception is usually complicated by the masking response, which is the direct effect of light on locomotor activity. Enucleating zebrafish or using eyeless mutants enables the study of behavioral mechanisms without the influence of ocular light perception. This allows the examination of light-dependent but non-ocular guided mechanisms. By using the visual motor response (VMR) setup to test locomotor activities in eyeless *chokh* mutants we discovered that these larvae react with a startle response upon a change from dark to bright light. This stands in contrast to a previous study that detected no light-dependent locomotor activities in these mutants (Emran *et al.*, 2007), and indicates that extraocular photoreceptors are involved in the light input pathway of startle ON-responses. The combination of such VMR studies with spectrally distinct LEDs allows the prediction of spectral properties of photopigments involved in light-guided locomotor behaviors. Using this approach, we could show that an extraocular photopigment absorbing light in the blue to green range drives the light ON-response, whereas OFF-responses likely involve a retinal photoreceptor. Although these results are all preliminary, they show the large potential of such straightforward studies in zebrafish larvae. More sophisticated experiments might narrow down the spectral sensitivities found to elicit specific behaviors and pave the way to unravel the mysterious photopigments involved in non-visual light perception. Besides that, it also shows how careful one has to be while rearing zebrafish, as already small differences in light conditions can have a major effect on the behavioral output.

To conclude, the zebrafish model system with its opportunities for genetic manipulation constitutes a versatile *in vivo* system in vision research. As we have shown in this study, it suits perfectly for studying signaling processes at the molecular level. Moreover, the raising availability of complex behavioral assays allows exploiting general mechanisms of light perception. In combination with the now emerging new genetic tools, future investigations will lead to a deeper understanding of light perceptive mechanisms in zebrafish which will convince even the last doubtful colleague about the usefulness of this little animal in science.

9.6 References

Amores, A., Force, A., Yan, Y.L., Joly, L., Amemiya, C., Fritz, A., Ho, R.K., Langeland, J., Prince, V., Wang, Y.L., Westerfield, M., Ekker, M. & Postlethwait, J.H. (1998) Zebrafish hox clusters and vertebrate genome evolution. Science, 282, 1711–1714.

Amsterdam, A., Lin, S. & Hopkins, N. (1995) The Aequorea victoria green fluorescent protein can be used as a reporter in live zebrafish embryos. Dev. Biol., 171, 123–129.

Audo, I., Bujakowska, K., Orhan, E., Poloschek, C.M., Defoort-Dhellemmes, S., Drumare, I., et. al. (2012) Whole-exome sequencing identifies mutations in GPR179 leading to autosomal-recessive complete congenital stationary night blindness. Am. J. Hum. Genet., 90, 321–330.

Balsalobre, A., Damiola, F. & Schibler, U. (1998) A serum shock induces circadian gene expression in mammalian tissue culture cells. Cell, 93, 929–937.

Bassi, C.J. & Powers, M.K. (1987) Circadian rhythm in goldfish visual sensitivity. Invest. Ophthalmol. Vis. Sci., 28, 1811–1815.

Bech-Hansen, N.T., Naylor, M.J., Maybaum, T.A., Sparkes, R.L., Koop, B., Birch, D.G., Bergen, A.A., Prinsen, C.F., Polomeno, R.C., Gal, A., Drack, A.V., Musarella, M.A., Jacobson, S.G., Young, R.S. & Weleber, R.G. (2000) Mutations in NYX, encoding the leucine-rich proteoglycan nyctalopin, cause X-linked complete congenital stationary night blindness. Nat. Genet., 26, 319–323.

Branchek, T. (1984) The development of photoreceptors in the zebrafish, brachydanio rerio. II. Function. J. Comp. Neurol, 224, 116–122.

Branchek, T. & Bremiller, R. (1984) The development of photoreceptors in the zebrafish, Brachydanio rerio. I. Structure. J Comp Neurol, 224, 107–115.

Cahill, G.M., Grace, M.S. & Besharse, J.C. (1991) Rhythmic regulation of retinal melatonin: metabolic pathways, neurochemical mechanisms, and the ocular circadian clock. Cell. Mol. Neurobiol., 11, 529–560.

Cao, Y., Posokhova, E. & Martemyanov, K.A. (2011) TRPM1 forms complexes with nyctalopin in vivo and accumulates in postsynaptic compartment of ON-bipolar neurons in mGluR6-dependent manner. J. Neurosci., 31, 11521–11526.

Cavallari, N., Frigato, E., Vallone, D., Fröhlich, N., Lopez-Olmeda, J.F., Foà, A., Berti, R., Sánchez-Vázquez, F.J., Bertolucci, C. & Foulkes, N.S. (2011) A blind circadian clock in cavefish reveals that opsins mediate peripheral clock photoreception. PLoS Biol., 9, e1001142.

Chaves, I., Pokorny, R., Byrdin, M., Hoang, N., Ritz, T., Brettel, K., Essen, L.-O., van der Horst, G.T.J., Batschauer, A. & Ahmad, M. (2011) The cryptochromes: blue light photoreceptors in plants and animals. Annu Rev Plant Biol, 62, 335–364.

Clark, K.J., Voytas, D.F. & Ekker, S.C. (2011) A TALE of two nucleases: gene targeting for the masses? Zebrafish, 8, 147–149.

Connaughton, V.P. (2011) Bipolar cells in the zebrafish retina. Vis. Neurosci., 28, 77–93.

Davies, W.I.L., Collin, S.P. & Hunt, D.M. (2012) Molecular ecology and adaptation of visual photopigments in craniates. Mol. Ecol., 21, 3121–3158.

Dhingra, A., Jiang, M., Wang, T.-L., Lyubarsky, A., Savchenko, A., Bar-Yehuda, T., Sterling, P., Birnbaumer, L. & Vardi, N. (2002) Light response of retinal ON bipolar cells requires a specific splice variant of Galpha(o). J. Neurosci., 22, 4878–4884.

Dibner, C., Schibler, U. & Albrecht, U. (2010) The mammalian circadian timing system: organization and coordination of central and peripheral clocks. Annu. Rev. Physiol., 72, 517–549.

Doyle, S.E., Grace, M.S., McIvor, W. & Menaker, M. (2002) Circadian rhythms of dopamine in mouse retina: the role of melatonin. Vis. Neurosci., 19, 593–601.

Dryja, T.P., McGee, T.L., Berson, E.L., Fishman, G.A., Sandberg, M.A., Alexander, K.R., Derlacki, D.J. & Rajagopalan, A.S. (2005) Night blindness and abnormal cone electroretinogram ON responses in patients with mutations in the GRM6 gene encoding mGluR6. Proc. Natl. Acad. Sci. U.S.A., 102, 4884–4889.

Ekker, S.C. (2008) Zinc finger-based knockout punches for zebrafish genes. Zebrafish, 5, 121–123.

Emery, P., So, W.V., Kaneko, M., Hall, J.C. & Rosbash, M. (1998) CRY, a Drosophila clock and light-regulated cryptochrome, is a major contributor to circadian rhythm resetting and photosensitivity. Cell, 95, 669–679.

Emran, F., Rihel, J., Adolph, A.R., Wong, K.Y., Kraves, S. & Dowling, J.E. (2007) OFF ganglion cells cannot drive the optokinetic reflex in zebrafish. Proc. Natl. Acad. Sci. U.S.A., 104, 19126–19131.

Engeszer, R.E., Patterson, L.B., Rao, A.A. & Parichy, D.M. (2007) Zebrafish in The Wild: A Review of Natural History And New Notes from The Field. Zebrafish, 4, 21–40.

Fernandes, A.M; Fero K.; Arrenberg, A.B; Bergeron, S.A; Driever, W.; Burgess, H.A (2012) Deep brain photoreceptors control light seeking behavior in zebrafish larvae. Current Biology. In press.

Foley, L.E., Gegear, R.J. & Reppert, S.M. (2011) Human cryptochrome exhibits light-dependent magnetosensitivity. Nat Commun, 2, 356.

Force, A., Lynch, M., Pickett, F.B., Amores, A., Yan, Y.L. & Postlethwait, J. (1999) Preservation of duplicate genes by complementary, degenerative mutations. Genetics, 151, 1531–1545.

Gegear, R.J., Casselman, A., Waddell, S. & Reppert, S.M. (2008) Cryptochrome mediates light-dependent magnetosensitivity in Drosophila. Nature, 454, 1014–1018.

Gesemann, M., Lesslauer, A., Maurer, C.M., Schönthaler, H.B. & Neuhauss, S.C.F. (2010) Phylogenetic analysis of the vertebrate excitatory/neutral amino acid transporter (SLC1/EAAT) family reveals lineage specific subfamilies. BMC Evol. Biol, 10, 117.

Grant, G.B. & Dowling, J.E. (1995) A glutamate-activated chloride current in cone-driven ON bipolar cells of the white perch retina. J Neurosci, 15, 3852–3862.

Grant, G.B. & Dowling, J.E. (1996) On bipolar cell responses in the teleost retina are generated by two distinct mechanisms. J Neurophysiol, 76, 3842–3849.

Gregg, R.G., Mukhopadhyay, S., Candille, S.I., Ball, S.L., Pardue, M.T., McCall, M.A. & Peachey, N.S. (2003) Identification of the gene and the mutation responsible for the mouse nob phenotype. Invest. Ophthalmol. Vis. Sci., 44, 378–384.

Guido, M.E., Garbarino-Pico, E., Contin, M.A., Valdez, D.J., Nieto, P.S., Verra, D.M., Acosta-Rodriguez, V.A., Zavalía, N. de & Rosenstein, R.E. (2010) Inner retinal circadian clocks and non-visual photoreceptors: novel players in the circadian system. Prog. Neurobiol., 92, 484–504.

Halford, S., Pires, S.S., Turton, M., Zheng, L., González-Menéndez, I., Davies, W.L., Peirson, S.N., García-Fernández, J.M., Hankins, M.W. & Foster, R.G. (2009) VA opsin-based photoreceptors in the hypothalamus of birds. Curr. Biol., 19, 1396–1402.

Hannibal, J. & Fahrenkrug, J. (2006) Neuronal input pathways to the brain's biological clock and their functional significance. Adv Anat Embryol Cell Biol, 182, 1–71.

Hattar, S., Lucas, R.J., Mrosovsky, N., Thompson, S., Douglas, R.H., Hankins, M.W., Lem, J., Biel, M., Hofmann, F., Foster, R.G. & Yau, K.-W. (2003) Melanopsin and rod-cone photoreceptive systems account for all major accessory visual functions in mice. Nature, 424, 76–81.

Hegarty, M.J. & Hiscock, S.J. (2008) Genomic clues to the evolutionary success of polyploid plants. Curr. Biol., 18, R435-44.

Hoegg, S. & Meyer, A. (2005) Hox clusters as models for vertebrate genome evolution. Trends Genet., 21, 421–424.

Imanishi, Y., Li, N., Sokal, I., Sowa, M.E., Lichtarge, O., Wensel, T.G., Saperstein, D.A., Baehr, W. & Palczewski, K. (2002) Characterization of retinal guanylate cyclase-activating protein 3 (GCAP3) from zebrafish to man. Eur. J. Neurosci., 15, 63–78.

Jackson, C.R., Ruan, G.-X., Aseem, F., Abey, J., Gamble, K., Stanwood, G., Palmiter, R.D., Iuvone, P.M. & McMahon, D.G. (2012) Retinal Dopamine Mediates Multiple Dimensions of Light-Adapted Vision. The Journal of neuroscience : the official journal of the Society for Neuroscience, 32, 9359–9368.

Kawakami, K. & Shima, A. (1999) Identification of the Tol2 transposase of the medaka fish Oryzias latipes that catalyzes excision of a nonautonomous Tol2 element in zebrafish Danio rerio. Gene, 240, 239–244.

Klooster, J., Blokker, J., Brink, J.B. ten, Unmehopa, U., Fluiter, K., Bergen, A.A.B. & Kamermans, M. (2011) Ultrastructural Localization and Expression of Trpm1 in the Human Retina. Invest. Ophthalmol. Vis. Sci.

Kobayashi, Y., Ishikawa, T., Hirayama, J., Daiyasu, H., Kanai, S., Toh, H., Fukuda, I., Tsujimura, T., Terada, N., Kamei, Y., Yuba, S., Iwai, S. & Todo, T. (2000) Molecular analysis of zebrafish photolyase/cryptochrome family: two types of cryptochromes present in zebrafish. Genes Cells, 5, 725–738.

Kojima, D., Mano, H. & Fukada, Y. (2000) Vertebrate ancient-long opsin: a green-sensitive photoreceptive molecule present in zebrafish deep brain and retinal horizontal cells. J. Neurosci., 20, 2845–2851.

Kojima, D., Torii, M., Fukada, Y. & Dowling, J.E. (2008) Differential expression of duplicated VAL-opsin genes in the developing zebrafish. J. Neurochem., 104, 1364–1371.

Krizaj, D., Gábriel, R., Owen, W.G. & Witkovsky, P. (1998) Dopamine D2 receptor-mediated modulation of rod-cone coupling in the Xenopus retina. J. Comp. Neurol., 398, 529–538.

Lavoie, J., Gagné, A.-M., Lavoie, M.-P., Sasseville, A., Charron, M.-C. & Hébert, M. (2010) Circadian variation in the electroretinogram and the presence of central melatonin. Doc Ophthalmol, 120, 265–272.

Li, L. & Dowling, J.E. (1998) Zebrafish visual sensitivity is regulated by a circadian clock. Vis. Neurosci., 15, 851–857.

Li, Y., Tsujimura, T., Kawamura, S. & Dowling, J. (2011) Bipolar Cell-Photoreceptor Connections in the Zebrafish Retina, ARVO Abstract Nr. 2573.

Lin, C. & Todo, T. (2005) The cryptochromes. Genome Biol., 6, 220.

Masland, R.H. (2001) The fundamental plan of the retina. Nat. Neurosci. 4 (9), 877–886.

Masu, M., Iwakabe, H., Tagawa, Y., Miyoshi, T., Yamashita, M., Fukuda, Y., Sasaki, H., Hiroi, K., Nakamura, Y., Shigemoto, R. & et al. (1995) Specific deficit of the ON response in visual transmission by targeted disruption of the mGluR6 gene. Cell, 80, 757–765.

Maurer, C.M. (2010) Aspects of retinal signaling and visual behavior in the zebrafish, Ph.D. Thesis, University of Zurich, Switzerland.

Mills, I., Adolph, A. & Dowling, J. (2009) Rods are Functional in 5-6 Day Old Larval Zebrafish, ARVO Abstract Nr. 4566.

Moens, C.B., Donn, T.M., Wolf-Saxon, E.R. & Ma, T.P. (2008) Reverse genetics in zebrafish by TILLING. Brief Funct Genomic Proteomic, 7, 454–459.

Morgans, C.W., Zhang, J., Jeffrey, B.G., Nelson, S.M., Burke, N.S., Duvoisin, R.M. & Brown, R.L. (2009) TRPM1 is required for the depolarizing light response in retinal ON-bipolar cells. Proc. Natl. Acad. Sci. U.S.A., 106, 19174–19178.

Neinstein A.G., Dhingra, A., Fina, M. & Vardi, N. (2012) Absence of Gβ3 from ON Bipolar Cells Reduces Expression of Postsynaptic and Presynaptic Proteins, ARVO Abstract Nr. 4315.

Nelson, R.F. & Singla, N. (2009) A spectral model for signal elements isolated from zebrafish photopic electroretinogram. Vis. Neurosci., 26, 349–363.

Ohno, S. (1999) Gene duplication and the uniqueness of vertebrate genomes circa 1970-1999. Semin. Cell Dev. Biol., 10, 517–522.

Ohuchi, H., Yamashita, T., Tomonari, S., Fujita-Yanagibayashi, S., Sakai, K., Noji, S. & Shichida, Y. (2012) A non-mammalian type opsin 5 functions dually in the photoreceptive and non-photoreceptive organs of birds. PLoS ONE, 7, e31534.

Orlandi, C., Posokhova, E., Masuho, I., Ray, T.A., Hasan, N., Gregg, R.G. & Martemyanov, K.A. (2012) GPR158/179 regulate G protein signaling by controlling localization and activity of the RGS7 complexes. J. Cell Biol., 197, 711–719.

Peachey, N.S., Ray, T.A., Florijn, R., Rowe, L.B., Sjoerdsma, T., Contreras-Alcantara, S., et. al. (2012) GPR179 is required for depolarizing bipolar cell function and is mutated in autosomal-recessive complete congenital stationary night blindness. Am. J. Hum. Genet., 90, 331–339.

Pearring, J.N., Bojang, P., Shen, Y., Koike, C., Furukawa, T., Nawy, S. & Gregg, R.G. (2011) A role for nyctalopin, a small leucine-rich repeat protein, in localizing the TRP melastatin 1 channel to retinal depolarizing bipolar cell dendrites. J. Neurosci., 31, 10060–10066.

Plautz, J.D., Kaneko, M., Hall, J.C. & Kay, S.A. (1997) Independent photoreceptive circadian clocks throughout Drosophila. Science, 278, 1632–1635.

Ribelayga, C., Cao, Y. & Mangel, S.C. (2008) The circadian clock in the retina controls rod-cone coupling. Neuron, 59, 790–801.

Rinner, O., Makhankov, Y.V., Biehlmaier, O. & Neuhauss, S.C.F. (2005) Knockdown of cone-specific kinase GRK7 in larval zebrafish leads to impaired cone response recovery and delayed dark adaptation. Neuron, 47, 231–242.

Ritz, T., Adem, S. & Schulten, K. (2000) A model for photoreceptor-based magnetoreception in birds. Biophys. J., 78, 707–718.

Rowan, M.J.M., Ripps, H. & Shen, W. (2010) Fast glutamate uptake via EAAT2 shapes the cone-mediated light offset response in bipolar cells. J. Physiol. (Lond.), 588, 3943–3956.

Sahar, S. & Sassone-Corsi, P. (2012) Regulation of metabolism: the circadian clock dictates the time. Trends Endocrinol. Metab., 23, 1–8.

Saszik, S., Alexander, A., Lawrence, T. & Bilotta, J. (2002) APB differentially affects the cone contributions to the zebrafish ERG. Vis. Neurosci., 19, 521–529.

Schröder, H.C., Krasko, A., Gundacker, D., Leys, S.P., Müller, I.M. & Müller, W.E.G. (2003) Molecular and functional analysis of the (6-4) photolyase from the hexactinellid Aphrocallistes vastus. Biochim. Biophys. Acta, 1651, 41–49.

Selby, C.P., Thompson, C., Schmitz, T.M., van Gelder, R.N. & Sancar, A. (2000) Functional redundancy of cryptochromes and classical photoreceptors for nonvisual ocular photoreception in mice. Proc. Natl. Acad. Sci. U.S.A., 97, 14697–14702.

Shen, Y., Heimel, J.A., Kamermans, M., Peachey, N.S., Gregg, R.G. & Nawy, S. (2009) A transient receptor potential-like channel mediates synaptic transmission in rod bipolar cells. J. Neurosci., 29, 6088–6093.

Shcherbakov, D., Winklhofer, M., Petersen, N., Steidle, J., Hilbig, R., Blum, M. (2005) Magnetosensation in zebrafish. In *Curr. Biol.* 15 (5), R161-2.

Stuart, G.W., McMurray, J.V. & Westerfield, M. (1988) Replication, integration and stable germ-line transmission of foreign sequences injected into early zebrafish embryos. Development, 103, 403–412.

Tamai, T.K., Vardhanabhuti, V., Foulkes, N.S. & Whitmore, D. (2004) Early embryonic light detection improves survival. Curr. Biol., 14, R104-5.

Tamai, T.K., Young, L.C. & Whitmore, D. (2007) Light signaling to the zebrafish circadian clock by Cryptochrome 1a. Proc. Natl. Acad. Sci. U.S.A., 104, 14712–14717.

Tarttelin, E.E., Bellingham, J., Hankins, M.W., Foster, R.G. & Lucas, R.J. (2003) Neuropsin (Opn5): a novel opsin identified in mammalian neural tissue. FEBS Lett., 554, 410–416.

Tse, D.Y., Chung, I. & Wu, S.M. (2012) Effects Of Glutamate Transporters On Bipolar Cell Responses In Dark-adapted Living Mice, ARVO Abstract Nr. 3160.

Tummala, S., Fina, M., Dhingra, A. & Vardi, N. (2012) Gαo1 is Required for the Proper Expression of mGluR6 Transduction Elements in ON-Bipolar Cells, ARVO Abstract Nr. 4314.

van der Horst, G.T., Muijtjens, M., Kobayashi, K., Takano, R., Kanno, S., Takao, M., Wit, J. de, Verkerk, A., Eker, A.P., van Leenen, D., Buijs, R., Bootsma, D., Hoeijmakers, J.H. & Yasui, A. (1999) Mammalian Cry1 and Cry2 are essential for maintenance of circadian rhythms. Nature, 398, 627–630.

van Genderen, M.M., Bijveld, M.M.C., Claassen, Y.B., Florijn, R.J., Pearring, J.N., Meire, F.M., McCall, M.A., Riemslag, F.C.C., Gregg, R.G., Bergen, A.A.B. & Kamermans, M. (2009) Mutations in TRPM1 are a common cause of complete congenital stationary night blindness. Am. J. Hum. Genet., 85, 730–736.

Vandepoele, K., Vos, W. de, Taylor, J.S., Meyer, A. & van de Peer, Y. (2004) Major events in the genome evolution of vertebrates: paranome age and size differ considerably between ray-finned fishes and land vertebrates. Proc. Natl. Acad. Sci. U.S.A., 101, 1638–1643.

Vardi, N., Duvoisin, R., Wu, G. & Sterling, P. (2000) Localization of mGluR6 to dendrites of ON bipolar cells in primate retina. J Comp Neurol, 423, 402–412.

Vihtelic, T.S., Doro, C.J. & Hyde, D.R. (1999) Cloning and characterization of six zebrafish photoreceptor opsin cDNAs and immunolocalization of their corresponding proteins. Vis. Neurosci., 16, 571–585.

Vitaterna, M.H., Selby, C.P., Todo, T., Niwa, H., Thompson, C., Fruechte, E.M., Hitomi, K., Thresher, R.J., Ishikawa, T., Miyazaki, J., Takahashi, J.S. & Sancar, A. (1999) Differential regulation of mammalian period genes and circadian rhythmicity by cryptochromes 1 and 2. Proc. Natl. Acad. Sci. U.S.A., 96, 12114–12119.

Wersinger, E., Schwab, Y., Sahel, J.-A., Rendon, A., Pow, D.V., Picaud, S. & Roux, M.J. (2006) The glutamate transporter EAAT5 works as a presynaptic receptor in mouse rod bipolar cells. J. Physiol. (Lond.), 577, 221–234.

Whitmore, D., Foulkes, N.S. & Sassone-Corsi, P. (2000) Light acts directly on organs and cells in culture to set the vertebrate circadian clock. Nature, 404, 87–91.

Witkovsky, P. (2004) Dopamine and retinal function. Doc Ophthalmol, 108, 17–40.

Wong, K.Y. & Dowling, J.E. (2005) Retinal bipolar cell input mechanisms in giant danio. III. ON-OFF bipolar cells and their color-opponent mechanisms. J. Neurophysiol., 94, 265–272.

Wong, K.Y., Adolph, A.R. & Dowling, J.E. (2005) Retinal bipolar cell input mechanisms in giant danio. I. Electroretinographic analysis. J Neurophysiol, 93, 84–93.

Wong, K.Y., Gray, J., Hayward, C.J.C., Adolph, A.R. & Dowling, J.E. (2004) Glutamatergic mechanisms in the outer retina of larval zebrafish: analysis of electroretinogram b- and d-waves using a novel preparation. Zebrafish, 1, 121–131.

Xu, Y., Dhingra, A., Fina, M.E., Koike, C., Furukawa, T. & Vardi, N. (2012) mGluR6 deletion renders the TRPM1 channel in retina inactive. J. Neurophysiol., 107, 948–957.

Yoshii, T., Ahmad, M. & Helfrich-Förster, C. (2009) Cryptochrome mediates light-dependent magnetosensitivity of Drosophila's circadian clock. PLoS Biol., 7,4.

Yu, W.-P., Rajasegaran, V., Yew, K., Loh, W.-L., Tay, B.-H., Amemiya, C.T., Brenner, S. & Venkatesh, B. (2008) Elephant shark sequence reveals unique insights into the evolutionary history of vertebrate genes: A comparative analysis of the protocadherin cluster. Proc. Natl. Acad. Sci. U.S.A., 105, 3819–3824.

Zeitz, C., van Genderen, M., Neidhardt, J., Luhmann, U.F.O., Hoeben, F., Forster, U., Wycisk, K., Mátyás, G., Hoyng, C.B., Riemslag, F., Meire, F., Cremers, F.P.M. & Berger, W. (2005) Mutations in GRM6 cause autosomal recessive congenital stationary night blindness with a distinctive scotopic 15-Hz flicker electroretinogram. Invest. Ophthalmol. Vis. Sci., 46, 4328–4335.

Zhu, H., Sauman, I., Yuan, Q., Casselman, A., Emery-Le, M., Emery, P. & Reppert, S.M. (2008) Cryptochromes define a novel circadian clock mechanism in monarch butterflies that may underlie sun compass navigation. PLoS Biol., 6,1.

V CURRICULUM VITAE

Personal Information

Name:	Marion Haug
Present address:	In Weizenächern 16, 8103 Unterengstringen
Phone:	+41 79 746 64 39
E-mail:	marion.haug@imls.uzh.ch
Date of birth:	19.08.1982
Place of origin:	Weiningen ZH
Citizenship:	Switzerland

Academic Education

1998 – 2002 09/2002	Secondary School, Kantonsschule Limmattal, Urdorf, Switzerland Matura Typus K
2003 – 2005	Undergraduate Studies of Biology, University of Zurich
2005 – 2008	Graduate Studies in Neuroscience, University of Zurich
01/2008	Master in Neuroscience, University of Zurich Master Thesis in the Laboratory of Prof. Dr. Stephan Neuhauss at the Institute of Zoology, University of Zurich: *Analysis of Metabotropic Glutamate Receptors in the Zebrafish Retina.*
2006 – 2010 06/2010	Teacher education, University of Zurich Certificate of teaching ability (teaching degree for secondary schools)
since 09/2008	PhD-Thesis in the Laboratory of Prof. Dr. Stephan Neuhauss at the Institute of Molecular Life Sciences (formerly Institute of Zoology), University of Zurich: *Molecular Dissection of Visual Sensitivity in Zebrafish.*

Professional Experience

05-07 2008	School teaching (secondary school) Kantonsschule Zürcher Unterland, Bülach, Switzerland

since 09/2008	International PhD-Program in Neuroscience Neuroscience Center Zurich (ZNZ), Zurich, Switzerland
since 09/2008	Teaching assistant Practical training in invertebrates for undergraduate students Neurobiology courses for undergraduate and gradutate students Practical training in genetics and developmental biology for medical students
10/2010 – 10/2011	Supervision of the Master Thesis of Viktor Lazovic
since 09/2011	Lecturer Bio 901: Master of Advanced Studies in Secondary and Higher Education, responsible for the didactical part of the term paper written by prospective high school teachers Bio 114: practical training in genetics for prospective high school teachers Practical training in molecular cell biology for medical students, part 14: Invertebrates

Presentation at Meetings (first authorships only)

2006, 2009-12	Various posters at the annual ZNZ-Symposium, Zurich, Switzerland
01/2007	Swiss Retina Meeting, Brunnen, Switzerland *Talk: Visual acuity in zebrafish*
01/2009	Swiss Eye Research Meeting, Brunnen, Switzerland *Talk: Genomic diversification and expression of metabotropic glutamate receptors in the zebrafish retina* Prize for best talk
04/2009	8th Goettingen Meeting of the German Neuroscience Society, Göttingen, Germany *Poster:* Role of Metabotropic Glutamate Receptors in the Zebrafish Retina
07/2009	6th European Zebrafish Meeting, Rome, Italy *Poster: Metabotropic glutamate receptors in the zebrafish retina*
04/2010	3rd Swiss Zebrafish Meeting, Zurich, Switzerland *Poster: Metabotropic glutamate receptors in the zebrafish retina*
05/2010	ARVO annual meeting, Fort Lauderdale, Florida, USA *Poster: Expressional and functional analysis of mGluR6 in the zebrafish retina*
05/2010	ZNZ annual retreat, Valens, Switzerland *Poster: Expressional and functional analysis of mGluR6 in the zebrafish retina*
06/2010	Young Researcher Vision Camp, Leibertingen, Germany *Talk: Expressional and functional analysis of mGluR6 in the zebrafish retina*

01/2011	IMLS Retreat, Wildhaus, Switzerland *Talk: Role of mGluR6 in teleost vision* Prize for best talk
01/2011	Swiss Eye Research Meeting, Biel, Switzerland *Talk: Glutamate signaling at the photoreceptor ON-bipolar synapse* Prize for best talk of a young scientist
07/2011	7th European Zebrafish Meeting, Edinburgh, Scotland *Poster: Role of mGluR6 at the zebrafish ON-bipolar cell synapse*
05/2012	ARVO annual meeting, Fort Lauderdale, Florida, USA *Poster: A glutamate transporter and the conserved mGluR6/TRPM1 pathway mediate the zebrafish ON-response*

List of Publications

Marion F. Haug*, Oliver Biehlmaier*, Kaspar P. Mueller, Stephan C.F. Neuhauss
Visual acuity in larval zebrafish: behavior and histology.
** These authors contributed equally*
Published in *Frontiers in Zoology*, 2010, Mar 1; 7:8.

Marion F. Haug*, Matthias Gesemann*, Ying-Yu Huang*, Stephan C.F. Neuhauss
Novel expression patterns of metabotropic glutamate receptor 6 in the zebrafish nervous system.
** These authors contributed equally*
Published *in PLoS One*, 2012, 7(4).

Marion F. Haug, Matthias Gesemann, Thomas Mueller, Ying-Yu Huang, Stephan C.F. Neuhauss
Identification, Phylogenetic Analysis and Expression Pattern Divergence of Metabotropic Glutamate Receptor Genes in the Brain of Zebrafish (Danio rerio)
Submitted to the *Journal of Comparative Neurology*

VI ACKNOWLEDGEMENTS

First and foremost I would like to thank my mentor Stephan Neuhauss for the constant support during my Ph.D. The joy and enthusiasm he has for his research was contagious and motivational, moreover, his encouragement and open-mindedness enabled this work and helped me to develop own ideas and projects beyond the daily lab routine.

Many thanks to the two other members of my Ph.D. committee, Christian Grimm and Steve Brown, for their supportive and open conversations during meetings.

In addition, all present and former members of the Neuhauss Lab have made the last years here very pleasant. Thanks for creating such a great working atmosphere, for encouraging discussions, and for the nice and funny time at trips and conferences. Special thanks go to Matthias and Edda: not only sharing medical stories during the last months of my Ph.D. but also Matthias' immense knowledge about bioinformatics and biochemistry and Edda's skilled advice concerning lab protocols or all other facets of life was of great help! It's a great pleasure working with you ☺. All the fish I used for my studies would have never had such a happy life without Kara, Fränzi, and the fishfeeders. Kara, thanks for your overwhelming energy in taking care of our fishroom and for keeping the lab working. I am grateful to Viktor, who was open-minded and intellectual master student and greatly promoted the Cryptochrome project, and to Röbi, my part-time master student, master of cloning and father of Glurs, Glursus, Nyccy, Nycole, and Nyco. Also many thanks to Corinne, Colette, and Valerie who were a great inspiration during my first years; to Sabina for sharing and discussing all problems concerning the life of a Ph.D. student; to Kaspar for his patience in solving all OKR or VMR problems; and to Irene for guiding us through the administrative jungle of the University.

Many thanks to my colleagues form the gym club and the ASVZ, and to Emina. The hours we spent sweating together either inside the gym hall or outside in nature helped balancing my work-life immensely!

Last but not least: Herzlichen Dank meiner Familie und Dani! Ihr wart meine Wurzeln während schlechten Zeiten und habt mich immer in all meinen Vorhaben unterstützt. Speziell möchte ich meinen Eltern danken, die mir das Interesse an die Natur weitergaben, das Studium überhaupt ermöglichten, meinen Entscheidungen vertrauten und sich immer für meine Arbeit interessierten. Vielen Dank!